Operational Planning and Optimisation in Active Distribution Systems for Flexible and Resilient Power Networks

Ahmad Asrul Bin Ibrahim

A Thesis presented for the degree of
Doctor of Philosophy

Department of Engineering
Durham University
England

2018

Dedicated to

My parents, wife and daughter

Operational Planning and Optimisation in Active Distribution Systems for Flexible and Resilient Power Networks

Ahmad Asrul Bin Ibrahim

Abstract

The electricity network is undergoing significant changes to cater to environmental-deterioration and fuel-depletion issues. Consequently, an increasing number of renewable resources in the form of distributed generation (DG) are being integrated into medium-voltage distribution networks. The DG integration has created several technical and economic challenges for distribution network operators. The main challenge is basically the problem of managing network voltage profile and congestion which is caused by increasing demand and intermittent DG operations. The result of all of these changes is a paradigm shift in the way distribution networks operate (from passive to active) and are managed that is not limited only to the distribution network operator but actively engages with network users such as demand aggregators, DG owners, and transmission-system operators. This thesis expands knowledge on the active distribution system in three specific areas and attempts to fill the gaps in existing approaches. A comprehensive active network management framework in active distribution systems is developed to allow studies on (i) the flexibility of network topology using modern power flow controllers, (ii) the benefits of centralised thermal electricity storage in achieving the required levels of flexibility and resiliency in an active distribution system, and (iii) system resiliency toward fault occurrence in hybrid AC/DC distribution systems. These works are implemented within the Advanced Interactive Multidimensional Modelling Systems (AIMMS) software to carry out optimisation procedure. Results demonstrate the benefit provided by a range of active distribution system solutions and can guide future distribution-system operators in making practical decisions to operate active distribution systems in cost-effective ways.

Declaration

The work in this thesis is based on research carried out at the Department of Engineering, Durham University, England. No part of this thesis has been submitted elsewhere for any other degree or qualification and it is all my own work unless referenced to the contrary in the text.

Acknowledgement

All praise to Allah for giving me the strength to be able to go through the tough times of completing this journey of PhD work. I am very thankful to my supervisor, Dr. Behzad Kazemtabrizi whose encouragement, guidance and support have motivated me to complete this work. I am very much indebted to his strong perseverance and motivation in encouraging me to complete my studies.

I would also like to dedicate my appreciation to my co-supervisor, Dr. Chris Dent who is never reluctant to share his comments and ideas. Also, I am thankful to all my colleagues in Research Office E215 for being such wonderful team members and very helpful throughout the years. To the Malaysian community in Durham, thank you for always being there for me whenever I need help and advice. I also owe my deepest gratitude to Universiti Kebangsaan Malaysia and ministry of higher education Malaysia for their financial support.

Lastly, I dedicate this PhD to my wonderful family members especially my parents who never stop supporting me and believing in me. To my wife for her love and support throughout the years. Finally to my wonderful daughter Amna, thank you for being my utmost encouragement and strength although it has been so difficult and trying at times. I would never have completed this PhD without all of you.

Contents

List of Figures

List of Tables

List of Abbreviations

AA-CAES	Advanced Adiabatic CAES
ABC	Artificial Bee Colony
AC	Alternating Current
ACO	Ant Colony Optimization
ADNEP	Active Distribution Network Expansion Planning
ADS	Active Distribution Systems
AE	Absolute Error
AIMMS	Advanced Interactive Multidimensional Modelling Systems
AMI	Advanced Metering Infrastructure
ANM	Active Network Management
ASIFI	Average System Interruption Frequency Index
BES	Battery Energy Storage
BPSO	Binary Particle Swarm Optimization
BTB	Back-to-Back
CAES	Compressed Air Energy Storage
CfD	Contracts for Difference
CSA	Cuckoo Search Algorithm
CSC	Current Source Converter
CVSR	Continuously Variable Series Reactor
DER	Distributed Energy Resource
DFIG	Doubly-Fed Induction Generator
DC	Direct Current
DE	Differential Evaluation
DG	Distributed Generation

DNO	Distribution Network Operator
DOPF	Dynamic Optimal Power Flow
DSA	Dynamic Security Assessment
D-SCOPF	Distribution Security Constrained Optimal Power Flow
DSO	Distribution System Operator
DSM	Demand Side Management
DSSR	Distribution System Security Region
ENS	Energy Not Supplied
ESS	Energy Storage System
ER	Engineering Recommendation
EU	European Union
EV	Electric Vehicle
FDIR	Fault Detection, Isolation and Reconfiguration
FES	Flywheel Energy Storage
FIT	Feed-In Tariff
GA	Genetic Algorithm
GSP	Grid Supply Point
HVDC	High Voltage Direct Current
ICT	Information and Communication Technology
IGBT	Insulated-Gate Bipolar Transistor
LAES	Liquid Air Energy Storage
LED	Light Emitting Diode
LIFO	Last-In First-Out
LP	Linear Programming
LTC	Load Tap Changer
MAE	Mean Absolute Error
MACS	Multi Agent Control System
MAIFI	Momentary Average Interruption Frequency Index
MC	Monte Carlo
MICP	Mixed-Integer Conic Programming

MIQCP	Mixed Integer Quadratically Constrained Programming
MINLP	Mixed Integer Non-Linear Programming
MISCOP	Mixed-Integer Second-order Cone Programming
MSE	Mean Square Error
MTS	Modified Tabu Search
MV	Medium Voltage
MVDC	Medium Voltage Direct Current
NERC	North American Electric Reliability Council
NLP	Non-Linear Programming
OLTC	On-Load Tap Changer
OPF	Optimal Power Flow
PCM	Phase Change Material
PCS	Power Conditioning System
PEV	Plug-in Electric Vehicle
PHES	Pumped Hydroelectric Energy Storage
PHEV	Plug-in Hybrid Electric Vehicle
PSO	Particle Swarm Optimization
PTES	Pumped Thermal Electricity Storage
PWM	Pulse Width Modulation
P2P	Point-to-Point
QCP	Quadratically Constrained Programming
QP	Quadratic Programming
RBSA	Risk-Based Security Assessment
RCS	Remotely Controlled Switch
RMSE	Root Mean Square Error
RTP	Real-Time Pricing
RO	Renewable Obligation
SA	Simulated Annealing
SAIFI	System's Average Interruption Frequency Index
SARFI	System Average RMS Variation Frequency Index

SCADA	Supervisory Control And Data Acquisition
SCES	Super-Capacitor Energy Storage
SCOPF	Security-Constrained Optimal Power Flow
SDP	Semi-Definite Program
SEDG	Sustainable Electricity and Distributed Generation
SFLA	Shuffled Frog Leaping Algorithm
SMES	Superconducting Magnetic Energy Storage
SoC	State of Charge
SOCP	Second-Order Cone Programming
SOP	Soft Open Point
SSE	Sum Square Error
SSSA	Steady-State Security Assessment
STATCOM	Static Compensator
SVC	Static VAR Compensator
SVR	Step-Voltage Regulator
SVS	Synchronous Voltage Source
TES	Thermal Energy Storage
TOPSIS	Technique for Order Preference by Similarity to Ideal Solution
TS	Tabu Search
TSC	Total Supply Capability
TSO	Transmission System Operator
VSC	Voltage Source Converter
VVC	Voltage/Var Control

Chapter 1

Introduction

In this chapter, an overview of the research questions addressed in this thesis has been outlined. The chapter also outlines the main aims of this research that were achieved through several objectives derived from the research questions. These objectives are the subject of subsequent chapters in this thesis. Meanwhile, a list of publications (published, under-review, and planned) is also outlined at the end of this chapter.

1.1 Background

Environmental concerns coupled with the rapid depletion of fossil fuel resources have led most countries across the world to move from conventional power plants to renewable and green resources. The electricity generated by renewable resources has shown a tremendous rise accounting for more than 465 TWh between 2006 to 2016 in the main EU countries as depicted in Figure 1.1 [1]. A rapid expansion trend can be observed in the quantity of electricity generated from wind and solar power generations which are 3.7 times and 44.4 times higher in 2016 than 2006, respectively. In the context of UK, total electricity generated by main renewable energy resources has increased more than 65 GWh (7.09 times) in a decade as shown in Figure 1.2 [2]. Apart from the large-scale renewable resource integration at the transmission levels, small scale renewable resources in form of distributed generation (DG) have also been integrated in distribution networks (medium and low voltage networks) to a

large extent [7]. Unlike transmission network, the distribution network generally operates in unidirectional power flow with a central supply point. On the other hand, renewable resources such as solar or wind are inherently intermittent which might be low during peak demand. High number of DG integration in distribution network, therefore, creates enormous technical challenges in terms of power quality, protection, stability and reliability, etc. [8–11]. This requires distribution network operator (DNO) to take proactive actions to face these challenges.

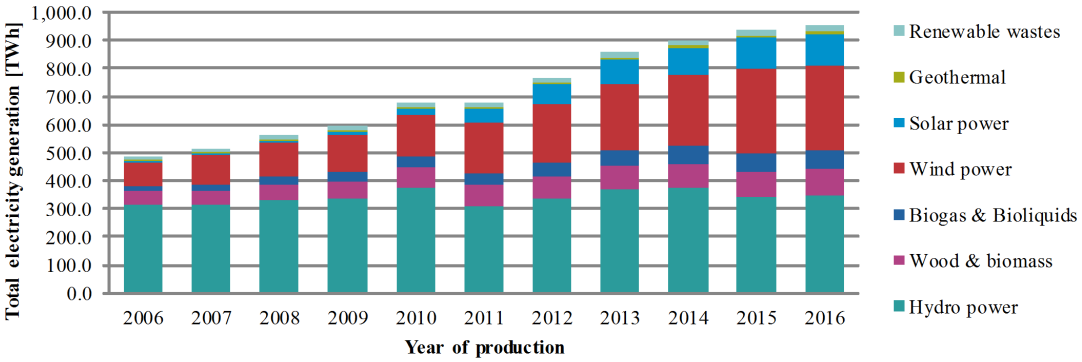

Figure 1.1: A growth of electricity generation from renewable resources in the EU-28 countries between year 2006 and 2016 [1]

A common practice to connect DG is based on the "fit and forget" concept where DG owners are required to carry out an assessment on the hosting capability of network for the intended DG installation that must not create technical problem under any circumstances. The worst-case scenarios, for example, DG output at maximum level and load at minimum level or vice versa, are usually considered in the assessment. The capacity of DG unit depends on site installation in the network. This challenge has been addressed in the literature using three different approaches; 1) identify the best location for predefined DG capacities [12], 2) calculate the optimal DG capacities at pre-defined locations [3, 13], and 3) determine the optimal DG capacities and locations [14–16]. The second approach is more realistic because renewable based-DGs are subjected to availability of resources and geographical constraints. Although the determination of DG capacity could avoid the technical problem, the level of DG penetration is further hindered by the relatively slow pace of network reinforcement and might increase cost and/or prevent achieving

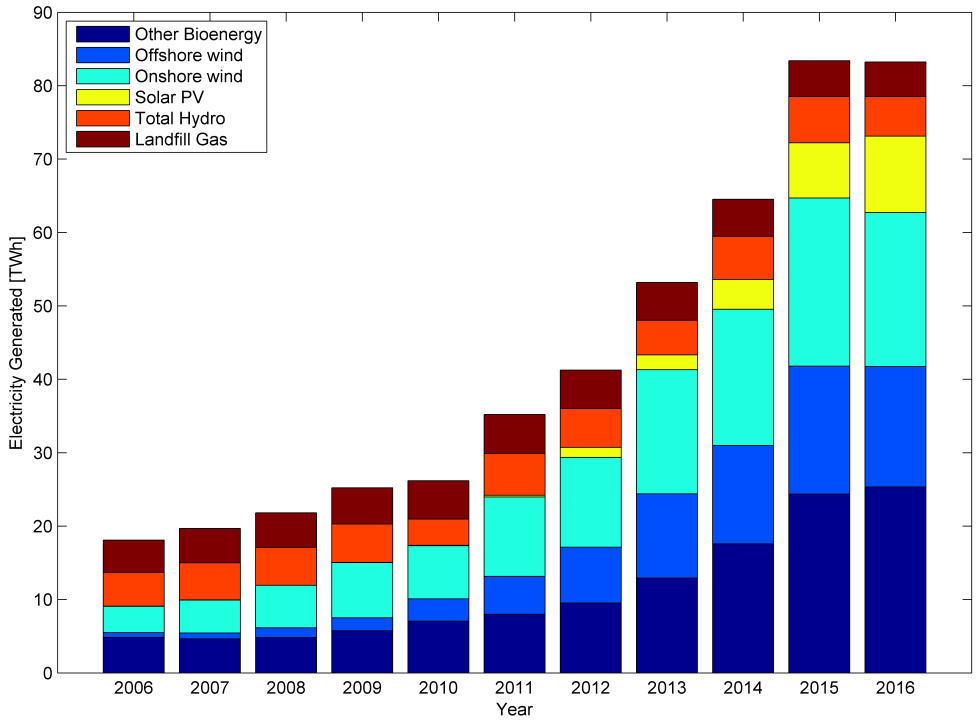

Figure 1.2: Electricity generation by main renewable resources in the UK between year 2006 and 2016 [2]

the renewable energy target. In addition, the occurrence probability of worst-case scenarios seems to be only few hours in a year [17] and thus, it is not beneficial to restrict the DG capacity for the due cause.

In another concept, known as the "fit and manage" concept, DG capacity is not restricted to a certain level as long as their outputs are controlled in a manner set by network operators in order to maintain stability and continuous safe operation of the distribution network [18]. This concept is not only limited to engagement with DG owners but includes other distribution network participants such as demand aggregators and the transmission system operator. More efficient, cost-effective and reliable electricity supply chain can be achieved from the incorporation of all participants via smart grid technologies (i.e, smart metering, digital communication, intelligence electronic devices, etc) [19]. This approach has brought more active components (i.e, flexible demand, non-firm generation, energy storage) into distribution network and creates the new challenge of managing these "active" distribution networks. This appears under the term "Active Distribution Systems (ADS)" as defined in [20]. De-

pending on the available network management schemes (commonly known as active network management or ANM), the ADS can be operated in a very similar fashion to how transmission systems are operated. In this context, term "Distribution System Operator (DSO)" is more suitable for future DNOs to cover the new dimension of their operation.

The ADS plays an important role to mitigate the occurrence of congestion issues (i.e., voltage and current congestion) from increasing demand and DG penetration in distribution networks. It has attracted enormous research interest to tackle the issues over the past few years. The research works have been done from different perspectives, for instance, coordinated volt-var control [21], coordinated dispatch of DGs [22–26] and network reconfiguration [6, 27, 28]. The management architecture used in these works can be classified into centralised and decentralised. The centralised approach is generally applied for the incoming day based on forecast information (i.e., demand and generation forecasting tool) to address wider network constraints. On the other hand, the decentralised approach lean towards real-time application and can be used to correct of any inaccuracies from the forecast data. This thesis mainly focuses on the centralised framework – known throughout this thesis as the "ANM framework" – which is based on a day-ahead optimisation. It is more suitable when considering energy storage applications as part of the congestion management scheme. Furthermore, demand side management requires an advance information for possible actions to achieve the network requirements. Although the day-ahead ADS planning framework has been widely discussed in the previous works, there are still some questions need to be answered.

1.2 Research Questions

The concept of ADS is generally understood and accepted by the research community. Arguments in the research mainly focus on the use of optimisation technique, objective function, variables of loads or generators, technology of energy resources, system constraints and taxonomy [29]. This thesis is looking into the application of new enabling technologies in distribution networks that could support ANM day-

ahead planning for improving flexibility, resiliency, and operation of a future ADS. Overall the following Research Questions (RQ) are identified:

RQ1 How should an ANM framework for day-ahead operational planning be modelled efficiently in terms of computational expenditure and complexity?

An ANM framework normally incorporates an optimisation procedure based on the multi-period optimal power flow formulation as presented in [13,30,31]. Several objective functions have been used for the optimisation problem to take environmental impacts into consideration [32–37], improve system voltages [38–40] and reduce network losses [3,41]. An ANM framework may therefore include multiple objective functions to address all of the aforementioned objectives. Meanwhile, the ANM framework should also incorporate different roles exerted by different actors (e.g. demand aggregators, DG owners) and enabling technologies (e.g. demand side management) within the network. These roles include DG power import/export [18, 42], incorporating demand response [43, 44] and rescheduling electrical vehicles charging times [45, 46]. The detailed model of the actors/enabling technologies is a complex problem and solved individually. Integrating them in a framework can lead to heavy computational burden. It is therefore essential to develop models that are computationally efficient and yet achieve the required performance. In this thesis RQ1 is the overarching theme of the thesis which is addressed in steps throughout Chapters 2 – 5. In Chapter 5, a unified ANM framework is introduced which is suitable for solving multi-period optimisation problems for a distribution network with any topology (radial and meshed, AC or DC), and with a variety of enabling technologies such as demand side management.

RQ2 How should an enhanced network reconfiguration scheme using power electronics control be integrated within an ANM framework?

One of the important ADS features is the ability to provide flexibility in distribution network configurations. This has been applied using network reconfiguration technique for added benefits in operation such as reducing system losses [41, 47–50], fulfilling voltage constraints [28, 51, 52] and improving reliability [53–55]. The network reconfiguration technique traditionally makes use

of the available normally open switches and sectionalising switches in the network. Statuses of the switches are alternated in a specific coordination so that power flow can be re-routed through feeders with less congestion and at the same time maintain the network radial topology. To obtain the best performance in the coordination, the switches are normally remotely controlled (i.e. they are called Remote Controlled Switches or RCS) [56]. Due to fluctuation in the demand and power injection especially from DG-based renewable resources, rapid changes of the switching statuses should be expected. This can lead to shorten the switch's life-time and increase maintenance costs. Static power electronics devices that are less subject to mechanical stress have witnessed increasing applications in distribution networks including static var compensators [57], power conditioning units [58] and soft normally-open points [59,60]. In this thesis, the use of such devices for fast network reconfiguration and voltage regulation is investigated. Their incorporation within an ANM is also studied and investigated. RQ2 is mainly the subject of Chapter 3.

RQ3 (a) What is the best way to model a realistic large-scale thermal energy storage? (b) How should such a model be integrated within an ANM framework without compromising tractability?

Energy storage system (ESS) technologies have special characteristics enabling them to operate either as generators or loads. It works as load in charging cycle by absorbing energy from distribution grid and when necessary it works as generator in discharging cycle by injecting energy back into the grid. With such flexible characteristics, the ESS could resolve the issue of mismatch between demand and generation. As a result, the use of ESS in ADS has seen a growing interest in recent research works [26,61,62]. An alternative ESS technology, known as pumped thermal electricity storage (PTES), is suggested in [63–65] to overcome geographical constraints with less impact to environment and low capital investment cost at a very long life cycle. The current model gives emphasis on thermodynamic studies that contains physical features of PTES in details. It is able to capture the behaviour of PTES in

every milliseconds which is not necessary for ADS applications. Too simple a model using fixed round-trip efficiency as used in [26] neglects the realistic operational characteristics of the PTES which in turn will be neglected when incorporated within an ANM framework. Therefore, an appropriate model of PTES is required which captures such details. Meanwhile, the model need be tractable for incorporation within the ANM framework. The subjects of RQ3 (modelling and integration) is addressed in Chapter 4.

RQ4 How should a hybrid AC/DC network be modelled and solved for purposes of ANM?

The renewable resources-based DG such as wind and solar generations often operate through an internal AC/DC/AC conversion stage. There are also different types of DC loads introduced in the market such as electric vehicle's charging facilities, DC data centres, LED lighting systems and variable-speed machines. It means more DC integration should be expected in the distribution networks. To reduce energy conversion steps and improve system efficiency, the distribution networks are suggested to operate in a full DC system [5]. However, the idea of converting MV distribution grids into DC systems cannot be done in totality due to the existence of many legacy AC equipment/infrastructure. Instead, it is more realistic to go through a gradual and step-by-step change from full AC to full DC. Consequently, a small portion of the existing distribution network will be converted to DC as more DC operated loads/DGs are integrated and operated as a hybrid AC/DC system. For the purposes of computational analysis (e.g. ANM framework) and modelling, AC and DC load flow formulations are different and therefore two separate platforms AC and DC need be developed and information exchanged between them to solve the hybrid AC/DC system [66]. This practice of solving AC and DC networks separately may however add to the computational burden and it is more straight forward computationally to solve the entire network in a unified manner. Thus, a unified formulation that is able to address both AC and DC problems should be formulated for the AC/DC hybrid system. RQ4 is the subject of Chapter 5.

RQ5 Can the security of supply be guaranteed in a flexible ADS?

The main challenge of system operator is to provide continuous service to the customer demand which can be measured as security of supply. The electricity service in power system is normally interrupted by unexpected events (e.g., equipment failures, lightning strikes, etc.) that lead to system outages and contingency conditions. The contingency conditions could cause circuit overloads and/or voltage violations. The issue has been widely addressed in previous works [67–71] by rescheduling generation units in a manner to provide adequate operating reserve that is able to avoid any network violations under pre-defined contingency conditions. The concept of security of operation is mostly applied for transmission networks and not investigated for distribution networks mostly due to their radial structure and passive operation. However, an ADS is expected to uphold the security of operation requirement. There are fundamental differences between an ADS and how it is operated through an ANM framework and a transmission system and therefore a new methodology for upholding the operational security need be developed for the ADS. RQ5 is addressed in Chapter 5 where a new improved ANM framework is introduced which not only optimises the coordination between actors but also guarantees a security of supply under all conditions.

1.3 Aim and Objectives

The main aim of this research is developing a new distribution system management scheme – known as ANM – using the state-of-the-art technologies for day-ahead planning at the presence of high levels of renewable resources while ensuring the security of supply. The overall objectives for this work are outlined as follows:

1. To develop a flexible distribution network configuration using power electronic control for application in day-ahead ADS operation and planning.

2. To establish an appropriate model of pumped thermal electricity storage for a centralised storage system in the medium-voltage distribution networks.

3. To investigate the benefits of hybrid AC/DC system using different configurations within an improved ANM framework and considering the operation security.

1.4 Thesis Structure

The main content of this thesis consists of 6 chapters including this introduction chapter. The rest of this thesis is organised and summarised as the following:

Chapter 2 describes the major challenges of the distribution network operation when considering high intermittent energy resources and demand fluctuations. Then, the concept of ADS is explained with the focus on its key components that can be used to address the afore-mentioned challenges. It also reviews different network management techniques and schemes that are relevant to the ADS concept. From the reviewed information, a model of active network management framework is developed within a simulation tool and applied on two selected benchmark distribution networks. The operating conditions of the networks are validated using a commonly used power simulation package. The case study presented at the end of this chapter shall be known as the "base case" throughout this thesis.

Chapter 3 explores the potential of flexible distribution network configuration using modern power flow controllers based on power electronics control. It starts with a review of the benefits of configuration flexibility using the existing conventional network reconfiguration methods. A modern power flow controller based on voltage source converters is introduced to replace mechanical switches that are used in the conventional approaches. An enhanced network reconfiguration method is then introduced based on the application of the power flow controllers. The enhanced network reconfiguration is then compared to the conventional network reconfiguration and the base case and the performance of each case is evaluated in terms of system loss, DG curtailment, voltage regulation, line loading, and total operational costs.

Chapter 4 develops a reduced model of pumped thermal electricity storage without neglecting its realistic operational characteristics for energy storage applications

when incorporated within the ANM framework. Meanwhile, a review of different energy storage technologies is given in the beginning of the chapter to distinguish their basic characteristics and give their performance overview for comparison purposes. The use of energy storage in the context of ADS applications in the previous works are reviewed and adopted in order to develop the reduced PTES model. The developed model is assessed with a detailed thermodynamic model and applied in one of the test network to showcase its performance when incorporated within an ANM framework. The analysis focuses on operational errors caused by fixed round-trip efficiency model as compared to the reduced model.

Chapter 5 studies the benefits of hybrid AC/DC systems to facilitate flexible operation whilst adhering to a pre-defined operational security criterion. This chapter starts with a brief review of the work done in literature on power systems operational security. It also highlights how the concept of ADS can help fulfil the security requirement within an improved ANM framework. This new security-constrained ANM is then applied to the hybrid AC/DC network. A unified formulation for both AC and DC systems is developed and applied within the new framework. One of the benchmark systems is used for this study and the performance are compared between different AC/DC system configurations.

Chapter 6 draws overall conclusions of the thesis. It also discusses the limitations of this work which can be used to derive potential directions for future work.

1.5 Publications

The outcomes of this thesis have been published or submitted for possible publications. A list of the publications and their relationship to chapters of the thesis is given in the following table.

Table 1.1: A list of publication

No	Publication	Thesis
1	Ahmad Asrul Ibrahim, Behzad Kazemtabrizi, Chris Dent. "Operational planning and optimisation in active distribution networks using modern intelligent power flow controllers" *In* ISGT Europe 2016 - IEEE PES Innovative Smart Grid Technologies, Europe, 2016	Chapter 3
2	Ahmad Asrul Ibrahim, Behzad Kazemtabrizi, Chiara Bordin, Chris J. Dent, Joshua D. McTigue, Alexander J. White. "Pumped thermal electricity storage for active distribution network applications" *In* 2017 IEEE Manchester PowerTech, 2017	Chapter 4
3	Javier Renedo, Ahmad Asrul Ibrahim, Aurelio Garca-Cerrada, Behzad Kazemtabrizi, Luis Rouco, Quanyu Zhao, Javier Garca-Gonzalez. "A simplified algorithm to solve optimal power flows in hybrid VSC-based AC/DC systems" *In* International Journal of Electric Power & Energy Systems (Under Review)	Chapter 5
4	Ahmad Asrul Ibrahim, Behzad Kazemtabrizi, Javier Renedo. "A new active network management framework for flexible hybrid AC/DC distribution networks" Under preparation	Chapter 5

Chapter 2

Distribution Systems Management

This chapter gives an overview of the distribution system management framework that will be used in this thesis. It covers a relevant background to the research problem, the main component of active distribution systems, different methods for active management and the working active network management framework. From the available information, the management framework is formulated as an optimal power flow problem. This chapter presents only the basic active network management scheme which can be derived from the previous works. Formulation for new applications to answer the research questions will be discussed in the following chapters. In the last section, the simulation packages and test systems for analysis in this thesis are explained. To ensure the distribution systems are modelled correctly, an evaluation procedure is carried out and presented in this chapter.

2.1 Driving Factors for an Active Network

The future medium-voltage distribution system is a system containing multiple distributed generation (DG) resources, and multiple actors (e.g. the aggregators, DG owners, consumers, and the system operators) all constantly and actively making decisions whilst coordinating their activities with other actors. In this thesis, such a network is collectively called an active distribution system. The increase in levels of intermittent distributed power generation coupled with an ever increasing erratic demand profiles (e.g. from integration of electric vehicles) inevitably introduce trying

challenges in the operation of such active networks. These challenges ultimately impose technical and economic constraints at planning and operational time frames. It is therefore imperative that these challenges are properly identified and their causes properly understood, particularly in operational time frames which is the scope of this thesis. In the subsequent sub-sections, the main technical and economic issues encompassing the operation of active distribution networks are properly identified and explained. The technical challenges that require a network-wide management solution will be the focal point of this thesis:

- bus voltage deviations due to intermittent resources and load fluctuations
- thermal capacity of network elements violations with high DG integrations
- energy losses due to unmatched between consumptions and productions
- power distortions due to unexpected contingencies and power quality issues
- protection system coordination might be interrupted by reversal flows

2.1.1 Voltage Deviations

According to standard EN 50160 [72], the permissible voltage magnitude variation ranges at the customers point of common coupling (PCC) in LV and MV distribution systems is between ±10% from the system nominal RMS voltage for 95% of the supplying time which is evaluated in 10-minute intervals for a week. In the UK, however, the limits for voltage below 132 kV should be kept between ±6% of their nominal value as stated by Electricity Safety, Quality and Continuity Regulations (ESQC) [73]. More rigorous range of voltage limits is defined by Engineering Recommendation (ER) P28 [74] between ±3% of nominal particularly for infrequent planned events, and ±6% for unplanned outages. In according to US standards, system bus voltages should be maintained within ±5% [75] and most of the IEEE test systems are based on the statutory limits. Therefore, appropriate limits should be applied accordingly.

The system voltages, however, fluctuate depending on the power operating conditions. Figure 2.1 depicts a simplified model of a radial distribution network to

explain voltage variation problem due to uncontrolled real and reactive power variations. In this model, a reactive power compensator is connected at the point of DG connection with reactive power injection, Q_C.

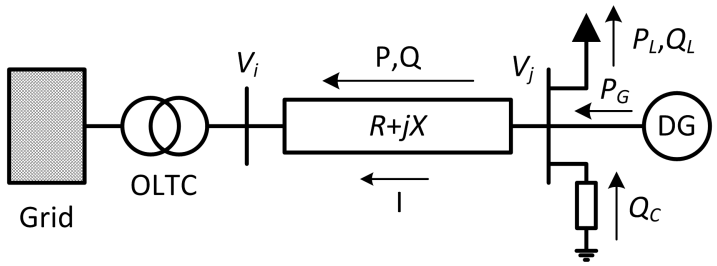

Figure 2.1: Two bus radial distribution network

The voltage drop across the line impedance shown in Figure 2.1 can be calculated as below [76]:

$$\begin{aligned} \triangle V_{ji} = \overline{V}_j - \overline{V}_i = \overline{I}^*_{ij}(R + jX) = \frac{\overline{S}^*_{ij}}{|V_j|}(R + jX) \\ = \frac{R(P) + X(Q)}{|V_j|} + j\frac{R(P) - X(Q)}{|V_j|} \end{aligned} \tag{2.1.1}$$

The voltage drop equation may be represented in phasor diagram as in Figure 2.2. Normally in realistic distribution networks the phase angle difference between the sending and receiving ends, θ is relatively small meaning that the imaginary part of equation (2.1.1) can be neglected and therefore this equation is approximated to:

$$\triangle V_{ji} \approx \frac{R(P) + X(Q)}{|V_j|} = \frac{R(P_G - P_L) + X(Q_C - Q_L)}{|V_j|} \tag{2.1.2}$$

From equation (2.1.1), it is clearly seen that the flow of both real (P) and reactive (Q) power will contribute to the voltage drop. This is generally due to the fact that in radial systems, the X/R ratio of the distribution cables are relatively low (≈ 0.3 at 400 V, ≈ 1 at 11 kV and ≈ 3 at 33 kV) [77]. Reactive power compensators, such as shunt capacitors, shunt reactors, or static VAR compensators (SVC), are normally used to manage the voltage by either injecting or absorbing the reactive power at their point of connection. The reactive power injection can be used to adjust power factor at the load point and becomes either inductive ($Q_C < Q_L$) or capacitive load ($Q_C > Q_L$). Figure 2.3 show how reactive power compensation can aid voltage regulation. As shown in the figure, a lagging power factor through reactive power

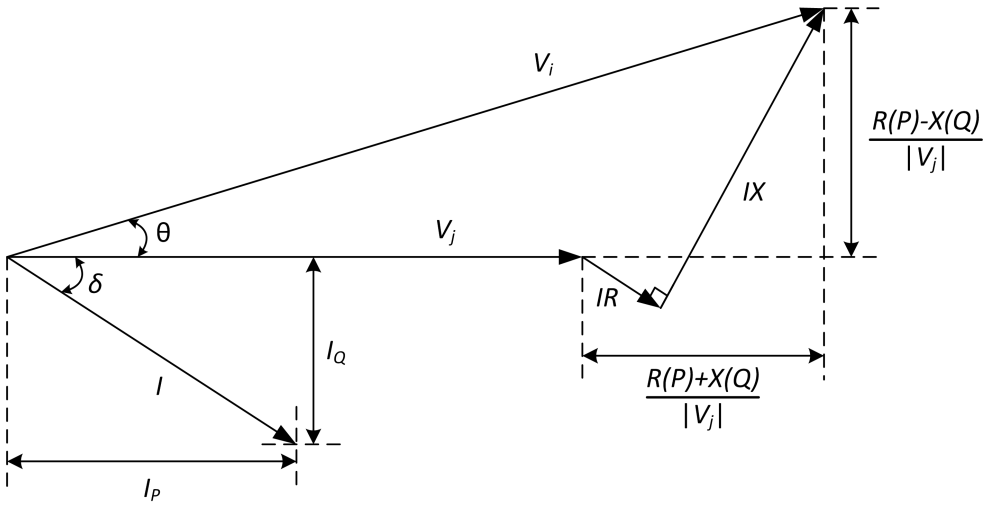

Figure 2.2: A phasor diagram representation of voltage drop

compensation makes voltage magnitude drops whereas a leading power factor makes voltage magnitude rises.

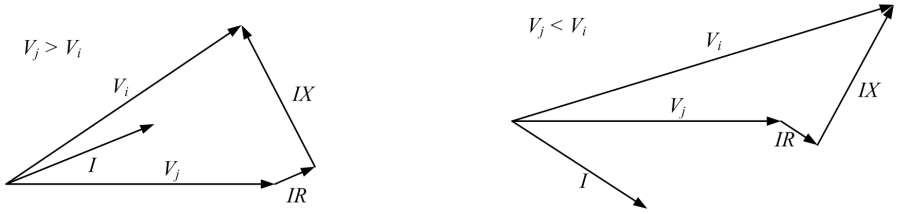

(a) Lagging power factor (b) Leading power factor

Figure 2.3: Reactive power compensation to regulate voltage

The power injection from DGs would create voltage problems such as voltage rise or voltage drop especially at end point of feeders and when generation is higher or lower than local demand, respectively. Similarly, feeders with no DGs connected may normally experience voltage drops when demand rises. This is even true for feeders with high penetration of DGs when the demand supersedes DG outputs. Figure 2.4 show an example of network with two feeders; feeder 1 having high DG penetration and feeder 2 is heavily loaded. The voltage fluctuations experienced in distribution systems are shown in Figure 2.4b. In order to tackle the voltage fluctuations at the end feeders, position of tap-changing transformer's taps – connected to the GSP – is normally adjusted to regulate voltage on the affected feeders [40]. The voltage regulation via the tap-changing transformer, however, might create voltage violation

on the other feeders to which it is connected. For example in Figure 2.4c, voltage rise caused by high power injection from DGs at Feeder 1 could be resolved by adjusting the tap position but resulting the voltage profile along the feeder with no DG (Feeder 2) drop below the statutory limits. Given such drastic fluctuations in the voltage, it is therefore imperative to develop new methods and solutions for managing voltage fluctuations in future flexible distribution networks.

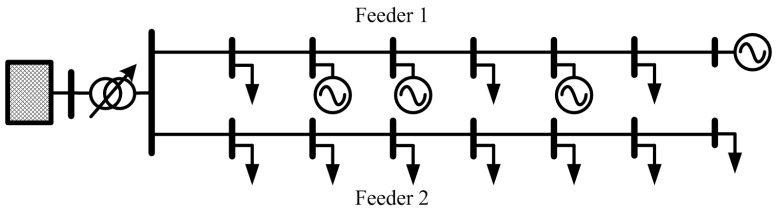

(a) A single diagram of exemplar network

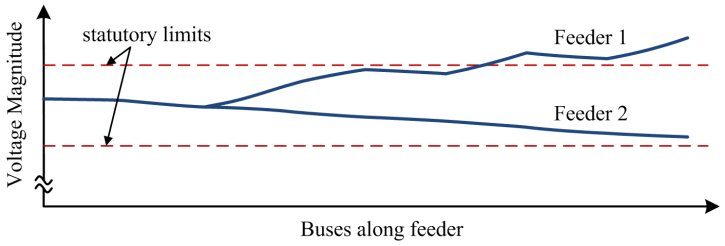

(b) Voltage profile before tap adjustment

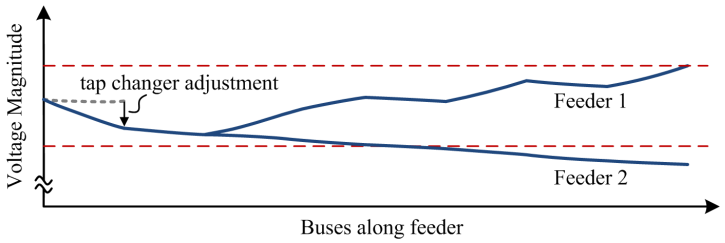

(c) Voltage profile after tap adjustment

Figure 2.4: A representative network with different load/generation conditions

2.1.2 Thermal Violations

All equipment in power networks (e.g., transformers, power cables, etc) are manufactured with particular properties. The maximum operating temperature (which is known as thermal limit) is one of the properties that directly constraints power transfer in the network operation. In the process of transferring power, the operating temperature increases proportionally with the amount of current flowing

through the power equipment (for instance, power cables). During congestion when excessive current flowing through a power cable (i.e., overload operation), insulation material of the cable will burn and its conductor might be melted. Power network is normally equipped with over-current relays and breakers to protect the equipment by disconnecting from power network when the thermal limit is exceeded in the events of a fault or otherwise excessive overload operation [78]. The action of the relay following by the breakers in isolating the fault will inevitably cause the loss of power in some parts of the network directly affected by fault since the feeders are radial.

Meanwhile, distribution networks are normally designed to carry current in one direction from the GSP to the load points. However, existence of DGs at particularly end points of feeders mean that there is reverse power flow in some feeders. The reverse power flows would increase current in the feeders which can cause over-current relay tripping [79]. It should be noted that even though the scenarios outlined above might be limited to a few feeders, it is nevertheless desirable to make use of the entire network and of feeders which are not as over-burdened particularly in emergency situations. A suitable power flow management scheme could negate the problem of thermal violations by distributing the loadings amongst the feeders more fairly.

2.1.3 Energy Losses

In network planning and operation, energy loss usually refers to the amount of dissipated energy (e.g., turning into heat as discussed earlier) in a process of transferring energy from supply to demand. In other words, the energy losses can be derived from total power loss of the lines depending on a particular operating time period. Figure 2.5 shows a well-known loss curve [3] describing its relationship with variations in generation and demand. According to the figure, the power loss could be minimised if all DGs meeting the local demand. This is mainly due to less power transfer when all demands are supplied locally. If all buses are installed with DG and their power production can be ensured to match power consumption at the connected bus, power loss could be totally avoided. However, this is unlikely to happen because DG installations are normally restricted to the availability resources and

placement sites or many other financial factors. Meanwhile, the energy losses highly depend on DG locations and its capacities as well as different used technologies [80]. Figure 2.5 also again clearly underlines the need and necessity for a more stringent energy/power management framework in an active network with high levels of DG penetration and flexible demand.

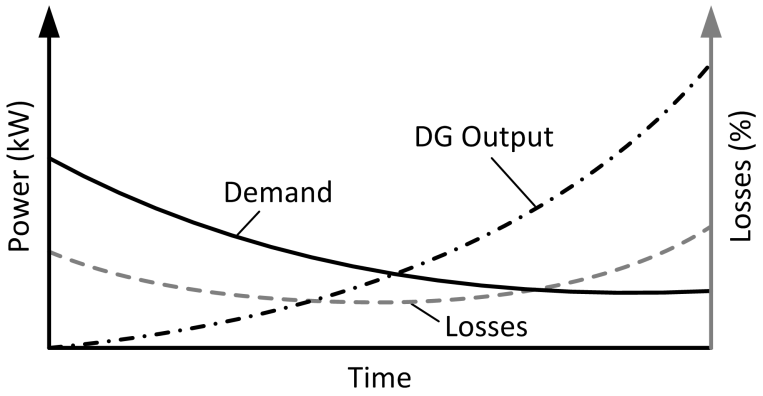

Figure 2.5: Power loss relative to generation and demand variations [3]

2.1.4 Power Distortions

Interconnection of electrical equipment into power network would distort voltage and/or current waveforms that cause deviations in their magnitude, frequency and/or shape (e.g. sinusoidal waveform). The power distortions degrade the quality of power, which is normally known as power quality, supply to consumers that might cause equipment malfunction or damage. Among of the power quality issues, voltage sag/swell, interruptions and harmonic distortion are found to be predominant problems in distribution networks with high penetration of DGs [81]. In normal operation, voltage sag and swell are mainly originated by the events discussed earlier in the Subsection 2.1.1. On the contrary, voltage interruptions are mostly caused by tripping of protective devices due to usual events such as lightning strikes, fire, human error or objects (trees, cars, etc) striking lines and/or poles. In some cases, thermal limit violation as described in the Subsection 2.1.2 would lead to voltage interruption as well due to equipment failure. In other words, the power quality can also be affected by undesirable demand and generation patterns due to the lack of a suitable network management scheme.

The increasing number of modern non-linear loads such as electric arc furnaces, static VAR compensators, converters, switch-mode power supplies, high efficiency lighting (e.g., compact fluorescent and LED bulbs) and motor drives within the power network would create harmonic distortion problem. Harmonics arise mainly because such loads draw a non-sinusoidal current from a sinusoidal voltage source. In the same fashion, DG integration which requires interface power converters can cause harmonic distortion in the power network. For instance, wind-based DG is driven by doubly-fed induction generators (DFIG) that contains rectifier-inverter blocks to adjust the operating frequency and phase angle whenever wind turbine speed changes. In another example, solar-based DG uses inverter to convert DC output before it can be injected to the network. The harmonic distortion in the network would result in overheating of cables and equipment (e.g., induction motors, transformers and capacitors) and neutral overloading [82]. Notwithstanding, problems due to harmonics normally are locally originated and can be resolved using filter. All equipment must be ensured not to generate harmonic more than standard limits, for instance, as defined by Engineering Recommendation (ER) G5/4-1 [83].

2.1.5 Protection Issues

As mentioned earlier, the distribution network is equipped with protective equipment. In the events of faults the role of the network protection is to isolate the impacted area to protect the rest of the network. It is obvious that the isolated area should be local to the fault as much as possible to minimise service interruption. This could be done through a suitable coordination between the protection equipment in the network. In radial distribution networks, the coordination of protection devices are largely designed for unidirectional flows (i.e. from the GSP to the loads). However, as described in Section 2.1.2, the power flows in the network is no longer unidirectional with the integration of DGs. Under those circumstances, the use of existing protection coordination schemes may lead to undesired actions by the protection scheme (e.g., tripping and/or re-closing breakers) [84]. Adaptive protection schemes have been developed to improve the coordination of protection devices by dividing distribution networks into multiple smaller sections [85]. Conse-

quently, the fault location can be detected separately in each section by measuring the fault current contributed by each DG. However, the protection coordination highly depends on network topology and DG locations which make it to be one of the most challenging tasks for distribution network operator.

2.2 Active Distribution Systems

The approach to planning, design and operation of distribution networks has to be significantly changed due to increasing DG penetration together with load growth, emergence of flexible demand technologies (such as plug-in electric vehicles) and expectations for higher quality of supply. In the last few years, research works dealing with the transition of distribution networks from 'passive' to 'active' have attracted interest among the system operators, manufacturers, consultants, research institutions, regulators and other stakeholders [28, 43, 54, 86–91]. The availability of advanced information and communication technologies (ICTs) has provided possibility to the distribution network operators (DNOs) to actively involve in control, operation and coordination of the integrated distributed energy resources (DERs) within the network under their responsibility. The CIGRE C6 Study Committee working on the implementation of the concept of active distribution management operation has revised and produced the following shared global definition of active distribution systems (ADSs) [20]:

"Distribution networks that have systems in place to control a combination of distributed energy resources (i.e., distributed generation, controllable loads or energy storage). Distribution System Operators (i.e., future distribution networks) have the possibility of managing the electricity flows using a flexible network topology. DERs take some degree of responsibility for system support, which will depend on a suitable regulatory environment and connection agreement".

Distributed energy resources which include distributed generations, energy storage systems and controllable loads under demand-respond are the enabling technologies for an active distribution system. Nonetheless, the flexibility of network topology has been highlighted in the aforementioned definition as an additional cri-

terion to the DERs coordination in order to achieve ultimate goal of providing energy efficiency, reducing harmful emissions, improving system reliability and enabling a transition to sustainable energy future. Therefore, each component is described in the following subsections to give better understanding of the underlying components of the ADS.

2.2.1 Distributed Generations

Distributed generation (DG) provides new challenges to the existing distribution operation. For integrating DGs into the distribution network normally, a hosting capacity assessment is carried out to ensure the intended DG installation will not create technical problem in any situations [92]. The hosting capacity assessment normally is driven by worst-case scenarios (e.g. cases with maximum DG output at minimum demand and vice versa) [87, 93, 94]. Although the determination of DG hosting capacity in this way could avoid the thermal limits and voltage constraints violations, the level of DG penetration is further hindered by the relatively slow pace of network reinforcement and might increase cost and/or prevent achieving the renewable energy target. Furthermore, the occurrence probability of worst-case scenarios seems to be only few hours in a year [17] and thus, as a result, the hosting capacity studies based on the worst-case scenario approach are rather conservative in their assessments. Alternatively, active power generation curtailment can be used as a means of avoiding the thermal limits and voltage constraints violations. In this way, it may be more profitable to curtail DG output (subject to specific agreements in place between the DNO and the DG owners) for limited periods if it means a larger hosting capacity [86, 88].

2.2.2 Controllable Loads

The total power drawn from the transmission system is the sum of distribution load demands and distribution loss. Reduction of loss is not the only option for decreasing the system total demand from the transmission system. The reduction in the total demand can also be achieved with the control of distribution system

loads. Demand side management (DSM) is one way to achieve such reductions [95]. In a DSM scheme, the utility company or an aggregator has direct control over certain loads that are covered under interruptible load contracts. A typical DSM action would interrupt or shift some loads including various (aggregated) residential loads, such as fridges, washing machines, air conditioners, space cooling/heating, water heating, etc. DSM can be effective for reducing the overall system demand; however, it requires the aggregator to have an infrastructure to remotely control these loads. The aggregator typically should have contracts with customers as a means to provide incentives for customers participating the DSM schemes [43].

The increase in electric vehicle related loads especially plug-in electric vehicles (PEVs) and plug-in hybrid electric vehicles (PHEVs) provide new opportunities for implementing DSM. Unlike other loads, PEVs or PHEVs have the capability to supply energy (through their batteries). The aggregator would encourage PEV and PHEV users to charge during high availability of energy and discharge to supply energy at peak loads during a power shortage using for example a price signal that is dynamically changing [89]. It is not only limited to electric vehicles but can be also applied to household users equipped with energy storage for self-scheduling of their consumption [96]. This scheme is different from the previous direct load control where end-users are motivated to make response through price changes (known as indirect control). Therefore, the aggregator does not require to have the remotely control infrastructure for direct engagement with the consumers. Unfortunately, it has less control to the demand response. Recently in [97], direct and indirect load control schemes are integrated to make use of the advantages can be gained from both methods.

2.2.3 Energy Storages

The growing number of DGs mainly from intermittent renewable energy sources has encouraged the use of energy storage systems (ESS) technologies in distribution networks [61,90,91,98]. It is used to convert electrical energy into a storable form during a period of surplus energy and then convert back into electrical energy when needed. Even though use of ESS technologies are limited by factors such as conversion loss,

and degradation of the storage medium (e.g. in batteries) [99], they are suitable for storing excess energy curtailed from DGs which could be used at a later time when needed. Without an appropriate storage technology energy curtailed from DGs would otherwise be lost. Instead of alleviating the intermittent of renewable based DGs, ESS could also yield energy reserve at distribution level to cater operation planning deficiencies in generation and consumption forecasts [100–102]. For that reason, a large-scale ESS is required for the system operator use that could provide the flexibility in managing the network operation. This topic will be discussed and explained more detail in the another chapter.

2.2.4 Flexible Network Topology

Most of the distribution networks normally operate in a radial topology in which loads are connected via main feeder to the substation. As mentioned earlier in this chapter, the radial topology creates numerous technical challenges in active networks with DGs and flexible demand (e.g. voltage fluctuations and reverse power flows). These challenges are normally due to the fact that DG outputs are intermittent and flexible demand profiles are varying. Normally, in distribution networks the end points of adjacent feeders are connected by mechanical tie-switched. These tie-switches only close in the event of faults in one feeder for continuous supply to the healthy portions of the feeders [103]. The tie-switches can also be used to reconfigure the network topology to better manage power fluctuations due to varying load/generation profiles in the network. This method has been applied to improve the reduce voltage sag propagation [53,55,104], manage thermal and voltage limits [28,51] and minimise system loss [49,54,105]. They could also be replaced by electronic switches for maximum flexibility. This application is another core part of the thesis that will be addressed in the following chapter.

2.3 Methods for Active Network Management

Active Network Management (ANM) refers to the collection of control schemes of the network resources with which a secure operation can be guaranteed at all times

[106]. The main purpose of the ANM is to operate the network at minimum cost while simultaneously complying to the technical operational requirements. There are several existing approaches developed for ANM of power distribution systems, which can be categorised as standalone [107–112], rule-based [113–119], analytical [3, 120–124] and heuristic approaches [125–130].

2.3.1 Standalone Approach

Standalone approach can be referred as a control framework using independent, individual or standalone devices that are installed or has control capability to improve the system operation. The devices such as voltage regulators, shunt capacitors and reactive power compensators are installed and controlled individually based on the local measurements (i.e., load currents, feeder voltages, power factor, etc). An early standalone technique using step-voltage regulators (SVRs) is presented in [107]. The study proposes a basic design of SVR and its applications using a microprocessor that involves both software and hardware for local voltage regulator control. It requires data sampling through communication facilities to decide whether to raise or lower the tap changer's position. During reverse power flow, all tap-changing operations are either ceased until the power flow resumes to its original direction or reversed the tap-changing directions using a different set of operating parameters. This work has demonstrated a conventional control framework which is among the earliest techniques for active network management.

In a later study, Kersting [110] introduces a compensator circuit to control SVR's tap position. The purpose for the compensator circuit is to allow for a local control scheme by representing the radial network with resistance and reactance settings in the circuit. The compensator circuit measures the system operating current and voltage constantly to give information to determine voltage needs to be increased or decreased. Then, the tap position will be adjusted accordingly to keep voltage at the regulation point which is predefined. The voltage is regulated in a discrete manner corresponding to the tap position and bounded to a certain bandwidth depending on tap changer's hard limits. This method is tested under three different load conditions; light, full and future (higher than base case when considering load

growth). Although the control scheme effectively maintains voltage at the predefined level, it might not be an optimal set point that could be fine-tuned along with other operating conditions of other network components.

Since network management using SVRs has control limit due to operating bandwidth, DG power curtailment is suggested in [111] as the last option to prevent over-voltage on sensitive feeders. This study uses the concept of droop based technique to control active power injection from photovoltaic using grid-tied inverter with maximum power point tracking. The active power control is determined by local voltage as alternative to frequency measurement to overcome problems especially during unintentional isolation from the main grid. In this control scheme, a unity power factor constraint is applied as to be in-line with the existing recommendation for DG installation and operation [131]. Although a constant power factor operation is necessary to avoid misleading of other control devices, there is an opportunity to make use of reactive power control capability for more sustainable operation. Therefore, reactive power support is applied in [112] along with active power control which is similar to the concept in [111]. Depending on local voltage measurements and available resources, power factor of inverters operation reduces proportionally with distance from the main substation.

Instead of managing DG operation, network operator traditionally invests on power factor correction techniques, for instance, adding shunt capacitors to overcome voltage problems (i.e., sags or swells). Power factor correction using microcontroller for automated local control is presented in [108]. The current and voltage are measured on site using current and potential transformers as input to the microcontroller. The micro-controller makes decisions either to open or close switches of the capacitor banks based on operating power factor from the measurement. The control signals are sent to relays for the switching action. McCarthy and Josken [109] showed that power factor control using shunt capacitors not only could improve the system voltage profile but reduce total losses for more efficient network operation.

The standalone approach as discussed in the aforementioned studies, unfortunately, only exerts local control and has a lack of knowledge of the entire system, which might cause conflicts between control actions of different local controllers.

Apart from that, the devices operation would also not be the optimal control settings for the entire distribution system. In addition, the standalone control is typically coordinated based on the conventional operation (e.g., unidirectional power flow) which is not necessarily appropriate for handling reverse power flows due to DG outputs. On the other hand, this approach is easy, low cost, does not require a separate communication infrastructure and scalable.

2.3.2 Rule-Based Approach

A rule-based approach is referred to a coordination between the distribution control devices that follow a set of predetermined rules to avoid counteractions among them. For example, a shunt capacitor is switched on when the power factor goes below 0.95 p.u. or tap position is lowered in a tap-changing transformer if voltage level at the end feeder goes above 1.05 p.u.. Typically, the rules of control actions are programmed in a centralised controller and all control devices in the network are handled through a Supervisory Control and Data Acquisition (SCADA) system [113]. The SCADA system is normally managed by the utility company who has responsibility to maintain network in secure operation. In order to deliver appropriate operating set points, all field measurements need to be sent to the control center. Therefore, it requires a two-way communication infrastructure to engage between the main controller and field devices.

A coordinated capacitor control using SCADA system by Virginia Electric and Power Company in [114] could be considered as one concept of the rule-based network management techniques for voltage regulation. A control algorithm is programmed in master computer to select which shunt capacitors need to be turned on and which ones turned off to maintain a level voltage profile across the network. The control decisions are made in every 15 minutes based on monitored input load data (i.e., bus voltages and reactive power flow between transmission and distribution networks) from the SCADA system. If there is a high level of reactive power flowing out into the transmission side, the relevant capacitors will be tripped to reduce the reactive power otherwise no action is taken, provided that this does not cause any voltage violations. A capacitor is selected based on the 'first in first out' rule where

previously tripped capacitors will be ignored in the next cycle. Furthermore, the number of capacitors switching in each cycle is limited to a certain level to reduce possible tear and wear costs. This work has showed a significant cost saving from both transmission and distribution sides.

Voltage regulator at the substation is coordinated together with capacitor control in [115] for an improved voltage regulation scheme. A voltage drop estimation based on typical impedance of the feeder is used in adjusting of the voltage regulators settings. On the other hand, the capacitor control is based on local measurements of power factor to reduce the amount of reactive power flow at the substation. This control framework decouples both problems in the supervisory controller of SCADA system. The controller adapts a set of pre-determined conditions for the control coordination. Similar to previous work, the control decision requires continuous load monitoring from the SCADA communication infrastructure. Reactive power support from DGs is suggested in [116] as alternative to the capacitor banks installation. In this control scheme, a small amount of reactive power injection takes place first and then the corresponding voltage changes are calculated for voltage regulators action. In the event that the actions by the voltage regulators are insufficient to bring down the system voltages within permissible limits, active power curtailment needs to be executed as a last resort.

A set of network management rules which are called expert system is introduced in [117]. The expert system can be divided into three distinct parts; knowledge base, inference engine and user interface. Knowledge base contains all rules that are derived from extensive knowledge of experienced engineers and technical information that make it capable of solving network operation problems. The user interface is referred to interaction with external environment such as control action signals, input measurement data and human recommendations. The inference engine uses various determination processes from information in the user interface and knowledge base to make network control decisions. Voltage regulators and capacitor control are fairly coordinated in the inference engine to perform network operation for maintaining system voltage limits with minimum operational costs. In this case, the cost includes system losses and tear and wear of the control devices. The expert system

configuration is then applied in a distribution test network for planning purposes as presented in [118]. This study has demonstrated a significant cost saving could be obtained from expert system application to actively manage the network.

A radial distribution network is suggested to be divided into small regions called control zones, according to the number of installed voltage regulators [119]. In each zone, a voltage regulator and DGs or capacitor banks are coordinated via a tree communication structure. The coordination requires local measurements at each installed DG or capacitor location and the information is shared with their neighbours. Each location is responsible to estimate voltage from both upstream and downstream sides and propagate the highest and lowest voltage information to the voltage regulator. Voltage is regulated by adjusting the tap position of the voltage regulator depending on the received information. In case of reducing the tap position might cause minimum voltage violation, DG active power at maximum voltage point needs to be curtailed. After all control zones are managed individually, the whole system could be ensured to operate within the permissible limits.

The rule-based technique has indicated that the counteracting problems in the standalone approach could successfully be resolved. However, the decision rules in this technique need to be pre-determined in a precise fashion and must follow a specified sequence. Therefore, the decision process will require longer times and solution is most likely not optimum if there is any flaw in determination of the rules. Moreover, the pre-determined rules in this technique would make it unable to adapt with any changes from the original network configuration at the time of the rules establishment. In other words, the rule-based algorithms that are designed for normal operation might not work in emergency conditions, for example, a line is tripped due to fault and supplied through an alternative route. Notwithstanding such limitations, the available communication infrastructure in SCADA system would allow a global network interaction and assessment which ultimately benefits network operation.

2.3.3 Analytical Approach

Analytical approach is used to develop a mathematical model of the whole power network for obtaining a possible whole-network optimal management solution. The model formulation considers the operating limits of the control devices as well as the nature of their control mechanism that could be modelled either as binary, integer or continuous domains. The optimal control settings are decided depending on requirements to either maximise or minimise an objective function which is defined by the system operator. The objective function is normally defined as a function of network operation cost which is to be minimised. Normally, in real network applications, the required information is gathered from the available communication infrastructure in SCADA system to estimate the network state within the next several hours or days. Based on the available data, an optimisation solver determines the optimal control settings and ensures no violations of the technical limits will be raised from the control decisions. The optimum settings in form of control signals are then delivered to all associated field devices in advance as reference inputs for their operation.

A discrete optimisation approach to coordinate and control capacitor banks and the tap changer transformer is presented in [120]. The optimisation algorithm is developed using the oriented discrete coordinate method, in which the control variables are updated from partial derivatives of an objective function. The partial derivative is defined as improvements of the objective with changing of control variables positions. A search direction is selected based on the largest partial derivative value and the updating process continues until no further improvement can be achieved. To ensure all constraints are fulfilled, a penalty function is imposed in the objective function to move away from the undesirable solution during the optimisation process. The optimisation algorithm is implemented in a centralised management framework to evaluate system performance at different objectives, including minimising supply power from the external grid, minimise reactive power flowing at substation transformer, and maximise revenue from energy sales and prime cost [121]. The framework is integrated with SCADA system to provide real-time data exchange between a central controllers and field devices (i.e., capacitor banks and transformer

tap changer) for the optimal operation. The results clearly show a lower level of energy imported from the external high voltage grid resulting in a 0.7% increase in the revenue for the network operator. This method, however, requires power flow calculation at every optimisation step to evaluate the system performance that causes major computational burden in the process. In large network applications, a simplified model is needed to perform the power flow calculation.

When considering high DG penetrations, analytical approach has also been used to manage the network operation in the most economic way whilst adhering to network operational boundaries and limiting DG power curtailment [122]. The power curtailment between DGs is coordinated using voltage- and loss-sensitivity factors to the DG power injections which can be analysed through the use of the Jacobian matrix of the network. The optimisation problem is then solved using a commercial package taking into account the cost of trading with the external grid supply as well as power curtailment of the DGs. Due to the intermittent nature of renewable resources and loads, Keane et al. [132] introduce the index of coincidence in the curtailment framework to assess the probability of voltage constraint breaches. The index is established from historical data and used to select any possible critical conditions (e.g., maximum generation and minimum load) that may cause over-voltage. A significant saving in the network operation cost could be attained through a proportional coordination between the DGs based on curtailment cost functions which are derived in relative to their power generation cost. This core framework is also used to investigate energy loss minimisation taking into account the time-varying characteristics of generation and load profiles in the network [3]. Analytical approaches normally require formulation of a multi-period AC optimal power flow (OPF) problem to find optimum operating points of network control devices.

The OPF problem can be solved as a mathematical optimisation problem using commercial solver packages capable of solving a wide class of optimisation problems from linear programming to mixed-integer non-linear programmes. A CPLEX solver, that uses simplex or barrier interior point algorithms, is commonly applied to solve LP problems [122, 132]. In this case, the OPF formulation is approximated as DC. The solver is also used for mixed integer quadratically constrained program-

ming (MIQCP) problems especially when taking into account discrete control of voltage regulators, capacitor banks and load tap changers (LTCs) for voltage regulation purposes [133]. DC model neglects important features such as deviations in voltage magnitudes. Full network models are used in AC OPF formulations. AC OPF formulations are non-linear and normally are more complex and computationally burdensome to solve when compared to DC formulations which are linear. Nevertheless, there are various non-linear solvers for solving non-linear programming (NLP) problems like the CONOPT solver which uses the generalised reduced gradient approach as applied in [3]. KNITRO is another example of a well-tailored solver for non-linear programming problems [123]. The NLP-formulated AC OPF, unfortunately, does not cater for integer control variables and they are typically approximated from continuous domain. It is possible to consider a MINLP approach to give better representation but this could potentially restrict the size of the problem and normally is not tractable for larger systems with many variables [124].

When compared with the standalone and rule-based approaches, the analytical approach is a more accurate and flexible way of producing optimum operating set-points for network control devices. Meanwhile, since in the analytical approach explicit network models are used, this approach could easily be tailored toward specific network problems. The main limiting factor in adopting analytical approaches is the relationship between model complication and size and the tractability of the problem. The network model representation, generally, involves a wide range of control variable domains (e.g., binary, integer and continuous. A purely analytical approach therefore many not be suitable for solving especially larger networks with a large pool of variables. Moreover, due to the inherent non-convex nature of power flow equations, the analytical approaches do not guarantee global optimum solutions.

2.3.4 Heuristic Approach

Heuristic method is an iterative process that combines different knowledge based concepts inspired by natural phenomenon in order to search for an optimal solution using limited information and often without the need for an explicit model for the

system. Learning strategies are used to sample and structure the information to effectively find the solution. As a result, less computational time is required which makes the heuristic approach more suited for real-time applications. Heuristic approach uses a similar control framework as in the analytical approach and yet the use of heuristic optimisation techniques make it different. In particular, the heuristic optimisation process does not require a closed-form of the model formulation as necessary in the analytical approach. Thus, this approach can overcome limitation in the classical analytical approach especially regarding non-convex and non-linear problems. Certainly, the heuristic approach can be adopted to cater for MINLP problems that are common in power system optimisation problems. There are numerous heuristic algorithms: Genetic Algorithm (GA) [125–127], Particle Swarm Optimization (PSO) [126, 129, 130], Ant Colony Optimization (ACO) [126], Artificial Bee Colony (ABC) [127], Differential Evaluation (DE) [127], Tabu Search (TS) [126–128] and Simulated Annealing (SA) [127] have found in the power network management applications.

Optimal voltage control and coordination of LTC, VSR and SVC in a distribution network with interconnected DG is solved using GA technique [125]. The GA is inspired by natural selection of genetic reproduction in the evolutionary process to produce better generation based on a survival of the fittest concept. The process is carried out by repeating such genetic operations (e.g., selection, crossover and mutation) until termination criteria can be found, then the solution is determined from the individual of the last generation. In this study, the GA is used to produce a fast optimal solution considering daily profiles of residential loads and solar generation for a network with a relatively large size. The time selection is identified according to critical scenarios such as peak load, minimum load, and peak generation. The strategy improves the voltage profile and reduces the distribution loss for the entire distribution power system using a combination of the voltage control devices (LTC, VSR, SVC). The GA method requires a reliable communication infrastructure and its application seems to provide the optimal solution with a sufficient degree of accuracy.

A daily voltage/Var control (VVC) optimisation for the distribution management

system using heuristic method based on ACO is presented in [126]. The management strategy requires load and generation forecast data for the next day profiles and decomposes them into several sequential operating conditions at specified time intervals. An ACO method is used to determine the active and reactive power injections from DGs, reactive power values of capacitors and tap positions of transformers for the next day operation. The ACO uses the concept of ant colony searching for food in which the solution is explored through stochastic iterative process biased by a set of parameters associated with graph components (known as pheromone model). The degree of bias is ranked from the best to worst performance according to operation cost of buying energy from the external grid supply and DG resources. Penalty factors are imposed to the objective function to ensure all equality and inequality constraints are fulfilled. This work shows that the solution obtained by the ACO method is more accurate and precise as compared to other heuristic methods (GA, TS and PSO).

An ABC optimisation is implemented in [127] to find the best distribution network configuration at minimum loss operation. Apart from the voltage and current constraints, network topology must be maintained radial at all times for effective co-ordination of their protective systems. Since there are many possible combinations of switching candidates for different configurations, the model is a complicated combinatorial, non-differentiable constrained optimisation problem. The problem is addressed using ABC algorithm inspired by intelligent foraging behaviour of honeybee swarm. Artificial bees in the optimisation process will attract others if they are performed better in minimising the losses. The optimal solution by ABC is converged at significant less computational time and more accurate in comparison to DE, SA, TS and GA. In a similar optimisation problem, Abdelaziz et al. [128] proposed a modified TS (MTS) to improve the computational time and solution accuracy. A dynamic tabu list with appropriate size and a multiplicative move are introduced respectively to escape from local minimum and diversify the search process toward unexplored regions. The MTS obtains better voltage profile and system losses than SA for regulating the network voltage.

Network management scheme with feeder reconfiguration control schemes in [129]

uses PSO to address a multi-objective problem. The objective function comprises the cost of buying power from the grid supply and DGs, number of switching actions, and voltage deviations. The PSO algorithm is inspired by the population of birds where the system is initialised with a population of random particles and the optimal solution is searched through interaction between the particles to follow the best among them. In this study, overall system losses, number of switching operation and voltage profile can be improved with dispatch-able DG application. The PSO is also applied together with voltage sensitivity method to regulate voltage in MV distribution systems by controlling reactive power injections from DGs [130]. The voltage sensitivity matrix is derived from imaginary part of impedance matrix and used to calculate suitable amount of the reactive power injections in order to return the system voltages inside the permitted range when necessary. The application PSO algorithm has improved the convergence rate in the optimisation process.

The heuristic approach uses a randomly acceptable process to prevent the solution to be trapped in a local optimum especially for non-convex problems. However, heuristic application in the literature indicates that the approaches do not guarantee solution to be the global optimum but sufficient for the immediate goals. Notably that it gives different solutions for every simulation runs. The heuristic approach can also be combined with analytical approach especially for solving non-convex MINLP problems. For example, a branch and bound algorithm, that uses heuristic and derivative techniques [134], is applied to search for optimal settings of control devices in distribution system with high DG penetrations taking into consideration the discrete control features [28].

2.4 Network Management Framework

Active Network Management requires a change in the traditional role of the Distribution Network Operator (DNO). The change effectively creates a new entity called the Distribution System Operator (DSO) which may be the network operator or a collection of network/asset operators coordinating and managing the operation in the network between various actors [135]. The DSO effectively performs a similar

role in the distribution network domain that the traditional Transmission System Operator (TSO) does in the transmission domain. The DSO implements an Active Network Management (ANM) framework similar to the TSO. Figure 2.6 shows a general often agreed-upon ANM framework for the managing the operation of the active distribution system of the future [20]. There are, at the moment, a few demonstrator projects that implement ANM, such as ADINE [136], ADDRESS [137], and GRID4EU [138] projects (all in the EU), Fort Collins (US) [139], ENMAX (Canada) [140]. There are also demonstration projects with regional companies in Japan and by the National High Technology Research and Development Program in China [141].

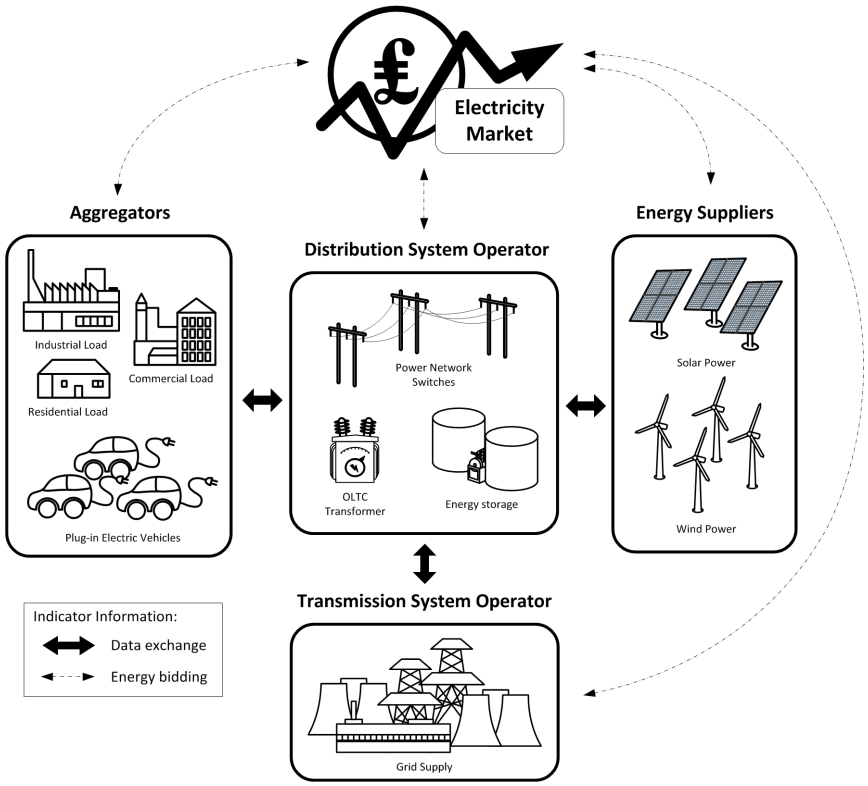

Figure 2.6: A conceptual ANM framework

2.4.1 Electricity Market Price

Depending on regulatory framework, there might be different paths with which pricing signals will travel within the ANM framework. Electricity prices generally fluctuate throughout a day that is determined by matching offers to sell and bids

to buy from all the network participants. With the available SCADA system and advanced metering infrastructure (AMI), real-time pricing (RTP) could easily be implemented. The RTP is an expected electricity rate which varies in corresponding to the electric utility's time varying costs of operation with given constraints considering fluctuation of demand and renewable resources [142]. The RTP has been applied in the last several years to enhance network operational management and improve social welfare [143–145]. In that works, the social welfare is addressed to give benefits for both power consumers and supplier through a mechanism where the consumers adjust their consumption to maximise profits according to the RTP set by the supplier. A look-ahead approach can be used to forecast the demand and resources as well as electricity price based on available information from weather and load forecast tools [146]. The forecast tools usually use historical patterns of consumption and production together with correlated parametric input from sensors to deal with the uncertainties in obtaining accurate prediction. With the forecast data in hand, optimal power flow (OPF) can be calculated at each time step for real-time network operation and planning [147].

2.4.2 Renewable Energy Curtailment

To encourage the deployment of renewable generation, the UK Government introduced two main incentive schemes which are the feed-in tariffs (FIT) for DG capacity up to 5 MW [148] and the renewable obligation (RO) for larger scale DG [149]. However, the RO scheme closed to all new generating capacity on 31 March 2017 and replace with the Contracts for Difference (CfD) scheme to continue support on the renewable generation development [149]. Under the current scheme, each renewable generation technology is set at a strike price to guarantee the return to DG owners. If the market price is lower than the strike price, the DG owners receive a payment for the difference or otherwise, the DG owners pay the difference. In the context of ANM, DG curtailment may be required to avoid any violations of operation constraints. The prevailing energy curtailment in UK distribution networks is a last-in first-out (LIFO) rule [150]. However, this approach would curtail output power from DGs at the bottom of the list regardless of whether any improvements

could be achieved or not. Alternatively, Kane & Ault [151] suggest that renewable energy suppliers or aggregators should involve in submitting bids to the electricity market balancing mechanism based on their willingness and an agreed compensation for the power curtailment which might be paid based on the RTP at the time of curtailment.

2.4.3 Demand Side Management

Demand side management application could be realised by aggregators to incorporate scattered bids coming from DGs and flexible loads at low voltage distribution networks. Aggregator are participating in energy market as retailers and managing their own business market with new electricity tariffs to coordinate consumers and DERs including EV users [152]. In the look-ahead energy market, DSO and TSO must guarantee a secure network operation under normal conditions (i.e., no technical violations). In certain circumstances, however, the promised operating points might be deviated and aggregators are receiving payment at regulation prices for demand response to overcome any potential problems could be originated from the deviation [153]. From DSO perspective, additional cost will be incurred to the balanced selling and buying prices between all involved parties as shown in Figure 2.6. Based on this conceptual framework, DSO could manage the MV distribution networks in effective way to reduce operation cost and further improve by introducing energy storage and flexible topology applications. The details explanation of the application will be discussed in the subsequence chapters.

2.5 Optimal Power Flow Formulation

This section presents formulation of the relevant models which are implemented in the multi-period optimal power flow formulation for look-ahead analyses. This multi-period OPF formulation is used for implementing a comprehensive ANM framework in this thesis. This work considered for the ANM framework either hourly (Chapter 3) or 30 minute (Chapter 4) interval time periods depending on the available data. The ANM framework has the same structure as shown in Figure 2.6. It should be

noted that these models can also be used for snapshot studies. Let N, G, W, S, L, O and T denote the set of respectively: nodes, grid supply points, wind-based DGs, solar-based DGs, power lines, lines with OLTC transformers and periods. An ANM for different purposes is normally developed using AC optimal power flow (OPF) [6, 13, 28, 154, 155]. An OPF is used to optimise power system operation while satisfying both network equality and inequality constraints as given in the following expression:

$$\min_{x,u} F(x,u) \tag{2.5.1}$$

subject to:

$$G(x,u) = 0 \tag{2.5.2}$$

$$H(x,u) \geq 0 \tag{2.5.3}$$

where, $F(x,u)$ is an objective function to determine all state variables, x and control variables, u in achieving a certain planning and operating criteria such as minimum generation cost. The problem can be properly addressed using different objectives depending on the requirements. The variables x, usually voltage magnitudes and angles, change depending on other known variables (i.e, power generations, loads, tap ratio, etc.) in a process to fulfil the equality constraints, $G(x,u)$. The equality constraints consist of power injection and power balance requirement that can be generalised as power flow equation. The variables u refer to some of the known variables such as DG operating points, demand responses and tap changer operation that can be adjusted to reach a goal as given by the objective function. The control variables, however operate within designated limitations which are defined as the inequality constraints, $H(x,u)$. The limitations are derived from physical characteristics of electrical equipment and regulatory requirements (i.e., voltage magnitudes).

The power flow equation contains some non-linear functions especially in the usual polar form formulation of power injection. The existence of non-linear functions in the equality constraints, however, makes the OPF problem non-convex and increase the possibility of solution to trap in local optima [156]. As a non-linear non-convex problem, the OPF can be a difficult problem to solve and requires an appropriate approach to get accurate solution. Before the problem can be solved,

it is important to understand its formulation. Therefore, the details formulation of OPF problem in this study will be presented in the following subsections.

2.5.1 Objective Function

The goal of the optimisation problem is to find a network state (i.e. the set of control settings for control devices as well as all network state variables) in which a certain objective function is at its minimum. Typically this is taken to the operation cost of the network incurred to the DSO. The objective function may be defined as:

$$F(P_{g,m}, \xi_{b,m}) = \sum_{m \in T} \Big[\sum_{g \in G} C_n P_{g,m} + \sum_{b \in N} C_p \xi_{b,m} P_{b,m} \Big] \tag{2.5.4}$$

where, C_n and C_p are the cost coefficients corresponding to the RTP energy market and the regulation prices, respectively. In all cases, C_p is always higher than C_n to encounter financial loss on selling electricity to consumers and compensation for demand shifting action.

In this formulation, operational cost due to power curtailment and system losses is already accounted in the cost of trading with TSO. If there is no power curtailment then more power could be exported to the external grid to reduce the operational cost. In other words, operational cost will increase depending on the particular period when DG output needs to be curtailed. Similarly, higher system losses causes more power import from the grid supply that increase the operational cost for buying more energy. Therefore, minimising the net import over export energy at the grid connection as given in equation (2.5.4) can directly reduce the operational cost. When a dynamic demand response mechanism is considered, $C_p - C_n$ is the imposed compensation amount for demand response (incurred to the DSO). The demand shift multiplier, ξ_b varies between 0 to a maximum value for no demand shift to maximum shift in demand respectively. The demand response mechanism can be implemented in cases where EV aggregators are present in the network.

2.5.2 Calculated Nodal Power Injections

In power flow analysis, it is compulsory to keep both active and reactive power balance at each node essentially satisfying Kirchoff's current law (KCL) at each

node in the network. Figure 2.7 depicts a general π model of the transmission line. The shunt susceptance in the figure can be normally ignored ($b_l^{sh} = 0$) in distribution networks as the length of lines are normally short (less than 50 km). Therefore, active and reactive power injections at sending ends (denoted as j) and receiving ends (denoted as k) of the line, $\forall l \in L$, at period $m \in T$ can be obtained from:

$$P_{j,m} = g_l V_{j,m}^2 - V_{j,m}V_{k,m}[g_l \cos(\theta_{j,m} - \theta_{k,m}) + b_l \sin(\theta_{j,m} - \theta_{k,m})] \tag{2.5.5}$$

$$Q_{j,m} = -b_l V_{j,m}^2 - V_{j,m}V_{k,m}[g_l \sin(\theta_{j,m} - \theta_{k,m}) + b_l \cos(\theta_{j,m} - \theta_{k,m})] \tag{2.5.6}$$

$$P_{k,m} = g_l V_{k,m}^2 - V_{j,m}V_{k,m}[g_l \cos(\theta_{k,m} - \theta_{j,m}) + b_l \sin(\theta_{k,m} - \theta_{j,m})] \tag{2.5.7}$$

$$Q_{k,m} = -b_l V_{k,m}^2 - V_{j,m}V_{k,m}[g_l \sin(\theta_{k,m} - \theta_{j,m}) + b_l \cos(\theta_{k,m} - \theta_{j,m})] \tag{2.5.8}$$

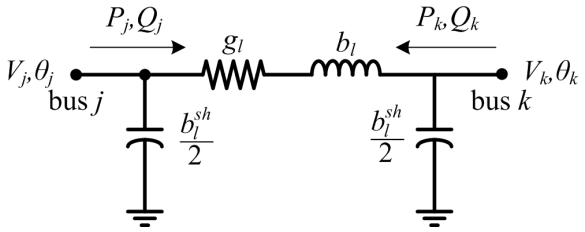

Figure 2.7: An equivalent power line based on π model

The power injection equations give sufficient information on power flow direction either entering or leaving the respective node. Depending on interconnection with other elements (i.e., supply point, DG, loads), the equality constraints for active and reactive power balance at bus, $\forall l \in L$, at each period $m \in T$ can be expressed as, respectively:

$$\sum_{g \in G} P_{g,m} + \sum_{w \in W} P_{w,m} + \sum_{s \in S} P_{s,m} = (1 - \xi_{b,m}) P_{d\{b\},m} + \sum_{l \in L} P_{j,m} + \sum_{l \in L} P_{k,m} \tag{2.5.9}$$

$$\sum_{g \in G} Q_{g,m} = (1 - \xi_{b,m}) Q_{d\{b\},m} + \sum_{l \in L} Q_{j,m} + \sum_{l \in L} Q_{k,m} \tag{2.5.10}$$

where, P_d and Q_d are active and reactive power consumptions. Although the aim is only to reduce active power, the demand response mechanism would affect the reactive power as well. For instance, some equipment that generate reactive power

will reduce the total aggregated reactive power when their operation are stopped or shifted. It is also important to note that DG integration is suggested to operate at fixed power factor in order to avoid conflict with the voltage regulation devices in the network. Therefore, all DGs are assumed to operate at unity power factor and there will be no reactive power injection from DGs as given in the equation (2.5.10).

Apart from the power balance constraints, maximum loading limits of line as mentioned in Section 2.1.2 should be also taken into account. The loading is normally measured in terms of flowing current that must be less than or equal to the line current rating, I_{rate} at all times, $\forall m \in T$, as follows:

$$(g_l^2 - b_l^2)[V_{j,m}^2 + V_{k,m}^2 - 2V_{j,m}V_{k,m}\cos(\theta_{j,m} - \theta_{k,m})] \leq I_{rate}^2 \forall l \in L \tag{2.5.11}$$

2.5.3 Optimisation Variables

As stated earlier, the OPF calculates the optimum operating points for all control devices. The control variables are normally, demand response multipliers, substation transformer tap positions, and power curtailment factors from DGs. The set of the control variables constraints at period $m \in T$ can be expressed as:

$$0 \leq \xi_{b,m} \leq \xi_b^{max} \qquad b \in N \tag{2.5.12}$$

$$0 \leq \zeta_{s,m} \leq \zeta_s^{max} \qquad s \in S \tag{2.5.13}$$

$$0 \leq \zeta_{w,m} \leq \zeta_w^{max} \qquad w \in W \tag{2.5.14}$$

where, ξ and ζ are the variable multipliers to illustrate degree of demand response (i.e. load shifting) and DG curtailment implemented within the ANM framework. Similar to demand response multiplier, ζ varies between the zero for no curtailment and ζ^{max} for full curtailment. In this case, both ξ^{max} and ζ^{max} must be less or equal to 1 (a complementary to the control action).

Regarding voltage regulation at substation transformer, OLTC is used to change tap position, α (which is the connection point along transformer winding) while the transformer is operated without any supply interruptions. The OLTC actual tap position is a discrete variable (but can be approximated as continuous for faster

solutions), the OLTC control variable at period $m \in T$ can be presented as:

$$\alpha_{o,m} \in \{\alpha_{min},..., \alpha_{max}\} \qquad o \in O \tag{2.5.15}$$

The OLTC tap, located on the primary winding as illustrated in Figure 2.8, is used to control voltage magnitude by switching tap from initial position to new position. The changes of voltage magnitude depend on the tap ratio step resolution, δV. The voltage magnitude at secondary side of the transformer for lines equipped with OLTC, $o \in O \subset L$, in period m can be calculated using:

$$V'_{j,m} = \frac{V_{j,m}}{\alpha'_{o,m}} = \frac{V_j(t)}{1 + [\alpha_{int} - \alpha_{o,m}]\delta V} \tag{2.5.16}$$

where, α_{int} is initial position (normally in the middle of the control range) that gives nominal setting. Therefore, active and reactive power injections of the corresponding lines need to be computed using the following expressions:

$$P_{j,m} = g_l[V'_{j,m}]^2 - V'_{j,m}V_{k,m}[g_l \cos(\theta_{j,m} - \theta_{k,m}) + b_l \sin(\theta_{j,m} - \theta_{k,m})] \tag{2.5.17}$$

$$Q_{j,m} = -b_l[V'_{j,m}]^2 - V'_{j,m}V_{k,m}[g_l \sin(\theta_{j,m} - \theta_{k,m}) + b_l \cos(\theta_{j,m} - \theta_{k,m})] \tag{2.5.18}$$

$$P_{k,m} = g_l V^2_{k,m} - V'_{j,m}V_{k,m}[g_l \cos(\theta_{k,m} - \theta_{j,m}) + b_l \sin(\theta_{k,m} - \theta_{j,m})] \tag{2.5.19}$$

$$Q_{k,m} = -b_l V^2_{k,m} - V'_{j,m}V_{k,m}[g_l \sin(\theta_{k,m} - \theta_{j,m}) + b_l \cos(\theta_{k,m} - \theta_{j,m})] \tag{2.5.20}$$

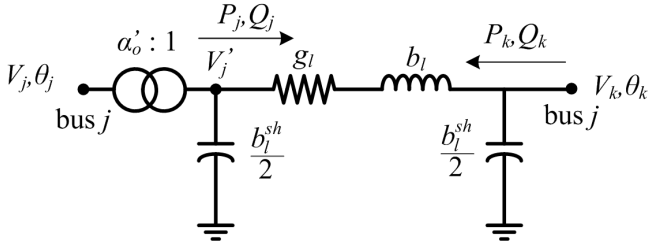

Figure 2.8: A power line model with OLTC control

After the control variables are specified, state variables can be analytically determined. The variables include voltage magnitude (V) and angle (θ) at load buses which can be obtained through the net power injection calculation at respective nodes to satisfy the active and reactive power balance constraints as given in the equations (2.5.9) and (2.5.10). As mentioned earlier, DGs are not involved in any voltage regulation and therefore, the corresponding nodes are assumed to be load

bus (with negative load convention). Apart from that, the grid supply point (GSP) is considered as slack bus and power injections at this node can be also categorised as state variables. The active and reactive power injections from GSP are governed to attain overall balance between generation and consumption in the system. All these variables are updated subject to the following inequality constraints:

$$V_{min} \leq V_{b,m} \leq V_{max} \qquad b \in N \tag{2.5.21}$$

$$P_{g,m}^2 + Q_{g,m}^2 \leq S_{g,max}^2 \qquad g \in G \tag{2.5.22}$$

where, voltage magnitudes are ensured to operate within the statutory limits as discussed the Section 2.1.1 and the GSP power injections are limited correspond to the substation transformer power rating, S_{max}.

2.6 Simulation Tools and Test Networks

This section gives an overview of the used simulation package and software tool for implementing the ANM framework. To evaluate the performance of its application, distribution test networks are required. There are two test networks, namely, modified 33-bus test network and HV-UG United Kingdom generic distribution system models have been considered for the analysis purposes in this research work. An explanation of the test networks is provided here to give better understanding of the case studies.

2.6.1 Software for Simulation Platform

The essential features of AC OPF require a modelling environment that is able to support non-linear constraints with mixed integer control variables. Advanced Interactive Multidimensional Modelling Systems (AIMMS) is an integrated combination of a modelling language, a graphical user interface and numerical solvers that offers advanced modelling capabilities for linear, mixed-integer and non-linear programming [157]. Therefore, the AIMMS modelling software is used as a platform in this work to develop, implement and analyse the ANM framework for multiple candidate test systems. The multi-period OPF as presented in Section 2.5 is

configured in AIMMS by the declaration of sets, parameters, variables, constraints and implementing the ensuing mathematical programme. The problem is solved in AIMMS using MINLP KNITRO solver that gives flexibility for solving both convex and non-convex problems.

In several cases, MATLAB environment is also used to establish a mathematical model and/or to carry out analysis for preliminary studies and verification purposes. For the verification purposes, MATPOWER toolbox introduced by Zimmerman et al. [158] is used. This work is carried out using MATPOWER version 5.0b1. The MATPOWER is a package of MATLAB M-files for solving power flow and optimal power flow problems. It is intended as a simulation tool for researchers that is easy to use and modify. MATPOWER is designed to give the best performance possible while keeping the code simple to understand. MATPOWER, however, can only be used for single period AC OPF and it requires some modifications to execute multi-period operation. Moreover, MATPOWER is also limited to solving AC systems (with minimal DC system modelling capabilities). Therefore, this package application is selected aiming to ensure the reliability of the obtained optimal scheduling solution.

2.6.2 Modified 33-bus Test Network

A benchmark radial 33-bus MV distribution network [159] is used to showcase the performance of proposed application in the network management framework. The network is a balanced 12.66 kV distribution system consisting of 33 nodes interconnected with 32 lines and 5 tie lines (dotted lines). The total active and reactive power peak loads in the network are 3.715 MW and 2.3 MVar, respectively. The test network has been widely used in many previous works [6, 28, 127, 130, 160, 161] for the purpose of network management application. The network is modified by including an OLTC transformer and 6 DGs in [28]. Two solar-based DGs and four wind-based DGs of 1 MW generation capacity are considered to simulate high renewable penetrations. The two solar-based DGs are allocated at nodes 13 and 18 whereas four wind-based DGs at nodes 6, 7, 28 and 33 as shown in Figure 2.9. Tap changer of the substation transformer has 11 steps upward and 13 steps downward

from the nominal settings to regulate voltage at 0.01 pu for every step transition. The system bus voltages are regulated within the statuary limits of ±5% and current rating of 5 p.u. is set to all interconnection lines and substation transformers.

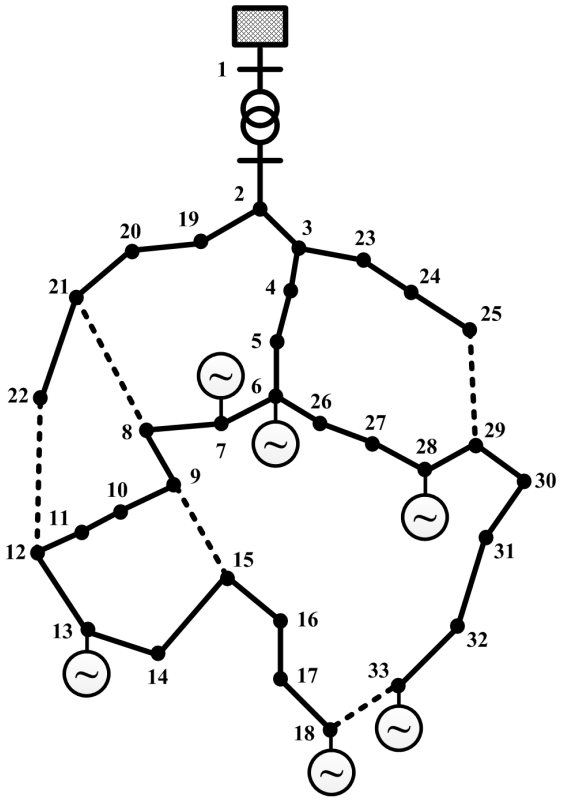

Figure 2.9: A modified 33-bus test network

2.6.3 HV-UG UK Generic Distribution System

The United Kingdom (UK) generic distribution system was developed by the Centre for Sustainable Electricity and Distributed Generation (SEDG) as representative of UK distribution networks [162]. The HV-UG model is an 11 kV urban distribution network fed from a 33 kV grid supply point through two main substations rated at 26.4 MVA. The network provides service to high customer density with total active and reactive loads of 24.274 MW and 4.8548 MVar, respectively. The HV-UG distribution network contains 75 nodes that are interconnected in radial topology by 75 lines with total length of 56.825 km underground cables and average thermal rating of 7.168 MVA. There are 22 identical generators are assumed to follow wind power behaviour with each generation capacity of 1.73 MW. A schematic diagram of

the network is depicted in Figure 2.10. A similar OLTC operation as in the modified 33-bus network is considered for this test system. The system voltage magnitudes follow the requirement as according to the Engineering Recommendation P28 [74].

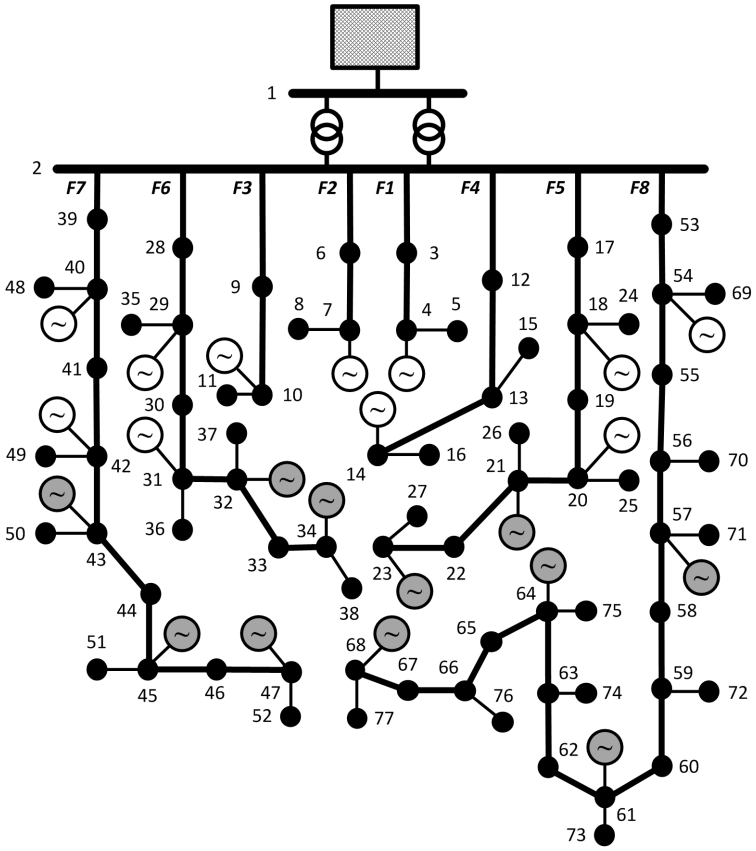

Figure 2.10: A HV-UG UK generic distribution system

2.6.4 Test Network Models Assessment

Preliminary assessments are conducted to evaluate how good the test network models have been developed for a power system analysis. In order to ensure all formulations in AIMMS are correct and provide accurate solution, a commonly used OPF problem, that is also designed in MATPOWER to minimise generation cost, is applied for assessment purposes. The assessment is carried out and compared in terms of voltage magnitudes and angles, active power injections from DG or GSP and line or transformer loadings. In this assessment, several indices are selected to showcase the accuracy of developed models in AIMMS as compared to MATPOWER. These indices are known as mean absolute error (MAE), mean square error (MSE) and root

mean square error (RMSE). In addition to these indices, minimum and maximum absolute error (AE_{min} and AE_{max}, respectively) are also provided to show the error distributions. The indices can be computed using the following expressions:

$$AE_{min} = \min_{n=1,\ldots,N} |y_n - \hat{y}_n| \tag{2.6.1}$$

$$MAE = \frac{1}{N}\sum_{n=1}^{N} |y_n - \hat{y}_n| \tag{2.6.2}$$

$$AE_{max} = \max_{n=1,\ldots,N} |y_n - \hat{y}_n| \tag{2.6.3}$$

$$MSE = \frac{1}{N}\sum_{n=1}^{N} (y_n - \hat{y}_n)^2 \tag{2.6.4}$$

$$RMSE = \sqrt{\frac{1}{N}\sum_{n=1}^{N} (y_n - \hat{y}_n)^2} \tag{2.6.5}$$

where, y and $\hat{y}$ are obtained solution from AIMMS and MATPOWER, respectively.

The two aforementioned models, modified 33-bus network and HV-UG UK distribution system, in AIMMS are compared to optimal solution obtained using MATPOWER and tabulated in Tables 2.1 and 2.2, respectively. The modified 33-bus network model show the errors less than 1×10^{-6} p.u., $4.7^{\circ} \times 10^{-5}$, $1.4 \times 10^{-5} MW$ and $3.35 \times 10^{-4}\%$ for comparison in terms of voltage magnitudes and angles, active power injections and element loadings, respectively. On the other hand, the parametric errors are less than 1.35×10^{-7} p.u., $6.96^{\circ} \times 10^{-7}$, $8.16 \times 10^{-8} MW$ and $3 \times 10^{-5}\%$ for the HV-UG UK distribution system model. The errors are relatively small within tolerance intervals of 10^{-5} – 10^{-8}. Therefore, the results indicate that the developed models in AIMMS are well represented as they consistence with MATPOWER solution and can be confidently used for further investigations.

Further investigations are carried out to understand the electrical and thermal behaviours of the original networks. For this purpose, a simulation is executed without ANM scheme where tap changer control, demand response and DG curtailment are not available. In other words, normal power flow is conducted with relaxed constraints of voltage and thermal limits. Figures 2.11a and 2.11b depict voltage magnitudes and element loadings in the modified 33-bus network, respectively. The voltage magnitude violated the statuary limits of $\pm 5\%$ without any

Table 2.1: Performance of modified 33-bus network model

Item	AE_{min} [$\times 10^{-7}$]	MAE [$\times 10^{-7}$]	AE_{max} [$\times 10^{-7}$]	MSE [$\times 10^{-12}$]	$RMSE$ [$\times 10^{-7}$]
Voltage magnitude (p.u.)	0.11	7.38	10.01	0.63	7.94
Voltage angle (°)	0	107.3	469.25	309.65	175.97
Power injection (MW)	28.28	51.71	139.47	40.02	63.26
Element loading (%)	0.55	1168.72	3343.2	27262.25	1651.13

Table 2.2: Performance of HV-UG UK distribution system model

Item	AE_{min} [$\times 10^{-7}$]	MAE [$\times 10^{-7}$]	AE_{max} [$\times 10^{-7}$]	MSE [$\times 10^{-12}$]	$RMSE$ [$\times 10^{-7}$]
Voltage magnitude (p.u.)	1.26	1.3	1.34	0.017	1.3
Voltage angle (°)	0	2.04	6.96	0.096	3.1
Power injection (MW)	0.01	0.24	0.82	0.001	0.32
Element loading (%)	0.91	74.79	299.59	126.74	112.58

thermally vulnerable of 5 p.u. current rating components in the modified 33-bus network. However, the power loading of the feeders are not well distributed and the highest loading is higher than 80% as shown in Figure 2.11b. This would lead to components especially for the element with the highest loading becoming thermally vulnerable during low demand and high generation if the network operation does not manage properly.

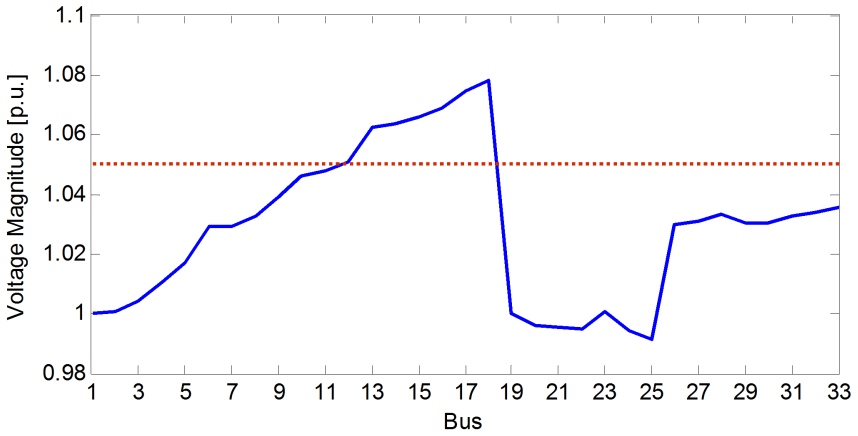

(a) Buses voltage magnitudes

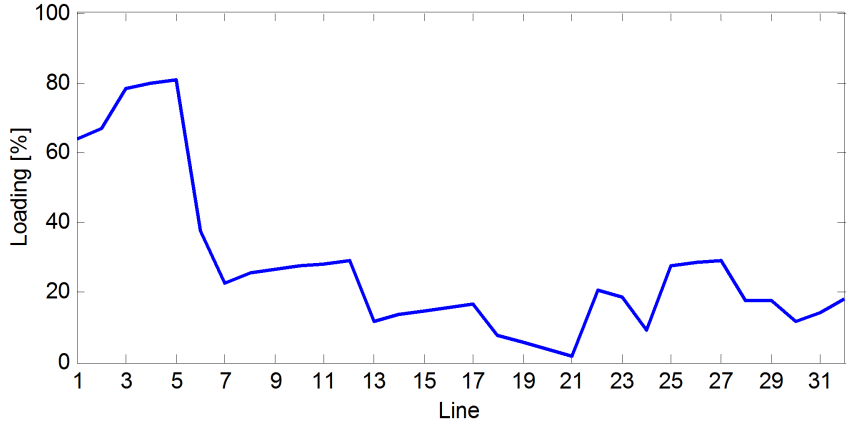

(b) Transformer and line loadings

Figure 2.11: Voltage magnitude and loading profiles of the modified 33-bus network

The investigation is also carried out on the HV-UG UK distribution system and the results are presented in Figure 2.12. Both voltage and loading profiles are operated within the required limits as shown in the figure. The distribution system shows that the highest voltage magnitude is slightly higher than 1.02 p.u. at bus 47. On the other hand, all network elements operate at low loading which is not even half of the loading capacity. In this situation, the network might not have any issue during worst case operating scenarios (i.e., low demand at high generation or high demand at low generation). However, the voltage statuary limits might be violated or the network elements overload during fault isolation at the worst operating scenarios. This indicates that the HV-UG UK distribution system is more suitable for power system security analysis.

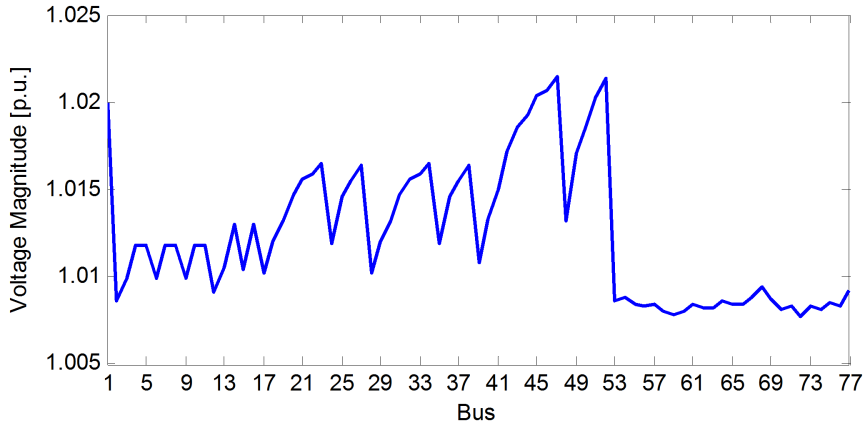

(a) Buses voltage magnitudes

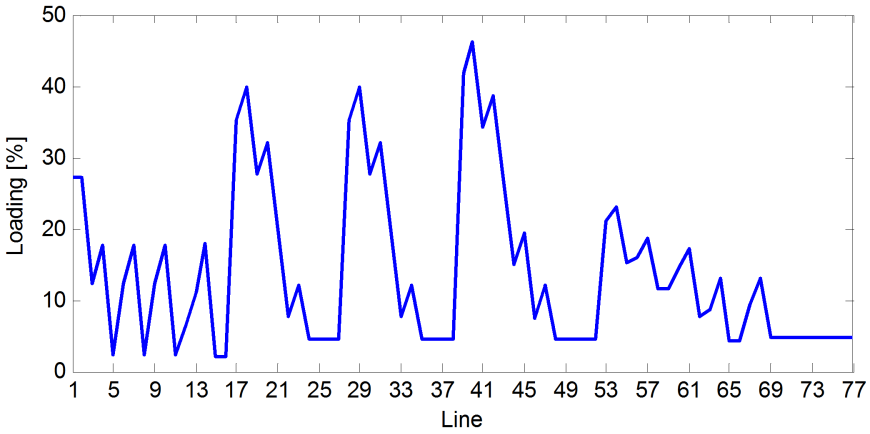

(b) Transformer and line loadings

Figure 2.12: Voltage magnitude and loading profiles of the HV-UG UK distribution system

2.7 Summary

In this chapter, a number of key issues that arise from the integration of renewable resources into the existing distribution network is reviewed. It is noticeable that renewable resources in form of DG connections create a wide range of technical problems and their influence on the power system performance cannot be neglected. To encourage more contribution from renewable energy, the philosophy of new distribution network planning and operation mechanism is introduced through the concept of active distribution systems. A literature survey of network management methods have been applied in the last few years for active distribution system are presented.

These methods can be divided into four categories, namely standalone, rule-based, analytical and heuristic approaches. Then, the concept of an active network management (ANM) framework is introduced as the main operational planning framework which will be investigated in this thesis. At the core of the ANM framework sits a multi-period non-linear non-convex OPF problem formulation for solving and determining optimum set points for various control devices throughout the network. Two candidate systems are introduced to showcase and test various ANM mechanisms and applications in realistic network operating conditions. These will be outlined in subsequent chapters.

Chapter 3

Active Network Management: Enhanced Network Reconfiguration

This chapter showcases the potential for implementing network reconfiguration methods as a viable active network management scheme, and for purposes of voltage constraint management, for future flexible active distribution systems with high levels of aggregated distributed generation (DG) resources. Network reconfiguration, as a cost effective way of improving network's operational performance (e.g. voltage profile), is reviewed briefly at the beginning of this chapter. In the latter part of this chapter, an enhanced network reconfiguration method, based on integration of voltage source converters, is introduced. The new reconfiguration method relies on integration of back-to-back VSC configurations (BTB-VSC) that act as controllable soft open points (SOP) between adjacent feeders, instead of using binary switches as used in conventional methods. The enhanced network reconfiguration method is then implemented within a day-ahead DSO active network management framework for purposes of voltage constraint management and load balancing.

3.1 Applications of Network Reconfiguration

Network reconfiguration in distribution systems is applied by altering the system topology through changing the status of sectionalising switches (normally closed) and tie-switches (normally open) that exist within the network. It is normally used to restore electricity supply to loads, which are isolated due to the existence of a fault (e.g. tripping of a line). Alternatively, it can also be used to reduce power losses by re-routing power flows to distribute loads between heavily loaded and lightly loaded feeders without violating the system security. The ensuing levels of flexibility promised by network reconfiguration, will improve system reliability by reducing system losses and improving its voltage profile. Furthermore, network reconfiguration can also reduce annual unavailability of the electricity supply contributing to a decrease of customer interruptions. The distribution network reconfiguration has been widely used in operational planning as well as real-time operation. For integrating within a day-ahead optimum operational planning framework, the network reconfiguration is modelled as a mixed integer non-linear optimisation problem which contains binary variables for the switching states and non-linearity terms in the power flow equations. Therefore, a distribution system with moderate number of switching options is computationally inefficient and impractical for even the day-ahead operational planning problems due to the number of switching perturbations. Consequently, various approaches have been proposed in the last decades to investigate any potential advantages of the network reconfiguration applications in conjunction with mitigating the computational issues in the ensuing optimisation problems.

3.1.1 Loss Reduction

Most of the previous works on network reconfiguration applications are mainly focused to reduce power losses or improve load balancing between the feeders in a radial distribution system operation. The earliest work for loss reduction using network reconfiguration is introduced by Merlin and Back [163]. A heuristic branch and bound algorithm had been applied in their work to find the best configuration

that gives the minimum power losses. In the searching procedure, all switches are initially closed to form a mesh network, and then a switch is opened in each time step until a radial structure is restored. The switches are selected to be open such that the power losses are minimised in the final configuration. Shirmohammadi and Hong [164] continued the previous approach and solved the problem by using branch flows calculation to determine which switch will be opened. This work introduced a computer program called distribution network optimization (DISTOP) to cater several drawbacks in [163] that includes the assumption of purely active loads and and neglecting voltage angle and network constraints. In the same year in 1989, Baran and Wu [159] introduced two power flow approximation methods to estimate loss reduction and load balancing in the system. In the first method that is called *forward update*, the power flow quantities (i.e., voltage magnitude, real and reactive power) at the receiving end of each branch are calculated from the same quantities at the sending end. In the second part of the approximation method which is known as *backward update*, the power flow quantities are determined in reverse direction (from the sending end to the receiving end). The updating process is carried out iteratively and used to approximate the total power loss reduction at every branch exchanges (after creating a new branch by closing and opening the respective switches). A meta-heuristic based on genetic algorithm is implemented in this work to search for the best configuration that gives the most load between the feeder loadings at minimum power losses.

The meta-heuristic algorithms, however, may not necessarily guarantee the global solution and their performance depends on the nature and complexity of the problem. Nevertheless, many different meta-heuristic algorithms have been found in minimising loss using network reconfiguration technique. Chiang and Jean-Jumeau [165,166] presented a two-stage methodology to improve the optimisation algorithm by using a simulated annealing as alternative to the genetic algorithm in [159]. The simulated annealing is another type of meta-heuristic algorithm that uses a probabilistic process for locating the global optimum of a given objective function in a large search space. The simulated annealing also applied on a similar optimisation problem in [167]. In contrast, Chang and Kuo [167] simplified load flow equations

to approximate the line loss and developed an efficient perturbation scheme and initialisation procedure to speed up the optimisation process. Ant colony algorithm is another type of meta-heuristic optimisation techniques that inspired by the foraging behaviour of ant colonies. The algorithm is employed in [168] to solve network reconfiguration for loss minimisation. This optimisation searching procedure is basically based on a population-based approach with exploration through a collection of cooperative agents called "ants" that looks for positive feedback (the near-optimal solution) until the convergence criteria is satisfied. In another research work [169], the ant colony search algorithm is used to solve both network reconfiguration and capacitor placement problems. Besides that, a particle swarm optimization algorithm has been applied in many literatures to solve network reconfiguration problems [170–173]. This algorithm is inspired by bird flocking behaviour when migrates to determine a search path based on particle self-assessment in terms of their velocity and position towards the leading particle of the swarm. In [173], the optimisation algorithm is modified by introducing a dynamic inertia weight to overcome the computational burden of obtaining a desired solution in the previous work [172]. Apart from the aforementioned algorithms, the problem of network reconfiguration has also been tackled using several different meta-heuristic approaches including Tabu search algorithm [128, 174], differential evaluation [175, 176] and harmony search algorithm [48, 177].

Notwithstanding the large use of meta-heuristics, conventional numerical approaches have also been used extensively to solve the network reconfiguration problem. References [47, 178] introduce a mixed integer linear programming problem formulation of the network reconfiguration. In order to ensure the connectivity and radiality of the network, a graph-based algorithm is embedded in the searching process. This approach, however, ignored the technical constraints of voltage variation due to linearisation of the power flow equations. On the other hand, Romero-Ramos et al. [179] presented a non-linear formulation of the network model that considers load flow equations, technical constraints of voltage magnitudes and line capacities and topological constraints, resulting in a mixed-integer quadratically constrained programming problem. The optimisation problem is then solved using a commercial

program solver. The exact loss modelling is used in [180] and solved using a Benders decomposition solution approach. The problem is partitioned into two sub-problems: master and slave. The master problem is modelled as a mixed-integer non-linear programming problem (MINLP) to determine the status of switches, whereas the slave problem is modelled as a non-linear programming problem (NLP) to seek for optimal feasible solution. These two level of problems are integrated using linear benders cuts. In the same direction, Taylor and Hover [181] introduced a convex formulation in modelling the reconfiguration problem. For comparison purposes, the model is formulated into three different problems; quadratic programming (QP), quadratically constrained programming (QCP), and second-order cone programming (SOCP). Among of these three formulations, the QP model provided relatively good solutions at the most efficient computational time. On the other hand, Jabr et al. [105] presented an exact mixed-integer conic programming (MICP) model using convex continuous relaxation to guarantee convergence at global optimal solution. Lee et al. [49] imposed the uncertainty of load variations as a two-stage problem where the network reconfiguration is determined in the first stage and the load variation in another. This optimisation problem is solved using the column-and-constraint generation algorithm, in which the master and sub-problems are transformed into an equivalent mixed-integer second-order cone programming (MISCOP).

3.1.2 Quality of Services

As discussed in the previous section, network reconfiguration is mainly applied for loss reduction but it also has been found to improve quality of service in terms of system reliability. System reliability level may be defined as the ability of the system to supply power to consumers at an acceptable quality and under a set of specified criteria. Voltage variations (i.e., interruptions, sags or swells) normally last for several hours after system faults have been cleared that may effect the reliability level. As a potential application to enhance network reliability, voltage variation propagation can be mitigated (or minimised) using network reconfiguration such that the number of affected consumers are minimised. In [182], the financial losses caused by voltage sag propagations are computed and used to indicate the best configuration

which yields the lowest customer interruptions. The optimal solution is obtained using genetic algorithm with enhanced features of double-point crossover and adaptive mutation for more efficient optimisation process. Two indices are introduced in [183] for system losses and reliability that can be used to address both issues together based on a Pareto optimal criterion. The criterion is important to give the best trade-off between the two considered objectives. An automated reconfiguration application based on fault detection, isolation and reconfiguration (FDIR) mechanism is suggested in [103] to improve the overall system reliability. The method used for FDIR is replicated from the concept of restoration process in transmission systems. In reality, the contingencies occurrence is uncertain. Therefore, Amanulla et al. [184] suggested probabilistic reliability models that can be derived from the respective component's history failure and the minimal cut sets of each load point. This study solves not only system reliability but together with power losses by using binary particle swarm optimization (BPSO). The uncertainty of contingencies occurrence is also imposed into demand and generation by Kavousi-Fard and Niknam [185] when consider the error of load forecast and wind speed variations. Network reconfiguration in their work is used to overcome a multi-objective problem with regard to system reliability, power loss and total operational cost.

3.1.3 Constraints Management

Although network constraints are considered in the literatures of the previous subsections, most of them focus on optimising the network configuration when there is no constraint violation during normal operation. In contrast, this subsection covers operating scenarios in normal condition that might violate network constraints especially thermal and voltage limits due to high penetration renewable distributed generation resources or in heavily loaded systems. A voltage constraints management is assessed by using different schemes including the network reconfiguration in [28]. This study has clearly showed that the penetration of renewable resources is limited by voltage constraints. In regards to this issue, Capitanescu et al. [6] studied the potential of dynamic network reconfiguration to improve hosting capacity of the distribution networks in addition to other active network management schemes.

A multi agent control system (MACS) is proposed in [51] to eliminate congestion and voltage violation while maintaining local state variables and the reactive power devices operate within the normal operating characteristics. Huang et al. [186] suggested the reconfiguration technique together with dynamic tariff to manage the congestion problem in distribution networks by taking advantage of electric vehicles. This study ultimately aims to reduce energy cost at minimum switching cost. In [50], a dynamic network reconfiguration is applied to assess the loss reduction in distribution systems with high renewable resources at different varying demand and generation profiles. It was found that network reconfiguration application becomes more worthy in systems with intermittent resources. Recently, a hierarchical and distributed congestion management concept is discussed in [187] to enable cost-effective network interconnection of DG and better utilisation of network assets. The hierarchy control consists of three levels; primary controllers operate independently based on field measurements, secondary controllers at substations provide optimal set points to their regional primary controllers, and tertiary controllers at the control center utilise forecast tools for day-ahead planning where the network reconfiguration is implemented. In order to enable on-line dynamic network reconfiguration that require fast computational process, [52] engaged a convex quadratic relaxations in the optimal power flow formulation. Meanwhile, the presence of harmonics in power systems can also result in increased heating in the conductors that would violate the thermal limit. The harmonic injections from non-linear loads are investigated in [188] to demonstrate the effectiveness of network reconfiguration to reduce power loss while keeping voltage magnitude and current flow within the required limits.

3.2 Integration of Power Flow Controllers

The network reconfiguration has been proven in the past research to be an effective technique to enhance network operation especially for active distribution systems application. Conventionally, network reconfiguration is centrally managed through operation of remotely controlled switches (RCSs). In the application of dynamic

network reconfiguration, the switches operate at a fast rate due to intermittent behaviour of demand and DG supplies that could shorten the device's lifetime. Consequently, solid-state devices are a better alternative to mechanical switches as they are not subject to the usual mechanical wear and tear of conventional RCSs when in rapid operation. In recent years, with the advances in power electronics technology as well as semiconductor technology, fully controlled power converters have also found applications in distribution systems. Power converters can generally be categorised into line-commutated and self-commutated [189]. The line-commutated converter uses thyristors in converting electric power that only can be turned on using a pulse control signal. In this case, it relies on the line voltage of AC system to enable for commutation between switches. A large inductor is usually installed in the DC side to operate at constant DC current flow behaving as a current source, thus the name current source converter (CSC). The self-commutated converter uses transistors, normally insulated-gate bipolar transistors (IGBTs), which can ideally operate as bi-directional switches. The DC voltage is kept constant by a capacitor acting as a constant voltage source, thus the name voltage source converter (VSC). The VSC can control independently both real and reactive power at its AC side, and can be used as a power flow controller in system applications.

The power converter applications in transmission systems are well known, for instance, high voltage direct current (HVDC) technology has been in service for more than 60 years [190,191]. In the context of distribution systems, power converters are typically implemented for interfacing DGs into the system. However, they can also be used in active network management schemes. Bloemink and Green in few publications [59,60,192,193] showed the benefits of power converter application in distribution systems to manage voltage constraints and thermal limits. In their work, they introduced a back-to-back (BTB) arrangement of VSCs to be installed at normally-open points between adjacent feeders within an otherwise radial distribution network. They call this arrangement a Soft Open Point (SOP). The SOP can control both active and reactive power flows at its interface terminals between the two interconnected feeders. It can therefore potentially be used as an alternative to binary mechanical RCSs for enhanced network reconfiguration and load balancing

in an active distribution system. However, the existing work in literature on SOPs often neglect the converter's actual operational limits. Furthermore, such studies typically do not consider suitable operational constraints to avoid undesired misconfiguration in the existing protection coordination schemes. The easiest way to address this issue at minimum cost and effort (to potentially modifying the protection regime) is by introducing a set of suitable operational constraints that would maintain the radial topology of the network [194]. In this chapter an enhanced network reconfiguration method is introduced that take advantage of the existence of fully controlled SOPs instead of conventional binary RCSs. The SOPs in this thesis are used not only for blocking power flows but also for providing voltage support to their AC terminals when needed, whilst adhering to the corresponding converter's operational constraints as well as network's radilaity constraint. Since, the SOPs specifically in this thesis, are basically back-to-back connection of voltage source converters, they are called BTB-VSCs to distinguish them from other types of devices that might be used as SOPs in other literature. Before introducing the details of the enhanced network reconfiguration, a brief overview of the VSC followed by a comprehensive model description is given. The steady-state fundamental frequency model of the VSC introduced in this chapter is suitable for integration into the enhanced network reconfiguration problem for purposes of incorporation within a day-ahead active network management framework.

3.2.1 Voltage Source Converters

There are several types of VSCs that employing the switching devices (typically IGBTs) in different topologies, for example, three-phase, two-level, six-pulse bridges or three-phase, three-level, twelve-pulse bridges. The two-level converter is generating the two voltage outputs; $-0.5E_{dc}$ and $+0.5E_{dc}$ (where E_{dc} is the DC voltage). On the other hand, the three-level converter comprises four valves in one arm of the converter which generates AC voltage comprising of three voltage levels $-0.5E_{dc}$, 0 and $+0.5E_{dc}$. In order to operate either the two or three-level topology in high voltage applications, series connection of IGBTs may be necessary. In each IGBTs valve, a number of connected devices and anti-parallel diodes are required to

suppress voltage spikes and accommodate return current when needed. The basic three-phase, two-level full bridge VSC as shown in Figure 3.1a forms the essence of the mathematical model presented in this work. As shown in the figure, the AC system and the controlled voltage source are connected via a phase reactor. It has been observed that for purposes of efficient computational modelling, the converter under a balanced three-phase system in Figure 3.1a could be represented by essentially an ideal transformer with complex tap ($\overline{m}_a = m_a e^{j\phi}$) as depicted in Figure 3.1b whose magnitude corresponds to the actual PWM amplitude modulation ratio and phase shift corresponds to the actual phase shift, relative to system reference, that can be exerted at the output AC voltage (RMS, line-line). It is important to note that the shunt branch, B_{sw} in the figure is used to impose a zero reactive power flow constraint on the DC circuit. This notional susceptance thus models the leading or lagging VAR operation through PWM switching action in the converter. For an actual VSC with a DC input voltage of line to ground, $V_{dc} = 0.5E_{dc}$, the AC output voltage magnitude at converter terminals then becomes:

$$\overline{V}_{cr} = \overline{m}_a \frac{\sqrt{3}V_{dc}}{\sqrt{2}} = k\overline{m}_a E_{dc} \tag{3.2.1}$$

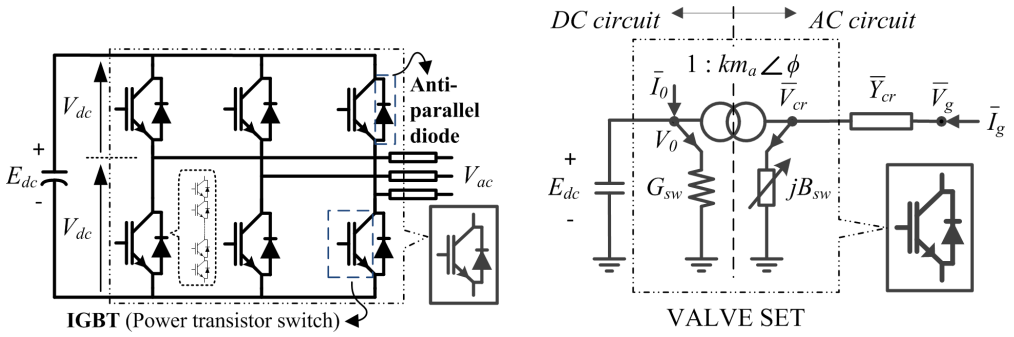

(a) A two-level converter (b) An equivalent model

Figure 3.1: Three-phase voltage source converter

where, E_{dc} is the DC line to line voltage which on a per-unit basis carries a value of 2 and $k = \sqrt{3/8}$ (≈ 0.612). This model can be extended for any type of converter at any switching level [195, 196]. The advantage of this model is that it combines both DC and AC sides on one single frame of reference for unified load flow calculations. It also does not neglect the operational limits imposed on the converter for linear

operation (i.e., $0 \leq m_a \leq 1$) [196]. The converter is then able to provide independent active and reactive power through controlling its AC output terminal voltage. Furthermore, using the ideal transformer model, a realistic operational capability curve for the VSC may also be derived which takes into account the limiting factors of the VSC operation, namely the switching devices (i.e., IGBTs) current limit, the DC bus voltage, E_{dc}, and the DC cable current limit [197]. With regards to the current limits, the active and reactive power injections of the VSC in a P-Q diagram for two different AC grid voltages V_{g1} and V_{g2}, where $V_{g1} < V_{g2}$ is illustrated in Figure 3.2a. Since DC voltage is kept constant, the operation limit due to the DC current limit is fixed and can be ignored if suitable DC cable size is used to make it equal or slightly higher than the maximum active power capability that is derived from the IGBT's current limit. With this condition, the VSC's power capability curve can only be represented by the IGBT's current limit. After all, the constant DC voltage creates another limitation on the power capability curve due to maximum voltage generated at the converter's terminal. Figure 3.2b illustrates the active and reactive power injections of the VSC into the power grid (AC system) at the maximum generated AC voltage (when modulation index at maximum point). It clearly shows that reactive power generated (leading power factor) varies depending on the difference between voltage at the connected grid, V_g and voltage at the converter's terminal, V_{cr}. Therefore, the voltage level at DC side would restrict the leading VAR operation especially when the grid voltage at high level. For this reason, using a constant MVA limit might neglect the converters actual voltage-dependent limiting factors.

Referring to Figure 3.1b, the operating power of the VSC can be derived from the nodal current equations with inclusion of the DC voltage limitation. The nodal current injections are given in the following expression [196, 198]:

$$\begin{bmatrix} \overline{I}_g \\ \overline{I}_0 \end{bmatrix} = \begin{bmatrix} \overline{Y}_{cr} & -km_a\overline{Y}_{cr}e^{\mathrm{j}\phi} \\ -km_a\overline{Y}_{cr}e^{-\mathrm{j}\phi} & G_{sw} + k^2m_a^2(\overline{Y}_{cr} + \mathrm{j}B_{sw}) \end{bmatrix} \begin{bmatrix} \overline{V}_g \\ E_{dc} \end{bmatrix} \tag{3.2.2}$$

Then, the nodal power injections can be calculated as below:

$$\begin{bmatrix} \overline{S}_g \\ \overline{S}_0 \end{bmatrix} = \begin{bmatrix} \overline{V}_g & 0 \\ 0 & E_{dc} \end{bmatrix} \begin{bmatrix} \overline{I}_g \\ \overline{I}_0 \end{bmatrix}^* \tag{3.2.3}$$

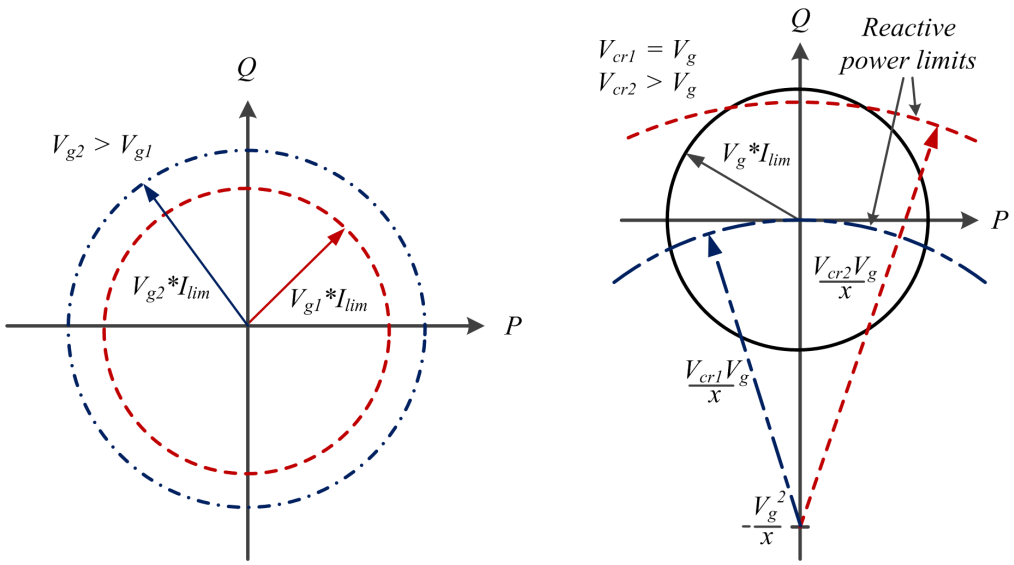

(a) Power curve at different AC voltages (b) Power curve at different DC voltages

Figure 3.2: Limiting factors of the converter operation

Substituting equation (3.2.2) into (3.2.3), the power injections at the connected grid and DC terminal can be expressed as:

$$\overline{S}_g = P_g + \mathrm{j}Q_g = \overline{Y}^*_{cr} V_g^2 - \overline{Y}^*_{cr} k m_a E_{dc} \overline{V}_g e^{-\mathrm{j}\phi} \tag{3.2.4}$$

$$\overline{S}_0 = P_0 + \mathrm{j}Q_0 = G_{sw} E_{dc}^2 + k^2 m_a^2 E_{dc}^2 (\overline{Y}^*_{cr} - \mathrm{j}B_{sw}) - \overline{Y}^*_{cr} k m_a E_{dc} \overline{V}_g e^{\mathrm{j}\phi} \tag{3.2.5}$$

where, $\overline{Y}_{cr} = G_{cr} + \mathrm{j}B_{cr}$ is the interface admittance and the shunt resistor (conductance, G_{sw}) to represent switching power loss of the VSC for a given PWM switching frequency. The notional susceptance, B_{sw}, is to provide a means for restricting a zero-reactive power flow at the DC side by imposing an appropriate constraint ($Q_0 = 0$). Let $\overline{V}_g = V_g e^{\mathrm{j}\theta}$, the B_{sw} variable can be determined by considering the imaginary part of the equation (3.2.5) at zero value that can be expressed as a function of modulation ratio and phase angle as such:

$$B_{sw} = -B_{cr} - \frac{V_g}{k m_a E_{dc}} [G_{cr} \sin(\phi - \theta) - B_{cr} \cos(\phi - \theta)] \tag{3.2.6}$$

On the other hand, the shunt resistance of the VSC, G_{sw} increases with the PWM switching frequency. When VSC operates at nominal current and rated DC voltage, the switching loss would be represented as a constant conductance, G_0. Although the DC voltage is kept constant, the operating current varies according

to the active and reactive power exchanged between the converter and the network. Then, the G_{sw} can be derived from the constant conductance and corrected by the quadratic of the operating current, I_{act} to the nominal current, I_{nom} which can be expressed as [198]:

$$G_{sw} = G_0(\frac{I_{act}^2}{I_{nom}^2}) \tag{3.2.7}$$

From power expressions derived, and as seen in Figure 3.2b, it is seen that the DC link voltage variations impose a limiting factor on the VSCs P-Q operational capability. On the other hand, the VSCs rated current is also a limiting factor to the P-Q capability curve, as seen in Figure 3.2a. Assuming that the DC cable has always higher ampicity than the IGBT's current rating, the following constraint can be derived from the magnitude of current injection from the connected grid (which gives the same magnitude of current at the converter's terminal on the AC side):

$$\begin{aligned} I_g^2 &= \overline{I}_g\overline{I}_g^* = \overline{Y}_{cr}\overline{Y}_{cr}^*(V_g e^{\mathrm{j}\theta} - km_a E_{dc}e^{\mathrm{j}\phi})(V_g e^{\mathrm{j}\theta} - km_a E_{dc}e^{\mathrm{j}\phi})^* \\ &= (G_{cr}^2 + B_{cr}^2)[V_g^2 + k^2 m_a^2 E_{dc}^2 - 2km_a E_{dc}V_g\cos(\theta - \phi)] \leq I_{rate}^2 \end{aligned} \tag{3.2.8}$$

3.2.2 Back-to-Back Configuration

As mentioned earlier, the power flow controller which ultimately is used for enhanced network reconfiguration purposes, is made out of a back-to-back connection of two VSCs sharing a common DC link. The ensuing BTB-VSC power flow controller is shown in Figure 3.3. In this application, the BTB-VSC is interfaced to an adjacent medium voltage line via a phase reactor, x_{cr} for power flow control purposes. The power flow through the device can be controlled by adjusting the modulation index and phase angle of each converter. However, some constraints that are relevant to the model configuration should be appropriately addressed.

Knowing (3.2.4), the nodal powers at the sending (j) and receiving ends (k) of the BTB-VSC power line can be derived as follows:

$$\overline{S}_j = P_j + \mathrm{j}Q_j = \overline{Y}_j^* V_j^2 - \overline{Y}_j^* km_a^{rec} E_{dc}\overline{V}_j e^{-\mathrm{j}\phi^{rec}} \tag{3.2.9}$$

$$\overline{S}_k = P_k + \mathrm{j}Q_k = \overline{Y}_k^* V_k^2 - \overline{Y}_k^* km_a^{inv} E_{dc}\overline{V}_k e^{-\mathrm{j}\phi^{inv}} \tag{3.2.10}$$

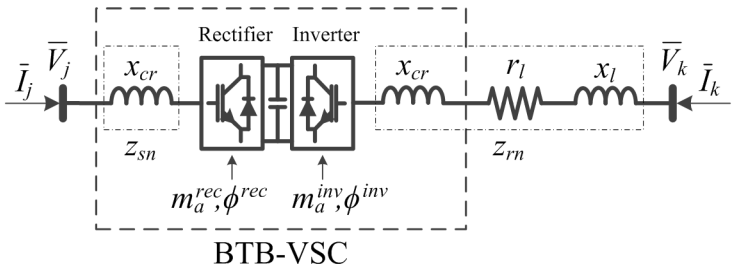

Figure 3.3: A BTB-VSC with the corresponding power line

In equations (3.2.9) and (3.2.10), the equivalent admittance as referred to Figure 3.3 can be computed by the following expressions:

$$\overline{Y}_j = G_{sn} + \mathrm{j}B_{sn} = -\mathrm{j}\frac{1}{x_{cr}} \tag{3.2.11}$$

$$\overline{Y}_k = G_{rn} + \mathrm{j}B_{rn} = \frac{r_l - \mathrm{j}(x_{cr} + x_l)}{r_l^2 + (x_{cr} + x_l)^2} \tag{3.2.12}$$

At the common DC link, the net power entering and leaving the link must be zero so as to avoid unnecessary over-voltages at the DC link (due to capacitor charging). Since, this is a back-to-back connection, the DC link loss is zero and therefore the power balance equation at the DC link can be expressed as below:

$$\Re\{\overline{S}_0^{rec}\} + \Re\{\overline{S}_0^{inv}\} = P_0^{rec} + P_0^{inv} = 0 \tag{3.2.13}$$

where, subscripts rec and inv denote rectifier and inverter, respectively. As shown in the equation, the DC power injections of rectifier, P_0^{rec} and inverter, P_0^{inv} can be extracted from the real part of the nodal power equation derived from (3.2.5). A complete formulation for the DC power injections of both converters are given in the following expressions:

$$P_0^{rec} = G_{sw}^{rec}E_{dc}^2 + G_{sn}k^2(m_a^{rec})^2E_{dc}^2 - km_a^{rec}E_{dc}V_j[G_{sn}\cos(\phi^{rec} - \theta_j) + B_{sn}\sin(\phi^{rec} - \theta_j)] \tag{3.2.14}$$

$$P_0^{inv} = G_{sw}^{inv}E_{dc}^2 + G_{rn}k^2(m_a^{inv})^2E_{dc}^2 - km_a^{inv}E_{dc}V_k[G_{rn}\cos(\phi^{inv} - \theta_k) + B_{rn}\sin(\phi^{inv} - \theta_k)] \tag{3.2.15}$$

In the above equations, terms $G_{sw}^{rec}E_{dc}^2$ and $G_{sw}^{inv}E_{dc}^2$ are referred to the switching power loss in the VSC. However, it is assumed that the switching loss of the VSCs is negligible (where, $G_{sw}^{rec} = G_{sw}^{inv} \approx 0$). For the completeness of the model, the

switching losses are taken into account in Chapter 5. Apart from that, the reactive power injections in DC circuit are kept at zero by imposing an appropriate constraint ($Q_0^{rec} = Q_0^{inv} = 0$). In order to fulfil the constraint, the values of B_{sw}^{rec} and B_{sw}^{inv} correspond to converter reactive power output as function of modulation ratio and phase angle as in expression (3.2.6). In other words, each converter controls reactive power independently between the rectifier and inverter which are given by B_{sw}^{rec} and B_{sw}^{inv}, respectively.

Referring to equations (3.2.9) and (3.2.10), it clearly shows that active power flow at the AC side can be blocked by matching the generated voltage magnitude, km_aE_{dc} and angle, ϕ with the voltage magnitude and angle at the adjacent connected grid bus. With the capability to block and allow active power flow, the BTB-VSC can be used to act like a switch and replace the mechanical RCSs. Moreover, the BTB-VSC could provide independent reactive power control at its corresponding AC terminals which result in an improved voltage management. Figure 3.4 shows an overall concept of the BTB-VSC that provides both network reconfiguration and voltage management. When open-circuited, the BTB-VSC through the use of VSC can provide reactive power support if needed to its terminals by operating it as a static compensator (STATCOM) providing only reactive power with zero active power exchange with system [199] as shown in Figure 3.4a. In contrast, there is no reactive power available when using the mechanical switch. On the other hand, BTB-VSC has the capability to inject different magnitudes of reactive power at different directions at the sending and receiving ends during closed circuit operation as depicted in Figure 3.4b. In case of using mechanical switches, reactive power at the receiving end highly depends on the sending end as to keep power balance according to Kirchoff's current law.

3.3 Enhanced Network Reconfiguration

In this section, the enhanced network reconfiguration scheme based on using BTB-VSCs as power flow controllers is introduced. An AC network can be turned into a series of smaller segments which are connected to each other via the BTB-VSCs.

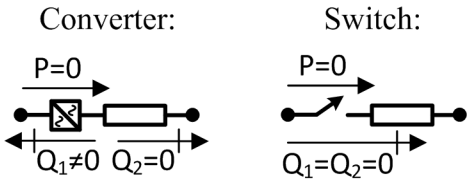

(a) Open circuit

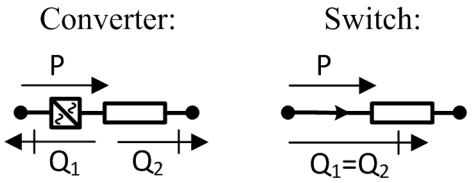

(b) Closed circuit

Figure 3.4: An operational comparison between BTB-VSCs and switches

The segmentation gives additional benefits in terms of resiliency towards power disturbances in the system. Furthermore, a potential for more efficient management could be achieved with regards only cover smaller area and can be controlled locally within the region. With regards the potential benefits, it is important to understand the modern power controller formulation within the ANM framework for its application on the enhanced network reconfiguration.

3.3.1 Reconfiguration Constraints

The main challenge in the enhanced network reconfiguration approach is that the network topology should be kept radial after altering the status of controlled switches for reconfiguration purpose. In order to achieve this condition, a similar approach as presented in [6] can be applied for the binary variable, s_c that models the on/off status of the controlled lines. In this approach, the sum of switches status must not change after reconfiguration. However, this constraint is insufficient to ensure all buses are linked to the grid supply point (GSP) that might result in some buses being isolated from the main grid especially zero-injection buses. This issue can be addressed by introducing a very small reactive power load (slightly higher than convergence tolerance) at the zero-injection bus as suggested in [28] that would not allow the power flow to converge as to keep the zero-injection buses connected.

Although this technique does help to keep all buses connected, the computational burden to obtain feasible combinations of the switch statuses could not be avoided. Therefore, this work imposes restriction on the combination of switch statues that ensures at least one path must be active to interconnection between the GSP and every bus in the network [179]. Since not all lines are controlled, this work uses regions (i.e., a group of buses) that are connected through a set of selected controlled lines (i.e. equipped with either RCSs or BTB-VSCs). This could avoid the checking of possible path for each bus that might give the same combinations of switch status. With that in mind, let Π^i be the set of possible paths to link between region i and the GSP region, $\Pi^i = \{\pi_1^i, \pi_2^i, \ldots, \pi_K^i\}$ in which π_k^i is one in case of an active k-th path or zero otherwise.

Now, it is possible to set the condition that each region must have at least one active path as in the following constraint:

$$\sum \Pi^i = \sum_{k=1}^{K} \pi_k^i \geq 1 \qquad \forall \Pi^i \tag{3.3.1}$$

where, the π_k^i can be obtained using boolean expression of the line status variable, $s_{c,m}$ associated with the path k. An illustrative example of possible paths with three controlled switches for network reconfiguration is depicted in Figure 3.5. In this example, there are two possible paths that link regions 1 and 2 to the GSP region. For the purpose of equation (3.3.1), these paths can be derived by the following expressions:

$$\text{Region 1:} \sum \Pi^1 = \pi_1^1 + \pi_2^1 = s_{1,m} + s_{2,m} \bullet s_{3,m} \tag{3.3.2}$$

$$\text{Region 2:} \sum \Pi^2 = \pi_1^2 + \pi_2^2 = s_{2,m} + s_{1,m} \bullet s_{3,m} \tag{3.3.3}$$

The above expressions are imposed to ensure all buses are connected to the GSP in order to avoid any isolated regions in the network. The mathematical expression to maintain network topology as radial can be written as [6]:

$$\sum_{c \in C} s_{c,m} = \sum_{c \in C} s_{c,0} \qquad \forall m \tag{3.3.4}$$

where, C is a set of controlled lines and $s_{c,0}$ is the initial condition of the radial network configuration. This expression clearly shows that the total number of deactivated lines should be gained back by activating the same number of lines that were

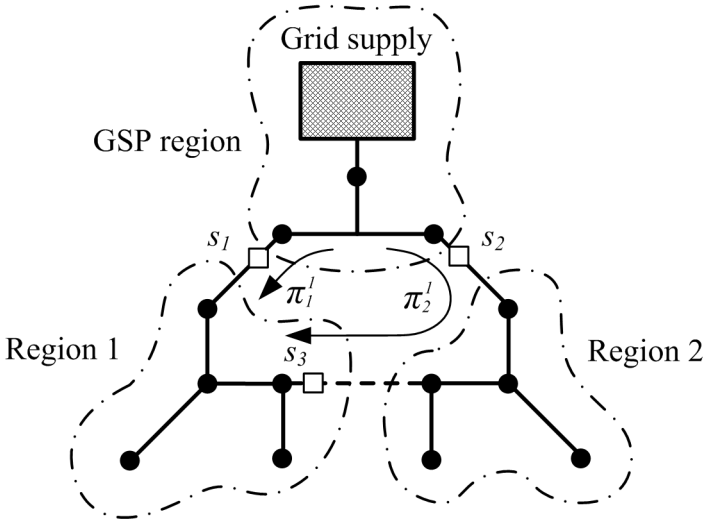

Figure 3.5: An example of possible paths for enhanced network reconfiguration

inactive before in order to maintain the radial topology. In that case, the sum of statuses of controlled lines from initial condition does not change after reconfiguration at every time period, m. With these constraints in place, searching for feasible combinations in order to fulfil the radiality constraint can be done separately without depending on the power flow computation.

3.3.2 Power Flow Formulation

Three explicit control variables namely, modulation index, phase angle and shunt susceptance that correspond to the converter VAR operation are used in each VSC as discussed previously. In addition to these variables, a binary variable, s_c is introduced in the previous section and used to enforce radiality constraint for enhanced network reconfiguration. The radiality constraint can be imposed into the power flow controller operation by enforcing a zero current injection constraint through the application of s_c in the equation (3.2.8) that can be expressed as given by (3.3.6). This can be done by producing a set of AC voltage magnitudes and angles at the converter's terminals, as given in (3.2.1), matching the system voltage phasor. As discussed in the Subsection 3.2.2, the BTB-VSC can provide reactive power control regardless of the state of the lines to which they are connected. Since the conductance in rectifier, G_{sn} is very small and can be neglected as shown in (3.2.11), the

current limits of rectifier and inverter can be updated and expressed in period m by the following expressions [200]:

$$B_{sn}^2[V_{j,m}^2 + k^2(m_{a\{c\},m}^{rec})^2 E_{dc}^2 - 2km_{a\{c\},m}^{rec} E_{dc} V_{j,m}\cos(\theta_{j,m} - \phi_{c,m}^{rec})] \leq I_{rate}^2 \tag{3.3.5}$$

$$(G_{rn}^2 + B_{rn}^2)[V_{k,m}^2 + k^2(m_{a\{c\},m}^{inv})^2 E_{dc}^2 - 2km_{a\{c\},m}^{inv} V_{dc} V_{k,m}\cos(\theta_{k,m} - \phi_{c,m}^{inv})] \leq s_{c,m} I_{rate}^2 \tag{3.3.6}$$

The BTB-VSC model is then incorporated within a day-ahead ANM framework using the following expressions given in equations (3.3.7) – (3.3.17). The AC active and reactive power injections at sending and receiving ends are given in (3.3.7) – (3.3.10), respectively. Equations (3.3.11) and (3.3.12) are used to compute the active power injections at the DC side of the rectifier and the inverter, respectively. The power balance equation in the DC link is shown in expression (3.3.13). On the other hand, the reactive power injections into the DC link from rectifier and inverter can be expressed in (3.3.14) and (3.3.15). These are kept zero using the zero-reactive power constraint. In order to restrict the reactive power injections from entering into the DC side, the variables $B_{sw\{c,m\}}^{rec}$ and $B_{sw\{c,m\}}^{inv}$ in the expressions can be calculated using equations (3.3.16) and (3.3.17), respectively.

$$P_{j,m} = -B_{sn} k m_{a\{c,m\}}^{rec} E_{dc} V_{j,m}\sin(\theta_{j,m} - \phi_{c,m}^{rec}) \tag{3.3.7}$$

$$P_{k,m} = G_{rn} V_{k,m}^2 - k m_{a\{c,m\}}^{inv} E_{dc} V_{k,m}[G_{rn}\cos(\theta_{k,m} - \phi_{c,m}^{inv}) + B_{rn}\sin(\theta_{k,m} - \phi_{c,m}^{inv})] \tag{3.3.8}$$

$$Q_{j,m} = -B_{sn} V_{j,m}^2 + B_{sn} k m_{a\{c,m\}}^{rec} E_{dc} V_{j,m}\cos(\theta_{j,m} - \phi_{c,m}^{rec}) \tag{3.3.9}$$

$$Q_{k,m} = -B_{sn} V_{k,m}^2 - k m_{a\{c,m\}}^{inv} E_{dc} V_{k,m}[G_{rn}\sin(\theta_{k,m} - \phi_{c,m}^{rec}) - B_{rn}\cos(\theta_{k,m} - \phi_{c,m}^{inv})] \tag{3.3.10}$$

$$P_{0\{c,m\}}^{rec} = G_{sw\{c,m\}}^{rec} E_{dc}^2 - B_{sn} k m_{a\{c,m\}}^{rec} E_{dc} V_{j,m}\sin(\phi_{c,m}^{rec} - \theta_{j,m}) \tag{3.3.11}$$

$$P_{0\{c,m\}}^{inv} = G_{sw\{c,m\}}^{inv} E_{dc}^2 + G_{rn} k^2 (m_{a\{c,m\}}^{inv})^2 E_{dc}^2 - k m_{a\{c,m\}}^{inv} E_{dc} V_{k,m} \times [G_{rn}\cos(\phi_{c,m}^{inv} - \theta_{k,m}) + B_{rn}\sin(\phi_{c,m}^{inv} - \theta_{k,m})] \tag{3.3.12}$$

$$P^{rec}_{0\{c,m\}} + P^{inv}_{0\{c,m\}} = 0 \tag{3.3.13}$$

$$\begin{aligned} Q^{rec}_{0\{c,m\}} = &-[B_{sn} + B^{rec}_{sw\{c,m\}}]k^2(m^{rec}_{a\{c,m\}})^2E^2_{dc} \\ &+B_{sn}km^{rec}_{a\{c,m\}}E_{dc}V_{j,m}\cos(\phi^{rec}_{c,m} - \theta_{k,m}) \end{aligned} \tag{3.3.14}$$

$$\begin{aligned} Q^{inv}_{0\{c,m\}} = &-[B_{rn} + B^{inv}_{sw\{c,m\}}]k^2(m^{inv}_{a\{c,m\}})^2E^2_{dc} - km^{inv}_{a\{c,m\}}E_{dc}V_{k,m} \\ &\times[G_{rn}\sin(\phi^{inv}_{c,m} - \theta_{k,m}) - B_{rn}\cos(\phi^{inv}_{c,m} - \theta_{k,m})] \end{aligned} \tag{3.3.15}$$

$$B^{rec}_{sw\{c,m\}} = -B_{sn} + \frac{B_{sn}V_{j,m}}{km^{rec}_{a\{c,m\}}E_{dc}}\cos(\phi^{rec}_{c,m} - \theta_{j,m}) \tag{3.3.16}$$

$$\begin{aligned} B^{inv}_{sw\{c,m\}} = &-B_{rn} - \frac{V_{k,m}}{km^{inv}_{a\{c,m\}}E_{dc}}[G_{rn}\sin(\phi^{inv}_{c,m} - \theta_{k,m}) \\ &-B_{rn}\cos(\phi^{inv}_{c,m} - \theta_{k,m})] \end{aligned} \tag{3.3.17}$$

3.4 Numerical Test Results

The application of the BTB-VSCs for enhanced network reconfiguration within a day-ahead ANM framework is presented in this section. The modified IEEE 33-bus system which was introduced in Chapter 2 was used as the test system for this section. The system is modified to accommodate aggregated distributed generation resources in form of solar power. Three operating scenarios are considered namely, the normal operation (day-ahead scheduling), and two worst case scenarios (high demand/no generation, and low demand/high generation). For comparative purposes, the ANM framework is implemented for a base case with no active controls except for the tap changers, a conventional network reconfiguration with RCSs integrated, and the enhanced network reconfiguration introduced in this chapter with BTB-VSCs in place of RCSs. The three case studies are shown in Table 3.1. All three cases will also consider DG curtailment as part of the ANM strategy implemented by the DSO. The case studies are then evaluated in terms of system losses, DG curtailment, tap changer operation, line loadings, control settings for BTB-VSCs and the subsequent operational cost.

Table 3.1: Summary of case studies

Case Study	Tap Control	Network Reconfiguration	Power Flow Control
Base case	Yes	No	No
Conventional network reconfiguration	Yes	Yes	No
Enhanced network reconfiguration	Yes	Yes	Yes

3.4.1 ANM Framework Formulation

As stated in Chapter 2, the ANM framework in this chapter is used for day-ahead scheduling of network services and thus is a multi-period OPF problem akin to the one formulated and presented in Chapter 2. The multi-period OPF simulation in this chapter is based on an hourly time interval. The objective function used in this chapter is given in equation (3.4.1).

$$F(P_{g,m}, \xi_{b,m}) = \sum_{m \in T} \Big[\sum_{g \in G} C_n P_{g,m} + \sum_{b \in N} C_p \xi_{b,m} P_{b,m} \Big] \tag{3.4.1}$$

where, C_n and C_p are the cost coefficients corresponding to the RTP energy market and the regulation prices, respectively. In all cases, C_p is always higher than C_n to encounter financial loss on selling electricity to consumers and compensation for demand shifting action. The multi-period OPF is subject to the constraints given in equations (2.5.12) – (2.5.13) taking into account tap changer controls, RCSs, and the BTB-VSC models. The equations for incorporating the BTB-VSCs are given in the preceding sub-section and are not repeated here. Meanwhile, the radiality constraint for each period m is given by equation (3.3.1).

The ensuing problem is then solved in AIMMS using KNITRO 9.0 on a PC of 3.5 GHz and 8 GB RAM. It also has been formulated in AMPL language [201] and solved using mixed integer nonlinear programming (MINLP) algorithm developed by Roger Fletcher and Sven Lyeffer within NEOS Server [202] for validating purposes. Both KNITRO 9.0 in AIMMS and MINLP in NEOS Server are converged to the

same solution in all cases. The average computational time by KNITRO 9.0 in AIMMS is 64 seconds.

3.4.2 Normal Operation Scenario

To investigate the effects of having BTB-VSCs, the network normal operation is firstly simulated. For each case study the multi-period OPF given above is solved taking into account the load and DG forecasts given in Figure 3.6 below.

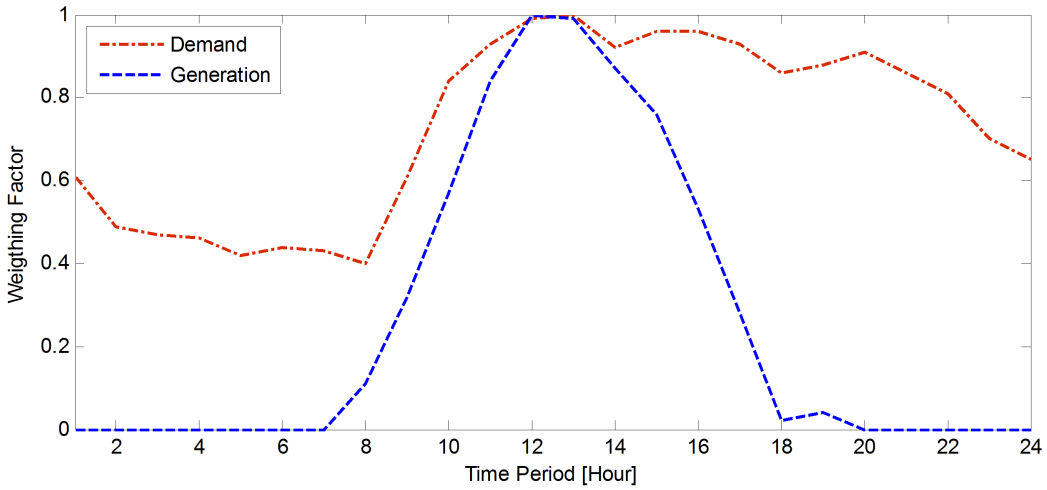

Figure 3.6: Daily demand and generation profiles

Table 3.2 summaries the network operation for the three case studies with the objective of minimising DG curtailment and power losses simultaneously as given in equation (3.4.1). The results show total energy of 43.2 kWh from renewable resources could be fully utilised when network reconfiguration is used. It is also apparent that when it comes to energy losses the BTB-VSC gives a much better performance in comparison to RCS. As a result, less dependency to the external grid could be achieved which has a potential to reduce carbon emissions from the conventional power plant. Ultimately, the enhanced network reconfiguration indicates a significant total cost reduction in terms of energy curtailment and losses up to 80.7% in the daily operation.

For discussing the results, two controlled points are selected within the test network, (i) the control point between buses 18 and 33 which operates as a normally open point, and (ii) the controlled point between buses 12 and 13 which operates

Table 3.2: Day-head Scheduling (Normal Operation)

Item	Case Study		
	Base Case	Conventional Network Reconfiguration	Enhanced Network Reconfiguration
Energy losses (kWh)	2561	1670	1086
Energy curtailed (kWh)	43.2	0	0
Total operation cost ($)	8.04	2.69	1.55
Total cost reduction	-	66.5%	80.7%

as a normally closed point within the 24-hour simulation period. The control points have RCS for conventional network reconfiguration scheme which are replaced by BTB-VSCs for implementation of enhanced network reconfiguration scheme. There are DGs connected to buses 18, 33, and 12. All DGs are modelled as solar power. Full information of the test system has been presented in Chapter 2.

Normally Open Point (buses 18-33)

In the base case, only the tap changer transformer at the grid supply point is providing any measures of active control in the system. Higher DG penetration during mid-day operation means that there is a slight rise in the voltage magnitude of bus 18 as shown in Figure 3.7a. Therefore, as seen in Table 3.2, that there should be a degree of DG curtailment in place to avoid any unnecessary voltage magnitude violations in the base case. However, when the ANM framework includes a measure of network reconfiguration – either by the use of RCSs or BTB-VSCs – it can be seen from Table 3.2 that no DG has been curtailed for the duration of the 24-hour simulation period and at the same time voltage magnitudes have been maintained within their respective boundaries.

Results clearly show that BTB-VSC are a better option to RCS where the BTB-VSC application can reduce line losses significantly by maintaining the nodal voltage at bus 18 close to its upper limit. This is made possible through reactive power injection of the VSC adjacent to bus 18. Figure 3.7b also shows the amount of shunt susceptance, B_{sw} as the control variable within the OPF, corresponding to

the required reactive power injection from the VSC connected to bus 18. It should also be noted that since the enhanced network reconfiguration maintains a radial topology, the active power flow between bus 18 and bus 33 has been suppressed through the action of the BTB-VSC. Practically, the BTB-VSC manages a zero active power flow by maintaining an identical phase angle between the VSCs and their corresponding adjacent AC nodes (i.e. buses 18 and 33).

Normally Closed Point (buses 12-13)

Since the BTB-VSC (or the RCS) between buses 12 and 13 operates as a normally closed point there can be active power exchange between the two nodes. As shown from Figure 3.8a, there is active power flow between buses 12 (sending end) and 13 (receiving end) between hours 8 and 17. This is the case for both RCS and BTB-VSCs. However, this is not the case when operating at base case since there are no active controls between 12-13 which may limit the active power exchange between these two nodes if needed. It should be noted that as apparent from Figures 3.8a and 3.8b, there is a significant difference between the active power exchange when using BTB-VSCs when compared to using RCSs. Similarly, the reactive power exchanges between the conventional network reconfiguration scheme and the enhanced network reconfiguraiton schemes differ as illustrated in Figure 3.8c and 3.8d. The reason for this observed different behaviour is that the ANM framework simply has more flexibility (i.e. degrees of freedom to move the system state variables) when using a fully controlled BTB-VSC rather than a mechanical RCS to achieve an optimum operating point. The results in Figure 3.8 therefore unequivocally showcase the superior impact of using BTB-VSCs to achieve higher levels of flexibility in the network operation. Moreover, similar to the normally open point case, the VSCs connected to buses 12 and 13 can also participate in voltage regulation by providing reactive power directly to their adjacent AC connected buses.

Furthermore, analysis on loading factors of the relevant equipment (e.g., OLTC and lines) for three case studies is carried out to highlight the benefits of using BTB-VSC and the enhanced network reconfiguration. Figure 3.9a illustrates the highest line loading in the system at each time period for all three cases. As can

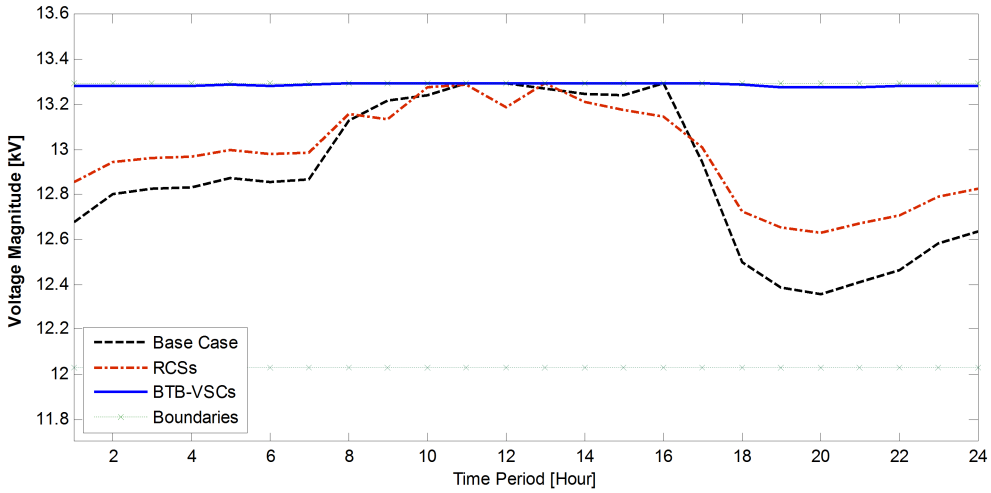

(a) Voltage magnitude at bus 18

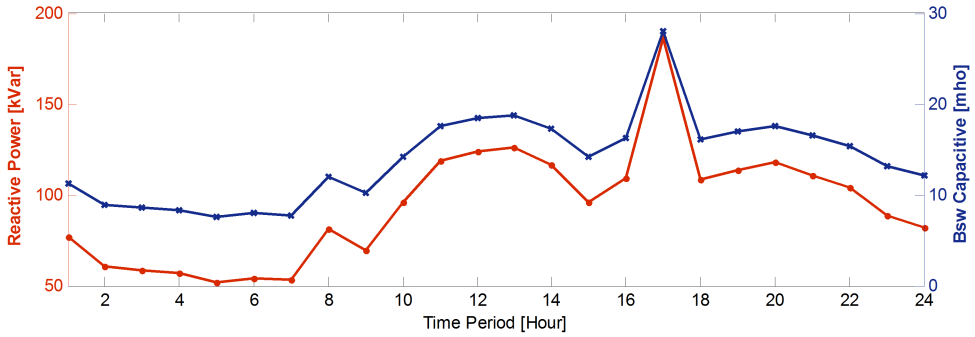

(b) Reactive power injection from the converter

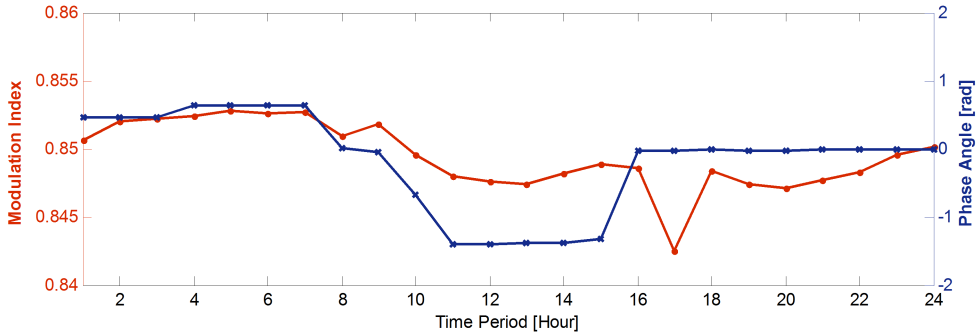

(c) The adjacent converter operation of bus 18

Figure 3.7: Normally Open Point Operation (buses 18-33)

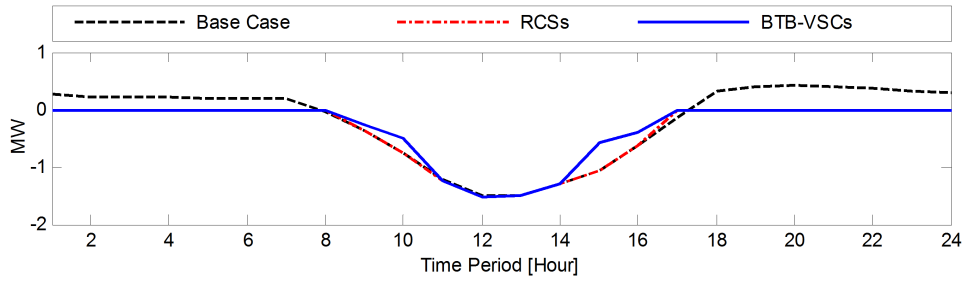

(a) Active power at sending end

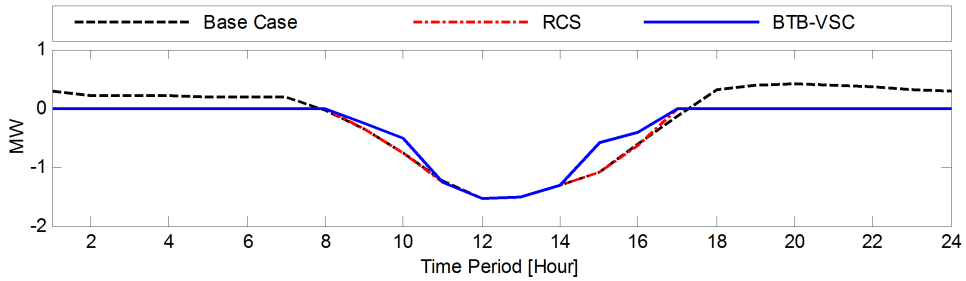

(b) Active power at receiving end

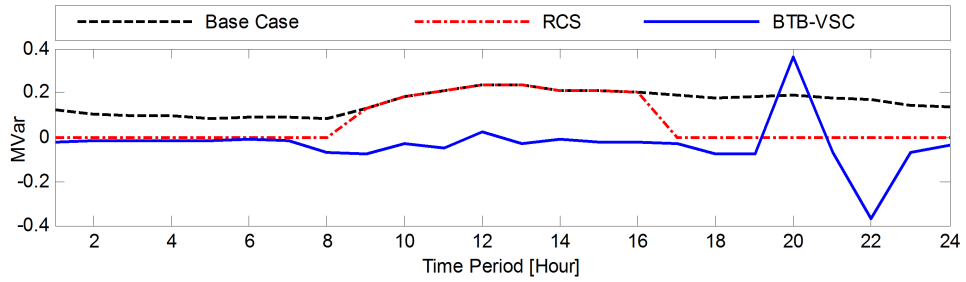

(c) Reactive power at sending end

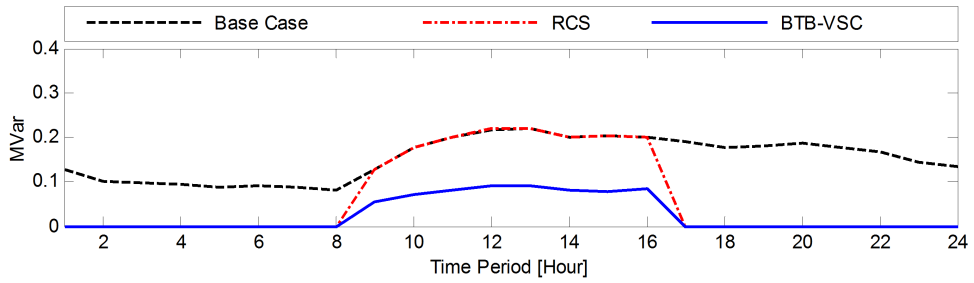

(d) Reactive power at receiving end

Figure 3.8: Normally Closed Point Operation (buses 12-13)

be observed in the figure, network reconfiguration using RCS provides almost same loading with base case except when DG output is higher than demand (hour 9 and 15). On the other hand, a significant line loading improvement can be seen at each time period when BTB-VSC is used to replace the RCS. The operation burden of OLTC transformer, indicated by changes of tap position, in daily operation is also compared between different cases as depicted in Figure 3.9b. Tap position is varying 8 steps in base case which is reduced to 5 steps using RCS and further reduced into 2 steps using BTB-VSC application. Therefore, the controllability of the BTB-VSC has a significant impact on relieving burden from the tap changer at the grid supply point. Moreover, this preliminary result suggested that the RCS has changed the status of line at least twice a day. In other words, annual operation requires at least 730 times (365 days 2 times/day) for applying conventional network reconfiguration for purposes of maintaining voltage constraints. Thus, the approach based on RCS is impractical as it will shorten the switchs lifetime due to rapid changes of the switch status in continuous operation.

3.4.3 Worst Case Scenario

In addition to the daily operation, two worst-case scenarios have also been presented, namely; a) high demand during periods of no generation, b) low demand during periods of high generation. Although the scenarios rarely occur in reality, they are worth investigating as their outcomes are potentially severe. The overall performance comparison is presented in Tables 3.3 and 3.4. It is clearly shown that the enhanced network reconfiguration could reduce burden on the OLTC operation. Referring to Table 3.3, the highest line loading is significantly improved in this case for a situation of high demand at no generation. During low demand at high generation, line loading might be violated if DG curtailment is not available in the base case. With DG curtailment of 910 kW, as shown in Table 3.4, the base case gives less line loading as compared to conventional network reconfiguration. Although higher line loading is observed using RCS, it can accommodate more power generation from the DGs. Instead, replacing RCSs with BTB-VSCs gives less line loadings at the same time DG output can be fully utilised. Furthermore, the overall system loss is

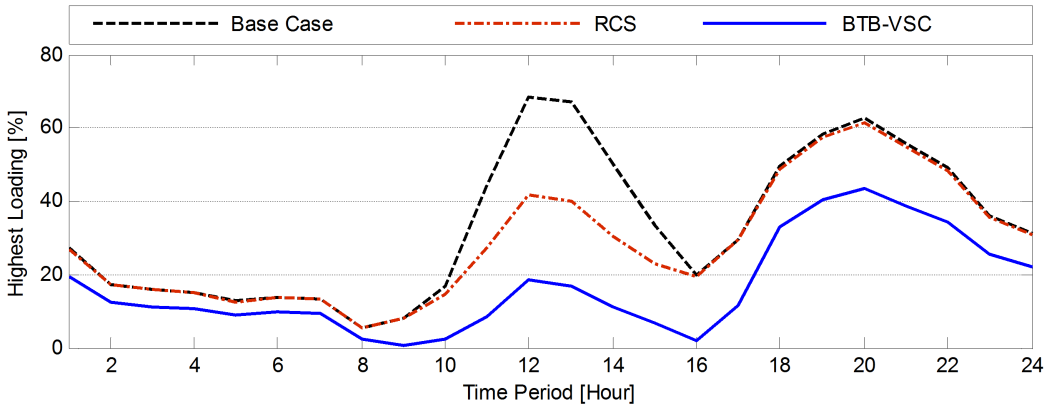

(a) The highest line loading in the network

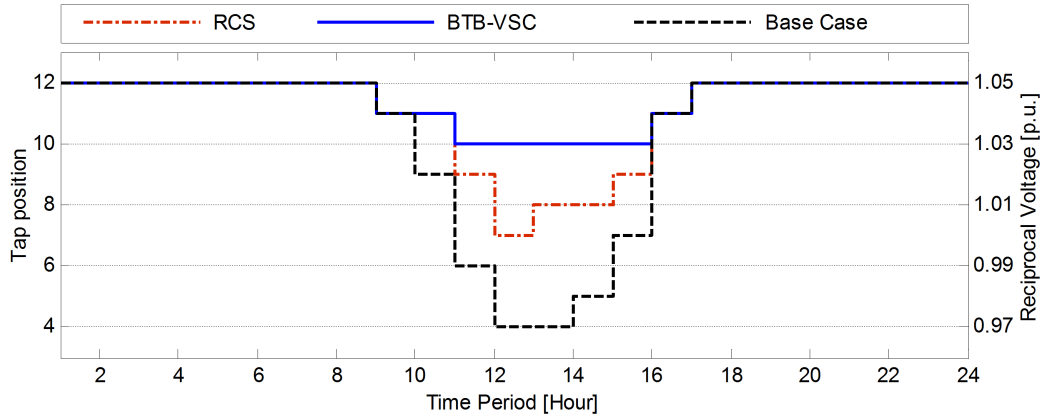

(b) Substation tap changer operation

Figure 3.9: Daily performance of line loading and tap operation

significantly improved in both scenarios when using the power controller. Moreover, the enhanced network reconfiguration introduced in this chapter also gives the best economic performance as is apparent from Tables 3.3 and 3.4.

Figure 3.10 shows an example of the BTB-VSC operation that is installed at line between buses 12 and 22 (later referred as line 35) in the two worst scenarios. For high demand and no generation case (Figure 3.10a), line 35 is decided to be deactivated where both active and reactive power flows through the line are suppressed. This can be achieved by adjusting modulation index and angle to generate phasor voltage at the inverter's terminal to match with the bus 22 as depicted in the figure. In the model, this condition can be obtained by restricting the current from flowing through the line as given by the constraint given in equation (3.3.6). Even thought,

Table 3.3: High Demand at No Generation (Worst Case Operation)

Item	Case Study		
	Base case	Conventional Network Reconfiguration	Enhanced Network Reconfiguration
Tap position	12	12	12
Highest loading	77%	75%	53%
Power loss (kW)	181	138	99
Operational cost ($)	0.58	0.28	0.17

Table 3.4: Low Demand at High Generation (Worst Case Operation)

Item	Case Study		
	Base case	Conventional Network Reconfiguration	Enhanced Network Reconfiguration
Tap position	3	4	9
Highest loading	72%	83%	71%
Power loss (kW)	306	250	222
Power curtailed (kW)	910	0	0
Operational cost ($)	23.69	0.66	0.55

there is zero reactive power injection at the converter terminal connected to bus 22, there is reactive power injection directly at bus 12 to support the nodal voltage further reducing system losses. The real and reactive power control of the two VSCs can be associated with the converters' modulation index and phase shift angles given in Figure 3.10a. For example, both converters maintain phase shift angles identical to their corresponding AC connected nodes which essentially results in zero active power exchange through the controlled line connecting bus 12 and 22. A similar argument could be said for reactive power exchange and its relationship with the converters' modulation indexes. On the other hand during low demand and high generation, as shown in Figure 3.10b, active power is now allowed in direction from bus 12 to bus 22. With negligible loss in the power controller, the entering and the leaving active powers are operated at the same amount to avoid energy from being

stored or consumed from the DC link. It can further be deduced by observing the converters operation in Figure 3.10 that both converters exert independent reactive power flow control. For example, as shown in Figure 3.10b, the reactive powers are not only operated at different amounts but also in opposite directions.

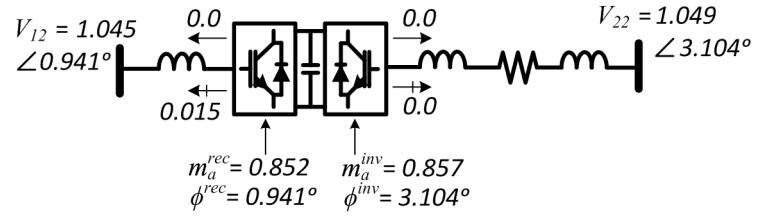

(a) High demand and no generation

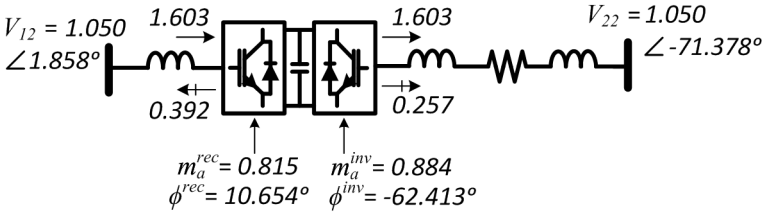

(b) Low demand and high generation

Figure 3.10: BTB-VSC operation at line 35 in worst case scenarios

3.5 Summary

This chapter illustrated the application of using voltage source converters for implementing ANM schemes. An enhanced network reconfiguration based on placement of back-to-back connections of VSCs was introduced in this chapter as a viable alternative to conventional network reconfiguration methods which use mechanical remote controlled switches (RCS). It clearly shows that the enhanced network reconfiguration can be applied to solve various problems (e.g. load balancing, and voltage regulation) in distribution networks with high levels of distributed generation resources. Use of BTB-VSCs can further be justified as it minimises the usual wear and tear associated with heavy usage of RCSs. A complete model was introduced for the voltage source converter to be incorporated in multi-period OPF formulations for a typical day-ahead scheduling ANM framework. The ANM framework was then tested on the modified IEEE 33-bus network introduced in the previous

chapter. The performance of the enhanced network reconfiguration scheme was compared to a base case and the conventional network reconfiguration scheme in terms of total operational cost to the operator (here the DSO), as well as various performance indices such as the decrease in line loadings, DG power curtailment, and total power loss in the network. In all cases, the enhanced network reconfiguration scheme fares better than the conventional approaches. The results show that using the BTB-VSCs instead of RCSs acting as both normally open and normally close switches would lead to far superior performance in terms of operational flexibility, which could ultimately reduce overall operational burden on network devices such as OLTC transformer and line operation. The results presented also show that the enhanced network reconfiguration scheme will reduce the DG curtailment and would be beneficial from an economic perspective encouraging toward more renewable DG resources at medium voltage levels.

Chapter 4

Active Network Management: Large-Scale Electricity Storage

This chapter discusses the potential for using large-scale electricity storage devices, mainly Pumped Thermal Electricity Storage (PTES), for purposes of active network management. The chapter starts with the importance of energy storage application and review on the current development in electrical storage system technologies. The discussion is continued with storage system applications in distribution networks from the previous works and a classical storage formulation is established for implementation in the ANM framework. Meanwhile, a new energy storage model for the PTES is introduced in this chapter. Based on a detailed thermodynamic model, a reduced model is developed for the PTES, which is computationally tractable for purposes of solving day-ahead optimisation problems (essentially OPF problems) for ANM purposes. The potential of using the reduced model for ANM applications is showcased in the last leg of this chapter through a series of case studies on the modified 33-bus network introduced in Chapter 2.

4.1 Energy Storage Technologies

The general concept of electric energy storage is to convert electrical energy into a form of storable energy such as mechanical, chemical or thermal. At a later time when necessary, the stored energy will be converted back into electrical en-

ergy to be utilised. Electricity storage plays an important role in active network management schemes to balance the intermittent renewable resources and power consumption from consumers. It helps reduce energy wastage by storing surplus energy during periods of high renewable generations which can be utilised at power shortage periods [203]. In general, using energy storage has many benefits, for example, it could help rise levels of renewable resource utilisation in lieu of conventional plants [204, 205], provide peak shaving mechanism by levelling between the peaks and the load curve valleys [206, 207], improve system reliability and energy stability from the additional energy reserve [100–102] and support the system operational planning and regulation [208, 209].

There are many technologies which can be classified according to the energy carriers or mediums as given in Figure 4.1. A detailed description of each type of technology will be given in the next subsections grouped into the categories given in the figure. This section only covers the most common technologies in each category which include pumped hydroelectric energy storage (PHES), compressed air energy storage (CAES), flywheel energy storage (FES), battery energy storage (BES), fuel cell, super capacitor, superconducting magnetic energy storage (SMES) and thermal energy storage. This brief discussion is mainly for the purposes of completeness and for giving an overview of the differences of these technologies and the benefits of their applications within the electric power system. The scope of the chapter, however, remains focused on the thermal energy storage category to which PTES belongs.

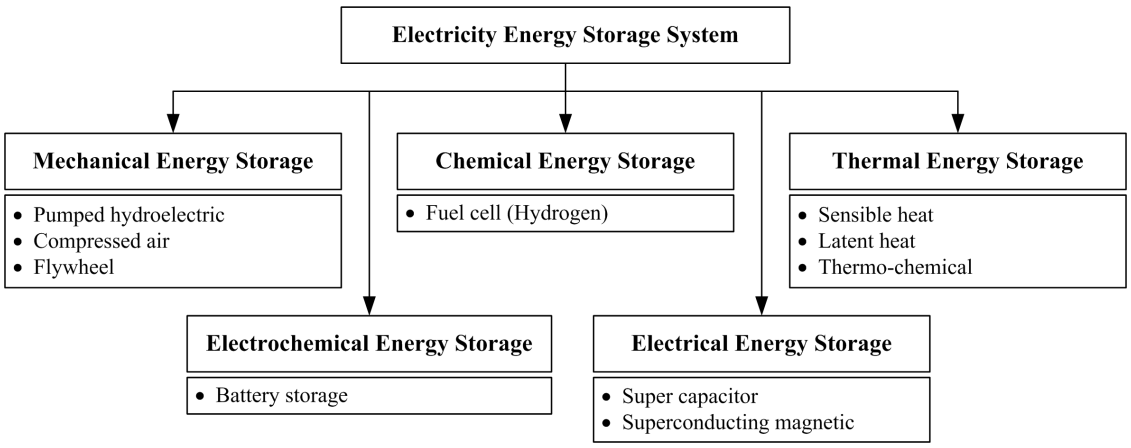

Figure 4.1: A classification of energy storage technologies

4.1.1 Mechanical Energy Storage

Pumped hydroelectric energy storage (PHES) is classified as mechanical due to the electricity energy being stored in form of gravitational potential energy. This method is considered as matured storage technology that has been widely used with an installed capacity of 127 GW worldwide [210]. A PHES system consists of two water reservoirs at different altitudes as shown in Figure 4.2. During low demand, an electrical machine is operated as motor to pump water from lower reservoir into upper reservoir which has greater potential energy. When necessary especially at high demand, the water at the upper reservoir is released to spin turbine units which drives the electrical machines to generate electricity. The storage capacity depends on the size of the reservoirs and the height difference between them whereas its power rating depends on the water flow rate and rated power of the electrical machines [211]. A typical PHES installation has a power rating from 1 MW to 3 GW, discharging its stored energy over a period of up to 10 hours, with approximately 71–85% cycle efficiency [99]. The application of PHES systems mainly involve energy management for load shifting, frequency control and supply reserve. However, PHES has long construction time and high capital investment due to geographical constraints that require adequate close land areas at appropriate elevation.

Another type of large-scale mechanical storage is a compressed air energy storage (CAES) where it can provide power more than 100 MW. Figure 4.3 illustrates a schematic diagram of CAES system. During the periods of excess energy, the electricity is used to drive a reversible electrical machine to run compressors for injecting ambient air to be stored under pressure in either an underground reservoir (large-scale) or aboveground tanks (small-scale) [4]. The underground reservoirs that can be used for the storage include hard rock caverns, salt caverns, depleted gas fields and aquifer. The pressurised air is then released as needed and heated in expansion turbine to drive the electrical machine that works as generator to produce electricity. With the pressurised air supply, CAES is capable of producing three times more electricity than a conventional gas turbine system. In order to improve CAES's cycle efficiency, the exhaust heat energy from the expansion turbine

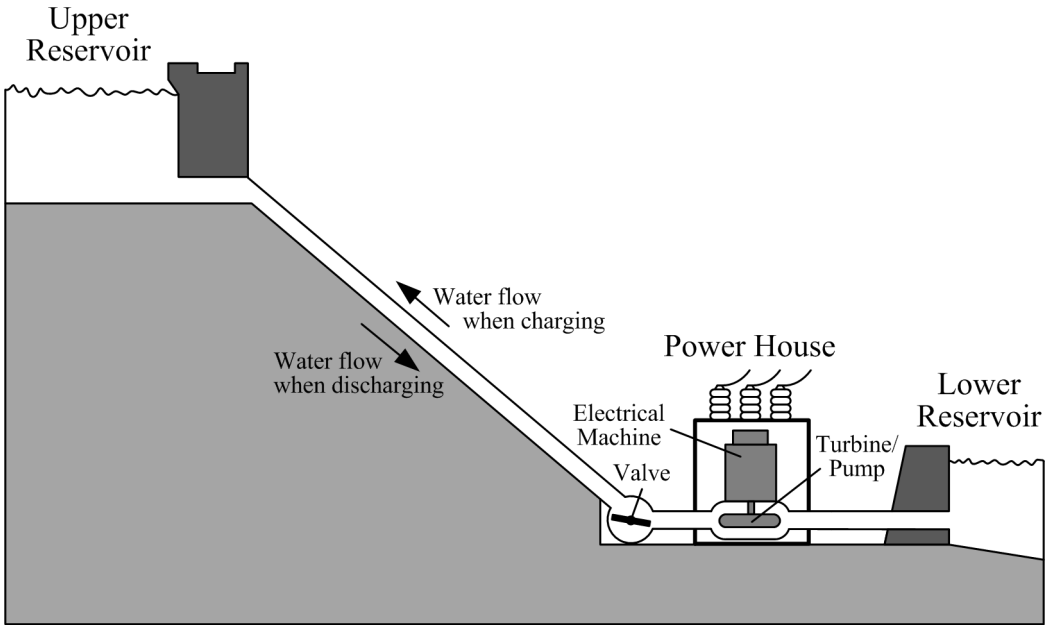

Figure 4.2: A layout of power hydroelectric energy storage

during generation process can be reused by a recuperator unit to capture the heat and deliver it to the combustion chambers. In general, the CAES system has a cycle efficiency of 70% with an expected lifetime of about 40 years [212]. The first CAES plant, the Huntorf power plant, was installed in 1978 to provide black-start power to nuclear units, back-up to local power systems and extra electrical power to fill the gap between the electricity generation and demand [213].

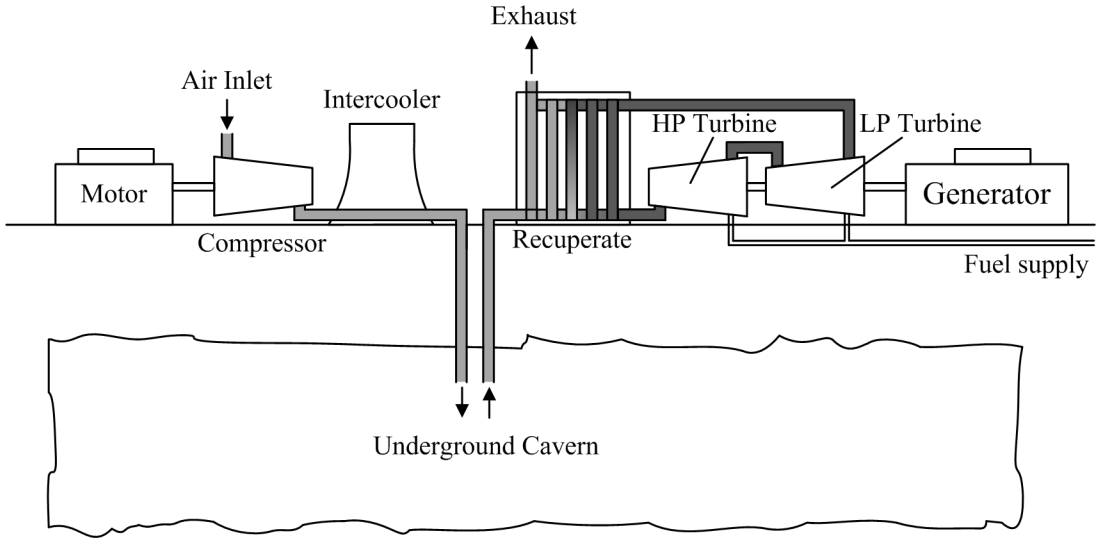

Figure 4.3: A schematic diagram of compressed air plant [4]

The large-scale CAES plants in grid applications can be used for load shifting, peak shaving and voltage control. In the previous works [214, 215], CAES is applied to smooth the intermittent power of wind energy. Similar to PHES, the process of identifying appropriate geographical locations to install the large-scale CAES plants will decide the main capital investment cost. Furthermore, low round trip efficiency as compared to other technologies is another barrier for the CAES implementation. To address the issue of efficiency, a new development of Advanced Adiabatic CAES (AA-CAES) is introduced via integration with a renewable source. The renewable power is used to help during the expansion mode so that carbon emission could be avoided. An international consortium headed by the German energy company RWE is currently working on the development of AA-CAES plant (which is called ADELE) with capacity of 360 MWh in Saxony-Anhalt, Germany [216]. The ADELE plant will be powered by wind energy for the compression process. Garrison and Webber [217] present a new configuration of wind and solar power to be integrated with AA-CAES system in order to achieve more steady power output. In this configuration, the compressed air is heated by concentrating solar thermal power instead of using fossil fuels.

Flywheel energy storage (FES) comprises of composite flywheel coupled with a reversible motor/generator unit and magnetic bearings inside a vacuum chamber to reduce friction in the system as given in Figure 4.4. Flywheels store electrical energy in the form of rotational kinetic energy. As an energy storage device, FES works in two common operating modes; charging and discharging. The FES system in charging mode is consuming the electrical energy by a motor to accelerate the flywheel (rotating mass) and stores energy in the flywheel's rotation. During the discharging mode, the rotational kinetic energy stored in the flywheel can be transferred via coupled shaft to rotate a generator that decelerates the rotation speed to produce the electrical energy. The reversible unit can be operated in both motor and generator operation where it acts as a motor during the charging mode while a generator during the discharging mode. Storage applications based on FES are suitable for grid applications due to their low maintenance cost, long life cycle, wide range of operating temperature, high efficiency and being environment friendly [218, 219].

However, the FES system is only suitable for short-term operation due to friction in the system. The friction causes reduction in the operation efficiency after long runs. For instance, the efficiency can drop roughly 7% after 5 hours and up to 40% after one day running in idle state [220].

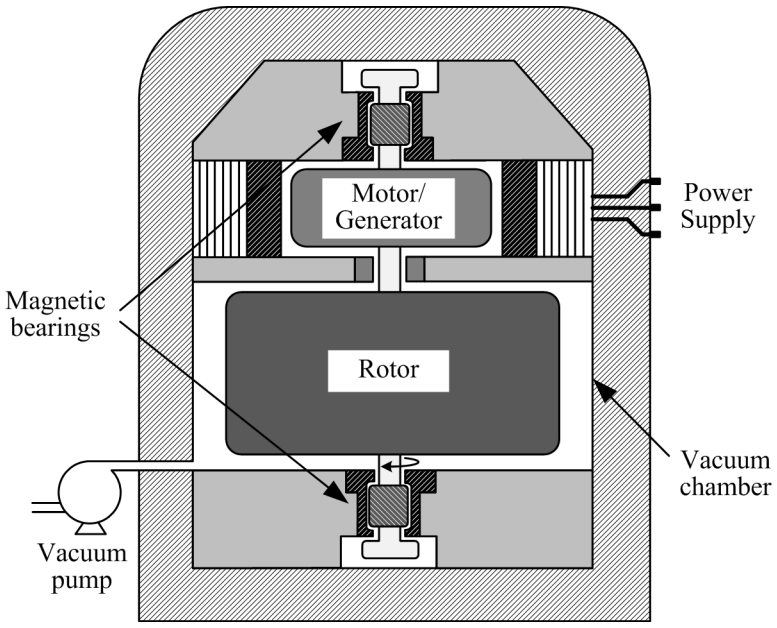

Figure 4.4: A conceptual structure of flywheel system [208]

4.1.2 Electrochemical Energy Storage

One of the most widespread storage technologies is the rechargeable battery that stores the electricity as chemical energy [221]. Figure 4.5 shows a typical schematic diagram of battery energy storage (BES) to explain its working principle. The BES system consists of multiple electrochemical cells connected in series and/or parallel in which each cell is constructed from two electrodes (anode and cathode) and an electrolyte. The electrolyte can be solid, liquid or viscous substance that separates the two electrodes and allows ions to migrate and complete the electrochemical reactions at the electrodes. The electrochemical cell can convert energy in a reversible process between electrical and chemical energy. When electrical force is applied across the terminals of the cell during charging as shown in the figure, positive charged ions (called cations) are attracted to the cathode to receive electrons while negative charged ions (called anions) are oxidised by releasing electrons at the an-

ode to form a combination of reversible chemical reactants. The reverse reactions happen to the chemical reactants during discharging where electrons are provided at the anodes and are collected at the cathode to create potential different between the terminals of the external circuit. The developed potential or voltage across the terminals depends on the electrochemical reactions between the chemical reactants and the electrodes.

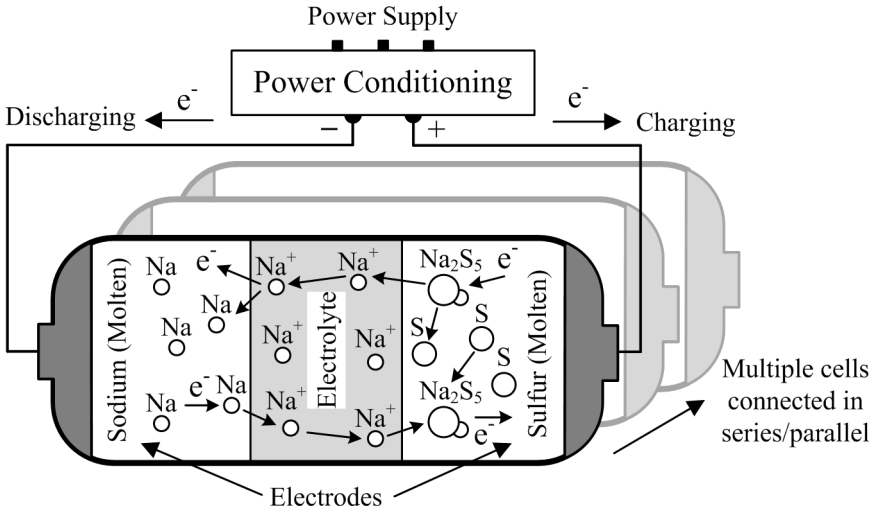

Figure 4.5: An example of battery storage operation

The BES technologies are built in different sizes with capacity ranging from less than 100 W to several megawatts. Their round trip efficiency is in the range of 60–90% depending on the operational cycle and the electro-chemistry type [222]. The BES can be used for different power system applications, such as power quality, energy management, ride-through power and transportation systems [223, 224]. Their application is not limited to power systems but also covers other sectors such as automotive (i.e, electric vehicles), marine and submarine missions, aerospace, portable electronic systems and wireless network systems. There are many different types of BES which include sodium sulphur battery, sodium nickel chloride battery, vanadium redox battery, iron chromium battery, zinc bromine battery, zinc air battery, lead acid battery, lithium ion battery, nickel cadmium battery, etc. In terms of installation, the BES systems take a relatively short time construction period and are not restricted to certain physical or geographical constraints. However, the main implementation barriers for this technology are relatively low life cycle

and high maintenance costs [222]. Furthermore, the storage capacity of many BES types cannot be fully utilised due to the depth-of-discharge limitation considered as one of the most critical degradation factors. Moreover, batteries cannot be disposed of or recycled in a straight forward manner. The toxic chemicals within the battery are essentially detrimental to the environment.

4.1.3 Chemical Energy Storage

A chemical energy storage technology covers the conversion process to produce chemical compounds which can be used to generate electricity when needed. There are several chemical compounds which are currently being considered for energy storage applications including hydrogen, methane, hydrocarbons, methanol, butanol and ethanol. Hydrogen is typically one of the most commonly used compounds for energy storage applications [218]. The hydrogen can be produced from water through an electrolysis process and stored either as compressed gas, liquefied gas, metal hydrides or carbon nano-structures [225]. A hydrogen energy storage (HES) uses fuel cell to convert hydrogen back into electricity. A complete cycle of the two separate processes for storing energy and electricity generation in the HES system is illustrated in Figure 4.6. The electricity generation using fuel cells has low noise, less pollution, and is more efficient than fossil fuel combustion engines when used for transportation [226]. Moreover, the HES systems offer flexible size for hydrogen production, storage and consumption (generate electricity) which independence to each other. However, the considerably high energy losses in each process create the major drawback to the HES system implementation. For instance, the hydrogen production through electrolysis process could currently achieve 60–75% efficiency, about 5–12% efficiency loss for storing and transporting the hydrogen and the fuel cell process to product electricity from hydrogen has efficiency up to 44% [227, 228]. Consequently, the round trip efficiency of the HES system is roughly at 30%.

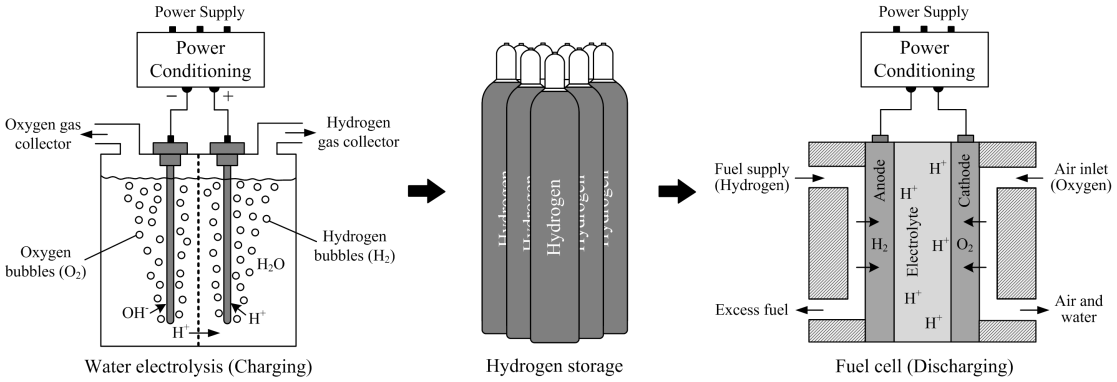

Figure 4.6: The processes in hydrogen energy storage

4.1.4 Electrical Energy Storage

A super-capacitor energy storage (SCES), also known as double-layer capacitor or ultra-capacitor, is composed of two electrodes separated by electrolyte and a porous membrane separator as shown in Figure 4.7. The energy is stored in the form of static electric field on the surfaces between the electrolyte and the two conductor electrodes [229]. Applying voltage to the SCES during charging creates two layers of charge (called electrical double-layers); one layer is developed from positive charged ions (cations) in the electrolyte which are attracted to the negative electrode and the other layer from opposite charged ions (anions) at the positive electrode. The developing layer's thickness which is known as Helmholtz plane at each electrode creates the potential difference. Unlike BES, there is no transfer of electrons at the electrodes where the layers are uniquely formed due to the electrostatic forces. When energy is consumed during discharging, the super-capacitor acts like current source in which the developed voltage drops at constant current linearly to reducing thickness of the Helmholtz plane. Since there is no chemical change involved, the charging and discharging of the SCES system could be done at very long times with high cycle efficiency about 84–95% [230]. However, the SCES system is not suitable for long term application due to high self-discharge rate which can be up to 40% energy losses in one day [99]. Furthermore, high capital cost would limit the installation capacity of the SCES system [229].

A superconducting magnetic energy storage (SMES) is another technology under the same type that uses magnetic field to store energy. The magnetic field is

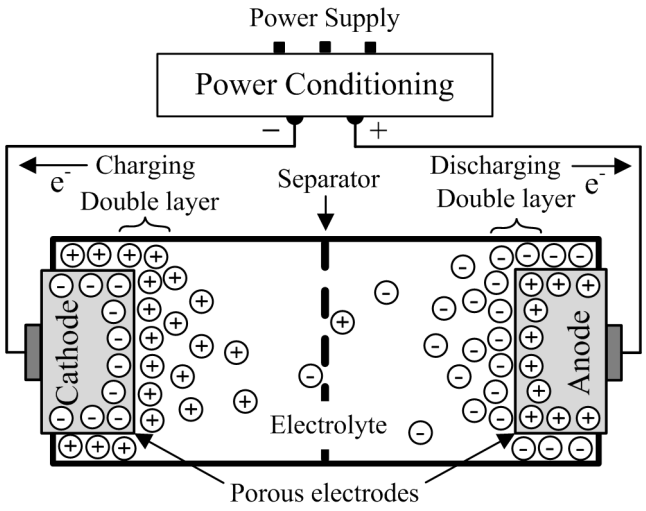

Figure 4.7: A super-capacitor energy storage system [212]

generated by DC current flow in a coil made of superconducting cables which has been cryogenic-ally cooled to a temperature below its superconducting critical temperature of 4.2 K [231]. A typical SMES system as shown in Figure 4.8 consists of three main parts; superconducting coil, power conditioning system and cryogenically cooled refrigerator [99]. The power conditioning system is used to transform AC into DC current during charging and convert back into AC when discharging. The DC current flowing through a coil develops magnetic field as well as dissipates heat due to resistance in the cables. If the cable is made of superconductor material, it can achieve superconducting state (no resistance) normally at very low temperature by the application of refrigerator unit. At this state, the electric energy can be stored in the magnetic field at almost no loss. The developed magnetic field can be released during discharging to induce electricity. The advantages of SMES system include very high overall efficiency (95-98%) [230], long lifetime (more than 20 years), rapid response time (in millisecond) level) and relatively high power density (up to 4 kW/L) [99]. On the contrary, the implementation of SMES system requires high investment cost and its operation causes negative environmental impact due to the strong magnetic field [232]. Moreover, a relatively high daily self-discharge rate makes it suitable only for short-term application such as smoothing the intermittent resources output [233].

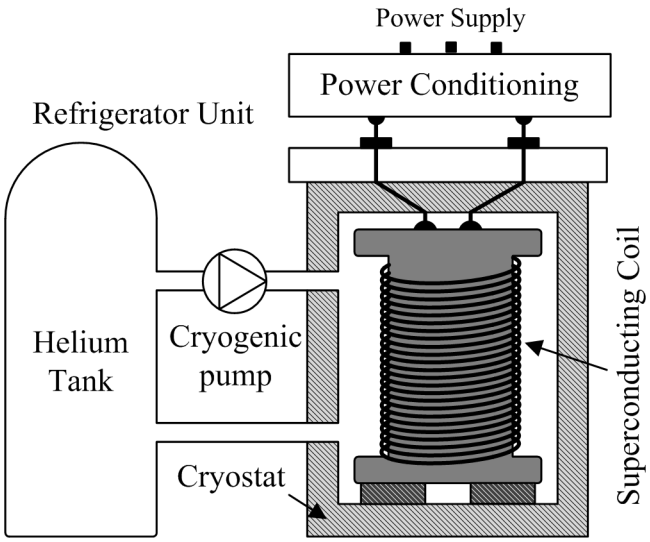

Figure 4.8: A schematic diagram of SMES system [208]

4.1.5 Thermal Energy Storage

A thermal energy storage (TES) is used to store electricity or other waste heat resources to be collected in form of thermal energy for later use to meet energy need. The TES systems can be categorised into three main storage methods that include: 1) sensible heating process through variations of temperature in storage material, 2) latent heating process that involves phase transition in the storage material known as phase change material (PCM), and 3) thermo-chemical reaction process that causes breaking or reforming in molecular bonds of the storage material after thermal energy absorbed or released, respectively [234, 235]. The TES system application has many benefits such as large scale storage capacity, less environmental effects, small daily self-discharge rate, high energy density and is economically viable with relatively low capital investment cost [99,220]. The TES performance characteristics are highly dependent on the type of the process used (as outlined above). It is therefore essential to understand the differences of each process in more detail.

A sensible heat storage system is the most utilised and matured form of working TES system. Sensible heat storage relies on the storage of heat in a solid or liquid with no change of phase or chemical reactions taking place [236]. Due to their low density, gases are not generally used for sensible heat storage. Materials used include water, rock, concrete, granite, molten salts, heat transfer oils, earth, etc.

Figure 4.9 illustrates an example of sensible heat storage system using a packed bed of rocks enclosed within insulated walls. This system requires a working fluid which can be liquid or gas to transport heat from source and transfer into the storage materials (i.e., rocks). During charging, heat is transferred from a hot working fluid when passing through the rocks causes temperature increase gradually in the storage medium. During discharging, heat is extracted to a cold working fluid when passing through the hot rocks in counterflow direction resulting in temperature reduction. The main advantage of sensible heat energy storage is low capital investment cost. However, the system losses are often increased significantly at high energy density. This issue can be tolerated through repetitive charging and discharging cycle which is most unlikely to have high energy density condition.

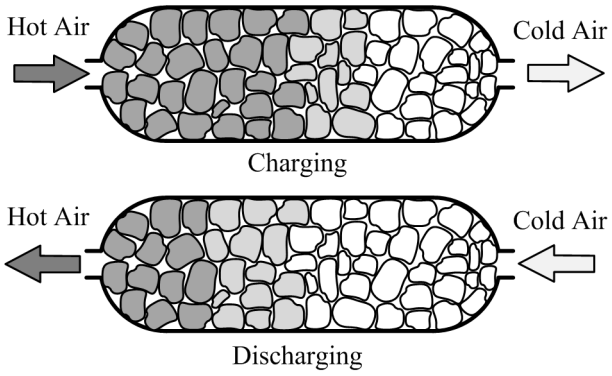

Figure 4.9: A concept of sensible heat storage

A latent heat storage system is stored heat by changing the phase of storage material in various ways either solidliquid, liquidgas or solidgas. The amount of heat stored in the storage material is proportional to the material mass, the fraction of material that undergoes the phase change and the material heat of fusion [234]. The material fusion into gas phase is associated with high volume effects which creates containment problems. For that reason, the solid-liquid type of materials have been widely used as their volume change is smaller. Upon storing heat in the storage material, the material begins to melt when the phase change temperature is reached and stays constant until the melting process is finished. During discharging, heat is released and solidified the storage material. Water is a simple example of latent heat storage material that operates at $0°C$ in which becomes liquid (water)

after absorbing heat and turns into solid (iced) when releasing heat. There are many other materials used in the latent heat storage system include aqueous salt solutions, paraffins, fatty acids, esters, glycols, salt hydrates and eutectic mixtures. These materials always achieve high potential for TES application than sensible heat storage material due to the high latent heat associated with the phase change.

A thermo-chemical storage system uses a reversible chemical reaction in two processes; the endothermic process where heat is consumed during charging to break down the molecular bonds between two reactants and the exothermic process where heat is released during discharging to reform the molecular bonds between the two reactants as depicted in Figure 4.10. As a result, the thermal energy is stored in form of product from the endothermic process in which the products are kept separately and mixed together when needed. The thermo-chemical TES materials have the highest energy density where it can store large quantities of heat in small volume [237]. Moreover, their storage period and transport are theoretically unlimited because there is no thermal loss during storage as the endothermic products can be stored at ambient temperature [212]. Some example of thermochemical TES material currently been investigated include metallic hydrides (MgH_2 and CaH_2), carbonates ($PbCO_3$ and $CaCO_3$), hydroxides ($Mg(OH)_2$ and $Ca(OH)_2$), oxides ($BaO2$ and CO_3O_4), ammonia system (NH_4HSO_4 and $NH3$) and organic systems (CH_4/H_2O, CH_4/CO_2, C_6H_{12}).

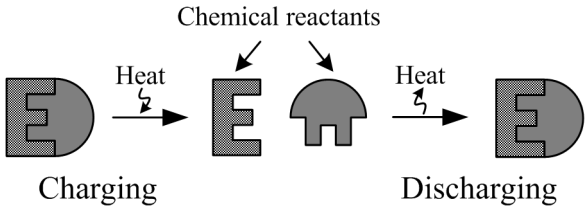

Figure 4.10: A process of thermo-chemical storage

There are many active research projects on TES applications currently developing in worldwide. A 20 MW commercial power plant using sensible heat storage called "Gemasolar Thermosolar Plant", is being built in Spain by Torresol Energy Investment in which uses molten salt as the storage medium to store thermal energy from a concentrating solar radiation [238]. A latent heat TES using an ice-based

cooling system for office building application was built in Beijing which can reduce peak electric energy consumption of 6100 kWh per month [239]. In bigger applications, the ice-based TES system with total capacity of 11,500 tons of chilled water is being built within a new central energy plant at the main campus of Nova Southeastern University (NSU) in South Florida. This project aims to improve the overall consumption of the campus by better managing the power consumption using the TES storage application. In particular focus on power system application for electrical storage, a pilot 2.5 MWh liquid air energy storage (LAES) plant, which is part of latent heat storage type, is developed by Highview Power Storage with a demonstration plant in Slough, UK [240]. The LAES system requires external heat source or in contact with thermal loads (i.e., air conditioning or refrigeration) in vaporisation to generate electricity. In more heat conservative system to reduce energy losses, a UK based company, Isentropic Ltd, has introduced a concept to store electrical energy by exploiting the high energy density of sensible heat contained in crushed and graded minerals which is called pumped thermal electricity storage (PTES) [203]. The PTES will be the focus of the remainder of this chapter.

4.2 ANM Framework: Classical Storage vs Realistic Models

There are many different storage technologies discussed in the previous section that are suitable for power system applications. With regards to the focus of this work, only storage applications in power distribution networks will be reviewed. The discussion here mainly is intended to understand how the energy storage can be applied and formulated within a day-ahead ANM framework similar to what was discussed in previous two chapters. The basic premise of the models presented in this chapter is a comparison between a widely used classical Energy Storage System (ESS) model and a more technology-specific PTES model which are both used within a day-ahead ANM framework. The classical ESS model is essentially invariant to the type of the technology used whilst adhering to the basic principles of energy storage operation whereas the PTES model is a direct adoption of the PTES realistic

operational characteristics, taken from the operational simulations of a complex thermodynamic model. The PTES model therefore is not necessarily in agreement with the operational characteristics generalisation of the classical ESS model. Before detailing the specifics of the two models, including their formulation within the ANM framework, a brief review of energy storage models used in literature for purposes of operational planning in power distribution systems is presented below.

4.2.1 Energy Storage in Power Distribution Systems: Computational Modelling Aspects

The electricity energy storage is considered as the catalyst for undergoing transition in the distribution system operation towards an active paradigm. This can be seen from increasing number of publications in the recent years that particularly focus on storage applications in the active distribution system. The studies can be categorised into short-term operational planning [26,61,62,90,98,241,242]and long-term expansion planning [91,243,244].

An application of battery storage in distribution networks with wind generation for short-term operational planning is studied in [61]. In the study, both active and reactive power flows in the power distribution system are optimised taking into account the capability of power flow control from the battery storage units. Each battery storage is equipped with power conditioning system (PCS) unit that can be employed to control active and reactive power injections into the power distribution. The controllability of active and reactive is also investigated in [62] for the context of micro-grids. A dynamic programming approach is suggested in this study to address numerical difficulties of gradient method in obtaining global solution especially when dealing with time-domain problems as such in the storage operation. In this case, active power is computed from the storage state using the dynamic programming based on backward recursive method and then, reactive power is calculated from the traditional power flow solver (i.e., Gauss-Seidel, Newton-Raphson, etc.) by assuming the storage unit as a P-V source that operates at constant voltage. The recursive process in the storage unit leads to more numerical complexity in power flow calculation especially when considering a number of storage devices. In [98], a

large distribution network with DGs and storage units are divided into several small regions and control actions are taken locally within the regions. In this situation, the storage unit is used to manage the energy in each region where the import/export are calculated from the total power generation/consumption including the storage operation (either charge or discharge). Then, the maximum power can be injected and received are evaluated for each region to establish its power regulating ranges. The overall optimal network operation can be determined using the power regulating ranges such that smaller number of variables will be computed in the general optimisation framework. Carr et. al [90] also emphasised that the network analysis becomes more difficult with the application of distributed storage (i.e., more than one unit) especially when considering its operational constraints. In their study, the analysis is conducted with unconstrained energy storage capacity to assess both centralised and distributed storage topologies in allowing more energy can be absorbed from wind-based generations. The study indicates both energy rating and power rating for distributed storage are generally larger than centralised storage that would reduce the levelised production cost. Although computational burden could be eased through relaxation in [90, 98], the storage operation is less dependent on network conditions and more on pre-defined external factors (i.e., prices) and inappropriate capacity limits. In [26], a dynamic optimal power flow (DOPF) similar to [62] is introduced to link the inter-temporal variables in storage with the overall power network operation. Instead of one variable for storage operating power, charge and discharging operations are treated as two separate variables in [26]. When storage efficiency is less than 1, it is most likely only one variable active at a time to achieve optimal operation where additional losses in the process could be avoided. Using almost the same storage model, Rahbar et al. [241] proposed a 'sliding-window' optimisation approach to manage energy storage operation in real-time. In addition, the study also investigated the effects of prediction error on the storage scheduling when considering the uncertainty factors in load and renewable resources. Other possible active devices that operate in discrete manner such as on-load tap changers, switch-able capacitor banks and voltage regulators are also included together with energy storage for active management schemes in [242]. A binary variable, that

works in similar fashion to other variables, is used to decide the storage operating state (i.e., charging or discharging).

Active network management schemes should also be considered in problems relating to distribution network expansion planning (i.e., long-term). For example, Xing et al. [243] introduced the concept of active distribution network expansion planning (ADNEP) that includes not only network management schemes but also the uncertainties from DGs and load during operation. Energy storage is considered as part of the active schemes in the study that can be deployed to reduce operation cost through the peak shaving mechanism. Since this is expansion planning framework, the installation of energy storage will be determined together with other elements such as DG installation, new lines, load buses and substations. On the other hand, Sedghi et al. [91] carried out analysis on the long-term planning for battery storage allocation in distribution grid taking into account the uncertainties of loads and wind generations. There is a special constraint applied to energy storage in this study where it only allows the battery unit to charge and discharge once in each day to reduce the replacement cost because of its lifetime limitations. The constraint is fulfilled via a condition that permits the battery to discharge only after it reached full charged and discharging power is regulated until state of charge goes to minimum allowed level towards end of the cycle. In the more recent study, Shen et al. [244] suggested to include both long-term investment and short-term operation in the ADNEP strategy. Similarly to [243], the long-term expansion planning covers the energy storage units installation and the network infrastructures reinforcement(lines and buses) for enhancing short-term daily operation strategies. The storage construction at two different options either centralised or distributed are investigated in [244] in terms of power reliability enhancement and peak load shifting. The study shows the centralised storage installation gives lower cost in terms of construction and operation but higher cost in general considering high potential of cables replacement and system losses.

Regardless the operational time-frame in the studies (either short-term or long-term), none of them looking into the effects of storage's efficiency at different stored energy levels and rather using a fixed round-trip efficiency which is called classical

model. Some discrepancies should be expected from the classical model when considering more realistic efficiency. A PTES system is adopted in this work since it has not been found in the literature for the active distribution network application. In order to appropriately model the PTES, a short-term operational planning analysis is taken as main references because it is more coherent with the ANM framework introduced in the previous chapter. The technique used to formulate storage model in [26,61,62,90,98,241,242] can be adopted to develop a new PTES model. However, an ancillary service from the reactive power support in [61, 62] would be inferior to the main storage function for energy management. Therefore, storage system is assumed to operate at unity power factor. A part from that, the storage constraints relaxation in [90, 98] will further hinder to represent a realistic storage operational capability. To address this issue, pre-defined constraints such as storage capacity and operational active power rating are used in this chapter as discussed in Section 4.3.2. Besides that, [26, 241, 242] treat the storage charging and discharging operations using two separate variables. This could cause both charging and discharging occur at the same time. To avoid such condition, an additional decision variable is imposed to the storage model then causes more non-convexity in the optimisation problem. Accordingly, a classical storage model based on the reviewed publication is represented in the following section that will be used as reference to reduce a complex thermodynamic PTES model into computationally tractable model for the purpose of solving optimal storage scheduling problem in the ANM framework.

4.2.2 Classical ESS Model Formulation

In this section, the so-called classical ESS model formulation is introduced. The classical model can be represented as a bi-directional device as shown in Figure 4.11. As shown in the figure, the energy storage has two operating states namely, motor mode (charging) or generator mode (discharging). There are two specific ways of representing this classical model in the literature by either using two separate variables for motoring (charging) and generating (discharging) models [26,61,98,241, 242,244] or combining them into one single variable [62,90,91,243,245]. In this study, one variable is used for the operating power of the ESS to ensure the storage system

does not operate in both states simultaneously. Consequently, a single variable of storage operating power is defined based on the generator convention where positive power represents discharging whereas negative power is for charging mode. The single variable ESS model is shown mathematically by the below expressions:

$$P_e^{min} \leq P_e(t) \leq P_e^{max} \tag{4.2.1}$$

$$P_e(t) = \begin{cases} P_{chr}(t) & \text{if } P_e(t) < 0 \\ P_{dis}(t) & \text{otherwise} \end{cases} \tag{4.2.2}$$

where, P^{min} and P^{max} are maximum discharging and charging rate, respectively.

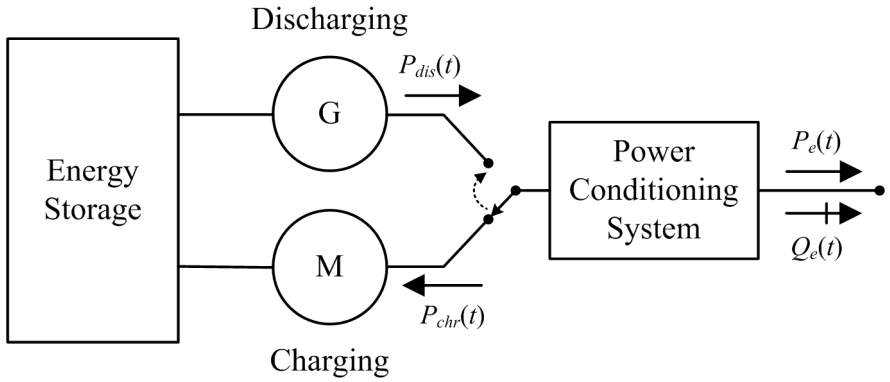

Figure 4.11: The classical ESS Model

An ESS is normally integrated to power distribution system through a PCS unit which allows active and reactive power injections control. The power injections, however, are limited to the device power rating, S_{rate}. It is important to consider the conversion losses in the storage unit which can be measured as system efficiency. With that in mind, the injected power during discharging into power grid is less than the actual discharging power from the storage. On the other hand, the consumed power during charging would be higher than the actual charging power but its operation is limited by the constraint in (4.2.1). Thus, the active and reactive power injections should obey the following constraints:

$$(\eta P_e(t))^2 + Q_e(t)^2 \leq S_e^{rate} \tag{4.2.3}$$

$$\eta = \begin{cases} \eta_c & \text{if } P_e(t) < 0 \\ 1/\eta_d & \text{otherwise} \end{cases} \tag{4.2.4}$$

where, η_c and η_d are discharging and charging efficiencies, respectively. The reactive power is not controlled through a source of reactive energy (i.e. a capacitor or inductor) but by purely electronic processing of the PCS unit and therefore does not contribute to the energy storage level in the storage device. In this way, the PCS can be thought of as a static synchronous voltage source (SVS), which by controlling its output voltage relative to the system voltage can be used to provide reactive power to the system or absorb reactive power from the system. This process is analogous to controlling internal excitation voltage in a rotating synchronous generator whilst in over-excited mode (i.e. internal excitation voltage magnitude is higher than system voltage magnitude) provides reactive power (or injects lagging current to the system) and whilst in under-excited model (i.e. internal excitation voltage magnitude is lower than system voltage magnitude) absorbs reactive power (or injects leading current to the system).

Although reactive power can be utilised to support the distribution system, the storage system in this study is assumed to operate at unity power factor especially to highlight its role in managing real power in the network. This condition is already explained in the ANM framework where all DGs are not allowed to inject or absorb reactive power in the system as mentioned in Chapter 2. Therefore, the ESS operating power can be simplified as $P_e^{min} \leq P_e(t) \leq \eta_d P_e^{max}$ by taking into consideration its overall power rating when defining the P^{min} and P^{max}. Apart from that, power losses during standby mode known as self-depleting rate, α (unit: percentage per hour) is another factor which impacts the energy level in the storage unit. The changes of energy level in the ESS unit usually measured in terms of the unit's state of charge (SoC) can be expressed as follows:

$$SoC_e(t+1) = SoC_e(t) - \alpha SoC_e(t)\tau - \frac{\eta P_e(t)\tau}{E_{max}} \tag{4.2.5}$$

$$\eta = \begin{cases} \eta_c & \text{if } P_e(t) < 0 \\ 1/\eta_d & \text{otherwise} \end{cases} \tag{4.2.6}$$

where, τ is the time interval of the operation in hour and E_{max} is a maximum amount of energy that can be stored in the unit and usually measured in kWh.

The SoC of the ESS unit, however, is restricted by its maximum capacity and

operational limits. Therefore, the net energy entering and leaving the storage system including energy losses during the process of charging and discharging must be balanced or equal to zero. This can achieved by ensuring that the SoC at start time, t_0 is equal to the SoC at final time, t_n for a specific operational time scale. These constraints can be expressed as the following:

$$SoC_{min} \leq SoC_e(t) \leq SoC_{max} \tag{4.2.7}$$

$$SoC(t_0) = SoC(t_n) \tag{4.2.8}$$

4.3 PTES: Reduced Model Development

As shown in the preceding section, the classical ESS model is essentially characterised by a constant round trip efficiency. In actuality, the efficiency however depends on many factors that could vary at different operating conditions. Too simple a storage model using fixed efficiency as presented in the ESS model previously might overestimate (or underestimate) the actual behaviour of the storage system. In this section, the process for developing a realistic model for the PTES is outlined. The salient point of this model is in its ability to reflect the realistic operational characteristics of the PTES whilst still be computationally tractable for integrating into the ANM framework. A comparison is then drawn between representing PTES as a classical ESS model or using the realistic PTES representation for ANM purposes. This section, first, outlines the process with which a reduced (computationally tractable) model for the PTES was developed from a detailed thermodynamic model. The detailed thermodynamic model is provided by researchers from the University of Cambridge as part of the EPSRC-funded research project called Pumped Thermal Electricity Storage (PTES). The reduced PTES model is then integrated within an ANM framework akin to the one used in previous chapter for short-term operational planning of the 33-bus network.

4.3.1 Application of PTES system

The battery energy storage (BES) is typically used in most of the works for distribution grid applications mainly because of its installation flexibility regardless

the geographical location. However, the BES is currently not economically viable for large-scale applications [246]. On the other hand, the use of large-scale energy storage systems such as PHES and CAES is severely limited by the geographical constraints (as described earlier) which make them unsuitable for integration to most MV networks. Thermal energy storage (TES) is a potential alternative to both the electrochemical and mechanical storages as it does not have the geographical limitations and has low capital cost per kWh at a very long life cycle [247]. There are few different storage methods in TES which have already been discussed in the Subsection 4.1.5 but this work mainly focuses on the sensible heat storage system. Many different materials can be used in the sensible heat TES system, such as water, molten salts and concrete. A PTES employs packed beds filled with pebbles and consequently exhibits lower environmental damage than batteries which contain toxic chemicals [63].

Figure 4.12 illustrates the PTES layout to give a fundamental understanding of its working principle. The PTES stores energy as sensible heat and cold in two thermal reservoirs as shown in the figure. The principle is to consume electricity from the grid by an electric machine that works as a motor to drive the two compression-expansion devices (CE and EC) during charging to pump heat from the cold reservoir to the hot reservoir. In this process, a hot thermal front propagates through high temperature of the pebbles in hot reservoir and simultaneously, a cold thermal front through low temperature of the pebbles in cold reservoir. The discharging process is then using the difference in temperature between the hot and cold reservoirs to operate the two reciprocal compression-expansion devices as heat engine that rotates the electric machine to work as generator and generates electricity back to the network. During the process, a working fluid (e.g., Argon) acts as heat carrier flowing in reverse direction to the charging process in order to release heat from hot to cold reservoir. This causes a warm front to diffuse in the cold reservoir and a cool front through the hot reservoir.

The detailed model of PTES system has been discussed in [64, 65] that studies the sensitivity of system efficiency to the various loss factors based on a hypothetical storage capacity and demonstrates rather complex influence of the numerous design

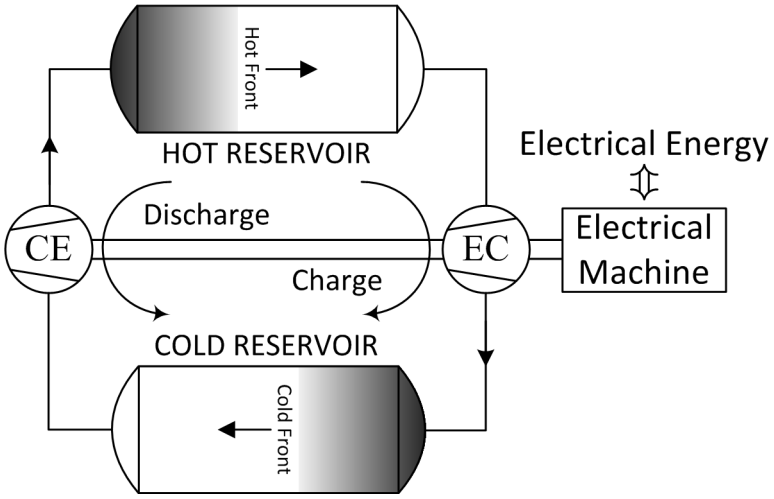

Figure 4.12: PTES working principle

variables. A number of physical processes act to reduce the PTES efficiency as described in [65]. For instance, frictional effects cause pressure losses in valves, pipes, and along the reservoirs. Conduction and heat transfer across a finite temperature difference are thermodynamically irreversible, and these effects are particularly significant in the reservoirs. Together these losses determine the temperature distribution along the reservoirs. The temperature distribution can consequently be seen to influence both the efficiency and the SoC. The model, however, is rather too detailed for integration within a day-ahead ANM framework which requires solving a non-linear optimisation problem (i.e. the OPF in this case) successively. The complexity of the model will mean it will become intractable as the size of the system (thus the ensuing problem) increases. Therefore, a reduced (tractable) PTES model need be developed which captures the operational characteristics of the real PTES (i.e. the variability in efficiency) yet be simple enough to be integrated successfully within the ANM framework as outlined in Chapter 2.

4.3.2 Development of Reduced PTES Model

The PTES efficiency depends on a number of factors, such as the operating power (charge and discharge), the SoC and temperature distributions. Furthermore, in thermal storage systems it is possible for the same SoC to be achieved with different temperature distributions in the reservoir. If the system is charged and discharged

with regular cycles, the system converges to a steady-state operation whereby the temperature distributions are the same from one cycle to the next. However, steady-state operation cannot be achieved with the irregular load cycles that may occur when PTES is operating part of a network. As a result, the temperature distributions can change significantly, and the SoC and efficiency of the current cycle are therefore affected by the historical operation of the system. In this work, the operating cycles do not differ significantly from one another, and this dependency on the history of operation is not particularly obvious. Therefore, it is possible to simplify the PTES characteristics using regression techniques based on the SoC and efficiency. The SoC can be calculated from the amount of useful energy that can be converted back into electricity relative to the temperature distribution in the reservoirs.

The useful energy stored within a storage system is influenced by the charge efficiency, discharge efficiency and self-discharge as given by (4.2.5). For a large-scale thermal storage systems with high insulation, the self-discharge rate is relatively small ($\approx 0.05 - 1\%$) [99, 220] and can be neglected. Therefore, the energy stored in a storage unit can be mainly determined by the operating power (either charging or discharging) as given in (4.3.1). According to the linear relationship between energy deviation and operating power, the charging and discharging efficiencies of the storage system can be derived using linear regression. Consequently, and through an iterative process depicted in Figure 4.13, a functional relationship can be drawn between the charge and discharge efficiencies of the PTES and its state of charge. This functional relationship is essentially the reduced PTES model and it still reflects the variability in the efficiency (as a function of its state of charge) captured by the detailed thermodynamic model. The detailed thermodynamic model is developed by collaborators from the University of Cambridge based on work in [65]. The PTES efficiency is modelled using linear regression by basically running the detailed thermodynamic model under a variety of operating conditions and recording the resultant operating profiles and calculating point efficiencies for each operating profile (see the process below). Once the reduced model is prepared, it is integrated within a simple optimal scheduling problem and is run. The ensuing optimum op-

erating cycles for the PTES obtained from the optimal scheduling problem is then validated by comparing the same operating cycles as run in the detailed model. This is described in more detail in the following sections.

$$\triangle E = -\eta P_e(t)\tau \tag{4.3.1}$$

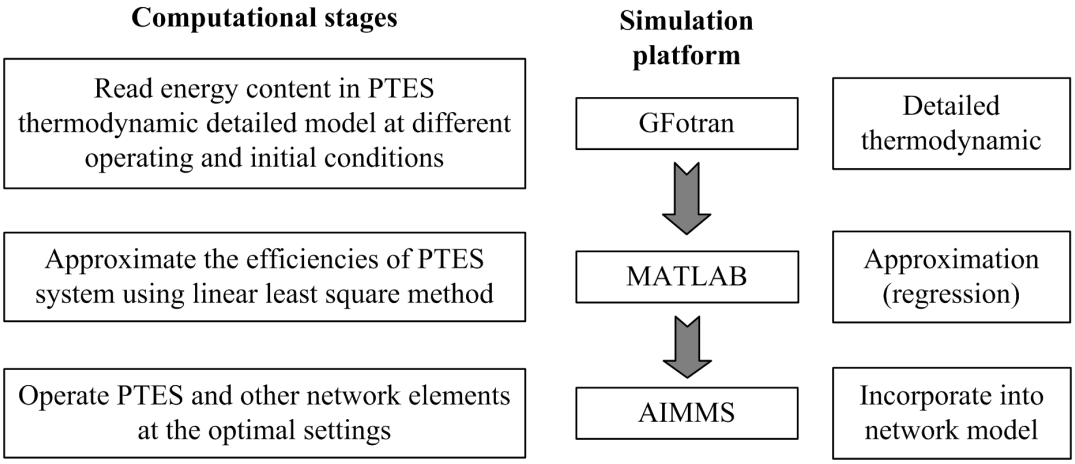

Figure 4.13: A process to simplify PTES for network application

Below, the detailed process of establishing the reduced PTES model is outlined. This process however is not limited to using the detailed PTES model for obtaining realistic operational profiles, rather it can also be used in conjunction of operating an actual PTES installation. For the purposes of this work and since there are no commercially available PTES test plants yet, a hypothetical 4.5 MWh PTES system at the maximum power rating of 1.25 MW has been considered in the detailed PTES thermodynamic model. The procedure is described in detail by the following steps and applied to create the reduced model of 4.5 MWh PTES system [248]:

1. Set an initial condition (state of charge) in the storage. This process depends on the historical charging and discharging cycles. Since historical data is not available, the state of charge is set by charging at a given power (e.g., 625 kW) for a certain period (starting with 100 minutes)

2. Charge at a given power (e.g., 125 kW) for 10 minutes

3. Calculate the quantity of energy that was stored in this time and the input energy (kWh). The ratio between these numbers is the charging efficiency for this power rating and initial state of charge.

4. Repeat steps 2 to 3 with different power ratings (e.g., using intervals of 125 kW)

5. Plot the stored energy against the input energy for each of these power ratings. Apply regression using linear least squares method and trust-region fitting algorithm to obtain the average efficiency for this initial state of charge. The regression technique will be discussed more details in the following subsection

6. Repeat steps 1 to 5 with different initial conditions (e.g., using longer charging period at intervals of 10 minutes)

7. Plot the efficiencies against the state of charge for each of these initial conditions. Apply linear regression based on least absolute residuals approach to derive a polynomial expression of the efficiency in a function of the initial state of charge

8. Repeat steps 1 to 7 for the discharging cycle

4.3.3 Parametric Regression Technique

The parametric regression technique is applied in this work to establish a parametric model of PTES system through a process of finding unknown parameters that describe the relationship between a dependent variables and independent variables (i.e., efficiency and operating power) from a given data. The data normally contains uncertainty component that can be represented as error due to many factors. However, systematic error could happen when the parametric model does not treat well all the input data. Therefore, a linear least square method is used to minimise the error and give the best fit to the data. The least square method is carried out in this work by using the regression function found in MATLAB's curve fitting toolbox [249]. In general, a linear regression of polynomial equation can be modelled in

the following expression:

$$\hat{y}_i = \sum_{k=0}^{K} \beta_k X_{ik} \tag{4.3.2}$$

where,

$\hat{y}_i$ An estimate value at observation i

X_{ik} A value of the k-th predictor function (e.g., x, x^2) at observation i

β_k A coefficient of the k-th predictor function

Assuming y_i are the observed values, the summed square of orthogonal errors (or residuals) is given by:

$$S = \sum_{i=1}^{n} (y_i - \hat{y}_i)^2 = \sum_{i=1}^{n} (y_i - \beta_k X_{ik})^2 \tag{4.3.3}$$

The minimum value of the function (so called the least square) can be obtained when the gradients of the function with respect to each unknown parameter ($\partial S/\partial \beta$) are equal to zero. Thus, the following partial derivatives should be fulfilled in order to get the least square solution:

$$\frac{\partial S}{\partial \beta_k} = 2 \sum_{i=1}^{n} (y_i - \sum_{j=1}^{m} \hat{\beta}_k X_{ij})(-X_{ik}) = 0 \qquad \forall k \tag{4.3.4}$$

The expression can be re-arranged into the normal equations and represented in matrix notation as in the following expressions, respectively:

$$\sum_{i=1}^{n} \sum_{j=1}^{m} \hat{\beta}_k X_{ij} X_{ik} = \sum_{i=1}^{n} X_{ik} y_i \qquad \forall k \tag{4.3.5}$$

$$\hat{\boldsymbol{\beta}} (\boldsymbol{X}^T \boldsymbol{X}) = \boldsymbol{X}^T \boldsymbol{y} \tag{4.3.6}$$

where, $\boldsymbol{X}^T$ is the transpose of the matrix $\boldsymbol{X}$. The solution is a vector $\hat{\boldsymbol{\beta}}$ which estimates the unknown coefficients, β_k as given by,

$$\hat{\boldsymbol{\beta}} = (\boldsymbol{X}^T \boldsymbol{X})^{-1} \boldsymbol{X}^T \boldsymbol{y} \tag{4.3.7}$$

In a process to determine charging and discharging efficiencies, the fitted model must intercept at the origin in order to make it similar form as expression in (4.3.1). Furthermore, the efficiency never goes beyond 100% or below zero. Therefore, the

model can be ensured is a good representation of the original system by applying the trust-region fitting algorithm. This algorithm is available in the Matlab toolbox that can be applied by specifying appropriate constraints for the respective coefficients. The trust-region is normally applied to solve difficult non-linear problems through an iterative procedure. This procedure approximates the nearest point (also known as trial step) and solution is updated if the square error reduces or otherwise, the current point remains unchanged [250]. Since the problem is linear, the unknown coefficients can be determined directly using (4.3.7). In this case, the trust-region finds the nearest settings within the feasible region.

The least squares fitting method is very sensitive to outliers in the data due to squaring error calculation as in (4.3.3) that magnifies the influence of these extreme points [249]. This issue becomes obvious in a higher order of polynomial fitting model especially to approximate the relationship between efficiency and state of charge as described in the previous section. In order to fit data using polynomials, an appropriate degree of the polynomial equation must be defined before the fitting is carried out. The resulting extrapolation gives odd curve shape when inappropriate order (too high or low) is used as shown in Figure 4.14. The effects can also be influenced by the squares of errors or residuals especially when using high order polynomials. The influence from the outliers can be reduced by using alternative regression approach which is called least absolute residuals (LAR). The LAR scheme finds a fitted model that minimises the summed of absolute errors instead the squared errors. As a result, the fitted model gives more balance treatment to all data.

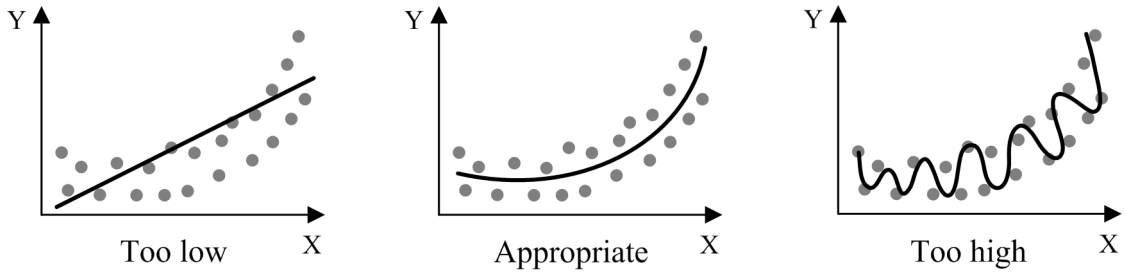

Figure 4.14: Solution at different order of polynomial models

4.3.4 Reduced PTES Model Establishment

The model development procedure to simplify the detailed PTES model as presented in Section 4.3.2 can be divided into two regression stages. In the first stage, a linear model is used to find the relationship between the changes of stored energy and charging/discharging energy. Figure 4.15 shows two examples of regression results at different initial SoCs. The average efficiency of the PTES system at various operating conditions can be determined from the gradient of the estimated line. It shows that PTES stores energy at a non-linear rate as the initial SoC increases. This trend is not as apparent when PTES is discharging. Power ratings have the greatest impact on the behaviour when the storage unit has a high SoC during charge, or a low SoC during discharge. An overall performance of the regression is indicated by sum square error (SSE), R-square and root mean square error (RMSE) for charging and discharging in average as tabulated in Table 4.1. Small average errors and high R-square values indicate that estimated efficiencies are acceptable.

Table 4.1: An overall performance of regression to estimate PTES efficiencies

Operation state	SSE	RSME	R^2
Charging	$8.17 \times 10^{-}4$	$4.07 \times 10^{-}3$	0.992
Discharging	$2.97 \times 10^{-}3$	$7.53 \times 10^{-}3$	0.997

In next stage of the reduced model development, the variations of estimated efficiencies are plotted against the initial SoC to obtain an explicit polynomial expression for the efficiency as a function of SoC. The relationships between the efficiency and SoC using the polynomial model is illustrated in Figure 4.16. In this case study, a degree of 4 has found to give the right polynomial fitting. The degree of the polynomial is determined via observation from the output curve after few trials at different degrees as described in Section 4.3.3. From this regression, the charging and discharging efficiency functions is derived as given in (4.3.8) and (4.3.9), respectively. The performance of this regressions is provided in Table 4.2. The results demonstrate that the efficiency decreases as the reservoirs become more fully charged. The temperature distribution along the reservoirs has a finite gradient

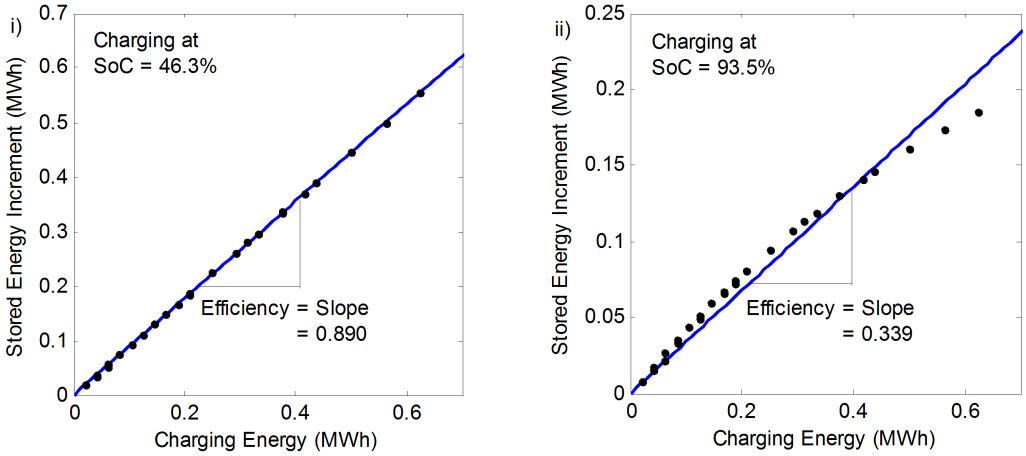

(a) Charging Efficiencies

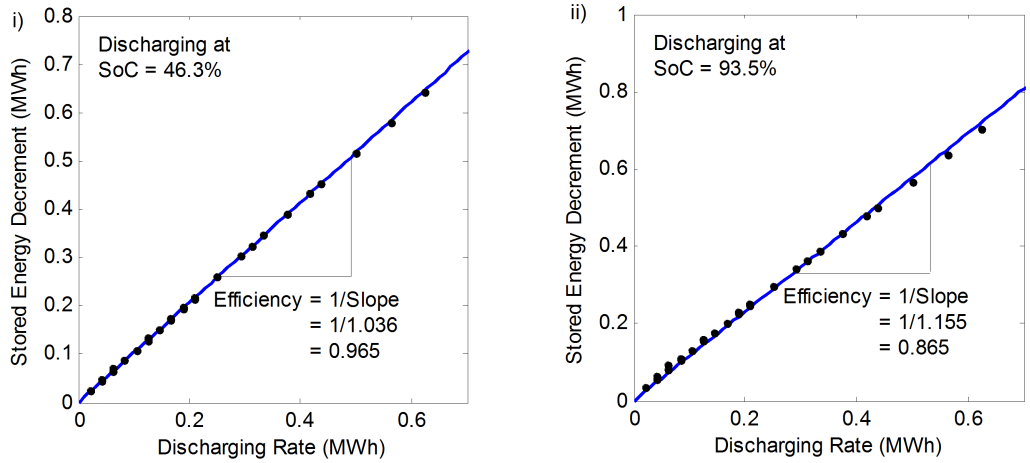

(b) Discharging Efficiencies

Figure 4.15: Regression results on the changes of stored energy against charging/discharging energy

rather than being a step-change. During charge, the hot reservoir outlet temperature increases, causing a so-called 'exit loss', and hence a reduction in efficiency.

$$\eta_c = -6.523SoC^4 + 9.946SoC^3 - 5.458SoC^2 + 1.29SoC + 0.7683 \quad (4.3.8)$$

$$\eta_d = -1.985SoC^4 + 3.4SoC^3 - 1.988SoC^2 + 0.4213SoC + 0.9503 \quad (4.3.9)$$

The reduced PTES model is validated by implementing the model for a simple optimal scheduling problem without any network constraints and with a simple market arbitrage objective (where the store sells when energy price is high and busy when it is low). The optimal power cycle is then fed into the detailed PTES

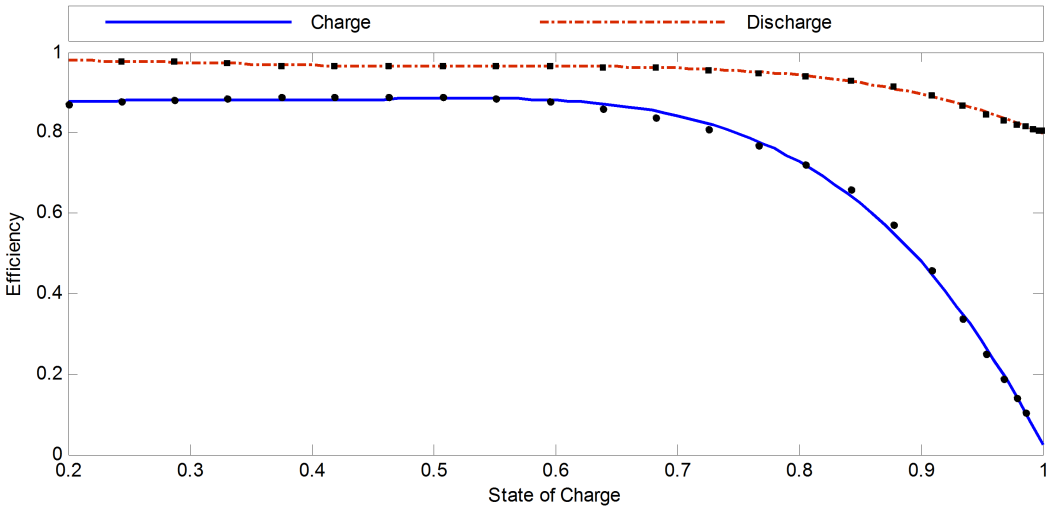

Figure 4.16: Regression results on the changes of stored energy against charging/discharging energy

Table 4.2: The performance of regression for PTES efficiencies and state of charge

Operation state	SSE	RSME	R^2
Charging	$2.18 \times 10^{-}3$	$9.96 \times 10^{-}3$	0.999
Discharging	$2.59 \times 10^{-}4$	$3.6 \times 10^{-}3$	0.998

thermodynamic model for comparison purposes. The simulation is run for twenty days due to computational limitations of the detailed model. Figure 4.17 depicts the comparison results between the reduced model and thermodynamic detailed model in terms of variations in the energy content. Based on the figure, the reduced model follows the detailed model quite closely with a small error during the idle states. The difference is mainly due to the fact that the detailed model includes the self-discharge in the reservoirs but as mentioned in Section 4.3.2, this is not included in the reduced model. The error in terms of SSE and RMSE are 0.365 and 0.0195, respectively. This indicates that the reduced PTES model is sufficient for network applications without neglecting its physical characteristics.

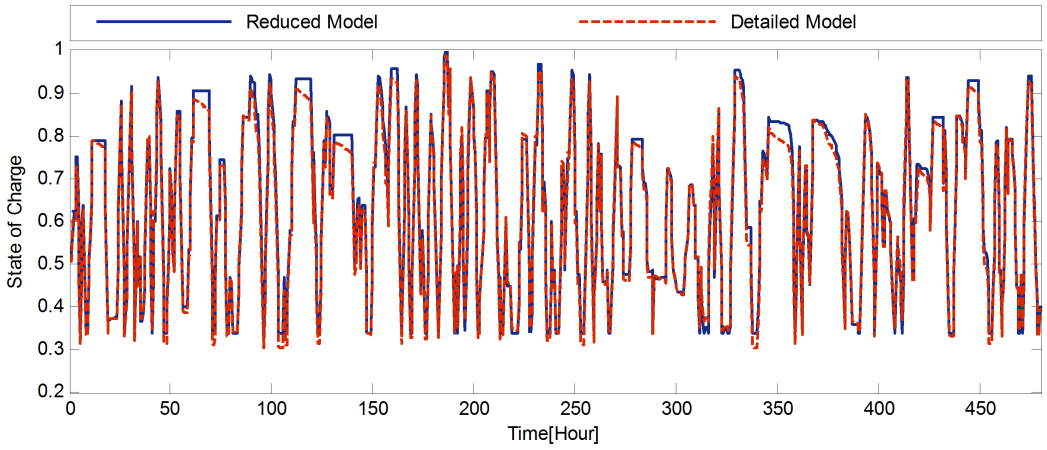

Figure 4.17: A comparison between the reduced and detailed models

4.4 Integration of PTES reduced model for Active Network Management

This section presents the application of integrating the reduced PTES model in an example distribution network for day-ahead operational planning based on the ANM framework which was described in detail in Section 2.4. In this application, the PTES is owned and managed by DNO to minimise the cost of buying electricity from the main substation or grid supply point (GSP). Accordingly, the DNO optimises all assets including storage (i.e, PTES) to achieve the target taking into account the costs of trading electricity with the grid supply, buying from DG owners, and supplying to consumer as depicted in Figure 4.18. Although power curtailment and load shifting schemes are available within the framework, only DG curtailment is considered especially to highlight the benefits of PTES for peak shaving. As mentioned earlier in this chapter, the performance of the PTES (variable efficiency) is compared to a classical representation of PTES (fixed efficiency) and comparison is drawn on their differences to highlight any drawbacks or shortcomings of the classical representation of storage systems for active network management problems.

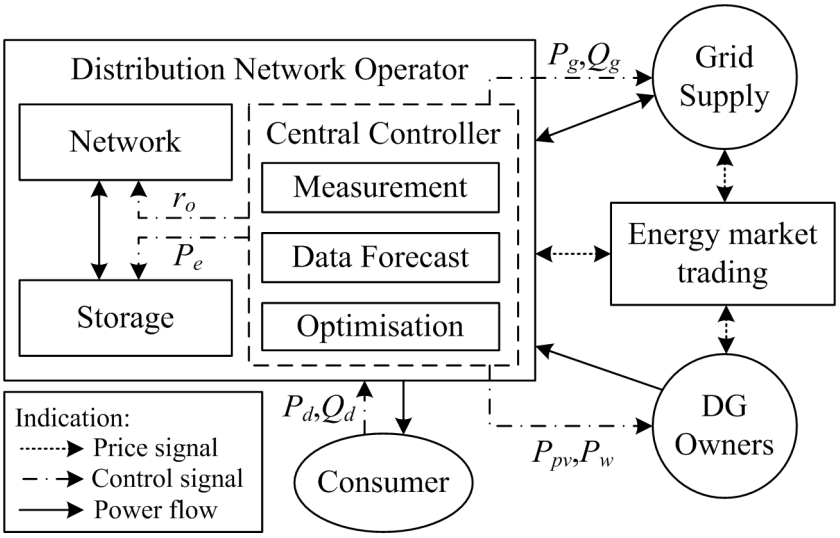

Figure 4.18: The ANM Framework including the Storage System

4.4.1 Case Study and Considerations

The reduced PTES model can be implemented in the ANM framework by including its power injections into the equality constraints of the optimal power flow formulation presented in Section 2.5. It is important to note that the unity power factor imposed to DGs should be also applied to the storage system. Therefore, only active power balance equation needs to be revised and the rest of the formulation will remain the same. In the equation, active power injection from PTES, P_e is considered as a control variable. The variable is optimised for each period, m throughout the simulation time (i.e., day-ahead) and bounded to each other via an inter-temporal variable, SoC as discussed earlier in this chapter. The additional expressions are applied to the ANM framework when considering the reduced PTES model can be

summarised as the following:

$$\sum_{g\in G} P_{g,m} + \sum_{w\in W} P_{w,m} + \sum_{pv\in PV} P_{pv,m} + \sum_{e\in E} P_{e,m} = (1-\xi_b)P_{d\{b\},m} + \sum_{l\in L} P_{j,} + \sum_{l\in L} P_{k,m} \tag{4.4.1}$$

$$SoC_{e,m+1} = SoC_{e,m} - \frac{\eta_m P_{e,m}\tau}{E_{max}} \tag{4.4.2}$$

$$\eta_m = \begin{cases} -6.523(SoC_m)^4 + 9.946(SoC_m)^3 - 5.458(SoC_m)^2 & \\ +1.29(SoC_m) + 0.7683 & \text{if } P_{e,m} < 0 \\ -1.985(SoC_m)^4 + 3.4(SoC_m)^3 - 1.988(SoC_m)^2 & \\ +0.4213(SoC_m) + 0.9503 & \text{otherwise} \end{cases} \tag{4.4.3}$$

where, τ is the period time step. It is important to note that the inequality and equality constraints as given in (4.2.1),(4.2.7)–(4.2.8) should be addressed accordingly together with these expressions.

The application is tested on the modified 33-bus benchmark test network as described in Section 2.6.2. In this study, we assume voltage limits of 0.97/1.03 p.u. (±3% of the nominal voltage) at all buses and thermal limit of lines, $S_{max} = 5$ MVA. A hypothetical 1.25 MW PTES unit at storage capacity of 4.3475 MWh is installed at bus 10. Figure 4.19 shows the time-variant of the energy market price [251], demand, wind and solar power profiles [99] in 24 hour periods with time interval of 30 minutes for the test case scenarios. Three different case studies are considered as summarised in Table 4.3. It should be noted that the fixed efficiency is referred to any storage model whose efficiency given in (4.4.3) is kept constant (i.e. the classical ESS model). The results are analysed in terms of energy losses, network operation that includes power exchange, tap ratio, storage unit operation and the total operational cost. The analysis can be divided into two different perspectives; a) power system performance: the potential improvement on network operation can be achieved through the PTES application, and b) storage system performance: the over/under-estimation of the storage operation when comparing the classical (i.e. fixed efficiency) with the reduced PTES (i.e. variable efficiency) models.

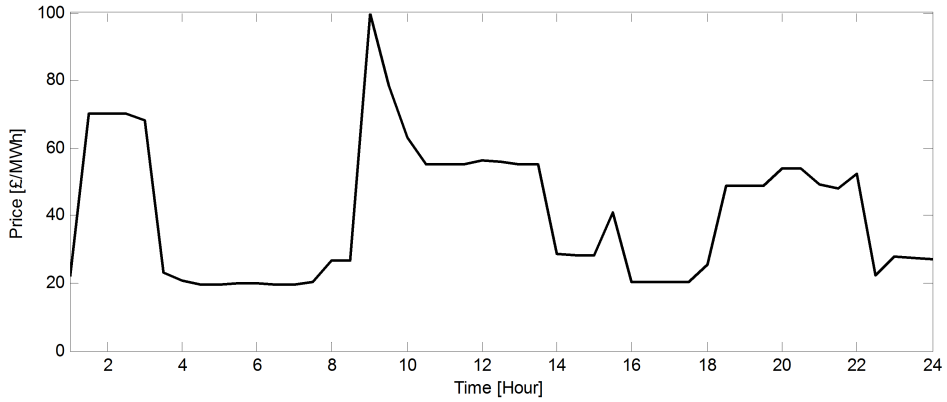

(a) Energy market price

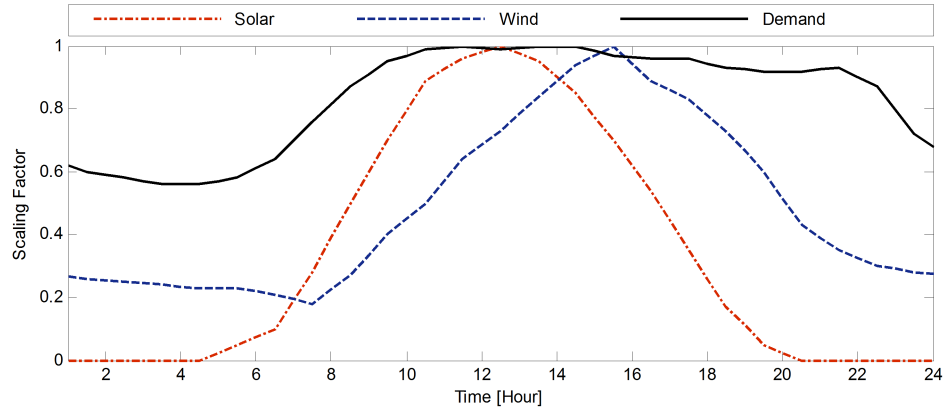

(b) DGs and demand profiles

Figure 4.19: Hourly energy market price, demand, wind and solar power profiles

Table 4.3: Test case studies for PTES application

Case Studies	Tap control	Storage control	Efficiency
No PTES system	Yes	No	N/A
Fixed Efficiency	Yes	Yes	Constant
Nonlinear Efficiency (The reduced PTES)	Yes	Yes	Non-linear

4.4.2 Power System Performance

The reduced PTES model is applied on the test network using daily profiles as described in the previous section. The performance of network operation at the three different case studies with the objective to minimise cost as given in (4.4.4) through

an arbitrage process (i.e., arbitrage is the process with which PTES buys energy from the grid when the price is low and sells back when it is high) are presented in Table 4.4. Although storage application shows higher power transfer losses and power curtailment regardless of the efficiency characteristic, it has gained more profit at lower costs from buying at low price and selling at high price. This indicates that the profit margins between high and low prices can cover the additional costs from the incurred losses when using PTES. It is also apparent that when it comes to energy losses within the storage unit, the reduced PTES model with varying efficiency gives better performance than the classical storage model with a fixed efficiency of 90% [64]. As a result, the PTES reduced model shows significant savings of more than 63% of operating costs, when compared to the network operation without PTES system and slightly higher than the fixed efficiency model (7.4% improved). The different performance of the reduced PTES model is due the non-linearity of PTES charge and discharge efficiencies (as shown in Figure 4.16) that give higher or lower efficiency depending on the operating cycles. In that case, the reduced PTES model operates at higher efficiency than average round-trip of the fixed efficiency model.

$$\sum_{m \in T} \Big[\sum_{g \in G} C_n P_{g,m} \tau \Big] \tag{4.4.4}$$

Table 4.4: Energy losses and operational cost

Case Studies	Energy Losses (MWh)			Total
	Network	Storage	Curtail	Cost ($)
No PTES system	4.522	N/A	2.225	587.39
Fixed Efficiency	5.216	3.151	2.879	228.99
Nonlinear Efficiency (The reduced PTES)	4.990	2.799	2.374	212.02

Figure 4.20 depicts a comparison of daily operation between the case study without PTES system, the classical fixed efficiency and the reduced PTES model as described in Table 4.3. Referring to the Figure 4.20a, there is minimal exchange of

power with the grid supply in the case study without PTES system, however both PTES application cases show a higher variation of power exchange due to the use of the storage device for buying energy at low price and selling at high price. The secondary voltage of substation transformer at the grid supply point is normally regulated at 1.03 p.u. as shown in Figure 4.20b. Nevertheless, high power injections from DGs have caused voltage rise at the connected terminals that lead to tap ratio decreases. At high price period during peak generation (between 8:30 and 10:30), PTES tends to discharge electricity that has been stored during lower price periods. Since PTES is located nearer to the grid supply, the discharging electricity from PTES results in voltage rise at the upstream buses. Hence, DG output (between 8:30 and 10:30) needs to be curtailed to avoid voltage rises as presented in Figure 4.20c. Instead, the surplus energy from DGs at low price periods (between 14 and 16) is absorbed and stored in the PTES to avoid curtailment. There is a significant different in DG curtailment between classical model and the reduced model at hour 12. Slightly higher price at this period as in Figure 4.19a has triggered the classical model to discharge the stored electricity. Higher power curtailment rate can be observed is mainly due to DG output at the highest generation. Unlike classical model, the reduced PTES is not scheduled to discharge at this period because the price is not significantly high as compared to the effect of efficiency drops (due to non-linear characteristic) when charging at low price periods. This effect limits the reduced PTES model to store more electricity and make it tends to not operate at hour 12. Figure 4.20 clearly shows the impact of ESS in providing a trade-off between energy price, demand and resource fluctuations for an optimum operation strategy.

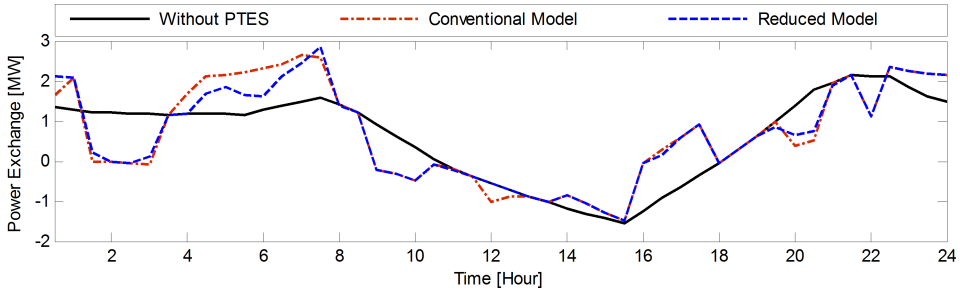

(a) Power exchange at the grid supply

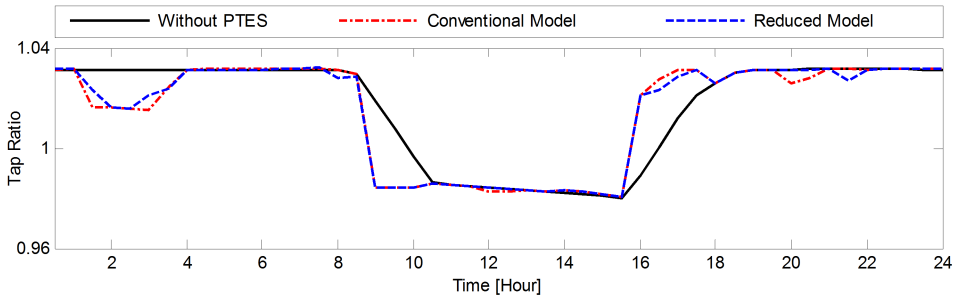

(b) Tap changer operation

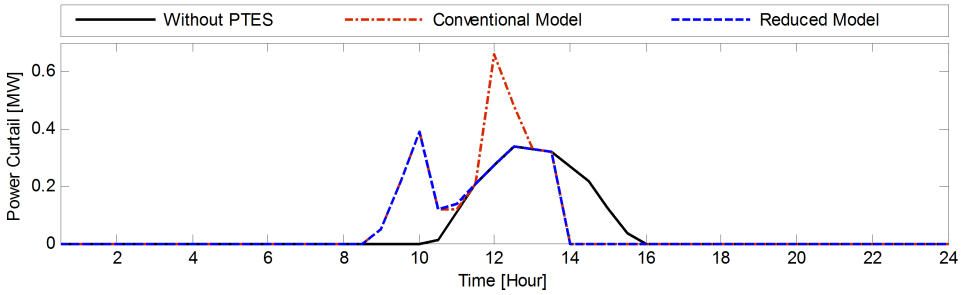

(c) Power DG curtailment

Figure 4.20: A performance comparison of daily operation

4.4.3 Storage System Performance

The daily operation of the reduced PTES model is analysed and compared to the classical fixed efficiency model as given in Figure 4.21. There are many significant differences in the operation between the classical and reduced PTES models between hours 3 to 7 and other several times at hours 12 and 21 as shown in Figure 4.21a. It is obvious that because of the non-linear efficiency characteristics, losses will increase when the reduced PTES model is fully charged. This has put a natural limit on how much PTES is charged/discharged at each point along the operation time as indicated in Figure 4.21b. In contrast, the fixed efficiency model allows the PTES

to be fully charged (SoC at 100%). In this case, the reduced PTES model maintains almost constantly a high round-trip efficiency (so operates within the normal region of the efficiency characteristic) to maintain a minimum cost solution as shown in Figure 4.21c. The exceptions would be at hour 17 where it is worth to charge at the expense of loss to reach high SoC due to low price for possible to discharge during high price in the next few hours. As a result, a dramatic loss in efficiency is observed. In overall, the PTES operating efficiency is slightly lower than the conventional model precisely due to the non-linear characteristic.

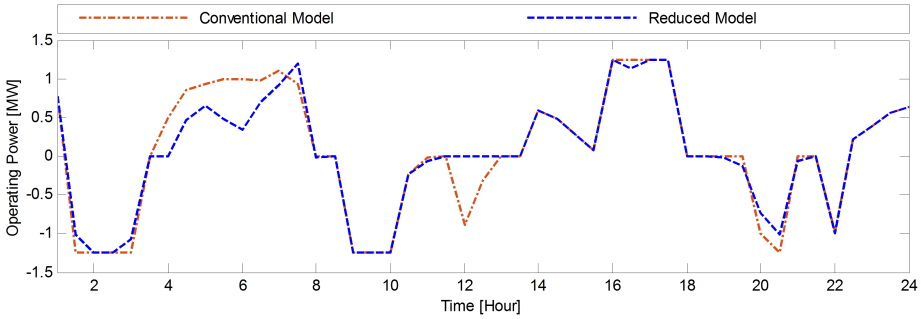

(a) Operating power

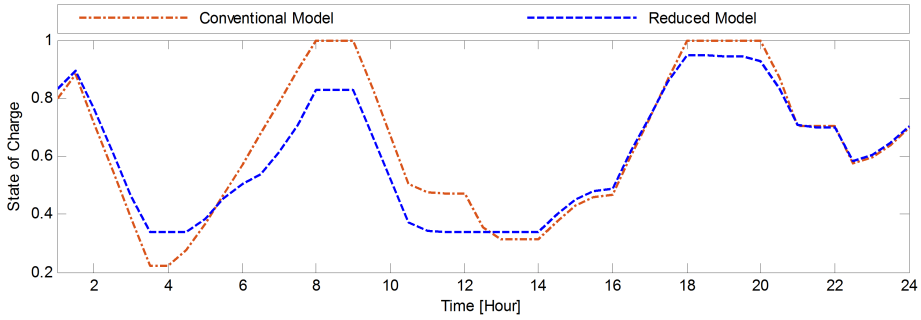

(b) State of charge

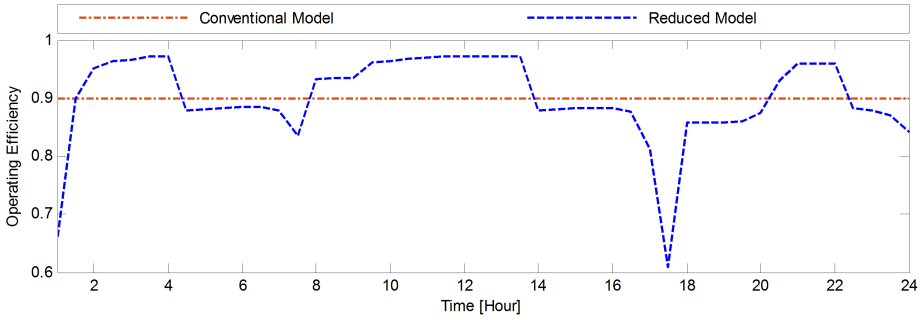

(c) Operating efficiency

Figure 4.21: A comparison between conventional and reduced PTES models

4.5 Summary

There are many different types of storage technologies applied in medium distribution networks but PTES has been found to be a good alternative for energy management in the ANM framework. This chapter introduces a method for developing a reduced (computationally tractable) model for a new thermal storage system called PTES which is computationally tractable to be included in day-ahead operational planning problem formulations for active network management purposes. The reduced PTES model as it was called in this chapter, still reflects the realistic operational characteristics of an actual PTES (i.e. its efficiency is a function of its state of charge reflecting the realistic loss process that exists in an actual PTES). The reduced PTES model is derived using two-stage regression technique; 1) linear regression to obtain efficiency at any operating power, and 2) polynomial regression to attain the variable efficiency as a function of SoC. The reduced PTES model is evaluated to show that it operates according to the PTES thermodynamic detailed model with a minute error due to the inclusion of reservoir self-discharge in the detailed model. This indicates the PTES can successfully be represented into a simplified form suitable for the power system operational planning studies. The reduced PTES model is applied on the modified 33-bus test network to showcase the operation performance in the ANM framework as compared to the conventional (classical) model based on fixed efficiency. From the network perspective, the reduced PTES model operates at slightly different points with better performance than the fixed 90% efficiency model. It will not fully charge as the efficiency drops at higher levels of SoC due to the non-linearity behaviour of the PTES efficiency. In conclusion, the PTES reduced model has provided a better representation of PTES characteristics that would be beneficial for accurate assessments of large-scale thermal storage integration and operational planning in medium voltage distribution networks application. Meanwhile, the methodology developed here can equally be extended to realistically representing any other type of large-scale storage device for purposes of operational planning within medium voltage networks.

Chapter 5

Security-Constrained Operational Planning for Distribution Systems

In this chapter, a security-constrained operational planning approach is introduced as an extension to the day-ahead ANM framework for future flexible distribution systems. To this end, the ANM framework introduced in Chapter 2 – Section 2.4 – and then extended in Chapters 3 and 4 is further modified to maintain an $N-1$ security criterion similar to the criterion applied to transmission systems. The main distinction, however, is that the $N-1$ criterion applied solely to a flexible, hybrid AC/DC, distribution network . This chapter begins with a brief review of previous works carried out on contingency and security assessments in power systems. A new Distribution Security Constrained OPF (D-SCOPF) is then introduced and implemented within the day-ahead ANM framework for secure operational planning in a hybrid AC/DC distribution system. The HV-UG UK generic distribution system introduced in Chapter 2 – Section 2.6.3 – is modified to a hybrid AC/DC network using an embedded DC network interface for ultimate flexibility of operation. The justification of this modification lies in the fact that most changes in distribution networks, such as integration of distributed generation as well as flexible loads such as electric vehicles or energy storage devices often requires a conversion stage (AC/DC/AC) which in time converts the network from a purely passive AC radial system to an active hybrid AC/DC radial-meshed system.

5.1 Security-constrained Operational Planning

An electric power system is expected to satisfy a continuous balance between generation and consumption while maintaining the quality of supply to consumers. However, system outages due to unexpected events such as lightning strikes, equipment failures, car-pole accidents or lines in contact with trees might cause an interruption of the electricity supply to the consumers. Under certain conditions, the electric power system is required to withstand the outages and keep the supply to consumers in the healthy regions. Therefore, the ANM framework in this work ultimately aims to withstand the loss of any one pre-defined contingency ($N-1$ criterion). Before going into more detail, the definition of secure operation in the context of system reliability must be firstly understood and different operating states in power system operation discussed. The discussion is followed by two main approaches applied for system security assessment. In the end of this section, a series of methods for optimum secure operation in both transmission and distribution networks are reviewed.

5.1.1 System Reliability Definition

The reliability can generally be referred to the ability of an item to perform a required function for a stated period of time. For example, a car would be considered as reliable if it does not breakdown often during its lifetime. However, the concept of power system reliability is extremely diverse and cannot be associated with a single specific definition [252]. North American Electric Reliability Council (NERC) [253] defines power system reliability as follows: "Reliability, in a bulk power electric system, is the degree to which the performance of the elements of that system results in power being delivered to consumers within accepted standards and in the amount desired. The degree of reliability may be measured by the frequency, duration, and magnitude of adverse effects on consumer service". The power system reliability studies can be quantified into two separate aspects: adequacy and security [254]. Adequacy deals with the capacity of the electric power system whereas security deals with the system operation. Adequacy covers the ability of power system to supply enough generation and transmission capacity to meet the customer requirements at

all times, taking into account contingencies. It focuses on long-term planning and investment. On the other hand, security covers the power system's ability to remain intact even after equipment failure occurrence. It deals with short-term operations and operational planning [254].

Within an ANM framework, the potential for outage events that can influence distribution system operation in a day-ahead planning should be also addressed. Therefore, this chapter deals with the system security because it is related to the short-term operations and planning. Distribution systems are usually 'radial' systems which means power flows from the grid supply point (i.e, a substation connected to the transmission system) downstream to customers distributed along the line. When any fault occurs, the faulted section will be isolated and the service to the downstream will be restored by closing a normally open switch. In this situation, the security of the current distribution system can be ensured when only one link of the primary feeders or substation transformers is out of service. Hence, the term 'security' in this work is referred to the ability of the system to withstand sudden disruptions that could cause circuit overload and/or voltage violation with respect to the $N-1$ security criterion. In line with the scope of steady-state analysis, the dynamic security assessment and control which refers to transient and oscillatory of system response is not addressed here. In that context, the security control is established from a basic framework as presented in [255], which can be represented in five different operating states namely, normal, alert, emergency,in extremes and restorative as shown in Figure 5.1.

The power flow computation contains two types of operation constraints; equality and inequality constraints as discussed in the Chapter 2. The different operating states in Figure 5.1 can be classified based on the fulfilment of these constraints. The system is considered in normal operating state when both the equality and inequality constraints are satisfied even during the loss of any element as specified by a certain criterion. The alert is similar to the normal state during pre-contingency but there is insufficient margin to withstand sudden disruption where some of the inequality constraints are violated during post-contingency. If a sufficiently severe disturbance takes place, the system may enter into emergency state when only equip-

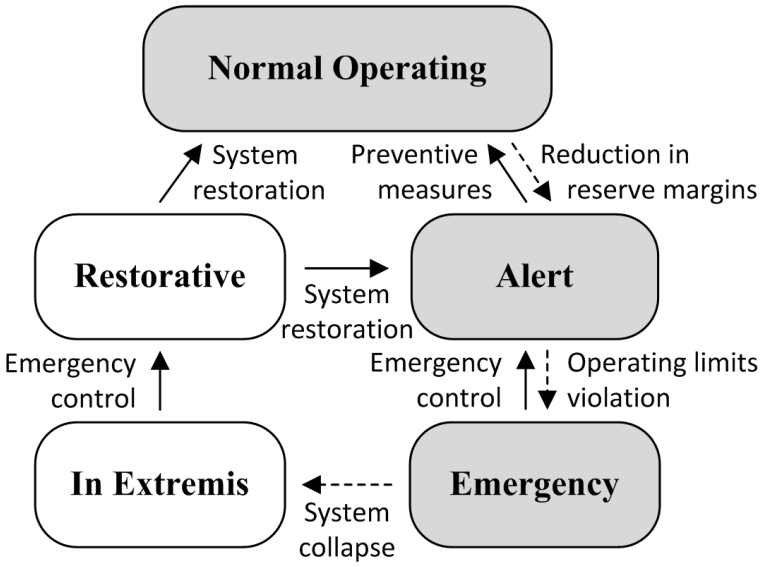

Figure 5.1: Power system operating states

ment operating constraints (i.e, inequality constraints) are violated and no load is curtailed (i.e, equality constraints are still satisfied). However, this operating state may transfer into an extreme emergency state or in extremis if control measures are not taken in time or render ineffective. In this state, equality as well as inequality constraints have been violated and load must be curtailed. When emergency control action is taken to avoid total collapse, the system may enter into a restorative state. The system still experiences loss of load (equality constraints are not satisfied) in restorative state. From this state, the system may transfer into either normal or alert states depending on circumstances, when control measures in place to pick-up all lost load [256].

5.1.2 System Security Assessment

A secure system operation can be achieved by ensuring the power system should always remain in the normal state in both operations and planning. Therefore, a security assessment (SA) is needed to determine whether or to what extent, a power system can meet specified reliability and security criteria for both steady-state (static) and dynamic (transient) conditions with regards to all critical contingencies [257]. In this context, the SA can be classified into steady-state security assessment (SSSA) and dynamic security assessment (DSA). The SSSA deals with

the system operation within security limits after transition to a new operating point due to contingencies. On the other hand, the DSA deals with the system performance as it progress during the transition [258]. The ANM framework in this thesis performs only steady-state analysis as demonstrated in the previous chapters and hence, this work is focused on the steady-state assessment. Two approaches are commonly applied for the SSSA; deterministic and probabilistic approaches. The deterministic approach refers to the system operation and planning procedure based on a contingency set that has been selected beforehand using worst case scenario, while the probabilistic approach accounts for the uncertainty of system conditions and quantify the likelihood of the contingency events.

The deterministic approach has been widely applied to ensure the system is able to withstand any selected contingency events by using performance indices. The indices are normally derived in terms of increment in the system element loadings and deviations in the bus voltages [259]. The deterministic approach has well-served the industry since it was first introduced in 1974 to support secure operation in the power systems. There are several recent studies that apply this approach for the system security assessment [259–264]. In [260], the deterministic approach is used to classify contingencies with different weighting factors in according to pre-defined levels of performance indices. As alternative to the existing indices, Chen et al. [261] introduce a new index to indicate the remaining margin for system secure operation after an outage occurrence (how far to be secure or become insecure). The index is established from the shortest Euclidean distance of post-contingency operating points to the security operating boundaries. High energy resources are connected and managed in distribution levels has brought Li et al. [262] to include information from distribution control centre into the transmission system security assessment loop instead of using passive load from the distribution system. The deterministic approach is used to train artificial neural networks in [259] for on-line remedial action when contingency happens. New margin-based and sensitivity-based performance indices are proposed in [263] for selection of critical contingencies. The deterministic approach is also applied in [264] to find an optimal placement of continuously variable series reactors (CVSRs) when considering $N-1$ security requirement.

The probabilistic approach has been used to find a trade-off between the severity and the probability of contingency events. For example, the worst contingency case might be very unlikely to happen but it could be very costly. To address the issue, the probabilistic approach combines the severity (which can be derived from the performance indices) and the probability of all contingency events in form of risk indices. More works using this approach has been found in the last few years to perform risk-based security assessment (RBSA) [265–269]. A hierarchical risk assessment in [265] is carried out to evaluate the reliability of transmission and distribution systems and improved the systems reliability by using standby DG units to supply local loads during contingencies. In [267], the RBSA is used to assess line overload risk with integration of wind power. Apart from normally used severity matrices (voltage and overload) for a power network with high wind integration, Negnevitsky et al. [266] carried out risk assessment on the system frequency response. Deng et al. [268] introduces a new risk index based on Markov chain and cumulant method to encounter the tail risk of extreme wind conditions for short-term scheduling plan. Recently, a fast system risk screening tool is proposed in [269] using the concept of severity function and detailed analysis on the risk regions for appropriate remedial actions. A Monte Carlo (MC) sampling is another research stream for probabilistic approach. In contrast to the methodology before, this technique randomly selects the contingency cases (not all contingencies are considered) for probabilistic reliability risk assessment in power system operation which is not limited to $N-1$ security criterion [270–272].

Although the sampling probabilistic analysis is able to capture the nature of system operation when considering many uncertainties (i.e., consumption, renewable generation and fault occurrence), the comparison results between different applications might give unfair representation as it randomly selects input case scenarios in the sampling process. This approach is more suitable to be applied on a standalone application especially for the purpose of realistic cost assessment. In contrast, the RBSA method is able to address the issue because all contingencies are taken into consideration and tackled according to their risk. However, the method would jeopardise the severe contingency cases due to very low probability of their occurrence

and the minimum security requirement of $N-1$ criteria might not be fully addressed. Nonetheless, additional information on outage and repair rates for each component must be available before the probabilistic approach can be applied. Since distribution system is normally operated in a passive way, such information are very limited and not available as such in the transmission system. There is not enough information can be used for the probabilistic approach from the considered test networks. Thus, this work uses deterministic approach for the security assessment.

5.1.3 Security Control and Management

In any power system security control and management scheme, there is normally a need to take into consideration of any event that could create network constraints violations. Therefore, additional constraints should be also applied in the optimal power flow calculation after outage of any element in the system (i.e., post-contingency events). This is known as security-constrained optimal power flow (SCOPF) problem. In the SCOPF problem, an objective function is optimised by adjusting the settings of control devices to ensure the security of system operation including at the post-contingency states. In other words, the control adjustment will restore the system from alert state to normal state and this leads to the implementation of preventive mode as depicted in Figure 5.1. This approach becomes a conservative way in managing the power system as the post-contingency control is not allowed. Alternatively, a corrective mode of SCOPF is suggested to allow emergency control immediately after the occurrence of contingency events. In that case, the system is permitted to operate in the alert state and the emergency control will be employed to restore the system from emergency state back to alert state at the post-contingency period.

The concept of SCOPF is firstly introduced by Alsac and Scott [273] where the normal problem of OPF was extended by adding constraints pertaining to contingency events (known as security constraints). Later the study in [274] showed that the preventive control in [273] is not economical and suggested the possibility of corrective actions after the contingency has occurred. The corrective and preventive control actions are combined in [68] and solved in a quasi steady-state simulation.

The simulation considers dynamic transition of system operation where any of the contingencies occurs in two consequent post-contingency stages namely, short-term and long-term. The preventive measures are applied during short-term due to delays in the system response (i.e., generator active power adjustment). After the delay (i.e, long-term period), corrective actions take place to reschedule power generation. This framework is used recently in [275] for multi-terminal HVDC applications. In this work, corrective actions from voltage source converters are employed in short-term period as their fast response can react immediately after the contingency occurrence. The SCOPF is more challenging compared to the traditional OPF problem as the size of optimisation constraints increase depending on the number of contingencies. This issue is addressed in [71] by using semi-definite program (SDP) through a convex relaxation to guarantee a global optimal solution. On the other hand, a typical DC formulation with linear representation of security constraints is used in [276] to tackle the issue on high computational cost of the SCOPF problem. Most recently, [277] introduces a mixed AC-HVDC test system that contains both AC and DC systems for evaluation of SCOPF.

Although the concept of SCOPF is widely used in the past few years, they are mostly for transmission networks. The concept has not been investigated for distribution networks mostly due to the nature of the network topology (i.e. radial feeders). Notwithstanding this, the operational security in distribution networks has been investigated in [50, 278] using network reconfiguration techniques by means of service restoration to all consumers at the healthy section. In [278], a distribution system security region (DSSR) has been introduced which is based on the concept of total supply capability (TSC) [279]. In this way, all operating points can be determined to ensure the system operates at an $N-1$ security criterion, considering the capacities of substation transformers, network topology and operational constraints. This concept is also applied in [50] for the case of substation transformer outages at varying load conditions. These studies, however, still require load interruption especially when TSC is less than total power consumption in the system. In order to improve the security of supply at a given $N-1$ criterion (i.e., link outages on the main feeders), the ANM framework used in this thesis can be improved further by

incorporating the SCOPF problem instead of the conventional OPF. In this chapter the variation of the SCOPF problem which is used for the distribution network is called Distribution Security Constrained OPF (D-SCOPF) and as discussed earlier in this chapter it upholds to an $N-1$ security criterion where the system is to withstand any one load interruptions.

5.2 DC Operation in Distribution System

The increasing trend of DC load integration in distribution systems such as electric vehicle's charging facilities, battery storage systems, LED lighting systems, DC data centres, and variable-speed machines has gradually been bringing forward the possibility of operating MV distribution networks as DC as well as AC [280]. Other than DC load integrations, the renewable resources-based DG such as wind and and solar generations operating with an internal DC bus. For instance, solar-based DG generates power in DC and it is converted into AC using an inverter before it can be supplied to the existing AC system. On the other hand, wind-based DG output is normally converted into DC in order to synchronise with frequency of the connected grid. This shows the necessity to have a DC platform that allows all DC loads and generators to be interconnected and operated as one system. DC operation will also lead to lower power losses due to the lack of reactive power loss thus improving the efficiency of the grid. Moreover, DC networks already has showed better performance in terms of system reliability and flexibility as reported in [281]. There are basically two ways with which DC operation at the MV levels can be realised namely, a full DC network or a hybrid AC/DC network. In the following sections, these are explained briefly.

5.2.1 A full DC system configuration

A full DC system refers to the whole or most part of the MV distribution grid that is developed to operate in DC. The grid network is normally supplied by a bidirectional AC/DC converter (i.e., rectifier) that converts AC supply from the existing high voltage grid into DC source or connected to high voltage DC (HVDC)

through a step-down DC converter (e.g., buck converter) [5]. All DC loads and DG technologies with internal DC bus can be connected directly to the grid and the system is operated in a similar fashion to the AC network. Some nearby AC loads and sources may connect to the DC network using inverter and rectifier, respectively. The full DC system configuration is illustrated as in Figure 5.2. This configuration is called a medium voltage direct current (MVDC) collection system because it is designated to gather all DC generations and loads in a platform that can be managed separately from AC system. The DC system still requires some information at the exchange points between AC and DC networks. Similar concepts have been found in large-scale wind farms or solar power parks [282,283] where all resources are collected using a DC system and converted into AC before it can be injected to the existing grid. This concept is therefore also known as a DC collector grid. This thesis uses term MVDC instead of collector grid because it covers a wider definition that gives a complete picture of DC system with generation, transmission and consumption.

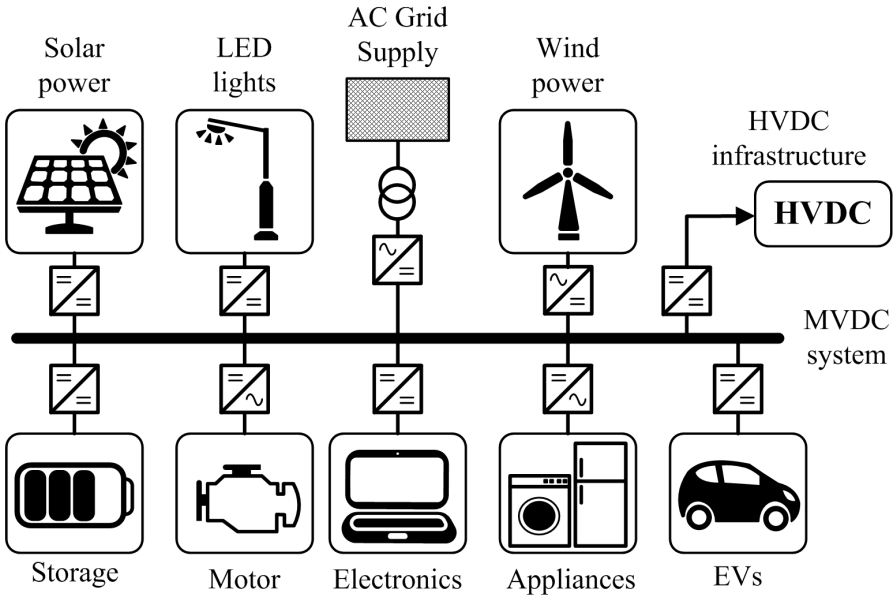

Figure 5.2: Possible future MVDC distribution grid [5]

There are already demonstrator projects for using a full DC configuration for distributing loads, for example a campus scale project is planned to be constructed at RWTH Aachen University in Germany [284–287]. There has also been studies on the operation of such topologies at the MV level. For example, in [284], a

simulation model of the MVDC grid is developed to investigate the dynamic and steady-state system operation. The MVDC grid is mainly supplied by the existing AC network without any generation in the DC network and managed using a master/slave strategy. Details on possible structure of the MVDC grid and topology of the power converters are presented in [285]. Apart from technical aspects, the study also explain in terms of legal constraints for the MVDC grid implementation that includes regulatory requirements, standard compliances and environmental impacts. In another work, Stieneker and De Doncker [286] conducted a comparison analysis between DC and AC operation in an urban MV distribution grid. The MVDC solution has shown superior ($\approx$ 5 times lower) than MVAC in terms of investment cost mainly due to the higher power rating for the AC-grid connection and higher cost for transformer which is expected to be more expensive than the cost for the DC/DC converters in the future. In [287], the MVDC supply grid is suggested to replace the existing MVAC grid in the urban railway system for more efficient with less effort (i.e., the use of inverters and filters) to install renewable energy sources.

5.2.2 A hybrid AC/DC configuration

The idea of converting the MV distribution grid from AC to DC operation may not be done in totality due to the existence of legacy equipment (and infrastructure) designed solely to operate in AC. For this very reason, an MVDC system topology is more likely to be embedded within an existing AC MV distribution grid acting as collector grid (or interface) between DC loads/DGs and the AC grid. Therefore, it is highly likely that the future MV distribution network be a hybrid AC/DC system. A version of an embedded DC grid infrastructure has already been discussed in Chapter 3 where normally-open point breakers where replaced by BTB-VSC interconnectors, seen in Figure 5.3a, for enhanced network reconfiguration. The resulting network as a whole can be considered as a hybrid AC/DC network. Figure 5.3b also shows a point-to-point DC interconnector. In both cases, it is clearly seen that only the adjacent feeders are involved in any coordinated control scheme. Nonetheless, such configurations, as already shown in Chapter 3, will result in improved flexibility of operation when used in an ANM framework for example. It can also help

with improving system reliability due to virtually instantaneous responses of the interfacing converters to any disturbances.

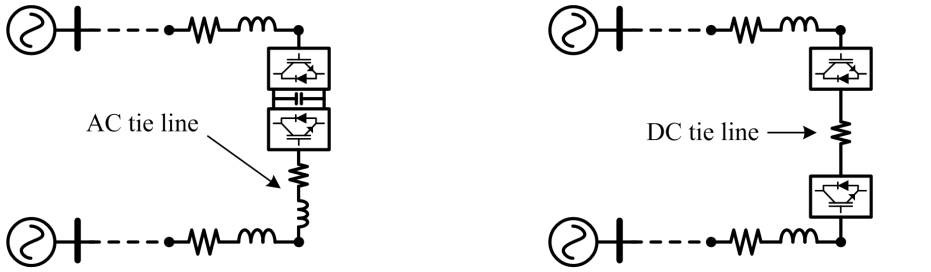

(a) A back-to-back configuration (b) A point-to-point configuration

Figure 5.3: Two Possible "Soft" Interconnector Points

However, the focus on this chapter is to improve the operation of the MV network even further by the introduction of an integrated MVDC interface which is essentially a DC collection grid comprising of multiple VSCs at all tie lines and they are interconnected to each other as shown in Figure 5.4 to attain higher levels of operational flexibility. Consequently, all DGs with internal DC links (wind and solar power) can be directly connected to the MVDC interface. The MVDC interface may also be used to connect all end feeders together to achieve a more seamless load transfer capability between the feeders thus providing improved voltage regulation (e.g. for loads at end feeders). Moreover, it is only by having such a configuration that a continuity of supply constraint can be guaranteed especially after outage of one line in the main feeder or substation transformer, thus as mentioned earlier in this chapter, a security-constrained operational planning scheme can be applied.

5.3 Unified AC/DC Hybrid Network Formulation

A unified AC/DC hybrid network model can be derived for solving power flow (and by extension the optimal power flow) equations using the same unified VSC modelling methodology introduced in Section 3.2.1 [288, 289]. Figure 5.5 below shows one feeder in the hybrid AC/DC network which was introduced earlier. For the integration line through a VSC between AC and DC systems as shown in the figure, the mathematical model which is derived in Section 3.2.1 can be applied.

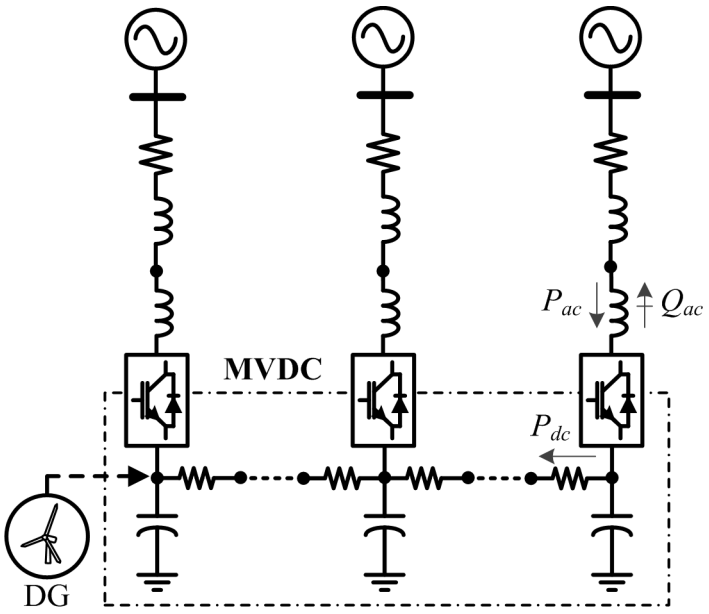

Figure 5.4: The Hybrid AC/DC Grid concept: AC MV network with an embedded MVDC Interface

Therefore, this section simply introduces a universal mathematical model for hybrid networks that can be used for inclusion of the MVDC interface.

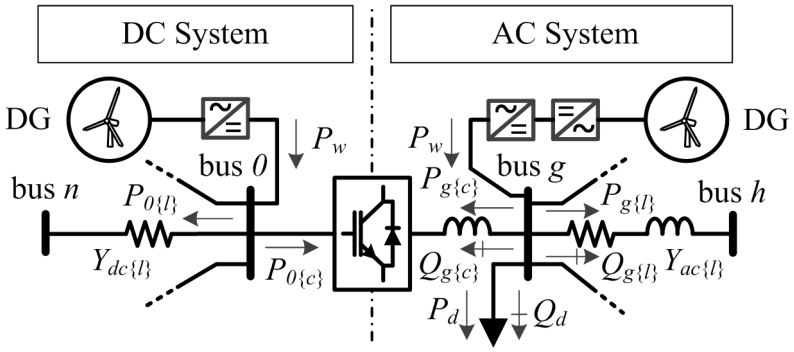

Figure 5.5: One feeder in the Hybrid AC/DC network with the MVDC interface

The entire hybrid network can be essentially modelled as notionally AC with one admittance matrix for which the following nodal power flow injections can be written as:

$$\boldsymbol{S} = diag(\boldsymbol{V}) \times (\boldsymbol{Y}^*_{ac/dc}\boldsymbol{V}^*) \tag{5.3.1}$$

In (5.3.1), the vector $\boldsymbol{V}$ denotes the vector of all nodal voltages (AC and DC) belonging to the set N and $\boldsymbol{Y}_{ac/dc}$ is the hybrid network admittance matrix. The entire network can be modelled using (5.3.1) as notionally AC and by assuming that

there is no reactance at the DC side. Referring to Figure 5.5 and using (5.3.1), the nodal power injections of the AC feeders at bus g can be expressed as:

$$\overline{S}_{g\{l\}} = \overline{Y}_{ac\{l\}}[V_g^2 - \overline{V}_g \overline{V}_h^*] \tag{5.3.2}$$

and, the power balance equations for the AC feeders (bus g) as:

$$P_{g\{c\}} + \sum_{l=1}^{nl} P_{g\{l\}} + P_{d\{g\}} - P_{w\{g\}} = 0 \tag{5.3.3}$$

$$Q_{g\{c\}} + \sum_{l=1}^{nl} Q_{g\{l\}} + Q_{d\{g\}} = 0 \tag{5.3.4}$$

where, nl is the total number of lines connected to bus g. The AC lines connected to bus g are denoted as $g\{l\}$ whereas the subscript $g\{c\}$ refers to AC side of the respective VSC that is connected to bus g. In that case, the complex power injection $\overline{S}_{g\{c\}}$ can be derived using (3.2.4) as presented in the earlier chapter. Besides that, the subscripts d and w are referred to loads and wind-based DGs at their respective buses.

For the DC side at bus 0, the following real and reactive power injections can be written by following the expression in (5.3.1):

$$P_{0\{l\}} = G_{dc\{l\}}[E_{dc\{0\}}^2 - E_{dc\{0\}}E_{dc\{n\}}\cos(\theta_0 - \theta_n)] = G_{dc\{l\}}E_{dc\{0\}}\triangle E_{dc} \tag{5.3.5}$$

$$Q_{0\{l\}} = -E_{dc\{0\}}E_{dc\{n\}}G_{dc\{l\}}\sin(\theta_0 - \theta_n)] = 0 \tag{5.3.6}$$

In (5.3.5) and (5.3.6), $\triangle E_{dc} = E_{dc\{0\}} - E_{dc\{n\}}$ and $Y_{dc\{l\}} = G_{dc\{l\}}$. By requiring a zero-reactive power injection condition as expressed in (5.3.6) the angles at the DC side will maintain their initial zero values (hence: $\theta_n = \theta_0 = 0$). The total nodal power injection at the DC side (bus 0) is therefore:

$$\sum_{l=1}^{nl} P_{0\{l\}} = \sum_{l=1}^{nl} G_{dc\{l\}}E_{dc\{0\}}\triangle E_{dc} \tag{5.3.7}$$

and, the power balance at the DC side (bus 0) can be expressed as:

$$P_{0\{c\}} + \sum_{l=1}^{nl} P_{0\{l\}} - P_{w\{0\}} = 0 \tag{5.3.8}$$

where, $P_{0\{c\}}$ is the active power injection at DC side of the respective VSC connected to bus 0 which can be derived from the expression in (3.2.5) of the earlier chapter.

In general term, the AC and DC lines can be defined as one set of power lines, L. By following the expression in (5.3.1) and based on the assumptions that in the hybrid network for any node, b, the power balance can be computed as below considering the nodal power injections for the converter, c, and the unified AC/DC line which are derived from (3.2.4),(3.2.5) and (5.3.2) for AC lines or (5.3.5) and (5.3.6) for DC lines, respectively:

$$\sum_{c\in C} P_{b\{c\}} + \sum_{l\in L} P_{b\{l\}} + P_{d\{b\}} - P_{w\{b\}} = 0 \qquad \forall b \in N \tag{5.3.9}$$

$$\sum_{c\in C} Q_{b\{c\}} + \sum_{l\in L} Q_{b\{l\}} + Q_{d\{b\}} = 0 \qquad \forall b \in N \tag{5.3.10}$$

This unified model formulation can now be implemented to achieve $N-1$ security operation in the ANM framework introduced in the next section.

5.4 Improved ANM Framework: D-SCOPF Formulation

An active network management (ANM) framework in distribution networks usually optimises operation without taking into account any post-contingency (faults) operating states as presented in [6]. This is apparent in the ANM framework used in the earlier chapters in this thesis (i.e. Chapters 3 and 4). An electricity security of supply should be addressed within the ANM framework to manage the system in advance. In this thesis, the ANM framework ensures a continuity of supply in the network even after the occurrence of any single faults in the primary feeders or substation transformers (to uphold an $N-1$ security criterion). The ANM framework runs a multi-period D-SCOPF, which will be introduced in detail later in this section. The D-SCOPF ensures the continuity of supply by maintaining operating constraints during both normal operation (pre-contingency) and abnormal (post-contingency) conditions [69]. It optimises the network operation for the day-ahead time horizon considering both preventive and post-contingency remedial control actions available to the DSO. A flowchart of the introduced ANM framework is shown in Figure 5.6. In this figure, $\boldsymbol{x}$ is the vector of state variables (voltage magnitudes

and angles), $\boldsymbol{u}$ is the vector of active scheme variables (demand shift and DG curtailment), and $\boldsymbol{w}$ is the vector of control variables. The control variables can be divided into slow corrective variables, $\boldsymbol{w}_s$ (tap changer operation) and fast control variables, $\boldsymbol{w}_f$ (modulation index and phase shift of VSCs).

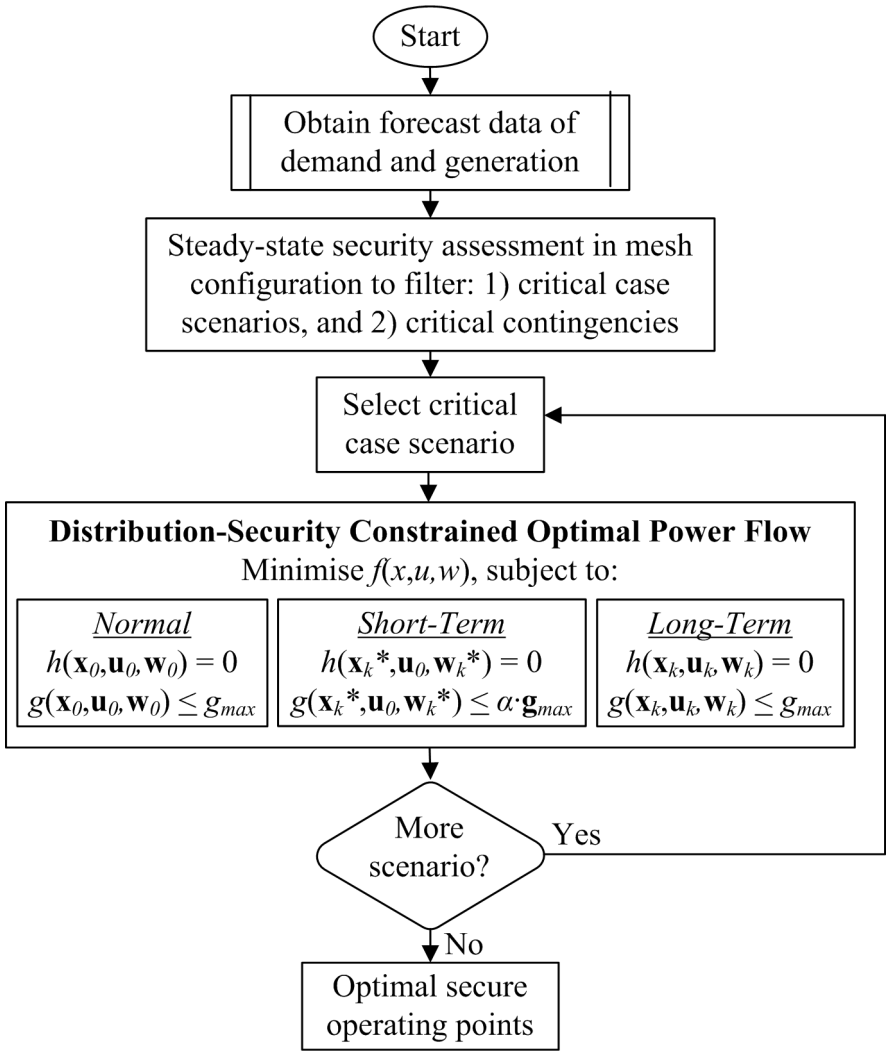

Figure 5.6: The flowchart of the introduced ANM Framework

In ANM framework, the availability of forecast tools is important to provide information on demand and generation to enable evaluation of the network capability in day-ahead planning. The information can be used to manage the network in advance and prepare for any possibility of contingency situations. It is assumed there is sufficient information available for reliable load/generation forecasting in this thesis. Compared to the ANM framework used in the previous chapters, there are two modifications made on the ANM framework in this chapter; 1) steady state security

assessment and 2) additional post-contingency constraints within the formulation as shown in Figure 5.6. Once operation is finalised using D-SCOPF algorithm, the control market agent engages with commercial aggregators to collect information and agree upon energy bids in the day-ahead flexibility energy market. The clearing energy price is then obtained to create its final schedule. More details explanation on the steady state security assessment and D-SCOPF framework are given in the following subsections.

5.4.1 Steady state security assessment

A steady-state security assessment is carried out to identify the critical contingencies from all of the expected demand and generation. The critical contingency case is selected from element outages that cause any operational constraints violation. In the context of security-constrained operational planning, the non-critical contingency cases will not give any different from normal optimal power flow calculation and they can be disregarded. The critical contingency selection is repeated at different operating points of demand and generation. In this procedure, critical case scenarios (i.e, demand and generation operating points binding with the critical contingency) can be also identified. The period of critical case scenarios should be identified in advance for possible actions (i.e., DG power curtailment or demand response) to ensure the system operating state always remains in the normal operation. Therefore, this step is essential to reduce the number of contingency cases and identify the coincidence period of demand and generation operating points that affect system secure operation. As a result, the size of optimisation problem can be reduced that could ease the computational burden.

In order to identify the set of critical contingencies and case scenarios, an iterative procedure is carried out in this step to assess for each time period. The simulation is performed in a meshed configuration (i.e., all tie switches are closed) to account for the worst conditions. The following iterative procedure is used in this assessment to select the potential critical contingency cases the actual execution of the D-SCOPF:

1. Let K be the contingency set with respect to which the system must be secure (i.e, line outages at the main feeder including the main substation transform-

ers). Set the critical contingency set, $K_c = \emptyset$ and the subset of critical case scenario, $M_c = \emptyset$.

2. Select a time period of the forecast data, $m \in M$ and solve OPF using base case constraints for the expected demand and generation. Let $\boldsymbol{P}_{0\{m\}}$ denote the optimal operating point at period m.

3. Simulate each contingency in K at $\boldsymbol{P}_{0\{m\}}$ by a conventional load flow program. If none of the contingency leads to any constraint violations, $\boldsymbol{P}_{0\{m\}}$ is a secure optimal solution. Otherwise, let $K \setminus K_c$ be the subset of critical contingencies (i.e., those leading to post-contingency violations) and time period of the expected demand and generation operating point is recorded as subset of critical case scenario.

4. Repeat steps 2 and 3 for next time period. The computation terminates after all time periods are executed.

5.4.2 D-SCOPF optimisation framework

In this stage, a multi-period D-SCOPF is solved for the day-ahead time horizon to determine the secure optimum settings for the various levels of control actions (both preventive and corrective) available to the DSO. Since in this thesis historic load/generation profiles are used rather than actual day-ahead time series values, for computational efficiency, only the critical case scenarios (i.e. the coincidence period of demand and generation variations leading to post-contingency violations) are considered in this stage. The D-SCOPF runs over the set of all critical contingencies but only for the selected critical case scenarios which are selected from the steady state security assessment as presented in the earlier subsection. The D-SCOPF formulation in this thesis is adopted from the preventive-corrective control framework in [68] that was applied for transmission networks. The actions available to the DSO can be divided into two consequence operating time scales namely, the short-term and the long-term after any contingency occurrence as shown in Figure 5.6. Fast response of the VSCs will then allow for provisions of short-term remedial

actions immediately following a contingency and before long-term corrective actions, by slower devices such as tap changers, take place.

In the ANM framework, the demand shift and DG curtailment should be treated as preventive measures which can be determined beforehand to be agreed upon. For the demand shift control scheme, the price π_{ds} will be paid to consumers to achieve the required demand shift targets, P_{shift}, for the DSO. The power demand shifting can be achieved through a demand shifting factor, ξ that is applied to the current demand as $P_{shift} = \xi P_d$. Similarly, DG curtailment is achieved by guaranteeing a buying price, π_{dg}, for a specific output, and paying the DG owner any compensation for any reduction of the guaranteed output, P_{curt}, at that price. The power reduction can be computed as $P_{curt} = P_{ava} - P_w$. On the other hand, we also assume the cost of power transfer losses, P_{loss}, at the forecast energy market price, π_{em}. It is reasonable to assume $\pi_{ds} > \pi_{dg}$ because from the optimisation perspective it is desirable to reduce the levels of demand shifting (compared to DG curtailment) due to concerns for consumer welfare. Consequently, the objective function can be formulated as shown in (5.4.1). For any period, $m \in M_c$, the optimisation formulation when considering MVDC interface application can be written as the following equations:

$$F = \sum_{m \in M_c} \Big[\sum_{w \in W} \pi_{dg} P_{curt\{w,m\}} + \sum_{b \in N} \pi_{ds} P_{shift\{b,m\}} + \sum_{l \in L} \pi_{em} P_{loss\{l,m\}} \Big] \tag{5.4.1}$$

$$P_g^{min} \leq P_g^m \leq P_g^{max} \quad \forall g \in G \tag{5.4.2}$$

$$Q_g^{min} \leq Q_g^m \leq Q_g^{max} \quad \forall g \in G \tag{5.4.3}$$

$$0 \leq P_w^m \leq P_{ava\{w\}}^m \quad \forall w \in W \tag{5.4.4}$$

$$\xi_b^{min} \leq \xi_b^m \leq \xi_b^{max} \quad \forall b \in N \tag{5.4.5}$$

$$r_o^{min} \leq r_o^m \leq r_o^{max} \quad \forall o \in T \tag{5.4.6}$$

$$V_g^m = 1 \quad \forall g \in G \tag{5.4.7}$$

$$\theta_g^m = 0 \quad \forall g \in G \tag{5.4.8}$$

$$V_{min} \leq V_b^m \leq V_{max} \quad \forall b \in N \tag{5.4.9}$$

$$\overline{Y}_l \overline{Y}_l^* (\overline{V}_{rn\{l\}}^m - \overline{V}_{sn\{l\}}^m)(\overline{V}_{rn\{l\}}^m - \overline{V}_{sn\{l\}}^m)^* \leq I_{max}^2 \quad \forall l \in L \tag{5.4.10}$$

$$\overline{Y}_{cr} \overline{Y}_{cr}^* (\overline{V}_{cr\{c\}}^m - \overline{V}_{sn\{c\}}^m)(\overline{V}_{cr\{c\}}^m - \overline{V}_{sn\{c\}}^m)^* \leq I_{nom}^2 \quad \forall c \in C \tag{5.4.11}$$

$$\Im(\overline{S}^{m}_{0\{c\}}) = 0 \quad \forall c \in C \tag{5.4.12}$$

$$P^{m}_{g\{b\}} + P^{m}_{w\{b\}} = \xi^{m}_{b}(P^{m}_{b} + \sum_{l\in L} P^{m}_{b\{l\}} + \sum_{c\in C} P^{m}_{b\{c\}} \quad \forall b \in N \tag{5.4.13}$$

$$Q^{m}_{g\{b\}} = \xi^{m}_{b}(Q^{m}_{b} + \sum_{l\in L} Q^{m}_{b\{l\}} + \sum_{c\in C} Q^{m}_{b\{c\}} \quad \forall b \in N \tag{5.4.14}$$

The active and reactive power limits that flow through the primary substation transformer (i.e. the grid supply point) are given in (5.4.2) and (5.4.3), respectively. The operating limits of DGs (in here all wind units) are given in (5.4.4) whereas the limits on the demand shifting factor, ξ, are given in (5.4.5). The demand shifting factor in the proportion of demand that can be shifted at any time. Meanwhile, the limits on the tap changer ratio, and voltage magnitude/phase angle for the grid supply point are given in equations (5.4.6) – (5.4.8). The nodal voltage magnitude limits are given in (5.4.9). Equations (5.4.10) and (5.4.11) impose the actual operating limits on lines and the converters which must always be respected. In these equations, $\{sn, rn, cr\} \in N$ are the sending and receiving ends of a line and the corresponding converter-connected nodes respectively. Moreover, the zero-reactive power limit is respected in (5.4.12) and finally the total nodal power balance equations at any node, b (regardless of AC or DC) is fulfilled in (5.4.13) and (5.4.14). The equality and inequality constraints in (5.4.2) – (5.4.14) which must be fulfilled in the three consequence time scales; pre-contingency, short-term and long-term post-contingency as illustrated in Figure 5.6. For all states, $k \in K_c$ the D-SCOPF can be generalised in the following expressions:

$$\min f(x, u, w) \tag{5.4.15}$$

subjected to:

$$h(x_0, u_0, w_{s\{0\}}, w_{f\{0\}}) = 0 \tag{5.4.16}$$

$$g(x_0, u_0, w_{s\{0\}}, w_{f\{0\}}) \leq g_{max} \tag{5.4.17}$$

$$h(x^{*}_{k}, u_0, w_{s\{0\}}, w^{*}_{f\{k\}}) = 0 \tag{5.4.18}$$

$$g(x^{*}_{k}, u_0, w_{s\{0\}}, w^{*}_{f\{k\}}) \leq \alpha g_{max} \tag{5.4.19}$$

$$h(x_k, u_0, w_{s\{k\}}, w_{f\{k\}}) = 0 \tag{5.4.20}$$

$$g(x_k, u_0, w_{s\{k\}}, w_{f\{k\}}) \leq g_{max} \tag{5.4.21}$$

The D-SCOPF program uses the objective function in (5.4.1) to minimise operational cost as expressed in (5.4.15). The function h is used to represent a group of equality constraints that include expressions in (5.4.7) – (5.4.8) and (5.4.12) – (5.4.13). On the other hand, the function g is used to represent a group of inequality constraints which are given by the remaining equations in (5.4.2) – (5.4.6) and (5.4.9) – (5.4.11). The parameter g_{max} indicates the limit of respective variables. The parameter α allows for relaxing of equipment limits during the short-term period immediately after the occurrence of the faults (known as emergency ratings). This condition is particularly applied to the equations (5.4.2) – (5.4.3) and (5.4.9) – (5.4.11). In the generalised expressions, the superscript '$*$' is used to denote that variables are also changed during short-term post-contingency period. Meanwhile, the subscripts 0 and k refer to variable settings at pre- (i.e., $k = 0$) and post-contingency, respectively.

Figure 5.7 illustrates changes of operation settings in a time-line of the three contingency states in the occurrence of system fault. The state variables, x include voltage magnitudes/angles and complex power injection from the substation $(V_b, \theta_b, P_g, Q_g)$ vary accordingly to the system operating conditions. Since the demand shift and DG curtailment schemes as denoted by u (given by ξ_b and P_w, respectively) are preventive control, they are kept at the same operating point in all states. The slow corrective variables, w_s such as tap changer setting (that gives r_o) normally takes few steps to move from current position to the optimal position. This work does not consider the transition process as it meant for steady state analysis and therefore, tap changer position assumes to remain unchanged ($w_{s\{0\}}$) until it reaches final setting ($w_{s\{k\}}$) just after the short-term period. As being highlighted earlier, the fast corrective action, w_f given by modulation index and phase shift of VSCs (generate AC voltages, $\overline{V}_{cr}$) at the MVDC interface allow emergency response within the short-term period (between period t_0 and t_1 as shown in Figure 5.7).

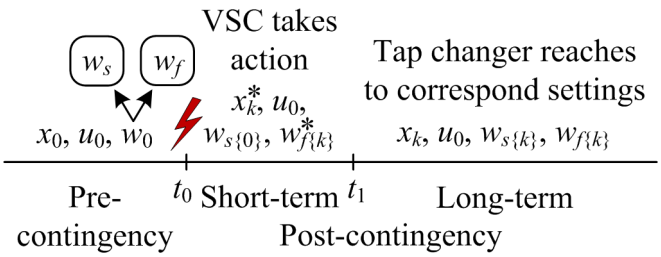

Figure 5.7: Changes of operation settings in post-contingency situation

5.5 Numerical Results and Discussion

The potential application of hybrid AC/DC system is studied in different configurations (e.g., point-to-point and MVDC interface) by considering an urban UK distribution system that operates under the improved ANM scheme. It adheres to a continuity of supply under the $N-1$ criterion where the system supply is not interrupted due to any one line outage in the main feeder or the main substation transformer.

5.5.1 Case studies and scenarios

An 11-kV urban 77-bus UK distribution generic system as introduced in the Chapter 2 is modified by including the MVDC interface at end of all feeders. The modified AC/DC network is seen in Figure 5.8. There are seven additional DC lines to form a hybrid AC/DC system in which four of the lines are considered as the existing tie lines (indicate with solid lines). These lines are assumed to be identical with thermal limit of 5 MVA and line resistance of 0.0665Ω. For the sake of comparison purposes, admittance of the existing AC tie lines are assumed at $0.0665 + j0.0512\Omega$. The voltage and thermal limits are relaxed at short-term emergency ratings of 0.94/1.06 p.u. for voltages and 20% higher than the normal ratings, respectively. The VSC parameter settings are provided in Table 5.1.

For the purposes of simulations in this thesis, the demand and generation profiles are used from historic demand and wind data corresponding to central Scotland in 2003 as presented in [6]. The data contains two sets of wind generation profiles (as a percentage of total generation capacity) and one set of demand profile (as a

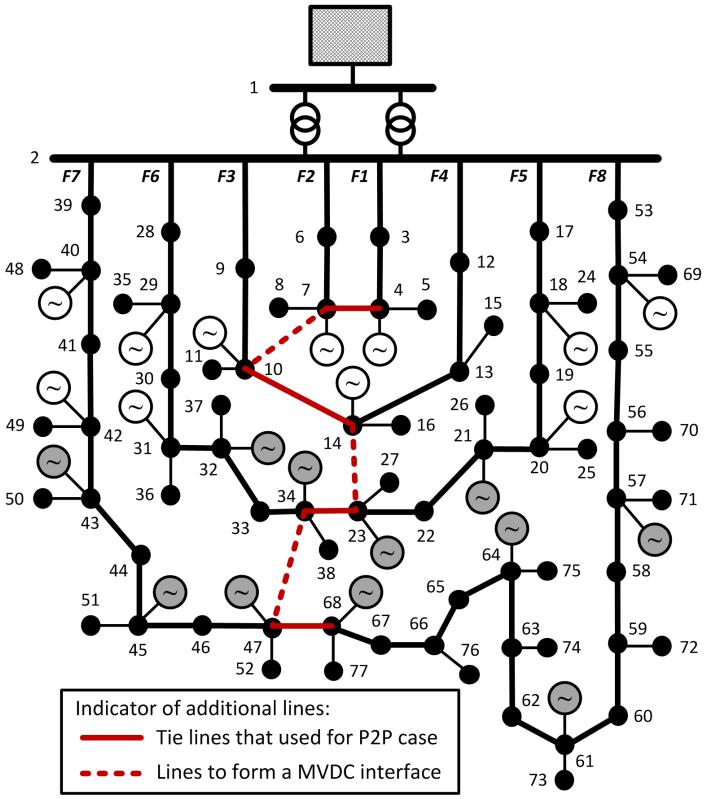

Figure 5.8: The modified hybrid AC/DC UK generic distribution system

Table 5.1: The converter parameter settings

Item	Parameter Settings
VSC rating	5 MVA
DC voltage	±33 kV
Phase reactor, x_{cr}	0.1 p.u.
Constant conductance, G_0	0.01 p.u.

percentage of the system peak load). The number of coincident hours (per year) for each operating point that occurred in the year is also provided. As described earlier in Section 5.4.1, a steady-state security assessment is performed on the test system with all AC tie lines are activated to identify critical contingencies and select only critical case scenarios. The critical case scenarios of load/generation profiles obtained using the steady-state security assessment are tabulated in Table 5.2. At the same time, there are 19 critical contingency cases identified as given in Table 5.3. The critical case scenarios and contingencies will be used for the modified hybrid

network as well. Table 5.3 clearly shows that outages of any line in the short feeders (F1 to F4) and tie-lines are not critical (i.e., does not create any post-contingency violation).

Three configurations are considered namely, base case (original AC configuration), point-to-point (P2P) and MVDC (modified hybrid configuration). The base case does not have VSCs and as a result only control actions available to the DSO are the LTC voltage control, DG curtailment and flexible demand shifting. For the P2P configuration VSCs are installed at end of the tie lines in P2P configuration as suggested and seen in Figure 5.3b. Finally, the operation of the hybrid network with MVDC interface is tested in the MVDC configuration. The MVDC interface acts as a platform for all DGs with internal DC links and loads as shown in Figure 5.5. The MVDC configuration can be considered as an extension of use of DC links in [290] with the same number of VSC stations. In both latter configurations, all available active network management schemes in the base case are also applied. The performances of the different configurations (base case and modified hybrid) are compared in terms of the overall system performance, demand shift, DG curtailment, line loadings and tap ratio optimal settings.

5.5.2 Overall performance comparison

The D-SCOPF presented in Section 5.4 is formulated in AIMMS modelling environment [157]. The problem is solved using CONOPT 3.14V on a PC of 3.5 GHz and 8 GB RAM. The performance comparison is presented in Table 5.4. It shows that the application of VSCs increases the overall system losses, since the switching action in the VSCs cause additional loss to the system. Notwithstanding this, the VSCs application either in P2P or MVDC configurations has shown improved performance in terms of shifted demand and DG curtailment when compared to the base case. Results show that the curtailed energy when using the MVDC interface is dramatically reduced by almost a factor of 3.5 comparing to the base case and twice when compared to the P2P configuration. Overall, as apparent from Table 5.4, the DSO can save over 80% of operational costs compared to the base case - when operating the network as a hybrid using the MVDC interface whilst facilitating a continuity

Table 5.2: The critical case scenarios of historical data in [6]

Case	Wind 1 (%)	Wind 2 (%)	Load (%)	No. of hours
1	0	0	70	114
2	0	0	80	78
3	0	0	90	39
4	0	0	100	2
5	0	10	80	49
6	0	10	90	14
7	10	10	80	238
8	10	10	90	100
9	10	10	100	8
10	10	20	90	56
11	10	20	100	3
12	20	20	90	22
13	20	20	100	6
14	20	30	100	8
15	100	0	80	10
16	100	0	90	11
17	70	90	50	16
18	80	90	50	48
19	80	100	60	18
20	90	100	40	2
21	90	100	50	54
22	90	100	60	144
23	90	100	70	212
24	100	100	50	63
25	100	100	60	249
26	100	100	70	555

of supply condition. Such high cost reduction is mainly due to the reduced levels of demand shifting as well as DG curtailment (which both burden a cost on the DSO

Table 5.3: The selected critical contingency cases

Feeder	Outages (lines)
F5	2-17, 17-18, 18-19 and 19-20
F6	2-28, 28-29, 29-30 and 30-31
F7	2-39, 39-40, 40-41 and 41-42
F8	2-53, 53-54, 54-55, 55-56, 56-57, 57-58 and 58-59

as described in Section 5.4) for upholding the secure of supply condition.

Table 5.4: A comparison in minimising the operation cost

Item	System Configurations		
	Base case	P2P	MVDC
System losses (MWh)	484.90	546.22	494.22
Demand shifted (MWh)	2161.82	576.43	445.78
DG curtailed (MWh)	2174.66	1125.83	620.28
Operational cost ($)	88,611.79	25,425.09	16,658.25
Total cost reduction	-	71.3%	81.2%

The detailed comparison in terms of demand shifting, DG power curtailment, line loadings and tap ratio settings will be discussed in the following subsections:

Demand shifting

Figures 5.9 and 5.10 show the percentage of maximum demand shift for each system configuration. Referring to Figure 5.9, the highest demand shift occurs during a period of high demand and low generation (load at 100% of peak demand and both wind generations are 0%). However, this scenario does not appear very often as shown in Figure 5.10. These figures clearly demonstrate that high demand shift in the base case (73.9%) can be reduced to 49.3% and 46.7% by using the two hybrid configurations (i.e. P2P and MVDC), respectively. The MVDC has shown better improvement than P2P where it reduces 5% maximum demand shift in average. This particularly can be seen in Figure 5.10 where maximum demand shift using

P2P ranges between 30-45% which can be significantly reduced to around 25-40% when using the MVDC interface.

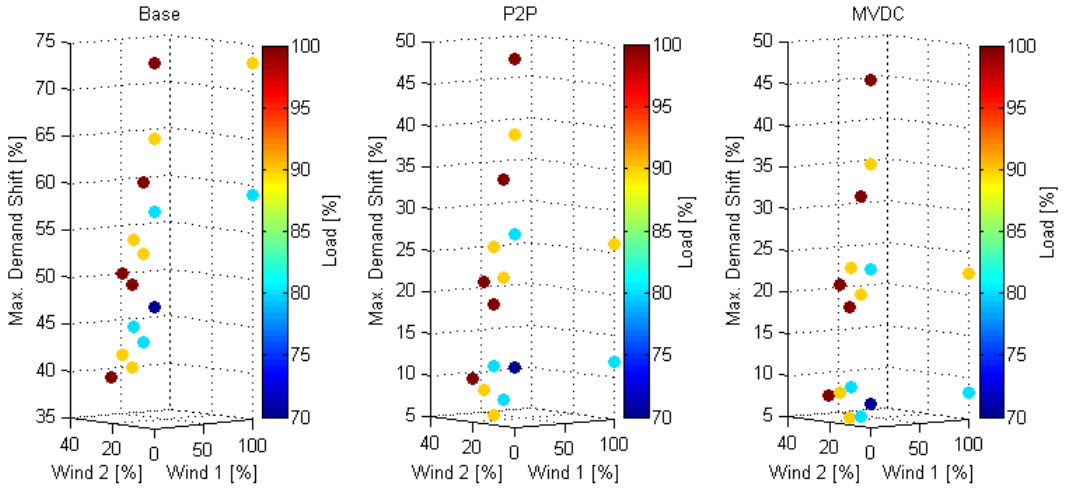

Figure 5.9: A comparison of maximum demand shift at different configurations

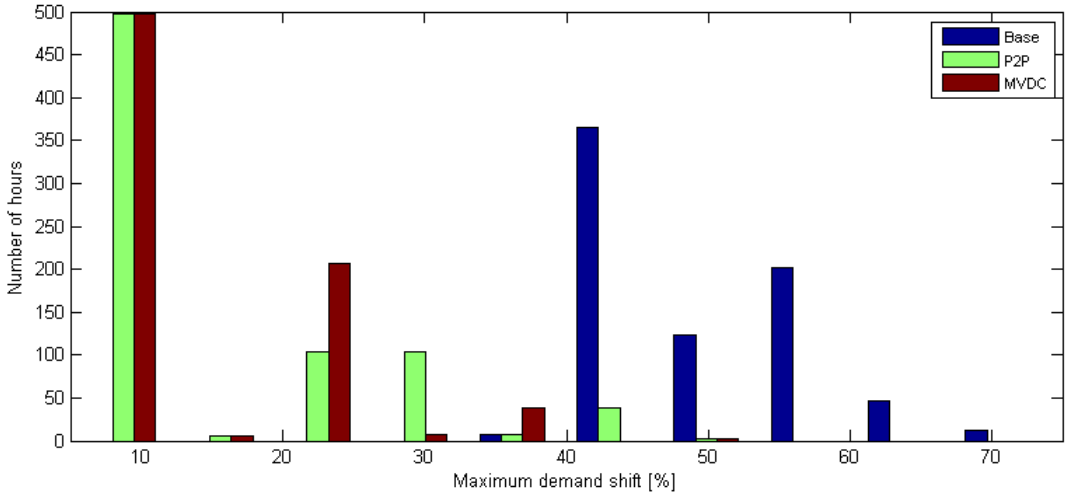

Figure 5.10: The distribution of maximum demand shift within the study period

DG curtailment

During low demand and high generation instances, power curtailment of DG output should be expected. Figures 5.11 and 5.12 show the total amount of DG curtailment for each system configuration. The highest total power curtailment for the base case (5.03 MW) is 15% reduced in P2P configuration (4.29 MW) whereas substantial

reduction of 59% can be achieved with the MVDC interface (2.05 MW) as illustrated in Figure 5.11. Moreover, the DG curtailment is at minimum when using the MVDC interface as apparent from Figure 5.12. The results clearly favour the application of the MVDC interface for maximising the usage of DG resources at distribution voltage levels.

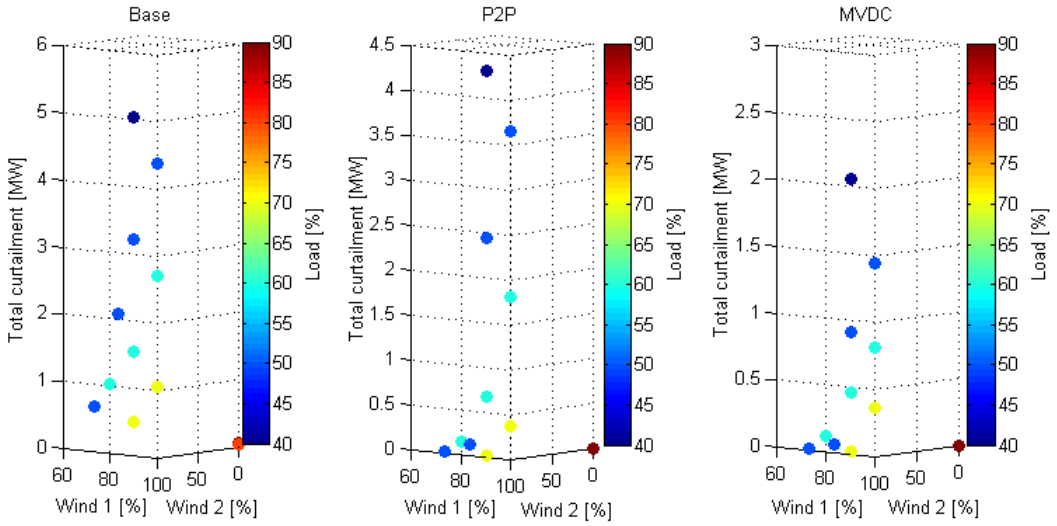

Figure 5.11: A comparison of total DG curtailment at different configurations

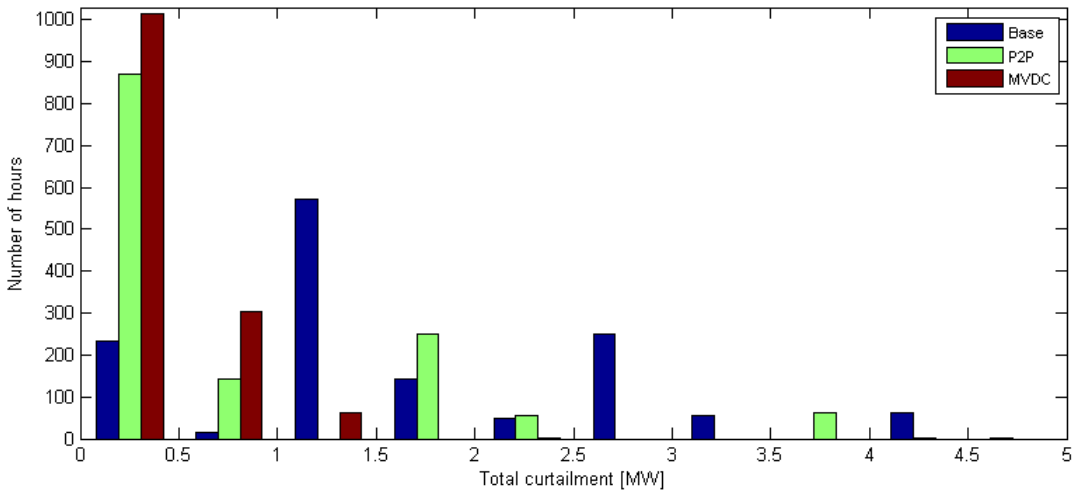

Figure 5.12: The distribution of total DG curtailment within the study period

Tap ratio setting

Figure 5.13 demonstrates the tap ratio deviations from average setting in all 26 critical case scenarios for each configuration. The average tap settings, $\hat{r}$ for base case, P2P and MVDC are 1.029, 1.025 and 1.029, respectively. The tap ratio deviations are calculated using $\Delta r = r - \hat{r}$. In all configurations, tap ratios are operated at higher settings at low generation (scenarios 1 – 16) compared to high generation periods (scenarios 17-26). The base case has shown the highest deviations in each case scenario. It is clearly shown that less tap ratio deviations can be observed for the hybrid configurations (i.e. P2P and MVDC). This signifies that fast remedial action using VSCs in the hybrid AC/DC system can provide reactive power support for system voltage regulation especially during the short-term periods. By contrast, the MVDC shows the least deviations due to the active power transfer flexibility between multiple feeders which is facilitated in the MVDC configuration.

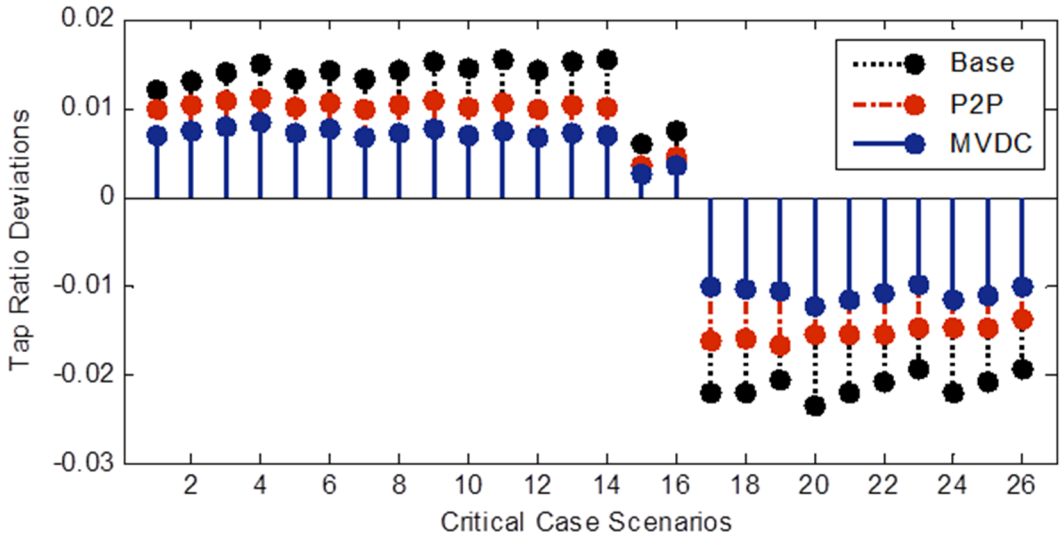

Figure 5.13: A comparison of tap ratio deviations at different case studies

Line loading

Deviations of the highest line loading operation from the base case using P2P and MVDC are compared and presented in Figure 5.14. The deviation is obtained using: Δ line loading (%) = selected case loading (%) – base case loading (%). The results indicate that P2P configuration has much higher line loading than base case

to maximize DG usage as well as demand shift. On the other hand, MVDC configuration not only has lower DG curtailment and demand shift (as seen previously) but also maintains lower line loading during high demand (scenarios 1 – 16) and further decreases the loading during high DG output (scenarios 17 – 26). This can be attained through load balancing between the feeders via the MVDC interface.

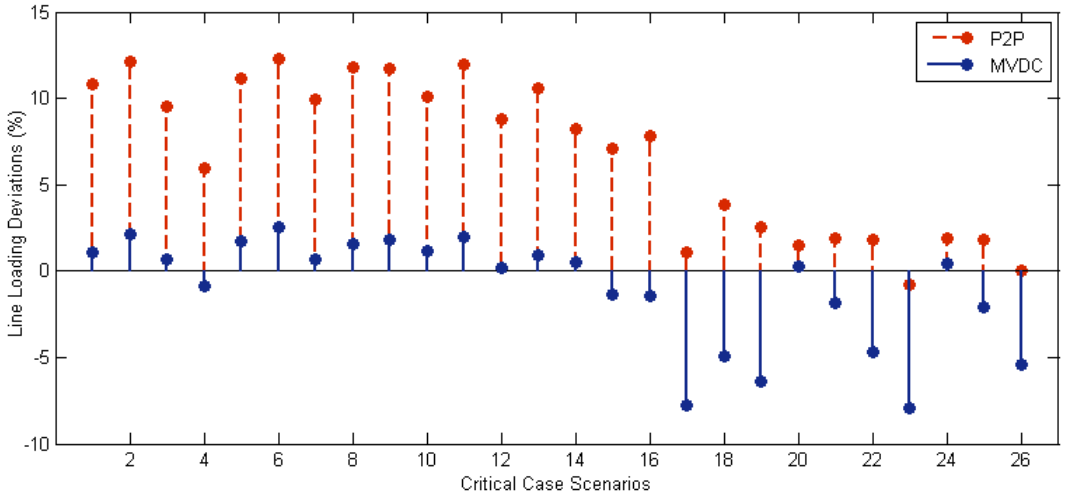

Figure 5.14: A comparison of line loadings at different case studies

5.5.3 Example of remedial actions

It is important to look into the effect on system operation when contingency occur at different case studies. This can be done by selecting one of the contingencies as an example to demonstrate the system operation in the three contingency stages; pre-contingency, short-term and long-term post-contingency. For this purpose, the worst contingency case of line 54–55 outage is selected. The case scenario when load at 80% of peak demand, wind profile 1 at full generation capacity (100%) and no generation from wind profile 2 is used in this example. This case scenario is chosen as the system in the base case requires both load shifting and DG curtailment to achieve $N-1$ secure operation. The results are discussed in terms of VSC operations, tap changer settings and line loadings.

VSC operation

Figures 5.15 and 5.16 illustrate the optimal power flows at the VSC stations in P2P and MVDC case studies, respectively. In these figures, DC voltages are measured across capacitor at each DC bus. Since DC lines in the P2P case are separated, the reference DC buses at the end of feeders F2, F4, F6 and F8 are considered. The optimal solutions are obtained by adjusting the modulation index, m_a and phase angle, ϕ and the reciprocal B_{eq} variable as explained in the Section 5.3. As can be seen, the reactive power injections from AC side of VSCs are actively controlled by the B_{eq} as remedial actions to the contingency stages. In a contingency event when line 54–55 in feeder F8 outage, more active powers are transferred through DC line to support unsupplied part of the feeder. This causes voltage drops in the respected AC bus. In order to avoid the voltage drops, more reactive powers are injected from VSCs. In P2P case, only feeder F7 is directly connected to the feeder F8. Therefore, VSCs at the end of feeders F7 and F8 operate nearly at full capacity as reaction to the contingency event but the rest of VSCs operation are almost the same as in the pre-contingency. Instead, in MVDC case, more distributed active power transfers from adjacent feeders can be obtained to reduce burden on one feeder (e.g., F7) especially during contingency. The different operations in the short-term and long-term post-contingency stages will be explained in the following discussion as they are related to the factor of tap changer operation.

Tap changer operation

Table 5.5 shows the optimal tap ratio operation in three different stages at the worst contingency case. As a slow control variable, tap changer remains at the same position during the period of short-term post-contingency. The base case has not demonstrated any significant changes on tap changer operation during the long-term post contingency. This indicates the tap changer would rather operate in preventive mode due to no other voltage regulation device can support during the short-term period. By contrast, the VSCs either in the P2P or MVDC application show a good coordination with the tap changer at substation. As can be observed in Figures 5.15 and 5.16, more reactive power are injected from VSCs during short-term period to

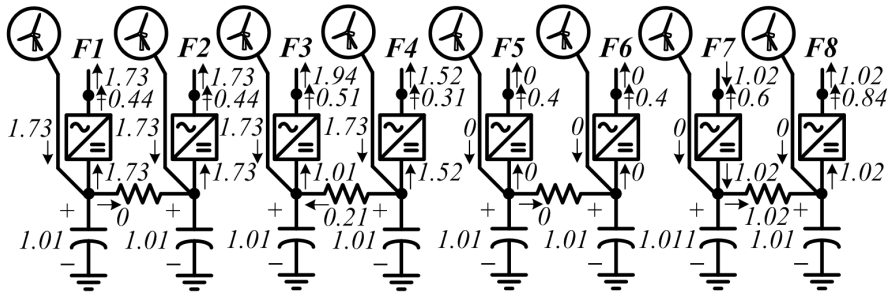

a) Pre-contingency operation

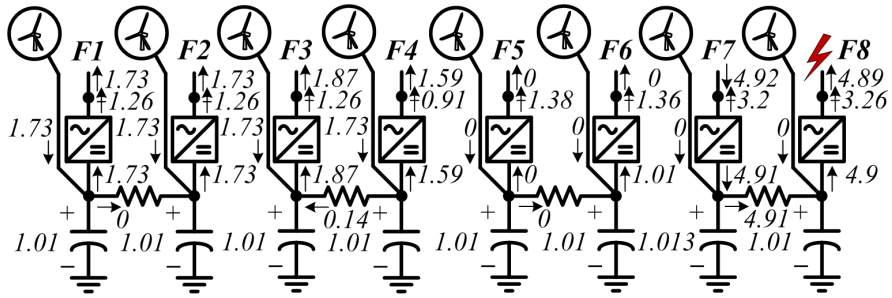

b) Post-contingency short-term operation

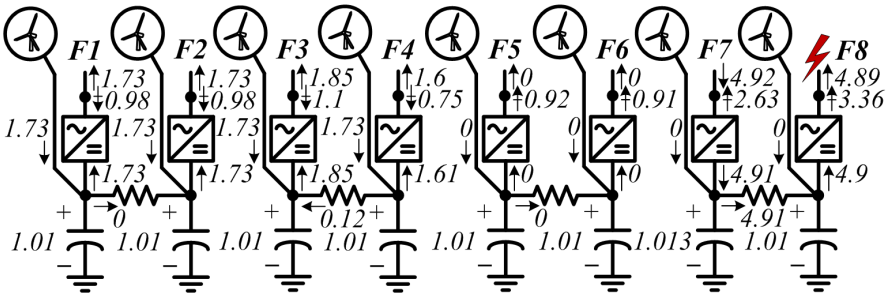

c) Post-contingency long-term operation

Figure 5.15: VSC operation of P2P configuration in the contingency situation

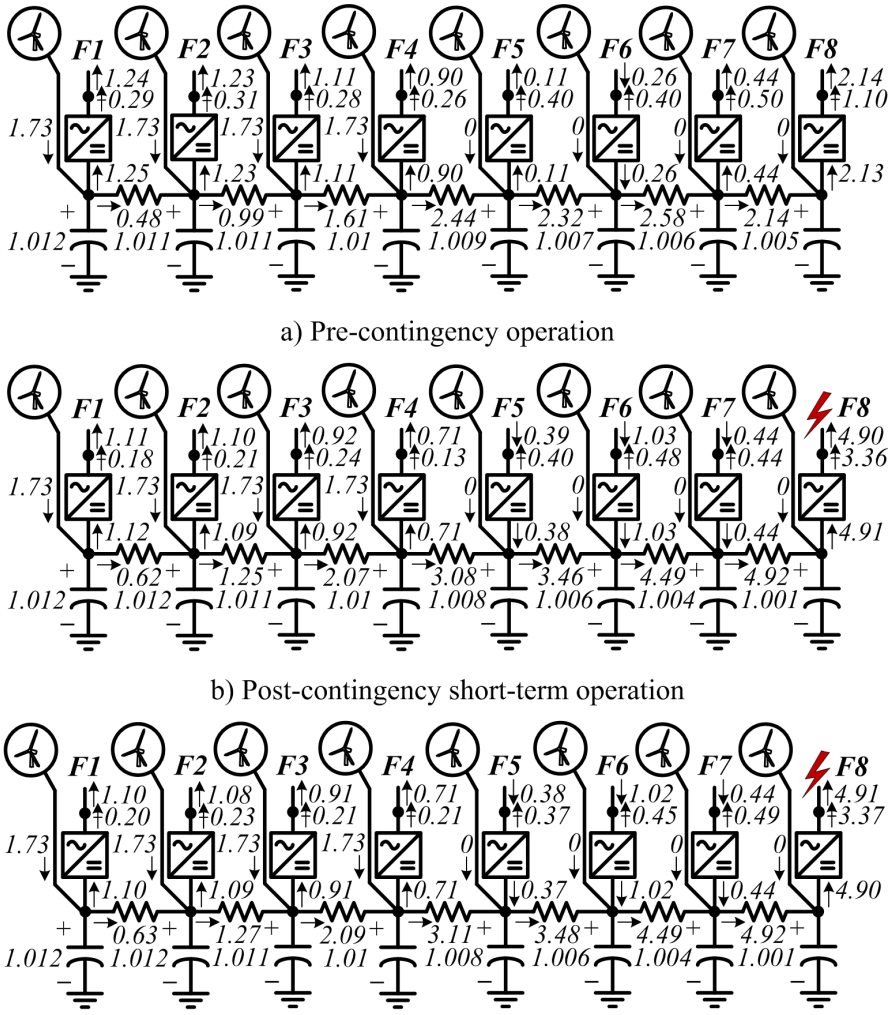

Figure 5.16: VSC operation of MVDC configuration in the contingency situation

regulate system voltages when tap changer not in action. Then, the reactive power decreases when tap change take action during the long-term period. The significant changes on tap charger are clearly showed in Table 5.5 for the P2P and MVDC cases. It is important to notice that MVDC has lower tap ratio deviation as compared to P2P. This signifies that the interconnection DC system in MVDC gives better support in terms of voltage regulation in the overall system.

Table 5.5: An example of optimal tap ratio setting in the contingency situation

Case study	Pre-contingency	Post-contingency		Δr (%)
		Short-term	Long-term	
Base Case	1.035	1.035	1.035	0.03
P2P	1.029	1.029	1.047	1.77
MVDC	1.031	1.031	1.026	0.49

Line operation

In order to demonstrate the changes on line loading in the three contingency stages, line 42-43 of feeder F7 is selected as an example. The loadings of line 42–43 at different case studies are given in Figure 5.17. This clearly shows that line loading increases drastically when contingency occurred. Then, it slightly decreases which can be observed in the P2P case when reaching the long-term period. The base case displays lower line loading than P2P due to less demand and most of DG output is curtailed. Despite this, the MVDC has shown the lowest loading along the contingency periods with higher supply capability (low DG curtailment or less demand shift).

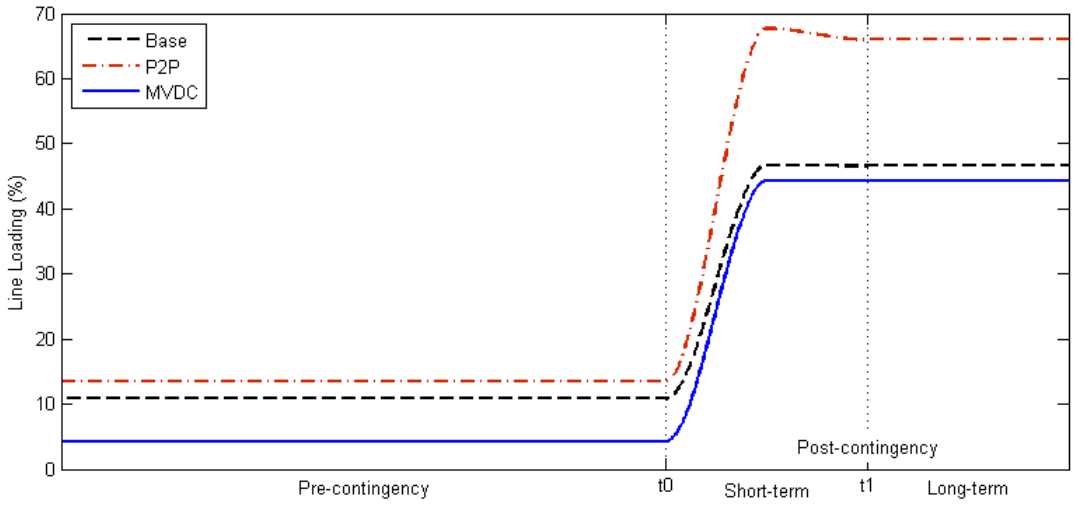

Figure 5.17: A time-line loading of line 42–43 in the contingency situation

5.6 Summary

This chapter introduces a framework for security-constrained optimal operational planning in active distribution networks using a flexible hybrid VSC-based AC/DC system whilst upholding a security of supply condition. A new Active Network Management (ANM) scheme is introduced and applied to a modified urban 75-bus UK generic distribution network. The results clearly show that operating a hybrid network will be beneficial. The MVDC interface configuration introduced in this thesis reduces demand shifting and DG curtailment when compared to normal AC or hybrid P2P configurations whilst upholding a continuity of supply condition. The MVDC interface also helps to improve line loadings and ease tap changer operation burden as it provides seamless load balancing between not just adjacent feeders but multiple feeders. Use of the MVDC interface shows significant savings to the DSO even when compared to P2P configuration with the same number of VSCs used.

Chapter 6

Conclusions

This final chapter draws the conclusion to the research as presented throughout the thesis. It outlines the key findings and highlights the contributions to knowledge from the research works discussed in precedent chapters. In addition, it lays out a path forward for future work based on this research. Overall, the intention of this thesis has been to outline the methods and paths for the realisation of active network management practices in future developments of distribution systems.

6.1 Key Results and Contributions

As stated in Chapter 1, the overarching goal of this thesis has been to develop a new active network management framework for enhanced flexibility and resiliency of operation of future active distribution systems. In achieving the main objectives, as outlined in Section 1.3, a series of research questions (RQ) were identified and outlined in Section 1.2 of this thesis. Chapter 3 covered the introduction of an enhanced network reconfiguration which was showed to improve significantly the voltage profile of a typical MV distribution network under DG/demand variations. Chapter 4 introduced a new energy storage device for reducing costly DG curtailment practices and further improving voltage profiles using active network management. Furthermore, Chapter 5 introduced novel topologies coupled with an enhancement of the active network management to provide a means for both flexible and yet secure operation of a future hybrid AC/DC MV distribution network. The application

of the active network management framework introduced in this thesis has been proven to improve network operation in terms of efficiency, reliability, hosting and supply capabilities. This work has developed models which are applicable within the management framework to help all involved parties including DSO, TSO, DG owners and demand aggregators so that they can cooperate and make practical decisions in more cost-effective ways without neglecting the importance of secure network operation. Further explanation on contributions of this work can be summarised in the following subsections.

6.1.1 A Novel ANM Framework (RQ1)

Existing network management schemes for active distribution systems often include one or two individual schemes for example, using DG curtailment to reduce voltage rise at the end feeders in periods of low demand or using technology for demand side management to reduce congestion in the system. Economically speaking, schemes such as DG curtailment and demand side management might not necessarily be related however they are not mutually exclusive and as showed throughout this thesis can be unified together under one active network management (ANM) framework.

At the core of the ANM framework sits a multi-period multi-objective OPF problem formulation which was introduced generally in Chapter 2 and then further expanded depending on the application in subsequent chapters. The ANM framework was showed to be able to (i) enhance voltage profile of the network even under high levels of renewable DG penetration, (ii) reduce the cost of network operation, e.g. import from the grid supply point, (iii) reduce and nearly eradicate the need for DG curtailment further reducing the viability of the DSO toward DG owners and (iv) provide for a secure and resilient network operation.

6.1.2 Enhanced Network Reconfiguration (RQ2)

An enhanced network reconfiguration scheme was introduced in Chapter 3. The scheme used a back-to-back VSC (BTB-VSC) power flow controller for fast network reconfiguration and voltage regulation. It provides for several improvements when

compared to conventional switching schemes using remote controlled mechanical switches. The new scheme (i) enhances the voltage profile by using direct reactive power control of the VSCs in the power flow controller, (ii) reduces the problem and costs associated with wear and tear due to the soft switching of IGBTs as opposed to mechanical switch operation, (iii) provides for regulated power flow control within the network to improve load balancing and eliminate DG curtailment, further enhancing DG hosting capacity at the MV levels.

Meanwhile, the power flow controller (BTB-VSC) was also modelled to reflect the realistic operational profiles of VSCs and the actual PWM control operation of the VSC for active and reactive power control. With the realistic model of the VSCs, the day-ahead active network management framework can still make use of the available reactive power injections and effective coordination with OLTC at the substation transformer to improve bus voltages at the end feeders and reduce DG curtailment.

6.1.3 Large-scale Energy Storage Systems (RQ3)

Energy storage system provides additional benefits in active distribution systems in terms of balancing generation and demand. In this thesis, a large-scale thermal energy storage system (PTES) was modelled and incorporated within the active network management framework. The so-called reduced model for the PTES device was developed to (i) be computationally tractable for non-linear multi-period OPF solutions and (ii) capture the realistic operational profile of the PTES device. The PTES model was compared to a generic so-called classical model with a fixed round-trip efficiency which immediately showed that for purposes of active network management and load balancing the classical model produces rather large errors which could have ramifications both technical and economical for the network operator. The novelty of this work was to develop a reduced model for the PTES which was then validated against a detailed model. The inclusion of the PTES showed clearly that DSO owned storage is a viable solution for economic operation of ADS especially for reducing costs of network operation (i.e. import from the grid and import/export from DG owners) and when considering dynamic pricing schemes.

6.1.4 Hybrid AC/DC Distribution System (RQ4)

Increasing number of DC loads and renewable resources-based DG especially those with internal DC bus has urged the distribution system to operate in DC. The DC system operation paradigm requires many changes in the existing AC distribution network and it is impractical to convert the whole system into DC operation. Instead, in this thesis a new DC system topology was introduced to the part of the network where the highest density of DC resources and loads that would create problems in radial distribution networks (i.e., the end feeders). The existing tie lines at the end feeders are interconnected and converted into DC using a VSC-based DC interface at medium voltage (MVDC) to act as a platform for the DC resources and loads interconnections. The MVDC interface is essentially an expansion of the BTB-VSC interfaces which were introduced in Chapter 3.

Meanwhile, for implementation of the ANM framework, a unified AC/DC OPF formulation was developed. The MVDC interface was then embedded within a realistic UK-based distribution network and compared with embedded P2P-VSC interconnections. The MVDC interface proved successful in (i) improving the overall flexibility of the network (ii) improving the utilisation of the DG resources (iii) enhancing of the voltage profile by providing direct reactive power and improved load balancing.

6.1.5 Security Constrained Operational Planning (RQ5)

Security constraints often are included in transmission systems rather than distribution systems. However, as it was showed in this thesis, the problem of security constraints is equally applicable in ADS especially in hybrid AC/DC networks which may operate in both radial and meshed fashion. In the last part of this thesis, therefore the aim was to enhance the ANM framework with the inclusion of security constraints to guarantee a continuity of supply even after the loss of any one feeder (i.e., upholding an $N-1$ criterion). To this end, a new unified D-SCOPF formulation was developed for the hybrid AC/DC MV distribution network. The demand and generation are arranged in advance (i.e., day-ahead) so that there would not cause

any interruptions on the agreed operating conditions in the event of contingencies. In the contingency situation, DSO uses the ANM facilities such as OLTC or power flow controllers to execute remedial actions to ensure the network constraints are fulfilled.

Two consequence constraints are imposed into the optimisation formulation for the short-term and long-term post-contingency stages at each operating state as presented in Chapter 5 to address different response times between the control devices. Tap changers are slower devices as compared to VSC-based power flow controllers. The post-contingency remedial action time frame is therefore divided into fast and slow stages.

6.2 Improvement and Future Works

The ensuing improved ANM framework in this thesis is the most comprehensive ANM framework with which a DSO (or a group of DSOs) can properly coordinate and manage the operation of a variety of actors (from DG owners to EV aggregators to storage operators) and schemes (demand side management, dynamic pricing) all in one unified framework for ultimate flexibility, resiliency, and reliability of operation. The development of such schemes will undoubtedly pave the way for industry to move further toward adopting innovative technologies/schemes for streamlining the transition of distribution systems from passive to active and realise the decarbonisation of the energy systems as a whole. Notwithstanding this, there is still room for further improvements and future avenues of research which can be explored after the conclusion of this thesis.

6.2.1 Degradation Effects on Storage

The storage model is developed using various operating cycles and states of charge that perform well in the network management framework. However, the storage technology has degradation effect. Since energy is stored thermally, the degradation effect being given by the temperature distribution along the reservoirs. The temperature distributions can change significantly with irregular charging and discharging

rates. In this work, the charging and discharging rates do not obviously differ from one another due to the stored energy is constrained to return to initial condition for the next 24 hours. This effect might be significant in case of long run simulations. Hence, further investigation is required to find the relationship between deviations in the operating cycles and state of charge or efficiency. This study, however, is more appropriate to be carried out for long-term planning framework.

6.2.2 Improved Computational Algorithms

The ANM framework introduced in this thesis can be computationally burdensome. Throughout this thesis, the computational expenditure was overcome through a series of solutions such as model reduction (Chapter 4) and unified formulation (Chapters 3 and 5). Further research into development and implementation of robust computational algorithms (e.g., use of convex optimisation methods) is needed to further enhance the computational efficiency and tractability of such problems.

6.2.3 Stochastic vs Robust Approaches

Throughout this thesis a robust approach was used to compare worst-case scenarios. To this end, for example, the security-constrained operational planning framework follows a deterministic security assessment in this work. For purposes of this thesis, the deterministic approach is deemed sufficient (as a robust worst-case scenario approach is adopted), however another avenue of research is to look at implementation of stochastic formulations of the same framework introduced in this thesis especially given uncertainties in weather forecast, demand variations, etc.

6.2.4 Advanced Multi-period Optimisation

Multi-period optimal power flow based on half-hourly or hourly time period interval has been used in this thesis to evaluate system performance for a day-ahead operation. Larger time interval would increase discrepancies between expected set-points and real-time operation mainly due to forecast errors. Hence, another research is required to study on the implementation of a smaller time period interval simulation

(says 1 or 5 minutes) in a sliding window fashion as an interface platform between the used day-ahead framework and real-time operation.

Bibliography

[1] Eurostat, "Renewable energy statistics," Available at http://ec.europa.eu/eurostat/statistics-explained/index.php/Renewable_energy_statistics [Accessed: 1 Febuary 2018].

[2] W. Evans, C. Michaels, M. Curds, N. Cartwright, J. Halliwell, S. Ashcroft, J. Hemingway, L. Waters, A. Annut, G. Haigh, and I. MacLeay, "Digest of united kingdom energy statistics 2017," Department for Business, Energy & Industrial Strategy, Tech. Rep., 2017.

[3] L. F. Ochoa and G. P. Harrison, "Minimizing energy losses: Optimal accommodation and smart operation of renewable distributed generation," *IEEE Transactions on Power Systems*, vol. 26, no. 1, pp. 198–205, Feb 2011.

[4] A. A. Akhil, G. Huff, A. B. Currier, B. C. Kaun, D. M. Rastler, S. B. Chen, A. L. Cotter, D. T. Bradshaw, and W. D. Gauntlett, "DOE/EPRI electricity storage handbook in collaboration with NRECA," *Sandia Report SAND2015-1002*, 2015.

[5] G. F. Reed, B. M. Grainger, A. R. Sparacino, R. J. Kerestes, and M. J. Korytowski, "Advancements in medium voltage DC architecture development with applications for powering electric vehicle charging stations," in *2012 IEEE Energytech*, May 2012, pp. 1–8.

[6] F. Capitanescu, L. F. Ochoa, H. Margossian, and N. D. Hatziargyriou, "Assessing the potential of network reconfiguration to improve distributed generation hosting capacity in active distribution systems," *IEEE Transactions on Power Systems*, vol. 30, no. 1, pp. 346–356, Jan 2015.

[7] M. Stewart, "Future energy scenarios: July 2017," Available at http://fes.nationalgrid.com/media/1363/fes-interactive-version-final.pdf [Accessed: 10 July 2018].

[8] W. Feero, D. Dawson, and J. Stevens, "White paper on protection issues of the microgrid concept," Consortium for Electric Reliability Technology Solutions, Tech. Rep., 2002.

[9] K. J. P. Macken, M. H. J. Bollen, and R. J. M. Belmans, "Mitigation of voltage dips through distributed generation systems," *IEEE Transactions on Industry Applications*, vol. 40, no. 6, pp. 1686–1693, Nov 2004.

[10] G. Quionez-Varela and A. Cruden, "Development of a small-scale generator set model for local network voltage and frequency stability analysis," *IEEE Transactions on Energy Conversion*, vol. 22, no. 2, pp. 368–375, June 2007.

[11] M. Al-Muhaini and G. T. Heydt, "Evaluating future power distribution system reliability including distributed generation," *IEEE Transactions on Power Delivery*, vol. 28, no. 4, pp. 2264–2272, Oct 2013.

[12] M. Ettehadi, H. Ghasemi, and S. Vaez-Zadeh, "Voltage stability-based DG placement in distribution networks," *IEEE Transactions on Power Delivery*, vol. 28, no. 1, pp. 171–178, Jan 2013.

[13] L. F. Ochoa, C. J. Dent, and G. P. Harrison, "Distribution network capacity assessment: Variable dg and active networks," *IEEE Transactions on Power Systems*, vol. 25, no. 1, pp. 87–95, Feb 2010.

[14] K. Nekooei, M. M. Farsangi, H. Nezamabadi-Pour, and K. Y. Lee, "An improved multi-objective harmony search for optimal placement of DGs in distribution systems," *IEEE Transactions on Smart Grid*, vol. 4, no. 1, pp. 557–567, March 2013.

[15] K. Mahmoud, N. Yorino, and A. Ahmed, "Optimal distributed generation allocation in distribution systems for loss minimization," *IEEE Transactions on Power Systems*, vol. 31, no. 2, pp. 960–969, March 2016.

[16] R. Sanjay, T. Jayabarathi, T. Raghunathan, V. Ramesh, and N. Mithulananthan, "Optimal allocation of distributed generation using hybrid grey wolf optimizer," *IEEE Access*, vol. 5, pp. 14 807–14 818, 2017.

[17] T. Boehme, G. P. Harrison, and A. R. Wallace, "Assessment of distribution network limits for non-firm connection of renewable generation," *IET Renewable Power Generation*, vol. 4, no. 1, pp. 64–74, January 2010.

[18] S. S. Al-Kaabi, H. H. Zeineldin, and V. Khadkikar, "Planning active distribution networks considering multi-DG configurations," *IEEE Transactions on Power Systems*, vol. 29, no. 2, pp. 785–793, March 2014.

[19] R. Bayindir, I. Colak, G. Fulli, and K. Demirtas, "Smart grid technologies and applications," *Renewable and Sustainable Energy Reviews*, vol. 66, pp. 499 – 516, 2016.

[20] F. Pilo, S. Jupe, F. Silvestro, C. Abbey, A. Baitch, B. Bak-Jensen *et al.*, "Planning and optimization methods for active distribution systems," CIGRE Working Group C6.19, Tech. Rep., 2014.

[21] S. Auchariyamet and S. Sirisumrannukul, "Optimal daily coordination of volt/VAr control devices in distribution systems with distributed generators," in *Universities Power Engineering Conference (UPEC), 2010 45th International*, Aug 2010, pp. 1–6.

[22] M. A. Kashem and G. Ledwich, "Multiple distributed generators for distribution feeder voltage support," *IEEE Transactions on Energy Conversion*, vol. 20, no. 3, pp. 676–684, Sept 2005.

[23] M. J. Dolan, E. M. Davidson, I. Kockar, G. W. Ault, and S. D. J. McArthur, "Distribution power flow management utilizing an online optimal power flow technique," *IEEE Transactions on Power Systems*, vol. 27, no. 2, pp. 790–799, May 2012.

[24] M. J. Dolan, E. M. Davidson, G. W. Ault, K. R. W. Bell, and S. D. J. McArthur, "Distribution power flow management utilizing an online constraint

programming method," *IEEE Transactions on Smart Grid*, vol. 4, no. 2, pp. 798–805, June 2013.

[25] G. Carpinelli, G. Celli, S. Mocci, F. Mottola, F. Pilo, and D. Proto, "Optimal integration of distributed energy storage devices in smart grids," *IEEE Transactions on Smart Grid*, vol. 4, no. 2, pp. 985–995, June 2013.

[26] S. Gill, I. Kockar, and G. W. Ault, "Dynamic optimal power flow for active distribution networks," *IEEE Transactions on Power Systems*, vol. 29, no. 1, pp. 121–131, Jan 2014.

[27] A. S. Bouhouras, G. C. Christoforidis, C. Parisses, and D. P. Labridis, "Reducing network congestion in distribution networks with high DG penetration via network reconfiguration," in *11th International Conference on the European Energy Market (EEM14)*, May 2014, pp. 1–5.

[28] F. Capitanescu, I. Bilibin, and E. R. Ramos, "A comprehensive centralized approach for voltage constraints management in active distribution grid," *IEEE Transactions on Power Systems*, vol. 29, no. 2, pp. 933–942, March 2014.

[29] P. S. Georgilakis and N. D. Hatziargyriou, "Optimal distributed generation placement in power distribution networks: Models, methods, and future research," *IEEE Transactions on Power Systems*, vol. 28, no. 3, pp. 3420–3428, Aug 2013.

[30] A. Borghetti, M. Bosetti, S. Grillo, S. Massucco, C. A. Nucci, M. Paolone, and F. Silvestro, "Short-term scheduling and control of active distribution systems with high penetration of renewable resources," *IEEE Systems Journal*, vol. 4, no. 3, pp. 313–322, Sept 2010.

[31] M. Falahi, S. Lotfifard, M. Ehsani, and K. Butler-Purry, "Dynamic model predictive-based energy management of DG integrated distribution systems," *IEEE Transactions on Power Delivery*, vol. 28, no. 4, pp. 2217–2227, Oct 2013.

[32] S. Agrawal, B. K. Panigrahi, and M. K. Tiwari, "Multiobjective particle swarm algorithm with fuzzy clustering for electrical power dispatch," *IEEE Transactions on Evolutionary Computation*, vol. 12, no. 5, pp. 529–541, Oct 2008.

[33] L. Zhang, X. Xu, S. Wang, M. Ma, C. Zhou, and C. Sun, "Solved environmental/economic dispatch based on multi-objective PSO," in *Intelligent Computation Technology and Automation (ICICTA), 2010 International Conference on*, vol. 3, May 2010, pp. 352–355.

[34] W. Qiu, J. Zhang, X. Jin, and X. Bai, "Using multi-objective differential evolution and TOPSIS technique for environmental/economic dispatch with security constraints," in *Electric Utility Deregulation and Restructuring and Power Technologies (DRPT), 2011 4th International Conference on*, July 2011, pp. 847–852.

[35] S. Krishnamurthy and R. Tzoneva, "Comparison of the lagrange's and particle swarm optimisation solutions of an economic emission dispatch problem with transmission constraints," in *2012 IEEE International Conference on Power Electronics, Drives and Energy Systems (PEDES)*, Dec 2012, pp. 1–8.

[36] T. Niknam, R. Azizipanah-Abarghooee, M. Zare, and B. Bahmani-Firouzi, "Reserve constrained dynamic environmental/economic dispatch: A new multiobjective self-adaptive learning bat algorithm," *IEEE Systems Journal*, vol. 7, no. 4, pp. 763–776, Dec 2013.

[37] B. Zhou, K. W. Chan, T. Yu, and C. Y. Chung, "Equilibrium-inspired multiple group search optimization with synergistic learning for multiobjective electric power dispatch," *IEEE Transactions on Power Systems*, vol. 28, no. 4, pp. 3534–3545, Nov 2013.

[38] B. R. Pereira Junior, A. M. Cossi, and J. R. S. Mantovani, "Multiobjective short-term planning of electric power distribution systems using NSGA-II," *Journal of Control, Automation and Electrical Systems*, vol. 24, no. 3, pp. 286–299, Jun 2013.

[39] T.-H. Chen, E.-H. Lin, N.-C. Yang, and T.-Y. Hsieh, "Multi-objective optimization for upgrading primary feeders with distributed generators from normally closed loop to mesh arrangement," *International Journal of Electrical Power & Energy Systems*, vol. 45, no. 1, pp. 413 – 419, 2013.

[40] D. Ranamuka, A. P. Agalgaonkar, and K. M. Muttaqi, "Online voltage control in distribution systems with multiple voltage regulating devices," *IEEE Transactions on Sustainable Energy*, vol. 5, no. 2, pp. 617–628, April 2014.

[41] G. J. Rosseti, E. J. de Oliveira, L. W. de Oliveira, I. C. Silva, and W. Peres, "Optimal allocation of distributed generation with reconfiguration in electric distribution systems," *Electric Power Systems Research*, vol. 103, pp. 178 – 183, 2013.

[42] P. Siano, P. Chen, Z. Chen, and A. Piccolo, "Evaluating maximum wind energy exploitation in active distribution networks," *IET Generation, Transmission Distribution*, vol. 4, no. 5, pp. 598–608, May 2010.

[43] M. Alizadeh, Y. Xiao, A. Scaglione, and M. van der Schaar, "Dynamic incentive design for participation in direct load scheduling programs," *IEEE Journal of Selected Topics in Signal Processing*, vol. 8, no. 6, pp. 1111–1126, Dec 2014.

[44] G. Mokryani, "Active distribution networks planning with integration of demand response," *Solar Energy*, vol. 122, pp. 1362 – 1370, 2015.

[45] X. Lin, J. Sun, S. Ai, X. Xiong, Y. Wan, and D. Yang, "Distribution network planning integrating charging stations of electric vehicle with V2G," *International Journal of Electrical Power & Energy Systems*, vol. 63, pp. 507 – 512, 2014.

[46] B. Zeng, J. Feng, J. Zhang, and Z. Liu, "An optimal integrated planning method for supporting growing penetration of electric vehicles in distribution systems," *Energy*, vol. 126, pp. 273 – 284, 2017.

[47] A. Borghetti, "A mixed-integer linear programming approach for the computation of the minimum-losses radial configuration of electrical distribution networks," *IEEE Transactions on Power Systems*, vol. 27, no. 3, pp. 1264–1273, Aug 2012.

[48] R. S. Rao, K. Ravindra, K. Satish, and S. V. L. Narasimham, "Power loss minimization in distribution system using network reconfiguration in the presence of distributed generation," *IEEE Transactions on Power Systems*, vol. 28, no. 1, pp. 317–325, Feb 2013.

[49] C. Lee, C. Liu, S. Mehrotra, and Z. Bie, "Robust distribution network reconfiguration," *IEEE Transactions on Smart Grid*, vol. 6, no. 2, pp. 836–842, March 2015.

[50] K. Chen, W. Wu, B. Zhang, S. Djokic, and G. P. Harrison, "A method to evaluate total supply capability of distribution systems considering network reconfiguration and daily load curves," *IEEE Transactions on Power Systems*, vol. 31, no. 3, pp. 2096–2104, May 2016.

[51] A. Elmitwally, M. Elsaid, M. Elgamal, and Z. Chen, "A fuzzy-multiagent self-healing scheme for a distribution system with distributed generations," *IEEE Transactions on Power Systems*, vol. 30, no. 5, pp. 2612–2622, Sept 2015.

[52] N. C. Koutsoukis, D. O. Siagkas, P. S. Georgilakis, and N. D. Hatziargyriou, "Online reconfiguration of active distribution networks for maximum integration of distributed generation," *IEEE Transactions on Automation Science and Engineering*, vol. 14, no. 2, pp. 437–448, April 2017.

[53] H. Shareef, A. Ibrahim, N. Salman, A. Mohamed, and W. L. Ai, "Power quality and reliability enhancement in distribution systems via optimum network reconfiguration by using quantum firefly algorithm," *International Journal of Electrical Power & Energy Systems*, vol. 58, pp. 160 – 169, 2014.

[54] T. T. Nguyen and A. V. Truong, "Distribution network reconfiguration for power loss minimization and voltage profile improvement using cuckoo search

algorithm," *International Journal of Electrical Power & Energy Systems*, vol. 68, pp. 233 – 242, 2015.

[55] N. G. Paterakis, A. Mazza, S. F. Santos, O. Erdinc, G. Chicco, A. G. Bakirtzis, and J. Catalao, "Multi-objective reconfiguration of radial distribution systems using reliability indices," in *2016 IEEE/PES Transmission and Distribution Conference and Exposition (T D)*, May 2016, pp. 1–1.

[56] S. Ray, A. Bhattacharya, and S. Bhattacharjee, "Optimal placement of switches in a radial distribution network for reliability improvement," *International Journal of Electrical Power & Energy Systems*, vol. 76, pp. 53 – 68, 2016.

[57] J. Lakkireddy, R. Rastgoufard, I. Leevongwat, and P. Rastgoufard, "Steady state voltage stability enhancement using shunt and series FACTS devices," in *Power Systems Conference (PSC), 2015 Clemson University*, March 2015, pp. 1–5.

[58] B. Kroposki, C. Pink, R. DeBlasio, H. Thomas, M. Simes, and P. K. Sen, "Benefits of power electronic interfaces for distributed energy systems," *IEEE Transactions on Energy Conversion*, vol. 25, no. 3, pp. 901–908, Sept 2010.

[59] J. M. Bloemink and T. C. Green, "Increasing distributed generation penetration using soft normally-open points," in *IEEE PES General Meeting*, July 2010, pp. 1–8.

[60] ——, "Benefits of distribution-level power electronics for supporting distributed generation growth," *IEEE Transactions on Power Delivery*, vol. 28, no. 2, pp. 911–919, April 2013.

[61] A. Gabash and P. Li, "Active-reactive optimal power flow in distribution networks with embedded generation and battery storage," *IEEE Transactions on Power Systems*, vol. 27, no. 4, pp. 2026–2035, Nov 2012.

[62] Y. Levron, J. M. Guerrero, and Y. Beck, "Optimal power flow in microgrids with energy storage," *IEEE Transactions on Power Systems*, vol. 28, no. 3, pp. 3226–3234, Aug 2013.

[63] T. Desrues, J. Ruer, P. Marty, and J. Fourmigu, "A thermal energy storage process for large scale electric applications," *Applied Thermal Engineering*, vol. 30, no. 5, pp. 425 – 432, 2010.

[64] A. White, G. Parks, and C. N. Markides, "Thermodynamic analysis of pumped thermal electricity storage," *Applied Thermal Engineering*, vol. 53, no. 2, pp. 291 – 298, 2013.

[65] J. D. McTigue, A. J. White, and C. N. Markides, "Parametric studies and optimisation of pumped thermal electricity storage," *Applied Energy*, vol. 137, pp. 800 – 811, 2015.

[66] F. Gonzalez-Longatt, J. M. Roldan, and C. A. Charalambous, "Solution of AC/DC power flow on a multiterminal HVDC system: Illustrative case supergrid phase i," in *2012 47th International Universities Power Engineering Conference (UPEC)*, Sept 2012, pp. 1–7.

[67] X. Bai and H. Wei, "Semi-definite programming-based method for security-constrained unit commitment with operational and optimal power flow constraints," *IET Generation, Transmission Distribution*, vol. 3, no. 2, pp. 182–197, February 2009.

[68] F. Capitanescu, T. V. Cutsem, and L. Wehenkel, "Coupling optimization and dynamic simulation for preventive-corrective control of voltage instability," *IEEE Transactions on Power Systems*, vol. 24, no. 2, pp. 796–805, May 2009.

[69] F. Capitanescu, J. M. Ramos, P. Panciatici, D. Kirschen, A. M. Marcolini, L. Platbrood, and L. Wehenkel, "State-of-the-art, challenges, and future trends in security constrained optimal power flow," *Electric Power Systems Research*, vol. 81, no. 8, pp. 1731 – 1741, 2011.

[70] D. Phan and J. Kalagnanam, "Some efficient optimization methods for solving the security-constrained optimal power flow problem," *IEEE Transactions on Power Systems*, vol. 29, no. 2, pp. 863–872, March 2014.

[71] R. Madani, M. Ashraphijuo, and J. Lavaei, "Promises of conic relaxation for contingency-constrained optimal power flow problem," *IEEE Transactions on Power Systems*, vol. 31, no. 2, pp. 1297–1307, March 2016.

[72] Standard EN50160, *Voltage Characteristics of Electricity Supplied by Public Distribution Systems*, Standard EN 50160 Std., 1994.

[73] Statutory Instruments, *The Electricity Safety, Quality and Continuity Regulations*, Statutory Instruments Std., 2002.

[74] Electricity Association, *Planning limits for voltage fluctuations caused by industrial, commercial and domestic equipment in the United Kingdom*, Electricity Association Engineering Recommendation P28 Std., 1989.

[75] American National Standards Institute, *American National Standard for Electric Power Systems and Equipment-Voltage Ratings (60 Hertz)*, American National Standards Institute Std., 1996.

[76] M. A. Mahmud, M. J. Hossain, H. R. Pota, and A. B. M. Nasiruzzaman, "Voltage control of distribution networks with distributed generation using reactive power compensation," in *IECON 2011 - 37th Annual Conference on IEEE Industrial Electronics Society*, Nov 2011, pp. 985–990.

[77] T. Green, R. Silversides, and T. Lüth, "Power electronics in distribution system management," HubNet Position Paper Series, Tech. Rep., 2015.

[78] S. Li, M. Ding, and S. Du, "Transmission loadability with field current control under voltage depression," *IEEE Transactions on Power Delivery*, vol. 24, no. 4, pp. 2142–2149, Oct 2009.

[79] H. Zhan, C. Wang, Y. Wang, X. Yang, X. Zhang, C. Wu, and Y. Chen, "Relay protection coordination integrated optimal placement and sizing of

distributed generation sources in distribution networks," *IEEE Transactions on Smart Grid*, vol. 7, no. 1, pp. 55–65, Jan 2016.

[80] V. H. M. Quezada, J. R. Abbad, and T. G. S. Roman, "Assessment of energy distribution losses for increasing penetration of distributed generation," *IEEE Transactions on Power Systems*, vol. 21, no. 2, pp. 533–540, May 2006.

[81] C. Battistelli, G. Carpinelli, U. D. Martinis, F. Mottola, and D. Proto, "Optimization methods with power quality issues for reactive power control of distribution networks with dispersed generation," in *2009 IEEE Bucharest PowerTech*, June 2009, pp. 1–8.

[82] M. Bollen, "What is power quality?" *Electric Power Systems Research*, vol. 66, no. 1, pp. 5 – 14, 2003.

[83] Energy Networks Association, *Engineering Recommendation G5/4-1: Planning Levels for Harmonic Voltage Distortion and the Connection of Non-Linear Equipment to Transmission Systems and Distribution Networks in the United Kingdom*, Energy Networks Association Std., 2005.

[84] A. D. Ko, G. M. Burt, S. Galloway, C. Booth, and J. R. Mcdonald, "Uk distribution system protection issues," *IET Generation, Transmission Distribution*, vol. 1, no. 4, pp. 679–687, July 2007.

[85] S. M. Brahma and A. A. Girgis, "Development of adaptive protection scheme for distribution systems with high penetration of distributed generation," *IEEE Transactions on Power Delivery*, vol. 19, no. 1, pp. 56–63, Jan 2004.

[86] W. Sun and G. P. Harrison, "Influence of generator curtailment priority on network hosting capacity," in *22nd International Conference and Exhibition on Electricity Distribution (CIRED 2013)*, June 2013, pp. 1–4.

[87] M. A. Mahmud, M. J. Hossain, and H. R. Pota, "Voltage variation on distribution networks with distributed generation: Worst case scenario," *IEEE Systems Journal*, vol. 8, no. 4, pp. 1096–1103, Dec 2014.

[88] M. Damarija and A. Keane, "Autonomous curtailment control in distributed generation planning," *IEEE Transactions on Smart Grid*, vol. 7, no. 3, pp. 1337–1345, May 2016.

[89] I. Momber, S. Wogrin, and T. G. S. Romn, "Retail pricing: A bilevel program for pev aggregator decisions using indirect load control," *IEEE Transactions on Power Systems*, vol. 31, no. 1, pp. 464–473, Jan 2016.

[90] S. Carr, G. C. Premier, A. J. Guwy, R. M. Dinsdale, and J. Maddy, "Energy storage for active network management on electricity distribution networks with wind power," *IET Renewable Power Generation*, vol. 8, no. 3, pp. 249–259, April 2014.

[91] M. Sedghi, A. Ahmadian, and M. Aliakbar-Golkar, "Optimal storage planning in active distribution network considering uncertainty of wind power distributed generation," *IEEE Transactions on Power Systems*, vol. 31, no. 1, pp. 304–316, Jan 2016.

[92] M. Rylander, L. Rogers, and J. Smith, "Distribution feeder hosting capacity: What matters when planning for DER?" The Electric Power Research Institute, Tech. Rep., 2015.

[93] N. C. Scott, D. J. Atkinson, and J. E. Morrell, "Use of load control to regulate voltage on distribution networks with embedded generation," *IEEE Transactions on Power Systems*, vol. 17, no. 2, pp. 510–515, May 2002.

[94] P. N. Vovos, A. E. Kiprakis, A. R. Wallace, and G. P. Harrison, "Centralized and distributed voltage control: Impact on distributed generation penetration," *IEEE Transactions on Power Systems*, vol. 22, no. 1, pp. 476–483, Feb 2007.

[95] R. Billinton and D. Lakhanpal, "Impacts of demand-side management on reliability cost/reliability worth analysis," *IEE Proceedings - Generation, Transmission and Distribution*, vol. 143, no. 3, pp. 225–231, May 1996.

[96] M.-G. Jeong, S.-I. Moon, and P.-I. Hwang, "Indirect load control for energy storage systems using incentive pricing under time-of-use tariff," *Energies*, vol. 9, no. 7, p. 558, 2016.

[97] A. Haque, M. Nijhuis, G. Ye, P. Nguyen, F. Bliek, and J. Slootweg, "Integrating direct and indirect load control for congestion management in LV networks," *IEEE Transactions on Smart Grid*, pp. 1–11, 2017, in Press.

[98] W. Yu, D. Liu, and Y. Huang, "Operation optimization based on the power supply and storage capacity of an active distribution network," *Energies*, vol. 6, no. 12, pp. 6423–6438, 2013.

[99] H. Chen, T. N. Cong, W. Yang, C. Tan, Y. Li, and Y. Ding, "Progress in electrical energy storage system: A critical review," *Progress in Natural Science*, vol. 19, no. 3, pp. 291 – 312, 2009.

[100] Y. Xu and C. Singh, "Power system reliability impact of energy storage integration with intelligent operation strategy," *IEEE Transactions on Smart Grid*, vol. 5, no. 2, pp. 1129–1137, March 2014.

[101] T. A. Taj, H. M. Hasanien, A. I. Alolah, and S. M. Muyeen, "Transient stability enhancement of a grid-connected wind farm using an adaptive neuro-fuzzy controlled-flywheel energy storage system," *IET Renewable Power Generation*, vol. 9, no. 7, pp. 792–800, 2015.

[102] W. Liu, S. Niu, and H. Xu, "Optimal planning of battery energy storage considering reliability benefit and operation strategy in active distribution system," *Journal of Modern Power Systems and Clean Energy*, vol. 5, no. 2, p. 177, 2016.

[103] D. Haughton and G. T. Heydt, "Smart distribution system design: Automatic reconfiguration for improved reliability," in *IEEE PES General Meeting*, July 2010, pp. 1–8.

[104] A. Asrari, T. Wu, and S. Lotfifard, "The impacts of distributed energy sources on distribution network reconfiguration," *IEEE Transactions on Energy Conversion*, vol. 31, no. 2, pp. 606–613, June 2016.

[105] R. A. Jabr, R. Singh, and B. C. Pal, "Minimum loss network reconfiguration using mixed-integer convex programming," *IEEE Transactions on Power Systems*, vol. 27, no. 2, pp. 1106–1115, May 2012.

[106] Energy Networks Association, "Active network management: Good practice guide," Available at http://www.energynetworks.org/assets/files/news/publications/1500205_ENA_ANM_report_AW_online.pdf [Accessed: 15 May 2016].

[107] T. N. Samuel and N. K. Nohria, "Digital control and instrumentation for step-voltage regulators," *IEEE Transactions on Power Apparatus and Systems*, vol. PAS-104, no. 1, pp. 194–199, Jan 1985.

[108] Y. V. Joshi, S. S. Deshpande, and S. G. Kahalekar, "Microprocessor based automatic power factor control," in *TENCON '93. Proceedings. Computer, Communication, Control and Power Engineering.1993 IEEE Region 10 Conference on*, vol. 5, Oct 1993, pp. 326–329 vol.5.

[109] C. A. McCarthy and J. Josken, "Applying capacitors to maximize benefits of conservation voltage reduction," in *Rural Electric Power Conference, 2003*, May 2003, pp. C4–1–C4–5.

[110] W. H. Kersting, "Distribution feeder voltage regulation control," *IEEE Transactions on Industry Applications*, vol. 46, no. 2, pp. 620–626, March 2010.

[111] R. Tonkoski, L. A. C. Lopes, and T. H. M. El-Fouly, "Coordinated active power curtailment of grid connected PV inverters for overvoltage prevention," *IEEE Transactions on Sustainable Energy*, vol. 2, no. 2, pp. 139–147, April 2011.

[112] E. Demirok, P. C. Gonzlez, K. H. B. Frederiksen, D. Sera, P. Rodriguez, and R. Teodorescu, "Local reactive power control methods for overvoltage

prevention of distributed solar inverters in low-voltage grids," *IEEE Journal of Photovoltaics*, vol. 1, no. 2, pp. 174–182, Oct 2011.

[113] L. L. Lai, "The impact of new technology on energy management systems and SCADA," in *IEE Colloquium on Advanced SCADA and Energy Management Systems*, Dec 1990, pp. 1–3.

[114] T. B. Girotti, N. B. Tweed, and N. R. Houser, "Real-time VAr control by SCADA," *IEEE Transactions on Power Systems*, vol. 5, no. 1, pp. 61–64, Feb 1990.

[115] M. E. Baran and M.-Y. Hsu, "Volt/Var control at distribution substations," *IEEE Transactions on Power Systems*, vol. 14, no. 1, pp. 312–318, Feb 1999.

[116] T. E. Kim and J. E. Kim, "Voltage regulation coordination of distributed generation system in distribution system," in *2001 Power Engineering Society Summer Meeting. Conference Proceedings (Cat. No.01CH37262)*, vol. 1, July 2001, pp. 480–484.

[117] M. M. A. Salama and A. Y. Chikhani, "An expert system for reactive power control of a distribution system. i. system configuration," *IEEE Transactions on Power Delivery*, vol. 7, no. 2, pp. 940–945, Apr 1992.

[118] J. R. P. R. Laframboise, G. Ferland, A. Y. Chikhani, and M. M. A. Salama, "An expert system for reactive power control of a distribution system. part 2: system implementation," *IEEE Transactions on Power Systems*, vol. 10, no. 3, pp. 1433–1441, Aug 1995.

[119] M. E. Elkhatib, R. El-Shatshat, and M. M. A. Salama, "Novel coordinated voltage control for smart distribution networks with DG," *IEEE Transactions on Smart Grid*, vol. 2, no. 4, pp. 598–605, Dec 2011.

[120] I. Roytelman, B. K. Wee, and R. L. Lugtu, "Volt/var control algorithm for modern distribution management system," *IEEE Transactions on Power Systems*, vol. 10, no. 3, pp. 1454–1460, Aug 1995.

[121] I. Roytelman, B. K. Wee, R. L. Lugtu, T. M. Kulas, and T. Brossart, "Pilot project to estimate the centralized volt/VAr control effectiveness," *IEEE Transactions on Power Systems*, vol. 13, no. 3, pp. 864–869, Aug 1998.

[122] Q. Zhou and J. W. Bialek, "Generation curtailment to manage voltage constraints in distribution networks," *IET Generation, Transmission Distribution*, vol. 1, no. 3, pp. 492–498, May 2007.

[123] C. Benoit, A. Mercier, Y. Bsanger, and F. Wurtz, "Deterministic optimal power flow for smart grid short-term predictive energy management," in *2013 IEEE Grenoble Conference*, June 2013, pp. 1–7.

[124] Y. M. Atwa, E. F. El-Saadany, M. M. A. Salama, and R. Seethapathy, "Optimal renewable resources mix for distribution system energy loss minimization," *IEEE Transactions on Power Systems*, vol. 25, no. 1, pp. 360–370, Feb 2010.

[125] T. Senjyu, Y. Miyazato, A. Yona, N. Urasaki, and T. Funabashi, "Optimal distribution voltage control and coordination with distributed generation," *IEEE Transactions on Power Delivery*, vol. 23, no. 2, pp. 1236–1242, April 2008.

[126] T. Niknam, "A new approach based on ant colony optimization for daily Volt/Var control in distribution networks considering distributed generators," *Energy Conversion and Management*, vol. 49, no. 12, pp. 3417 – 3424, 2008.

[127] R. S. Rao, S. Narasimham, and M. Ramalingaraju, "Optimization of distribution network configuration for loss reduction using artificial bee colony algorithm," *International Journal of Electrical Power and Energy Systems Engineering*, vol. 1, no. 2, pp. 116–122, 2008.

[128] A. Abdelaziz, F. Mohamed, S. Mekhamer, and M. Badr, "Distribution system reconfiguration using a modified tabu search algorithm," *Electric Power Systems Research*, vol. 80, no. 8, pp. 943 – 953, 2010.

[129] J. Olamaei, T. Niknam, and G. Gharehpetian, "Application of particle swarm optimization for distribution feeder reconfiguration considering distributed

generators," *Applied Mathematics and Computation*, vol. 201, no. 12, pp. 575 – 586, 2008.

[130] B. B. Zad, H. Hasanvand, J. Lobry, and F. Valle, "Optimal reactive power control of DGs for voltage regulation of MV distribution systems using sensitivity analysis method and PSO algorithm," *International Journal of Electrical Power & Energy Systems*, vol. 68, pp. 52 – 60, 2015.

[131] T. W. Eberly and R. C. Schaefer, "Voltage versus VAr/power-factor regulation on synchronous generators," *IEEE Transactions on Industry Applications*, vol. 38, no. 6, pp. 1682–1687, Nov 2002.

[132] A. Keane, Q. Zhou, J. W. Bialek, and M. O'Malley, "Planning and operating non-firm distributed generation," *IET Renewable Power Generation*, vol. 3, no. 4, pp. 455–464, December 2009.

[133] H. Ahmadi and J. R. Marti, "Linear current flow equations with application to distribution systems reconfiguration," *IEEE Transactions on Power Systems*, vol. 30, no. 4, pp. 2073–2080, July 2015.

[134] B. Borchers and J. E. Mitchell, "An improved branch and bound algorithm for mixed integer nonlinear programs," *Computers & Operations Research*, vol. 21, no. 4, pp. 359 – 367, 1994.

[135] R. Smith, "System operability framework 2016: UK electricity transmission," National Grid, Tech. Rep., 2016.

[136] O. Samuelsson, S. Repo, R. Jessler, J. Aho, M. Krenlampi, and A. Malmquist, "Active distribution network demonstration project adine," in *2010 IEEE PES Innovative Smart Grid Technologies Conference Europe (ISGT Europe)*, Oct 2010, pp. 1–8.

[137] E. Peeters, D. Six, M. Hommelberg, R. Belhomme, and F. Bouffard, "The address project: An architecture and markets to enable active demand," in *2009 6th International Conference on the European Energy Market*, May 2009, pp. 1–5.

[138] D. Stein, L. Consiglio, and J. Stromsather, "Enel's large scale demonstration project inside grid4eu: The challenge of res integration in the mv network," in *22nd International Conference and Exhibition on Electricity Distribution (CIRED 2013)*, June 2013, pp. 1–4.

[139] M. Panwar, G. P. Duggan, R. T. Griffin, S. Suryanarayanan, D. Zimmerle, M. Pool, and S. Brunner, "Dispatch in microgrids: Lessons from the fort collins renewable and distributed systems integration demonstration project," *The Electricity Journal*, vol. 25, no. 8, pp. 71 – 83, 2012. [Online]. Available: http://www.sciencedirect.com/science/article/pii/S1040619012002151

[140] D. Craig and C. Befus, "Implementation of a distributed control system for electric distribution circuit reconfiguration," in *IEEE Power Engineering Society General Meeting, 2005*, June 2005, pp. 2436–2441 Vol. 3.

[141] J. Liu, H. Gao, Z. Ma, and Y. Li, "Review and prospect of active distribution system planning," *Journal of Modern Power Systems and Clean Energy*, vol. 3, no. 4, pp. 457–467, 2015.

[142] P. Finn and C. Fitzpatrick, "Demand side management of industrial electricity consumption: Promoting the use of renewable energy through real-time pricing," *Applied Energy*, vol. 113, no. Supplement C, pp. 11 – 21, 2014.

[143] W. Zhang, G. Chen, Z. Dong, J. Li, and Z. Wu, "An efficient algorithm for optimal real-time pricing strategy in smart grid," in *2014 IEEE PES General Meeting — Conference Exposition*, July 2014, pp. 1–5.

[144] L. Jia and L. Tong, "Dynamic pricing and distributed energy management for demand response," *IEEE Transactions on Smart Grid*, vol. 7, no. 2, pp. 1128–1136, March 2016.

[145] Y. Okawa and T. Namerikawa, "Distributed dynamic pricing based on demand-supply balance and voltage phase difference in power grid," *Control Theory and Technology*, vol. 13, no. 2, pp. 90–100, May 2015.

[146] R. Weron, "Electricity price forecasting: A review of the state-of-the-art with a look into the future," *International Journal of Forecasting*, vol. 30, no. 4, pp. 1030 – 1081, 2014.

[147] A. Papavasiliou, "Analysis of distribution locational marginal prices," *IEEE Transactions on Smart Grid*, vol. PP, no. 99, pp. 1–1, 2017.

[148] Ofgem, "Feed-in tariff : Annual report 2016," The Office of Gas and Electricity Markets, Tech. Rep., 2016.

[149] ——, "Renewable obligation: Annual report 2015-16," The Office of Gas and Electricity Markets, Tech. Rep., 2017.

[150] R. A. F. Currie, G. W. Ault, C. E. T. Foote, N. M. McNeill, and A. K. Gooding, "Smarter ways to provide grid connections for renewable generators," in *IEEE PES General Meeting*, July 2010, pp. 1–6.

[151] L. Kane and G. Ault, "A review and analysis of renewable energy curtailment schemes and principles of access: Transitioning towards business as usual," *Energy Policy*, vol. 72, pp. 67 – 77, 2014.

[152] R. J. Bessa, M. A. Matos, F. J. Soares, and J. A. P. Lopes, "Optimized bidding of a EV aggregation agent in the electricity market," *IEEE Transactions on Smart Grid*, vol. 3, no. 1, pp. 443–452, March 2012.

[153] D. A. Sbordone, E. M. Carlini, B. D. Pietra, and M. Devetsikiotis, "The future interaction between virtual aggregator-TSO-DSO to increase DG penetration," in *2015 International Conference on Smart Grid and Clean Energy Technologies (ICSGCE)*, Oct 2015, pp. 201–205.

[154] B. Kroposki, P. K. Sen, and K. Malmedal, "Optimum sizing and placement of distributed and renewable energy sources in electric power distribution systems," *IEEE Transactions on Industry Applications*, vol. 49, no. 6, pp. 2741–2752, Nov 2013.

[155] S. H. Lee and J. W. Park, "Optimal placement and sizing of multiple DGs in a practical distribution system by considering power loss," *IEEE Transactions on Industry Applications*, vol. 49, no. 5, pp. 2262–2270, Sept 2013.

[156] W. A. Bukhsh, A. Grothey, K. I. M. McKinnon, and P. A. Trodden, "Local solutions of the optimal power flow problem," *IEEE Transactions on Power Systems*, vol. 28, no. 4, pp. 4780–4788, Nov 2013.

[157] J. Bisschop and M. Roelofs, *AIMMS Language Reference, Version 3.12*, 2011.

[158] R. D. Zimmerman, C. E. Murillo-Sanchez, and R. J. Thomas, "MATPOWER: Steady-state operations, planning, and analysis tools for power systems research and education," *IEEE Transactions on Power Systems*, vol. 26, no. 1, pp. 12–19, Feb 2011.

[159] M. E. Baran and F. F. Wu, "Network reconfiguration in distribution systems for loss reduction and load balancing," *IEEE Transactions on Power Delivery*, vol. 4, no. 2, pp. 1401–1407, Apr 1989.

[160] W. Cao, J. Wu, and N. Jenkins, "Feeder load balancing in MV distribution networks using soft normally-open points," in *IEEE PES Innovative Smart Grid Technologies, Europe*, Oct 2014, pp. 1–6.

[161] M. R. Dorostkar-Ghamsari, M. Fotuhi-Firuzabad, M. Lehtonen, and A. Safdarian, "Value of distribution network reconfiguration in presence of renewable energy resources," *IEEE Transactions on Power Systems*, vol. 31, no. 3, pp. 1879–1888, May 2016.

[162] C. Foote, P. Djapic, G. Ault, J. Mutale, and G. Strbac, "United kingdom generic distribution system (UKGDS): Defining the generic networks," DTI Centre for Distributed Generation and Sustainable Electrical Energy, Tech. Rep., 2005.

[163] A. Merlin and H. Back, "Search for a minimal-loss operating spanning tree configuration in an urban power distribution system," in *Proc. 5th Power System Computation Conference (PSCC)*, Cambridge, U.K., Sep. 1975.

[164] D. Shirmohammadi and H. W. Hong, "Reconfiguration of electric distribution networks for resistive line losses reduction," *IEEE Transactions on Power Delivery*, vol. 4, no. 2, pp. 1492–1498, Apr 1989.

[165] H. D. Chiang and R. Jean-Jumeau, "Optimal network reconfigurations in distribution systems. i. a new formulation and a solution methodology," *IEEE Transactions on Power Delivery*, vol. 5, no. 4, pp. 1902–1909, Oct 1990.

[166] ——, "Optimal network reconfigurations in distribution systems. ii. solution algorithms and numerical results," *IEEE Transactions on Power Delivery*, vol. 5, no. 3, pp. 1568–1574, Jul 1990.

[167] H.-C. Chang and C.-C. Kuo, "Network reconfiguration in distribution systems using simulated annealing," *Electric Power Systems Research*, vol. 29, no. 3, pp. 227 – 238, 1994.

[168] C.-T. Su, C.-F. Chang, and J.-P. Chiou, "Distribution network reconfiguration for loss reduction by ant colony search algorithm," *Electric Power Systems Research*, vol. 75, no. 2, pp. 190 – 199, 2005.

[169] C. F. Chang, "Reconfiguration and capacitor placement for loss reduction of distribution systems by ant colony search algorithm," *IEEE Transactions on Power Systems*, vol. 23, no. 4, pp. 1747–1755, Nov 2008.

[170] H. T. Yang, Y. T. Tzeng, and M. S. Tsai, "Loss-minimized distribution system reconfiguration by using improved multi-agent based particle swarm optimization," in *2010 Asia-Pacific Power and Energy Engineering Conference*, March 2010, pp. 1–6.

[171] A. Swarnkar, N. Gupta, and K. R. Niazi, "Reconfiguration of radial distribution systems with fuzzy multi-objective approach using adaptive particle swarm optimization," in *IEEE PES General Meeting*, July 2010, pp. 1–8.

[172] S. Sivanagaraju, J. V. Rao, and P. S. Raju, "Discrete particle swarm optimization to network reconfiguration for loss reduction and load balancing," *Electric Power Components and Systems*, vol. 36, no. 5, pp. 513–524, 2008.

[173] A. Abdelaziz, F. Mohammed, S. Mekhamer, and M. Badr, "Distribution systems reconfiguration using a modified particle swarm optimization algorithm," *Electric Power Systems Research*, vol. 79, no. 11, pp. 1521 – 1530, 2009.

[174] D. Zhang, Z. Fu, and L. Zhang, "An improved TS algorithm for loss-minimum reconfiguration in large-scale distribution systems," *Electric Power Systems Research*, vol. 77, no. 5, pp. 685 – 694, 2007.

[175] C.-T. Su and C.-S. Lee, "Network reconfiguration of distribution systems using improved mixed-integer hybrid differential evolution," *IEEE Transactions on Power Delivery*, vol. 18, no. 3, pp. 1022–1027, July 2003.

[176] J.-P. Chiou, C.-F. Chang, and C.-T. Su, "Variable scaling hybrid differential evolution for solving network reconfiguration of distribution systems," *IEEE Transactions on Power Systems*, vol. 20, no. 2, pp. 668–674, May 2005.

[177] R. S. Rao, S. V. L. Narasimham, M. R. Raju, and A. S. Rao, "Optimal network reconfiguration of large-scale distribution system using harmony search algorithm," *IEEE Transactions on Power Systems*, vol. 26, no. 3, pp. 1080–1088, Aug 2011.

[178] E. R. Ramos, A. G. Exposito, J. R. Santos, and F. L. Iborra, "Path-based distribution network modeling: application to reconfiguration for loss reduction," *IEEE Transactions on Power Systems*, vol. 20, no. 2, pp. 556–564, May 2005.

[179] E. Romero-Ramos, J. Riquelme-Santos, and J. Reyes, "A simpler and exact mathematical model for the computation of the minimal power losses tree," *Electric Power Systems Research*, vol. 80, no. 5, pp. 562 – 571, 2010.

[180] H. M. Khodr, J. Martinez-Crespo, M. A. Matos, and J. Pereira, "Distribution systems reconfiguration based on OPF using benders decomposition," *IEEE Transactions on Power Delivery*, vol. 24, no. 4, pp. 2166–2176, Oct 2009.

[181] J. A. Taylor and F. S. Hover, "Convex models of distribution system reconfiguration," *IEEE Transactions on Power Systems*, vol. 27, no. 3, pp. 1407–1413, Aug 2012.

[182] S. Bahadoorsingh, J. V. Milanovic, Y. Zhang, C. P. Gupta, and J. Dragovic, "Minimization of voltage sag costs by optimal reconfiguration of distribution network using genetic algorithms," *IEEE Transactions on Power Delivery*, vol. 22, no. 4, pp. 2271–2278, Oct 2007.

[183] J. E. Mendoza, M. E. Lopez, C. A. C. Coello, and E. A. Lopez, "Microgenetic multiobjective reconfiguration algorithm considering power losses and reliability indices for medium voltage distribution network," *IET Generation, Transmission Distribution*, vol. 3, no. 9, pp. 825–840, September 2009.

[184] B. Amanulla, S. Chakrabarti, and S. N. Singh, "Reconfiguration of power distribution systems considering reliability and power loss," *IEEE Transactions on Power Delivery*, vol. 27, no. 2, pp. 918–926, April 2012.

[185] A. Kavousi-Fard and T. Niknam, "Multi-objective stochastic distribution feeder reconfiguration from the reliability point of view," *Energy*, vol. 64, pp. 342 – 354, 2014.

[186] S. Huang, Q. Wu, L. Cheng, and Z. Liu, "Optimal reconfiguration-based dynamic tariff for congestion management and line loss reduction in distribution networks," *IEEE Transactions on Smart Grid*, vol. 7, no. 3, pp. 1295–1303, May 2016.

[187] A. Kulmala, M. Alonso, S. Repo, H. Amaris, A. Moreno, J. Mehmedalic, and Z. Al-Jassim, "Hierarchical and distributed control concept for distribution network congestion management," *IET Generation, Transmission Distribution*, vol. 11, no. 3, pp. 665–675, 2017.

[188] S. Jazebi, M. M. Hadji, and R. A. Naghizadeh, "Distribution network reconfiguration in the presence of harmonic loads: Optimization techniques and analysis," *IEEE Transactions on Smart Grid*, vol. 5, no. 4, pp. 1929–1937, July 2014.

[189] T. K. Abdel-Galil, A. E. Abu-Elanien, E. F. El-Saadany, A. Girgis, Y. A.-R. I. Mohamed, M. M. A. Salama, and H. H. M. Zeineldin, "Protection coordination planning with distributed generation," CETC Varennes, Natural Resources Canada, Tech. Rep., 2007.

[190] N. C. Hingorani, "Power electronics: Advances in the application of power electronics in generation, transmission, and distribution systems," *IEEE Power Engineering Review*, vol. 15, no. 10, p. 13, October 1995.

[191] Y. Wang and B. Zhang, "A novel hybrid directional comparison pilot protection scheme for the lcc-vsc hybrid hvdc transmission lines," in *13th International Conference on Development in Power System Protection 2016 (DPSP)*, March 2016, pp. 1–6.

[192] J. M. Bloemink and T. C. Green, "Increasing photovoltaic penetration with local energy storage and soft normally-open points," in *2011 IEEE Power and Energy Society General Meeting*, July 2011, pp. 1–8.

[193] ——, "Required VSC efficiency for zero net-loss distribution network active compensation," in *2016 IEEE 7th International Symposium on Power Electronics for Distributed Generation Systems (PEDG)*, June 2016, pp. 1–8.

[194] S. A. M. Javadian, R. Tamizkar, and M. R. Haghifam, "A protection and reconfiguration scheme for distribution networks with DG," in *PowerTech, 2009 IEEE Bucharest*, June 2009, pp. 1–8.

[195] E. Acha and B. Kazemtabrizi, "A new statcom model for power flows using the newtonraphson method," *IEEE Transactions on Power Systems*, vol. 28, no. 3, pp. 2455–2465, Aug 2013.

[196] B. Kazemtabrizi and E. Acha, "An advanced STATCOM model for optimal power flows using newton's method," *IEEE Transactions on Power Systems*, vol. 29, no. 2, pp. 514–525, March 2014.

[197] S. G. Johansson, G. Asplund, E. Jansson, and R. Rudervall, "Power system stability benefits with VSC DC-transmission systems," in *CIGRE conference*, 2004, pp. 1–8.

[198] E. Acha, B. Kazemtabrizi, and L. M. Castro, "A new VSC-HVDC model for power flows using the newton-raphson method," *IEEE Transactions on Power Systems*, vol. 28, no. 3, pp. 2602–2612, Aug 2013.

[199] N. G. Hingorani and L. Gyugyi, *Understanding FACTS: Concepts and Technology of Flexible AC Transmission Systems*. Wiley-IEEE press: Chichester, West Sussex, 2000.

[200] A. A. Ibrahim, B. Kazemtabrizi, and C. Dent, "Operational planning and optimisation in active distribution networks using modern intelligent power flow controllers," in *2016 IEEE PES Innovative Smart Grid Technologies Conference Europe (ISGT-Europe)*, Oct 2016, pp. 1–6.

[201] R. Fourer, D. M. Gay, and B. W. Kernighan, *AMPL: A mathematical programming language*, second edition ed. Duxbury-Thomson, 2003.

[202] J. Czyzyk, M. P. Mesnier, and J. J. Moré, "The network-enabled optimization system (NEOS) server," 1996.

[203] R. Jonathan, "Energy storage technologies," *Ingenia*, pp. 27–32, 2013.

[204] G. Plemann, M. Erdmann, M. Hlusiak, and C. Breyer, "Global energy storage demand for a 100vol. 46, pp. 22 – 31, 2014, 8th International Renewable Energy Storage Conference and Exhibition (IRES 2013).

[205] A. Castillo and D. F. Gayme, "Grid-scale energy storage applications in renewable energy integration: A survey," *Energy Conversion and Management*, vol. 87, pp. 885 – 894, 2014.

[206] S. U. Agamah and L. Ekonomou, "Peak demand shaving and load-levelling using a combination of bin packing and subset sum algorithms for electrical energy storage system scheduling," *IET Science, Measurement Technology*, vol. 10, no. 5, pp. 477–484, 2016.

[207] G. Mokhtari, G. Nourbakhsh, G. Ledwich, and A. Ghosh, "A supervisory load-leveling approach to improve the voltage profile in distribution network," *IEEE Transactions on Sustainable Energy*, vol. 6, no. 1, pp. 245–252, Jan 2015.

[208] F. Luo, K. Meng, Z. Y. Dong, Y. Zheng, Y. Chen, and K. P. Wong, "Coordinated operational planning for wind farm with battery energy storage system," *IEEE Transactions on Sustainable Energy*, vol. 6, no. 1, pp. 253–262, Jan 2015.

[209] Y. Wang, K. T. Tan, X. Y. Peng, and P. L. So, "Coordinated control of distributed energy-storage systems for voltage regulation in distribution networks," *IEEE Transactions on Power Delivery*, vol. 31, no. 3, pp. 1132–1141, June 2016.

[210] D. Rastler, *Electricity energy storage technology options: a white paper primer on applications, costs and benefits*. Electric Power Research Institute, 2010.

[211] F. C. Figueiredo and P. C. Flynn, "Using diurnal power price to configure pumped storage," *IEEE Transactions on Energy Conversion*, vol. 21, no. 3, pp. 804–809, Sept 2006.

[212] T. Kousksou, P. Bruel, A. Jamil, T. El Rhafiki, and Y. Zeraouli, "Energy storage: Applications and challenges," *Solar Energy Materials and Solar Cells*, vol. 120, pp. 59–80, 2014.

[213] S. Succar, R. H. Williams *et al.*, "Compressed air energy storage: theory, resources, and applications for wind power," *Princeton environmental institute report*, vol. 8, 2008.

[214] R. Madlener and J. Latz, "Economics of centralized and decentralized compressed air energy storage for enhanced grid integration of wind power," *Applied Energy*, vol. 101, pp. 299 – 309, 2013.

[215] S. Succar, D. C. Denkenberger, and R. H. Williams, "Optimization of specific rating for wind turbine arrays coupled to compressed air energy storage," *Applied Energy*, vol. 96, pp. 222 – 234, 2012.

[216] R. Power, "ADELE–adiabatic compressed-air energy storage for electricity supply," *RWE Power AG, Essen/Koln*, 2010.

[217] J. B. Garrison and M. E. Webber, "An integrated energy storage scheme for a dispatchable solar and wind powered energy system," *Journal of renewable and sustainable energy*, vol. 3, no. 4, p. 043101, 2011.

[218] T. Mahlia, T. Saktisahdan, A. Jannifar, M. Hasan, and H. Matseelar, "A review of available methods and development on energy storage; technology update," *Renewable and Sustainable Energy Reviews*, vol. 33, pp. 532 – 545, 2014.

[219] Z. Zhou, M. Benbouzid, J. F. Charpentier, F. Scuiller, and T. Tang, "A review of energy storage technologies for marine current energy systems," *Renewable and Sustainable Energy Reviews*, vol. 18, pp. 390 – 400, 2013.

[220] H. Ibrahim, A. Ilinca, and J. Perron, "Energy storage systems - characteristics and comparisons," *Renewable and Sustainable Energy Reviews*, vol. 12, no. 5, pp. 1221 – 1250, 2008.

[221] R. Huggins, *Energy Storage*. Springer Science & Business Media, 2010.

[222] X. Tan, Q. Li, and H. Wang, "Advances and trends of energy storage technology in microgrid," *International Journal of Electrical Power & Energy Systems*, vol. 44, no. 1, pp. 179 – 191, 2013.

[223] K. Divya and J. stergaard, "Battery energy storage technology for power systems: An overview," *Electric Power Systems Research*, vol. 79, no. 4, pp. 511 – 520, 2009.

[224] A. Joseph and M. Shahidehpour, "Battery storage systems in electric power systems," in *2006 IEEE Power Engineering Society General Meeting*, 2006, pp. 1–8.

[225] A. S. Biris, A. R. Biris, D. Lupu, D. Buzatu, J. Darsey, and M. K. Muzumder, "Use of carbon nanostructures for hydrogen storage for environmentally safe

automotive applications," in *Conference Record of the 2004 IEEE Industry Applications Conference, 2004. 39th IAS Annual Meeting.*, vol. 2, Oct 2004, pp. 953–956.

[226] A. Ozarslan, "Large-scale hydrogen energy storage in salt caverns," *International Journal of Hydrogen Energy*, vol. 37, no. 19, pp. 14 265 – 14 277, 2012.

[227] M. Balat, "Potential importance of hydrogen as a future solution to environmental and transportation problems," *International Journal of Hydrogen Energy*, vol. 33, no. 15, pp. 4013 – 4029, 2008.

[228] C. Lamy, "From hydrogen production by water electrolysis to its utilization in a PEM fuel cell or in a SO fuel cell: Some considerations on the energy efficiencies," *International Journal of Hydrogen Energy*, vol. 41, no. 34, pp. 15 415 – 15 425, 2016.

[229] F. Daz-Gonzlez, A. Sumper, O. Gomis-Bellmunt, and R. Villaffila-Robles, "A review of energy storage technologies for wind power applications," *Renewable and Sustainable Energy Reviews*, vol. 16, no. 4, pp. 2154 – 2171, 2012.

[230] S. C. Smith, P. K. Sen, and B. Kroposki, "Advancement of energy storage devices and applications in electrical power system," in *2008 IEEE Power and Energy Society General Meeting - Conversion and Delivery of Electrical Energy in the 21st Century*, July 2008, pp. 1–8.

[231] K. E. Nielsen and M. Molinas, "Superconducting magnetic energy storage (SMES) in power systems with renewable energy sources," in *2010 IEEE International Symposium on Industrial Electronics*, July 2010, pp. 2487–2492.

[232] M. Beaudin, H. Zareipour, A. Schellenberglabe, and W. Rosehart, "Energy storage for mitigating the variability of renewable electricity sources: An updated review," *Energy for Sustainable Development*, vol. 14, no. 4, pp. 302 – 314, 2010.

[233] C. Liu, C. Hu, X. Li, Y. Chen, M. Chen, and D. Xu, "Applying SMES to smooth short-term power fluctuations in wind farms," in *2008 34th Annual Conference of IEEE Industrial Electronics*, Nov 2008, pp. 3352–3357.

[234] A. Sharma, V. Tyagi, C. Chen, and D. Buddhi, "Review on thermal energy storage with phase change materials and applications," *Renewable and Sustainable Energy Reviews*, vol. 13, no. 2, pp. 318 – 345, 2009.

[235] A. Gil, M. Medrano, I. Martorell, A. Lzaro, P. Dolado, B. Zalba, and L. F. Cabeza, "State of the art on high temperature thermal energy storage for power generation. part 1: Concepts, materials and modellization," *Renewable and Sustainable Energy Reviews*, vol. 14, no. 1, pp. 31 – 55, 2010.

[236] A. Fernandez, M. Martnez, M. Segarra, I. Martorell, and L. Cabeza, "Selection of materials with potential in sensible thermal energy storage," *Solar Energy Materials and Solar Cells*, vol. 94, no. 10, pp. 1723 – 1729, 2010.

[237] J. Cot-Gores, A. Castell, and L. F. Cabeza, "Thermochemical energy storage and conversion: A-state-of-the-art review of the experimental research under practical conditions," *Renewable and Sustainable Energy Reviews*, vol. 16, no. 7, pp. 5207 – 5224, 2012.

[238] C. Amadei, G. Allesina, P. Tartarini, and W. Yuting, "Simulation of GEMASOLAR-based solar tower plants for the chinese energy market: Influence of plant downsizing and location change," *Renewable Energy*, vol. 55, pp. 366 – 373, 2013.

[239] J. Clark and H. York, "Thermal energy storage," *Handbook of Heat Transfer*, vol. 2, 2010.

[240] R. Morgan, S. Nelmes, E. Gibson, and G. Brett, "Liquid air energy storage - analysis and first results from a pilot scale demonstration plant," *Applied Energy*, vol. 137, pp. 845 – 853, 2015.

[241] K. Rahbar, J. Xu, and R. Zhang, "Real-time energy storage management for renewable integration in microgrid: An off-line optimization approach," *IEEE Transactions on Smart Grid*, vol. 6, no. 1, pp. 124–134, Jan 2015.

[242] L. H. Macedo, J. F. Franco, M. J. Rider, and R. Romero, "Optimal operation of distribution networks considering energy storage devices," *IEEE Transactions on Smart Grid*, vol. 6, no. 6, pp. 2825–2836, Nov 2015.

[243] H. Xing, H. Cheng, Y. Zhang, and P. Zeng, "Active distribution network expansion planning integrating dispersed energy storage systems," *IET Generation, Transmission Distribution*, vol. 10, no. 3, pp. 638–644, 2016.

[244] X. Shen, M. Shahidehpour, Y. Han, S. Zhu, and J. Zheng, "Expansion planning of active distribution networks with centralized and distributed energy storage systems," *IEEE Transactions on Sustainable Energy*, vol. 8, no. 1, pp. 126–134, Jan 2017.

[245] Y. Tan, Y. Cao, Y. Li, K. Y. Lee, L. Jiang, and S. Li, "Optimal day-ahead operation considering power quality for active distribution networks," *IEEE Transactions on Automation Science and Engineering*, vol. 14, no. 2, pp. 425–436, April 2017.

[246] Y. Yang, Q. Ye, L. J. Tung, M. Greenleaf, and H. Li, "Integrated size and energy management design of battery storage to enhance grid integration of large-scale pv power plants," *IEEE Transactions on Industrial Electronics*, vol. 65, no. 1, pp. 394–402, Jan 2018.

[247] M. McManus, "Environmental consequences of the use of batteries in low carbon systems: The impact of battery production," *Applied Energy*, vol. 93, pp. 288 – 295, 2012.

[248] A. A. Ibrahim, B. Kazemtabrizi, C. Bordin, C. J. Dent, J. D. McTigue, and A. J. White, "Pumped thermal electricity storage for active distribution network applications," in *2017 IEEE Manchester PowerTech*, June 2017, pp. 1–6.

[249] I. MathWorks, *Curve fitting toolbox for use with Matlab: User's guide version 1.* MathWorks, 2001.

[250] T. Coleman, M. A. Branch, and A. Grace, *Optimization toolbox for use with Matlab: User's guide version 2.* MathWorks, Inc., 1999.

[251] ELEXON, "NETA: Balancing mechanism reporting system," Available at http://www.bmreports.com/bwx_home.htm [Accessed: 13 June 2016].

[252] R. Billinton and R. Allan, "Basic power system reliability concepts," *Reliability Engineering & System Safety*, vol. 27, no. 3, pp. 365 – 384, 1990.

[253] North American Electric Reliability Council (NERC), *Reliability Assessment Guidebook: Version 1.2*, T. Burgess, J. Mitchell, C. Smart, B. Williams, E. Weber, B. Bojorquez, R. Hubbert, M. Johannis, M. Lauby, and J. Moura, Eds. North American Electric Reliability Council, 2008.

[254] A. A. Ebrahim, "Evaluation of power system reliability: adequacy and security considerations," in *The Cigre 2004 Session*, 2004.

[255] R. Billinton and S. Aboreshaid, "A basic framework for composite power system security evaluation," in *IEEE WESCANEX 95. Communications, Power, and Computing. Conference Proceedings*, vol. 1, May 1995, pp. 151–156 vol.1.

[256] L. H. Fink and K. Carlsen, "Operating under stress and strain," *IEEE Spectrum*, vol. 15, no. 3, pp. 48–53, March 1978.

[257] K. Morison, L. Wang, and P. Kundur, "Power system security assessment," *IEEE Power and Energy Magazine*, vol. 2, no. 5, pp. 30–39, Sept 2004.

[258] H. Kim and C. Singh, "Steady state and dynamic security assessment in composite power systems," in *Circuits and Systems, 2003. ISCAS '03. Proceedings of the 2003 International Symposium on*, vol. 3, May 2003, pp. 320–323.

[259] P. Sekhar and S. Mohanty, "An online power system static security assessment module using multi-layer perceptron and radial basis function network,"

International Journal of Electrical Power & Energy Systems, vol. 76, no. Supplement C, pp. 165 – 173, 2016.

[260] B. Cintula, . Eleschov, and A. Beln, "Methodology of global assessment of operational states of power system using deterministic approach," in *2015 16th International Scientific Conference on Electric Power Engineering (EPE)*, May 2015, pp. 127–131.

[261] S. Chen, Q. Chen, Q. Xia, H. Zhong, and C. Kang, "N-1 security assessment approach based on the steady-state security distance," *IET Generation, Transmission Distribution*, vol. 9, no. 15, pp. 2419–2426, 2015.

[262] Z. Li, J. Wang, H. Sun, and Q. Guo, "Transmission contingency screening considering impacts of distribution grids," *IEEE Transactions on Power Systems*, vol. 31, no. 2, pp. 1659–1660, March 2016.

[263] E. Polymeneas and A. P. S. Meliopoulos, "Margin-based framework for online contingency selection in unbalanced networks," *IEEE Transactions on Power Systems*, vol. 32, no. 1, pp. 30–38, Jan 2017.

[264] X. Zhang, K. Tomsovic, and A. Dimitrovski, "Security constrained multi-stage transmission expansion planning considering a continuously variable series reactor," *IEEE Transactions on Power Systems*, vol. 32, no. 6, pp. 4442–4450, Nov 2017.

[265] H. Jia, W. Qi, Z. Liu, B. Wang, Y. Zeng, and T. Xu, "Hierarchical risk assessment of transmission system considering the influence of active distribution network," *IEEE Transactions on Power Systems*, vol. 30, no. 2, pp. 1084–1093, March 2015.

[266] M. Negnevitsky, D. H. Nguyen, and M. Piekutowski, "Risk assessment for power system operation planning with high wind power penetration," *IEEE Transactions on Power Systems*, vol. 30, no. 3, pp. 1359–1368, May 2015.

[267] X. Li, X. Zhang, L. Wu, P. Lu, and S. Zhang, "Transmission line overload risk assessment for power systems with wind and load-power generation correla-

tion," *IEEE Transactions on Smart Grid*, vol. 6, no. 3, pp. 1233–1242, May 2015.

[268] W. Deng, H. Ding, B. Zhang, X. Lin, P. Bie, and J. Wu, "Multi-period probabilistic-scenario risk assessment of power system in wind power uncertain environment," *IET Generation, Transmission Distribution*, vol. 10, no. 2, pp. 359–365, 2016.

[269] M. D. Jong, G. Papaefthymiou, and P. Palensky, "A framework for incorporation of infeed uncertainty in power system risk-based security assessment," *IEEE Transactions on Power Systems*, vol. PP, no. 99, pp. 1–1, 2017.

[270] P. Henneaux and D. S. Kirschen, "Probabilistic security analysis of optimal transmission switching," *IEEE Transactions on Power Systems*, vol. 31, no. 1, pp. 508–517, Jan 2016.

[271] E. Heylen, W. Labeeuw, G. Deconinck, and D. V. Hertem, "Framework for evaluating and comparing performance of power system reliability criteria," *IEEE Transactions on Power Systems*, vol. 31, no. 6, pp. 5153–5162, Nov 2016.

[272] R. Fernndez-Blanco, Y. Dvorkin, and M. A. Ortega-Vazquez, "Probabilistic security-constrained unit commitment with generation and transmission contingencies," *IEEE Transactions on Power Systems*, vol. 32, no. 1, pp. 228–239, Jan 2017.

[273] O. Alsac and B. Stott, "Optimal load flow with steady-state security," *IEEE Transactions on Power Apparatus and Systems*, vol. PAS-93, no. 3, pp. 745–751, May 1974.

[274] A. Monticelli, M. V. F. Pereira, and S. Granville, "Security-constrained optimal power flow with post-contingency corrective rescheduling," *IEEE Power Engineering Review*, vol. PER-7, no. 2, pp. 43–44, Feb 1987.

[275] J. Cao, W. Du, and H. F. Wang, "An improved corrective security constrained OPF for meshed AC/DC grids with multi-terminal VSC-HVDC," *IEEE Transactions on Power Systems*, vol. 31, no. 1, pp. 485–495, Jan 2016.

[276] M. Chvez-Lugo, C. R. Fuerte-Esquivel, C. A. Caizares, and V. J. Gutierrez-Martinez, "Practical security boundary-constrained DC optimal power flow for electricity markets," *IEEE Transactions on Power Systems*, vol. 31, no. 5, pp. 3358–3368, Sept 2016.

[277] F. Sass, T. Sennewald, A. K. Marten, and D. Westermann, "Mixed AC high-voltage direct current benchmark test system for security constrained optimal power flow calculation," *IET Generation, Transmission Distribution*, vol. 11, no. 2, pp. 447–455, 2017.

[278] J. Xiao, W. Gu, C. Wang, and F. Li, "Distribution system security region: definition, model and security assessment," *IET Generation, Transmission Distribution*, vol. 6, no. 10, pp. 1029–1035, October 2012.

[279] J. Xiao, F. Li, W. Z. Gu, C. S. Wang, and P. Zhang, "Total supply capability and its extended indices for distribution systems: definition, model calculation and applications," *IET Generation, Transmission Distribution*, vol. 5, no. 8, pp. 869–876, August 2011.

[280] S. H. Lee, Y. C. Kang, and J. W. Park, "Optimal operation of multiple DGs in DC distribution system to improve system efficiency," *IEEE Transactions on Industry Applications*, vol. 52, no. 5, pp. 3673–3681, Sept 2016.

[281] A. Kaur, J. Kaushal, and P. Basak, "A review on microgrid central controller," *Renewable and Sustainable Energy Reviews*, vol. 55, no. Supplement C, pp. 338 – 345, 2016.

[282] S. Chuangpishit, A. Tabesh, Z. Moradi-Shahrbabak, and M. Saeedifard, "Topology design for collector systems of offshore wind farms with pure dc power systems," *IEEE Transactions on Industrial Electronics*, vol. 61, no. 1, pp. 320–328, Jan 2014.

[283] H. A. B. Siddique and R. W. D. Doncker, "Evaluation of DC collector-grid configurations for large photovoltaic parks," *IEEE Transactions on Power Delivery*, vol. 33, no. 1, pp. 311–320, Feb 2018.

[284] F. Mura and R. W. D. Doncker, "Design aspects of a medium-voltage direct current (MVDC) grid for a university campus," in *8th International Conference on Power Electronics - ECCE Asia*, May 2011, pp. 2359–2366.

[285] M. Stieneker, J. Butz, S. Rabiee, H. Stagge, and R. W. D. Doncker, "Medium-voltage DC research grid aachen," in *International ETG Congress 2015; Die Energiewende - Blueprints for the new energy age*, Nov 2015, pp. 1–7.

[286] M. Stieneker and R. W. D. Doncker, "Medium-voltage DC distribution grids in urban areas," in *2016 IEEE 7th International Symposium on Power Electronics for Distributed Generation Systems (PEDG)*, June 2016, pp. 1–7.

[287] A. Hinz, M. Stieneker, and R. W. D. Doncker, "Impact and opportunities of medium-voltage DC grids in urban railway systems," in *2016 18th European Conference on Power Electronics and Applications (EPE'16 ECCE Europe)*, Sept 2016, pp. 1–10.

[288] E. Acha and L. M. Castro, "A generalized frame of reference for the incorporation of, multi-terminal vsc-hvdc systems in power flow solutions," *Electric Power Systems Research*, vol. 136, pp. 415 – 424, 2016. [Online]. Available: http://www.sciencedirect.com/science/article/pii/S0378779616300566

[289] E. Acha, T. Rubbrecht, and L. M. Castro, "Power flow solutions of ac/dc micro-grid structures," in *2016 Power Systems Computation Conference (PSCC)*, June 2016, pp. 1–6.

[290] J. Yu, K. Smith, M. Urizarbarrena, N. MacLeod, R. Bryans, and A. Moon, "Initial designs for the ANGLE DC project; converting existing AC cable and overhead line into DC operation," in *13th IET International Conference on AC and DC Power Transmission (ACDC 2017)*, Feb 2017, pp. 1–6.

[291] M. R. Bussieck and A. Pruessner, "Mixed-integer nonlinear programming," *SIAG/OPT Newsletter: Views & News*, vol. 14, no. 1, pp. 19–22, 2003.

Appendix A

Optimisation Problem

Mathematical models with discrete variables and non-linearities in the objective function and constraints are considered as Mixed Integer Nonlinear Programming (MINLP) [291]. Since full AC optimal power flow contains non-linear objective function and constraints, it can be formulated as MINLP when considering discrete behaviour of element operation such as switch transitions or tap position. Apart from optimal power flow, MINLPs have been used in various other applications including the process industry, financial, engineering, management science and operations research sectors [291]. The needs in such diverse areas have motivated researchers in the field to develop and improve MINLP solver in handling large-scale, highly combinatorial and non-linear problems. The general form of a MINLP:

$$\min f(x, y) \tag{A.0.1}$$

subjected to:

$$g(x, y) \leq 0 \tag{A.0.2}$$

$$x \in X \tag{A.0.3}$$

$$y \in Y \text{intenger} \tag{A.0.4}$$

The functions $f(x, y)$ and $g(x, y)$ are non-linear objective function and constraint function, respectively. The variables X and Y are the decision variables, where one of them (e.g., Y) is required to be integer. If the model is restricted to contain only linear functions (e.g., functions $f(x, y)$ and $g(x, y)$ are linearised), it can be reduced to a Mixed Integer Linear Programming (MILP).